Complexity of 3–manifolds
Geometric and Topological Perspectives

James Edward Morgan

A thesis submitted in fulfilment of
the requirements for the degree of
Doctor of Philosophy

The School of Mathematics and Statistics
Faculty of Science
The University of Sydney

January 2026

Statement of originality and authorship

This is to certify that, to the best of my knowledge, the content of this thesis is my own work. This thesis has not been submitted for any other degree or purpose.

I certify that the intellectual content of this thesis is the product of my own work, and that all assistance received in preparing this thesis and all sources have been acknowledged.

I certify that no generative AI was used in any stage of the production of this thesis.

James Edward Morgan 30 September 2025

Financial support

The research in this thesis was supported by the award of an Australian Government Research Training Program (RTP) Scholarship to the candidate, together with the Australian Research Council's Discovery funding scheme (project number DP190102259), University of Sydney Postgraduate Research Support Scheme (PRSS), and Philipp Hofflin International Research Travel Scholarship.

Authorship Attribution

The material in Chapter 2 was done in collaboration with Jonathan Spreer and is available as the preprint [**MS25**]. This work has been accepted for publication. The research direction and overall mathematical analysis were developed jointly. I substantially contributed to the writing of the manuscript, creation of figures, and the development and proof of key results.

The material in Chapter 3 is in preparation as [**MT**] in collaboration with Stephan Tillmann. The research direction and overall mathematical analysis were developed jointly. My substantial contributions are as above, with an additional in depth exploratory analysis of minimal triangulations in the `Regina` census. This exploratory analysis lead to the development of the algorithm presented in Chapter 4. The final algorithm, its proof of correctness, and the results obtained from an implementation are my own work.

James Edward Morgan 30 September 2025

As supervisor for the candidature upon which this thesis is based, I can confirm that the authorship attribution statements above are correct.

Stephan Tillmann 30 September 2025

Acknowledgements

This thesis would not have been possible without the support and guidance of so many people, especially my supervisors Stephan Tillmann and Jonathan Spreer. Stephan and Jonathan, thank you both so much for all of the mentorship over the past 4 years. I consider myself especially lucky to have had two supervisors who have taken such an active role in my PhD. Stephan – your knack for having a picture for absolutely every situation still boggles my mind, especially considering they never fail to be informative! Jonathan – your seemingly bottomless bag of algorithmic solutions and constructions for every situation has never failed to enlighten and entertain me. To both of you, thank you. I really couldn't have done it without you.

Thank you to the many people from the mathematics community that I have engaged with over the past four years. I don't think I have ever found such a welcoming and warm community, and I'm not sure I will ever find another. To the people at SMRI, AustMS, AMSI, and Matrix – you help foster such a vibrant mathematics community that involves people at all stages of their mathematical careers and it truly makes a world of difference.

A particularly big thanks must go to Zsuzsanna Dansco for all of the encouragement, mentorship, motivation, tea, chocolate, and baked goodies. Ben Burton and Jessica Purcell also have to get a large thanks too. Both of you have been endless pools of wisdom, support, and encouragement throughout my candidature. To the other academics, both near and far, who have given me their time - thank you. Hans Boden, Eric Chesebro, Daryl Cooper, Dionne Ibarra, Adele Jackson, Marc Kegal, Marc Lackenby, Joan Licata, Dan Matthews, Vanessa Robins, Eric Sedgewick, Francis Su, Kate Turner, and many others whose names are escaping me – thank you for the many insightful discussions which have helped not only inform this thesis, but shape me as a mathematician.

To Grace and Yossi. I couldn't have asked for a better pair of PhD siblings. You have both encouraged me from day dot, been there for me through the emotional roller coaster that is a PhD, and been two of the best friends I could ask for. To Em and Alex. The list of things I have learned from both of you is quite long at this point. Collaborating with you was a complete joy (I cannot draw octagons without thinking of you both) and to have gone through my PhD with you both has been a truly wonderful experience.

I have encountered so many amazing peers throughout my PhD. To the $(GT)^2$ community and, especially, my fellow organisers – Alex, Elena, Em, Grace, and Yossi: thank you for the shared

strength, insight, and laughs. To the geometric structures working group, MaPS, the level 4 Carslaw crew, and those at SMRI: I truly believe that, beyond a shadow of a doubt, I chose the best place to do my PhD. Special shout outs go to: Alec, Alex, Ash, Chris L., Damian, Daniel, Ellie, Georg, Grace, Jack, Joe, Justin, Lucy, Mei, Mitch, Nalini, Nelson, Nick, Pieter, Sam, Sophie, Thomas, Tilda, and Will. To anyone who I have forgotten to mention, I sincerely apologise.

Outside of mathematics, so many people have supported me on this journey. Cheyenne E. and Cheyenne H. – words cannot express how much you have been there for me. You have supported my every endeavour and been there through the hard times. Truly, thank you. To my family, my parents Anne and Barry, my sister Amie, and my brother*, Blake. Thank you all for encouraging me down this path, supporting me at every turn, and doing your best to try and understand what it is I actually do. I am forever indebted to you.

To my D&D gang – Alex, Anne, Cheyenne, and Paul – thank you for always giving me a distraction when I need it, something play to balance the work. Maybe now that the thesis is done, we can get you all to level 3? Alex and Paul, every minute spent gaming, laughing, and crying with you has made the past four years so much easier. Eric and Jack, the two best eggs – thank you for all of the brunches, dinners, and, especially, Yum Chas. My housemate, Nick: living with you has made the past two years a lot easier than they could have been. I'll always think of you every time a Harley goes past.

For the many others, who I will attempt to list now, thank you. Thank you for being a friend, for being up for a chat, for reading anything I've sent you, for listening to me rant about mathematics when you definitely have no idea what's going on: Adi, Al, Alex T., Annie, Brendan, Brittany, Chris, Connie, Cynthia, Dean, Jen, Lucy, Lecheng, Qas, Rhuaidi, Rodd, Sandra, Sara.

Thank you.

*in law.

Abstract

Minimal triangulations of 3–dimensional manifolds offer key insights to topological and geometric properties of the underlying manifold. We study minimal triangulations through two lenses – one geometric, and one topological. The lens of geometry allows us to utilise properties such as volume to understand the underlying topology. The lens of topology allows us to use a more flexible theory to dissect the underlying subcomplexes.

In the former case we study geometric triangulations of hyperbolic 2–bridge link complements. Using the hyperbolic structure induced on the triangulations, we are able to establish new lower bounds on the complexity of infinitely many 2–bridge link complements. The main tool we use for this is hyperbolic volume by way of angle structures.

In the latter case, we utilise normal surface theory together with layered and 0–efficient triangulations to explore the anatomy of minimal triangulations by way of the $\mathbb{Z}_2$–Thurston norm. Our main result bounds the number of edges of degree three within such triangulations and hence gives us a method of analysing their subcomplexes intersecting layered solid tori. As an application, we determine new infinite families of minimal triangulations.

CONTENTS

Introduction

This thesis exists in the world of low-dimensional topology, at the intersection between topology, geometry, and combinatorics. We study triangulations of 3–manifolds with a focus towards minimal triangulations. We give our attention to both material triangulations of closed 3–manifolds and ideal triangulations of cusped hyperbolic 3–manifolds[†] and employ techniques from 3–manifold topology and hyperbolic geometry to examine their anatomy.

Why minimal triangulations?

Triangulations have proven to be a powerful tool in understanding 3–manifolds since the following landmark result of Moise.

Theorem [Moi52] *Every closed 3–manifold admits a triangulation.*

In the context of Moise's work, a 'triangulation' was a simplicial triangulation. We, however, will focus on pseudo–simplicial triangulations. Further work of Moise [Moi54] and Bing [Bin54] extended this result to include compact 3–manifolds with boundary. In the language of this thesis, the triangulations stemming from these results were material triangulations. Later work of Casler [Cas65], focusing on special spines, implied the existence of ideal triangulations for the interior of a 3–manifold with boundary.

All of this still does not answer the question of why we are interested in *minimal* triangulations.

For a given 3–manifold M, there are infinitely many ways in which we may triangulate it. Depending on the application, some of these choices will be notably better than others. For an instructive example, consider the 2–sphere. The three simplicial platonic solids – the tetrahedron, the octahedron, and the icosahedron – have, as boundaries, the three triangulations of the 2–sphere with the maximum number of symmetries per triangle. The tetrahedron is the simplicial triangulation with the smallest number of pieces, the octahedron is the smallest triangulation with central symmetry, and the icosahedron is the smallest triangulation covering a simplicial triangulation of the real projective plane. It seems reasonable that these triangulations should be "good" in most contexts. In 3–dimensions, it seems reasonable that the "best" triangulations of 3–manifolds feature those that have the smallest number of tetrahedra, that is, are minimal.

[†]The author would like to think that both are given an approximately equal amount of attention, though this may not be true.

The complexity $c(M)$ of a 3–manifold M is the minimum number of tetrahedra required in a triangulation of M. In the case that M is closed and irreducible, this definition agrees with the complexity defined by Matveev in terms of spines [**Mat90**] unless the manifold is S^3, $\mathbb{R}P^3$, or $L(3,1)$. If a triangulation $\mathscr{T}$ of a 3–manifold M realises the complexity, that is $|\mathscr{T}| = c(M)$, then the triangulation is minimal. Complexity acts as the organising principle when enumerating manifolds as only a finite number of 3–manifolds can achieve a given complexity. It also offers a measure as to how topologically complicated a given 3–manifold is.

In addition, minimal triangulations have many advantages in computations, especially since algorithmic solutions to topological problems often scale exponentially in the size of the input triangulation (see [**HLP99**] for an example).

A geometric perspective. The main focus of the geometric perspective in this thesis is on geometric ideal triangulations of cusped hyperbolic 3–manifolds. Whilst all of these terms are defined in due course, the main idea is that we take an inherently topological object (an ideal triangulation) of an inherently geometric object (a cusped hyperbolic 3–manifold) in a way that we can leverage the underlying geometry to analyse the topology.

In the context of minimal ideal triangulations, Thurston [**Thu80**] established a one-sided inequality connecting the volume of a complete hyperbolic 3–manifold of finite volume and its complexity:

$$c(M) \geq \frac{\mathrm{Vol}(M)}{v_3}$$

where $v_3 \approx 1.0149\ldots$ is the maximum volume of a hyperbolic ideal tetrahedron. Indeed, through Mostow-Prasad rigidity [**Mos68, Pra73**] the volume itself is a topological invariant of M. The difficulty remains in computing (or estimating) the volume of a hyperbolic 3–manifold.

Thurston [**Thu80**] also devised two sets of gluing equations – one a set of complex polynomials and one a set of linear equations – which, when satisfied, guarantee that a set of hyperbolic ideal tetrahedra will glue together to induce a hyperbolic structure (not necessarily complete) on the resulting triangulation. Whilst this provides a starting point for leveraging the underlying geometry, we ideally want to induce a complete hyperbolic structure on our triangulation which agrees with the structure on the underlying 3–manifold. Casson and Rivin [**Riv94**] provided a connection between the set of linear equations and the existence of this complete hyperbolic structure on the triangulation. The main tools of this work are angle structures and volume maximisation. Angle structures provide a method by which the volume of a hyperbolic tetrahedron may be calculated [**Mil82**]. Using these, combined with Thurston's lower bound, an avenue for computing lower bounds on the complexity is revealed and, perhaps unsurprisingly, traversed in this thesis.

A topological perspective. The main focus of the topological perspective in this thesis is on minimal triangulations of closed, orientable, irreducible, connected 3–manifolds which admit a colouring by some rank–2 subgroup of $H^1(M;\mathbb{Z}_2)$. The theory of such minimal triangulations has been developed since work of Jaco, Rubinstein, and Tillmann [**JRT09**]. The main tool used is the $\mathbb{Z}_2$ analogue of Thurston's norm [**Thu86**]. The $\mathbb{Z}_2$–Thurston norm [**JRT13**] is defined in terms of embedded surfaces in a manifold. By passing to a triangulation, this theory offers a prime example of understanding the anatomy of 3–manifolds by studying the surfaces embedded within a triangulation.

A particularly pleasing aspect of this theory is its use of normal surface theory, layered triangulations, and 0–efficient triangulations. By colouring a triangulation with a rank–2 subgroup, we may define a special class of normal surfaces dual to the colouring. By examining the properties of the surfaces in a minimal triangulation, we are able to distil the essence of its anatomy.

The combination of these surfaces with the additional assumption of 0–efficiency allows a systematic study of the subcomplexes which may arise within minimal triangulations. Subcomplexes which are combinatorially equivalent to layered solid tori play a particularly important role and their intersections are controlled within a 0–efficient triangulation. Using these as a springboard, we can describe and classify more general subcomplexes within these triangulations.

Organisation of the thesis.

The background required for this thesis is covered in Chapter 1. We define concretely what we mean by a triangulation, a material triangulation, and an ideal triangulation (Section 1.1). We then survey the landscape of minimal triangulations (Section 1.2). Normal surface theory (Section 1.3) is introduced as a method by which we can study triangulations of 3–manifolds via embedded surfaces. Special types of triangulations are introduced in Section 1.4. Layered triangulations (Section 1.4.1) are ubiquitous in the study of both material and ideal triangulations, in particular through layered solid tori. In the topological setting, 0–efficient triangulations (Section 1.4.4) arise naturally when studying minimal triangulations. Finally, we introduce the necessary hyperbolic geometry and define geometric triangulations in Section 1.5. Of particular importance in this section are angle structures, as these play a fundamental role in our work.

Chapter 2 presents the geometric perspective in this thesis. We study the Sakuma–Weeks triangulations of hyperbolic 2–bridge link complements. These triangulations are geometric and thus we may utilise tools from hyperbolic geometry to study the topology and combinatorics of the underlying 3–manifold. In Section 2.1 we introduce the construction and notation of a 2–bridge link and follow with Section 2.2 in which we define the Sakuma–Weeks triangulations focusing on their construction from a link diagram. In Section 2.3 we provide a necessary condition for the Sakuma–Weeks triangulation to be minimal and show that 'most' of them are in fact not minimal. Finally, we present our main contribution in Section 2.4. We utilise angle

structures on the triangulations together with their combinatorics to provide lower bounds on the complexity of the 2–bridge links whose Sakuma–Weeks triangulation satisfies the necessary condition for minimality. Our main contribution is the following result providing a multiplicative lower bound on the complexity of these manifolds.

Theorem 2.20 Let $L = L(\Omega)$ be the 2-bridge link associated to the word $\Omega = RL^{a_1} \cdots (L^{a_n}R \mid R^{a_n}L)$ where $a_i \in \{1,2\}$ for all $1 \leq i \leq n$ and $n \geq 1$. Let $M = S^3 \backslash L$ and $\mathscr{T} = \mathscr{T}(M)$ be the Sakuma-Weeks triangulation of M and let $c(M)$ denote the complexity of M. Then,

$$0.8|\mathscr{T}| \leq c(M) \leq |\mathscr{T}|$$

Chapter 3 presents the topological perspective in this thesis. We continue the study of minimal triangulations of closed, orientable, irreducible, connected 3–manifolds using the $\mathbb{Z}_2$–Thurston norm started by Jaco, Rubinstein, and Tillmann [**JRT09**, **JRT13**]. After reviewing the necessary background in Sections 3.1 and 3.2 we move to understand the general anatomy of rank–2 coloured minimal triangulations in Section 3.3. This section culminates in our main technical result which provides an upper bound on the number of edges of degree 3 in a rank–2 coloured minimal triangulation. In particular, we reveal a link between the complexity of M, the efficiency of surfaces representing homology classes, and the degrees of homologically trivial edges.

Theorem 3.1 Let M be a closed, orientable, irreducible, connected 3–manifold with minimal triangulation $\mathscr{T}$. Suppose that all edge loops are coloured by the rank–2 subgroup H of $H^1(M;\mathbb{Z}_2)$, $\mathscr{T}$ is $(\Delta_{qq},4)$–free with respect to the colouring and that $|\mathscr{T}| = (2+k) + \sum_{\varphi \in H} \|\varphi\|$. Letting $\mathfrak{e}_d$ denote the number of H–even edges of degree d, we have:

$$\mathfrak{e}_3 \leq k + 2\sum_{i=1}^{3} d_{\varphi_i} + \sum_{d=5}^{\infty} (d-4)\mathfrak{e}_d.$$

One important aspect of this result is that it places constraints on the existence of layered solid torus subcomplexes within a minimal triangulation. In Section 3.4 we apply this result to conduct a detailed analysis of 3–manifolds satisfying additional assumptions on their complexity. We conclude this chapter by describing two new infinite families of 3–manifolds in Section 3.5.

The final chapter of this thesis, Chapter 4, describes an algorithm for computing the $\mathbb{Z}_2$–Thurston norm for non-trivial classes $\varphi \in H^1(M;\mathbb{Z}_2)$ using a 0–efficient triangulation. Importantly, this algorithm does not rely on the triangulation being minimal. Having implemented this algorithm using `Regina` [**BBP+23**], we provide several summary tables of data available in the current `Regina` census of closed, orientable 3–manifolds up to 11 tetrahedra [**Bur**]. We expect that the code and data will contribute to the discovery of further results.

CHAPTER 1

Minimal triangulations in geometry and topology

In this chapter we lay the groundwork for this thesis, providing background on the geometry and topology of 3–manifolds. We define both material and ideal triangulations in Section 1.1 and introduce the `Regina` gluing table. In Section 1.2 we define the complexity of 3–manifolds and provide a summary of work done in classifying minimal triangulations and enumerating minimal triangulations in the creation of censuses. We finish this section with a set of combinatorial moves, called Pachner moves, which allow for the modification of triangulations. The content of these sections (Sections 1.1 and 1.2) will be used throughout the thesis.

In Sections 1.3 and 1.4 we focus on topological aspects of triangulations. Section 1.3 introduces Haken's theory of normal surfaces, providing us with a finite set of building blocks for properly embedded surfaces within a given triangulation. In Section 1.4 we define layered triangulations and, with the language of normal surface theory, 0–efficient triangulations. These types of triangulations play a fundamental role in the analysis of minimal triangulations, with many subcomplexes being layered and most* closed, orientable, irreducible 3–manifolds having 0-efficient minimal triangulations. The content of these sections is used in Chapters 3 and 4.

In Section 1.5 we focus on geometric aspects of triangulations in the setting of cusped, hyperbolic 3–manifolds. We define both topological and geometric ideal triangulations, focusing on the latter. Through the use of angle structures, we conclude with a theorem by Casson and Rivin which provides necessary and sufficient conditions for a topological ideal triangulation equipped with an angle structure to be geometric. The content of this section provides a basis for the work presented in Chapter 2.

1.1. Generalised triangulations

Let M be an orientable, connected 3–manifold. Intuitively, a triangulation is a decomposition of M into finitely many tetrahedra together with a set of gluing instructions which describe how their triangular faces are identified in pairs. In this thesis we concern ourselves with both *material* triangulations of closed 3–manifolds and *ideal* triangulations of cusped hyperbolic 3–manifolds. Whilst the treatment of each of these types of triangulations is broadly the same, we define each type of triangulation separately.

*The only excluded 3–manifolds are $\mathbb{R}P^3$ and $L(3,1)$.

Definition 1.1 A **(generalised) triangulation** is a triple $\mathscr{T} = (\widetilde{\Delta}, \Phi, p)$ consisting of the union of a finite collection of pairwise disjoint 3–simplices, $\widetilde{\Delta} = \sigma_1 \cup \cdots \cup \sigma_t$, a family of affine isomorphisms, Φ, which pair faces of the simplices in $\widetilde{\Delta}$, and a natural quotient map $p : \widetilde{\Delta} \to \widetilde{\Delta}/\Phi$, where the space $\widehat{M} = \widetilde{\Delta}/\Phi$ is endowed with the identification topology.
The quotient map p is injective on the interior of each 3–simplex in $\widetilde{\Delta}$ and we thusly refer to the image of a 3–simplex as a **tetrahedron**. Similarly, p is injective on faces and we further require that it is injective on edges[‡]. We refer to the images of the k–simplices as the **vertices**, **edges**, and **faces** of the triangulation for $k = 0,\ 1$, and 2, respectively. ◇

Unless it is necessary, we suppress the triple and simply write $\mathscr{T}$ to denote a triangulation. A triangular face which remains unpaired is termed a **boundary face** of the triangulation, and similarly for the edges and vertices incident with it [ST80].

Definition 1.2 Given a triangulation $\mathscr{T} = (\widetilde{\Delta}, \Phi, p)$ of $\widehat{M} = \widetilde{\Delta}/\Phi$, the **k–skeleton** of $\mathscr{T}$ is the set of images of the k–simplices in $\widetilde{\Delta}$. Letting $\sigma^k \subset \widetilde{\Delta}$ denote a k–simplex in $\widetilde{\Delta}$, we write this formally as

$$\widehat{M}^{(k)} = \left\{ p(\sigma^k) \in \widehat{M} \mid \sigma^k \subseteq \widetilde{\Delta} \right\}$$

◇

We sometimes refer to an edge $e \in \widehat{M}^{(1)}$ as an **edge class** when we need to distinguish between e and an edge in $p^{-1}(e)$. This language is prevalent in Chapter 2. For an edge $e \in \widehat{M}^{(1)}$ we define its **degree**, denoted $\deg(e)$, to be the number of pairwise distinct 1–simplices in the preimage $p^{-1}(e)$.

The term *generalised* in our definition is to emphasise that we do not require our triangulations to be simplicial[†]. This allows greater flexibility in that two triangular faces of a single 3–simplex may be identified with each other.

Our definition of a triangulation makes no reference to 3–manifolds thus far, and this is intentional. This is to emphasise triangulations as *combinatorial* objects and not just topological ones. For a triangulation of $\widehat{M}$ to describe a 3–manifold there are additional conditions which must be satisfied.

Definition 1.3 Let v be a vertex of a triangulation $\mathscr{T}$. The **link** of v is the surface S that is the boundary of a small regular neighbourhood of v. This surface is termed a **vertex–linking** surface. ◇

[‡]Requiring that p is injective on the edges allows us to avoid the situation where an edge is identified with itself but in the opposite direction.

[†]Mathematicians have used many names for these types of triangulations – *pseudosimplicial* triangulations, *semi-simplicial* triangulations, *singular* triangulations, *topological* triangulations, and *loose* triangulations, to name a few.

We now discuss the allowed vertex links and use these to determine when a triangulation is homeomorphic to a 3–manifold. If the link of v is a sphere or disc, then v is termed a **material** vertex. If the link of v is any other surface, then we term v an **ideal** vertex. When every vertex is material, we say that $\mathscr{T}$ is a **material triangulation**. When every vertex is ideal, we say that $\mathscr{T}$ is an **ideal triangulation**.

Given a triangulation $\mathscr{T}$, the points at which the quotient space $\widehat{M} = \widetilde{\Delta}/\Phi$ may fail to be a manifold are contained in $\widehat{M}^{(0)}$ and we call $\widehat{M}$ a **3–dimensional pseudomanifold**. Details on pseudomanifolds can be found in [**ST80**, Chapter 3]. When $\mathscr{T}$ is a material triangulation the neighbourhood of each vertex in $\widehat{M}$ is homeomorphic to the neighbourhood of a point in 3–dimensional Euclidean space or the neighbourhood of a point on the boundary of 3–dimensional Euclidean half–space.

If $\widehat{M}$ contains no boundary vertices, then it is a **closed 3–dimensional pseudomanifold**; otherwise it is a **compact 3–dimensional pseudomanifold with boundary**. When $\mathscr{T}$ is an ideal triangulation the space $\widehat{M}\backslash\widehat{M}^{(0)}$ is a topologically finite, non–compact 3–manifold (possibly with non–empty boundary). The elements of $\widehat{M}^{(0)}$ and $\widehat{M}^{(1)}$ are termed the ideal vertices and ideal edges of $\widehat{M}\backslash\widehat{M}^{(0)}$, respectively.

When working with material triangulations we will adopt the notation $M = \widehat{M}$. Similarly, when working with ideal triangulation we will adopt the notation $M = \widehat{M}\backslash\widehat{M}^{(0)}$ and hope this does not cause any confusion.

Example 1.4 The lens space $L(7,2)$ has a material triangulation consisting of two tetrahedra. The complement of the figure-8 knot has an ideal triangulation consisting of two ideal tetrahedra. These are illustrated in Figure 1.1.

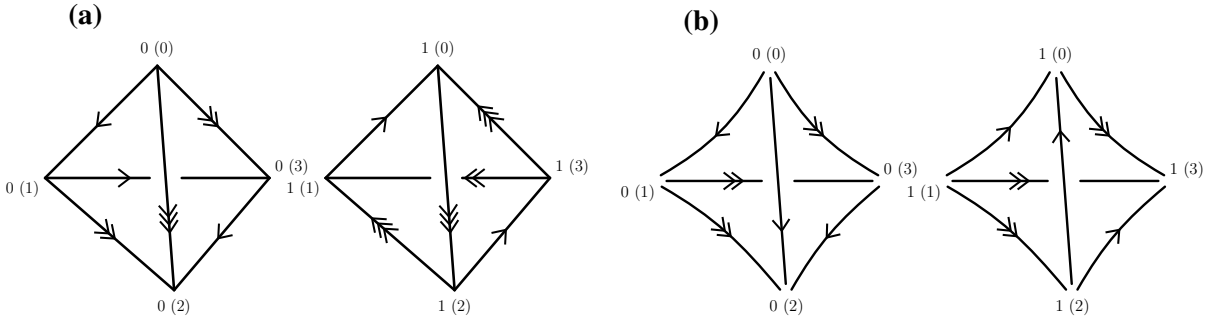

FIGURE 1.1. (a) Material triangulation of the lens space $L(7,2)$; (b) Ideal triangulation of the figure-8 knot complement. Labels on the vertices denote tetrahedron index and, in parentheses, the vertex index. That is, 0 (0) denotes tetrahedron 0 (vertex 0).

1.1.1. Triangulations with `Regina`. One key advantage of viewing a 3–manifold as a combinatorial object is that we may develop algorithms and computational tools to aid our investigations. The software packages `Regina` [BBP+23] and `SnapPy` [CDGW] provide many tools examining both the geometry and topology of 3–manifolds via their triangulations. More specialised software packages, such as `Veering` [PSS25], have also been developed utilising the tools available from both `Regina` and `SnapPy` which allow for the analysis of more specialised classes of triangulations.

The work presented in this thesis utilises `Regina` for both exploratory analysis and constructing explicit examples. We present below a standard gluing table utilised by `Regina` for representing a triangulation.

Example 1.5 The construction of a standard gluing table requires a labelling of each tetrahedron and its vertices. For each face of each tetrahedron, the gluing table describes which face of which tetrahedron it is paired with via a permutation of the vertices. Tables 1.1 and 1.2 provide the gluing tables for the triangulations presented in Figure 1.1.

Tetrahedron	Face 012	Face 013	Face 023	Face 123
0	1 (231)	0 (132)	1 (301)	0 (031)
1	1 (320)	0 (230)	1 (210)	0 (201)

TABLE 1.1. Gluing table for the triangulation of $L(7,2)$ illustrated in Figure 1.1.

Tetrahedron	Face 012	Face 013	Face 023	Face 123
0	1 (203)	1 (103)	1 (102)	1 (132)
1	0 (203)	0 (103)	1 (102)	0 (132)

TABLE 1.2. Gluing table for the triangulation of the figure-8 knot complement illustrated in Figure 1.1.

1.2. Minimal triangulations

At the core of this thesis are *minimal triangulations*. For a given 3–manifold M, a triangulation $\mathscr{T}$ is considered minimal if there does not exist another triangulation of M with fewer tetrahedra.

Definition 1.6 The **complexity** of a 3–manifold M is the number of tetrahedra in a minimal triangulation of M. We denote this quantity $c(M)$. ◇

The notion of complexity for 3–manifolds was first defined by Matveev [Mat88, Mat90] as the number of vertices in a special spine. Termed the *Matveev complexity*, much of what is currently known about the complexity of 3–manifolds is in terms of the Matveev complexity. Combinatorially, special spines are dual to triangulations and the two definitions of complexity

agree for all irreducible 3–manifolds except S^3, $\mathbb{R}P^3$, and $L(3,1)$; their Matveev complexities all being 0 but their complexities being 1, 2, and 2, respectively.

Loosely speaking, the complexity of M measures how combinatorially difficult M is to describe. For every $n \in \mathbb{N}$, the number of 3–manifolds of complexity at most n is finite and thus complexity provides low-dimensional topologists with a useful tool for organising and systematically studying 3–manifolds.

Given a 3–manifold, the task of determining its complexity precisely is, in general, difficult. For example, the Weber-Seifert dodecahedral space [**WS33**] is a closed, orientable hyperbolic 3–manifold for which the complexity remains unknown. Burton, Rubinstein, and Tillmann [**BRT12**] have provided an explicit triangulation of this space (available with `Regina`) consisting of 23 tetrahedra. A triangulation with fewer tetrahedra has not been found.

There are very few results which determine the complexity for infinite families of manifolds. Work of Jaco, Rubinstein, and Tillmann determined the complexity for several infinite families of lens spaces [**JRT09**]. Building on the methods developed in this work, Jaco, Rubinstein, Spreer, and Tillmann provided a global lower bounds on the complexity of all closed, orientable, irreducible, connected 3–manifolds M with non-trivial $H^1(M;\mathbb{Z}_2)$ by using the $\mathbb{Z}_2$-Thurston norm [**JRT13**, **JRST20b**] with Nakamura [**Nak17**] establishing the same result independently. From this, they have determined the complexity of all such 3–manifolds which achieve these lower bounds when the rank of $H^1(M;\mathbb{Z}_2)$ is exactly one or two.

Shifting our attention to finite volume, cusped, orientable hyperbolic 3–manifolds we still observe sparseness in the results which determine the complexity for infinite families of manifolds. Perhaps one of the most studied manifolds here are the 2–bridge link complements. Geometric triangulations of these manifolds were first described by Sakuma and Weeks [**SW95**] with upper bounds on the complexity being determined by Ishikawa and Nemoto [**IN16**]. This upper bound proved to be exact for a certain family of 2–bridge links, which we describe in Section 2.4.3. Work of Morgan and Spreer [**MS25**] provides a necessary condition for the minimality of the Sakuma-Weeks triangulations and establishes both multiplicative and additive lower bounds on their complexity. Recent work of Aribi, Guéritaud, and Piguet-Nakazawa [**BAGPN23**] constructed ideal triangulations for twist knots (a certain type of 2–bridge knot) with approximately half the number of tetrahedra than the upper bound established by Ishikawa and Nemoto.

Jaco, Rubinstein, Spreer, and Tillmann [**JRST20a**] extended their work with the $\mathbb{Z}_2$–Thurston norm to the setting of cusped hyperbolic 3–manifolds and established a lower bound on the complexity when the rank of $H^1(M;\mathbb{Z}_2)$ is at least two. The immediate application of this theory was to show that the monodromy ideal triangulations of once-punctured torus bundles over the circle are minimal. Rubinstein, Spreer, and Tillmann [**RST24**] further utilised this theory to construct another infinite family of minimal triangulations of once-cusped hyperbolic

3–manifolds which arise from certain Dehn surgeries on the complement of the 3-component link 8^3_9.

Outside of these results, most research has generated bounds on the complexity of certain classes of 3–manifolds. Notably, complexity bounds for Dehn-fillings have been determined by Cha [**Cha16a**, **Cha16b**, **Cha18**], and in more special cases in [**JRST25**].

1.2.1. Enumeration and censuses. Prior to the introduction of Matveev complexity, the work of Matveev and Savvateev [**MS74**] provided an enumeration of all 61 closed, orientable, irreducible, connected 3–manifolds of complexity at most 5. This was extended further over the next three decades through works of Matveev [**Mat90**] and Martelli and Petronio [**MP01**]. These censuses were developed utilising spines rather than triangulations.

The first census of all closed orientable 3–manifold triangulations of complexity at most 9 was first reported by Burton [**Bur10**] and extended to all such manifold triangulations of complexity at most 11 [**Bur11a**]. At the time of writing, the work of Matveev and Tarkaev [**MT20**] has extended the census of closed, orientable, irreducible 3–manifolds to include all those of complexity at most 13.

Work of Amendola and Martelli [**AM03**, **AM05**] provided the first censuses of closed non-orientable 3–manifolds. Their census revealed that there were no such manifolds achieving a complexity less than 6 and found that there were only eight achieving a complexity of at most 7. Work of Burton [**Bur07**] independently found these manifolds and provided their 41 minimal triangulations.

Attention has also been given to cusped hyperbolic 3–manifolds of finite volume, with the work of Hildebrand and Weeks [**HW89**] generating the `SnapPea` census – the first census of minimal ideal triangulations of cusped hyperbolic 3–manifolds containing at most 5 ideal tetrahedra. Together with Callahan [**CHW99**], they extended this census to include all those minimal ideal triangulations containing at most 7 ideal tetrahedra. Thistlethwaite [**Thi10**] extended it further to 8 ideal tetrahedra. At the time, however, this census was not guaranteed to be complete in that its construction relied upon inexact calculations and some unproven assumptions. Burton [**Bur14a**] rectified this, proving that the `SnapPea` census indeed captured all minimal ideal triangulations of cusped hyperbolic 3–manifolds with complexity at most 8 and further extended the census to include such manifolds with complexity 9.

The final census that we mention is the Hodgson-Weeks census of closed hyperbolic 3–manifold triangulations [**HW94**]. This census approximates the set of all closed hyperbolic 3–manifolds of volume strictly less than 6.5 and systole length at least 0.15.

All of the above mentioned triangulation censuses are shipped with `Regina` and/or `SnapPy`. The development of these censuses over the past 50 years highlights the deep connection between low-dimensional and algorithmic topology.

1.2.2. Modification of triangulations. Given a 3–manifold M with triangulation $\mathscr{T}$, certifying that $\mathscr{T}$ is minimal is not an easy task as we have already mentioned. Of course if M is in a census of minimal triangulations, then we need only check if $\mathscr{T}$ is one of the listed triangulations in the census. Otherwise, we are left with a lower bound on $c(M)$ from the appropriate census and an upper bound from the number of tetrahedra in $\mathscr{T}$. For example, the Weber-Seifert dodecahedral space does not appear in the census of Matveev and Tarkaev [**MT20**]. We know from this that it must have a complexity of at least 14. An upper bound of 23 on the complexity is provided by Burton, Rubinstein, and Tillmann [**BRT12**] via an explicit construction.

For a given triangulation *not* in any census, we may attempt to modify it by a sequence of *elementary*, or **Pachner moves** [**Pac91**]. These moves adjust a subcomplex of the triangulation whilst preserving the manifold.

The only Pachner move we will encounter in this thesis is the **3–2 move**. This takes three pairwise distinct tetrahedra glued around a degree 3 edge and replaces it with two tetrahedra glued along a triangular face. The inverse of this move is the **2–3 move**. These are illustrated in Figure 1.2.

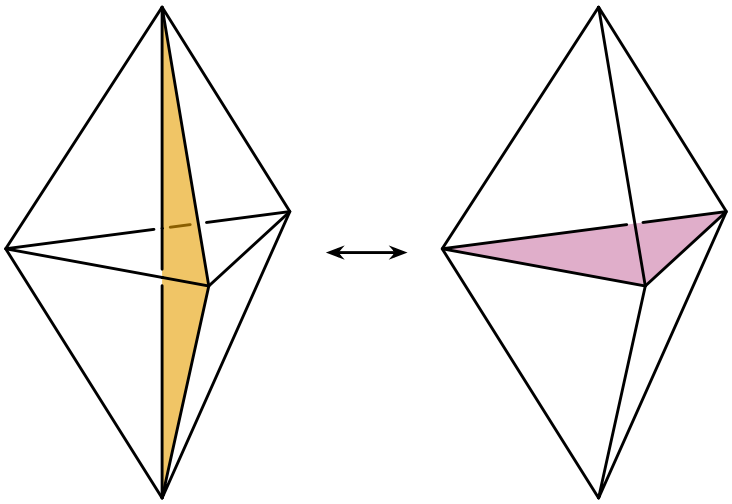

FIGURE 1.2. The Pachner 3–2 and 2–3 moves. The 3–2 move replaces the three tetrahedra on the left with the two tetrahedra on the right.

The other elementary move we will encounter in this thesis is the aggregate **4–4 move**. A square bipyramid can be triangulated with four pairwise distinct tetrahedra by inserting an edge of degree 4 between a pair of opposite vertices. The 4–4 move replaces this edge with one of the other two possible edges. We illustrate this in Figure 1.3. We consider this move to be

'aggregate' as it is achieved by performing a 2–3 move followed by a 3–2 move. Importantly, this means the 4–4 move preserves the number of tetrahedra in $\mathscr{T}$.

A key observation of the 4–4 move is that whilst it preserves the number of tetrahedra, it alters the degrees of edges incident to the four tetrahedra. The degrees of the equatorial edges always increase by 1 whilst the degrees of the four edges opposite the new axis decrease by 1. We have marked these decreases on the appropriate edges in Figure 1.3.

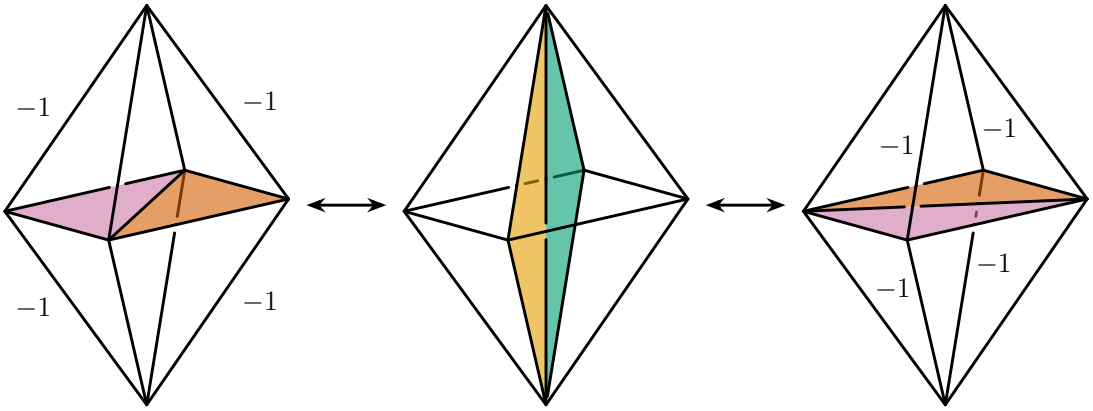

FIGURE 1.3. The aggregate 4–4 move. The negative degree changes are marked for each of the two possible retriangulations.

The elementary moves are also defined on special spines and they are generally considered easier to visualise in this context. The following result, proved by Amendola [**Ame05**], establishes the importance and power of the 3–2 and 2–3 moves.

Theorem 1.7 (Amendola) *Let M be a 3–dimensional manifold or pseudomanifold. The set of all triangulations of M with a fixed number of material vertices, including zero, is connected under 3–2 and 2–3 moves, excluding those triangulations consisting of a single tetrahedron.*

This result by itself is already powerful; combined with Theorem 1.17 it tells us that, in the case of closed, orientable, irreducible 3–manifolds, we only need to consider one vertex triangulations if we are searching for minimal triangulations. The triangulations excluded by this result are those with only a single tetrahedron. Thankfully, these triangulations can be enumerated easily. In the closed setting there are two triangulations of S^3, one of $L(4,1)$, and one of $L(5,2)$. In the ideal setting, there is one triangulation of the Gieseking manifold – a non-orientable, cusped hyperbolic 3–manifold of finite volume.

1.3. Normal surface theory

The concept of a normal surface was first introduced by Kneser in 1929 [**Kne29**]. Haken, in 1961, extended this theory and developed an algorithm for detecting the unknot [**Hak61**,

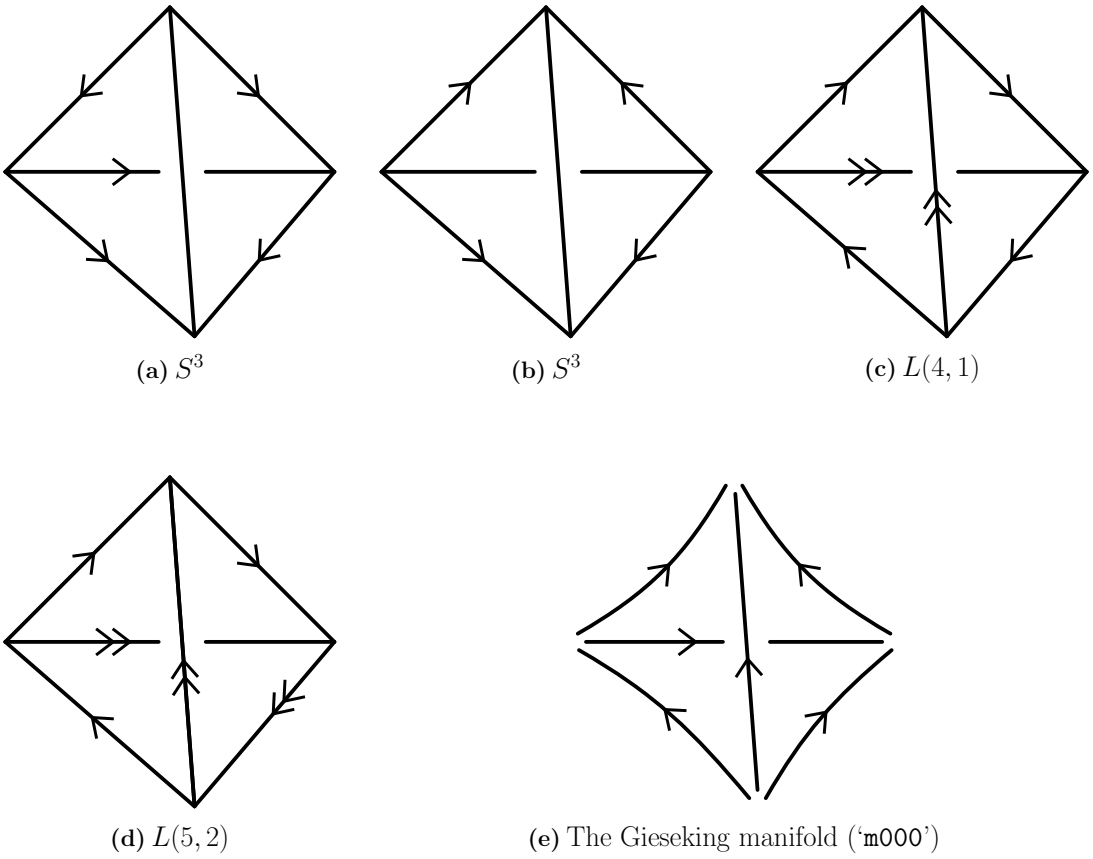

(a) S^3 (b) S^3 (c) $L(4,1)$

(d) $L(5,2)$ (e) The Gieseking manifold (‘m000’)

FIGURE 1.4. The five 3–manifolds which can be triangulated with a single tetrahedron. (a)-(d) are material triangulations of closed orientable 3–manifolds. (e) is an ideal triangulation of a cusped, non-orientable hyperbolic 3–manifold.

Hak62], marking the start of the construction of an algorithmic solution to the homeomorphism problem for certain classes of 3–manifold and establishing this theory as a core component of algorithmic topology. Haken's methods were not without their complications when it came to implementation. Work of Jaco and Oertel [JO84] resolved these complications leading to the development of the first finite time algorithm that could solve the homeomorphism problem for closed, irreducible 3–manifolds containing a properly embedded, incompressible, two-sided surface. In the thirty years since, normal surfaces have played a central role in many practical algorithms and are used extensively in `Regina`.

Haken's approach was to decompose a 3–manifold M into simple pieces and consider the surfaces which may be constructed from ‘elementary discs’ within these pieces. The two main decompositions used in normal surface theory are triangulations and handle decompositions. As our focus is on triangulations, we will not discuss handle decompositions. The definitions and results we cover here can be found in [Mat07]. We assume that a surface mentioned is in **general position** with respect to the triangulation, which is to say that it does not intersect the vertices and it intersects the edges transversely.

Definition 1.8 Let σ be a face in a triangulation $\mathscr{T}$ of a 3–manifold. A **normal arc** on σ is a properly embedded arc whose endpoints lie on distinct edges of σ. ◇

Definition 1.9 Let Δ be a tetrahedron in the triangulation $\mathscr{T}$. A **normal disc** in Δ is a properly embedded disc whose boundary consists of a sequence of normal arcs and meets each face of Δ in at most one normal arc. ◇

There are seven types of normal discs within a tetrahedron: four triangle discs, each separating one of the four vertices; and two quadrilateral discs, each separating a pair of opposite edges. The seven normal disc types are illustrated in Figure 1.5 below.

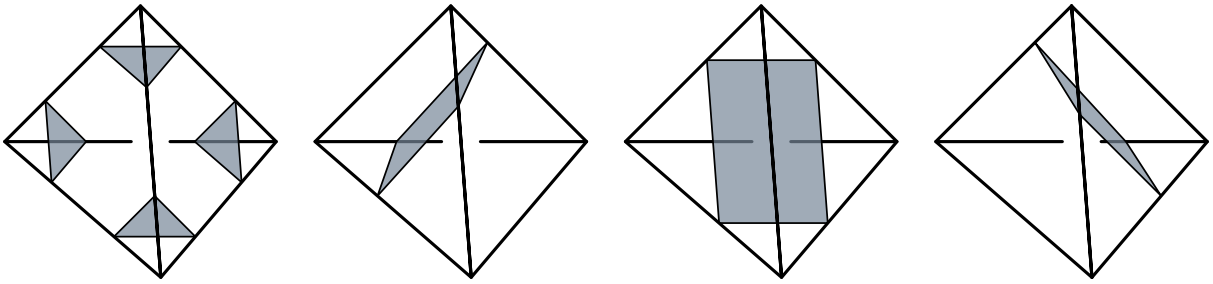

FIGURE 1.5. The seven types of normal disc in a tetrahedron.

Having defined the elementary discs of Haken's scheme, we are able to define a normal surface in the following, perhaps obvious, way. As a note to the reader, only closed surfaces will play a role in this thesis and we accordingly restrict our attention to closed normal surfaces.

Definition 1.10 Let S be a properly embedded closed surface in a triangulation $\mathscr{T}$. S is a **normal surface** with respect to $\mathscr{T}$ if and only if it intersects each tetrahedron in a finite number of normal discs. ◇

Given a triangulation $\mathscr{T}$ of a 3–manifold M, it is unlikely that any properly embedded surface $S \subset M$ chosen will be a normal surface with respect to $\mathscr{T}$. A core result of Haken's theory informs us that we can always 'normalise' a surface S with respect to $\mathscr{T}$. The following result can be found as Theorem 3.3.21 in [**Mat07**].

Theorem 1.11 *Let M be a 3–manifold with triangulation $\mathscr{T}$ and let S be any properly embedded surface in M. Then S can be realised as a, possible empty, normal surface F with respect to $\mathscr{T}$ by a finite number of compressions, isotopies, and boundary compressions.*

We now turn our attention to the use of normal surfaces in algorithms. Let $\mathscr{T}$ be a triangulation consisting of n tetrahedra which we label $\Delta_1, \ldots, \Delta_n$. The seven normal disc types in Δ_i can be represented by the vector $\mathbf{x}_i = (t_{i,1}, t_{i,2}, t_{i,3}, t_{i,4}, q_{i,1}, q_{i,2}, q_{i,3}) \in \mathbb{R}^7$, where each $t_{i,r}$ records the number of normal triangles of type r and each $q_{i,s}$ records the number of normal quadrilaterals

of type s. Extending this to all tetrahedra in $\mathscr{T}$ we obtain a vector $\mathbf{x} \in \mathbb{R}^{7n}$ with entries $t_{i,r}$ and $q_{i,s}$ for $1 \leq i \leq n$.

Given any vector $\mathbf{x} \in \mathbb{R}^{7n}$, we need a method to certify whether or not it corresponds to a valid normal surface in $\mathscr{T}$. The first observation we make is that a normal surface is an embedded surface. This is not true if we allow more than one normal quadrilateral disc type to exist within a single tetrahedron. The **admissibility conditions** we impose on $\mathbf{x}$ are that for each $1 \leq i \leq n$ at most one of $q_{i,1},\ q_{i,2},\ q_{i,3}$ is non-zero. We call the vector $\mathbf{x}$ **admissible** if it satisfies the admissibility conditions.

Let Δ_i and Δ_j be two tetrahedra in $\mathscr{T}$ which are identified along the face σ^2. The intersection of a normal disc and this face is a normal arc. For any pair of edges incident with σ^2 there is one type of normal triangle and one type of normal quadrilateral which meet both edges. Let $t_{i,r}$ and $q_{i,s}$ denote the quantities of the corresponding disc types in Δ_i and let $t_{j,r'}$ and $q_{j,s'}$ denote the corresponding disc types in Δ_j. This condition can be written as $t_{i,r} + q_{i,s} = t_{j,r'} + q_{j,s'}$. Adding the requirement that $t_{i,r}, q_{i,s} \geq 0$ we arrive at the matching equations:

$$\begin{aligned} t_{i,r} + q_{i,s} &= t_{i,r'} + q_{i,s'} \\ t_{i,r}, q_{i,s}, t_{i,r'}, q_{i,s'} &\geq 0 \\ 0 \leq i &\leq n \end{aligned}$$

The matching equations and admissibility conditions transform the problem of finding all $\mathbf{x} \in \mathbb{R}^{7n}$ which define a valid normal surface in $\mathscr{T}$ into a linear programming problem. A fundamental result of Haken's scheme establishes a bijective correspondence between the set of admissible solutions to the matching equations and the set of normal surfaces in $\mathscr{T}$.

Theorem 1.12 (Haken's Hauptsatz [**Hak61**]) *Let $\mathscr{T}$ be a triangulation consisting of n tetrahedra. A vector $\mathbf{x} \in \mathbb{R}^{7n}$ represents a normal surface in $\mathscr{T}$ if and only if each of the following conditions holds:*

(i) $\mathbf{x}$ *is a solution to the matching equations;*

(ii) the entries of $\mathbf{x}$ *are integers; and*

(iii) $\mathbf{x}$ *is admissible.*

A pleasant property of normal surfaces is that we may combine them by adding their corresponding vectors together. Let S_1 and S_2 be two normal surfaces with corresponding vector representation $\mathbf{v}_1$ and $\mathbf{v}_2$, respectively. We say that S_1 and S_2 are **compatible** if the vector $\mathbf{v} = \mathbf{v}_1 + \mathbf{v}_2$ represents a normal surface in $\mathscr{T}$. This new normal surface is written $S = S_1 + S_2$. We similarly define the surface kS, for integer $k > 0$, to be the normal surface with vector representation $k\mathbf{v}$.

Definition 1.13 Let S be a normal surface in a triangulation $\mathscr{T}$ with vector representation $\mathbf{v}$. The surface S is called a **fundamental surface** if it cannot be written as the sum $S = S_1 + S_2$ for any non–empty normal surfaces.

The surface S is called a **vertex surface** if there are no positive integer solutions to $kS = k_1S_1 + k_2S_2$ for any non–empty surfaces S_1 and S_2 which are not multiples of S. ◇

Fundamental and vertex solutions play an important algorithmic role. For any triangulation, the set of fundamental surfaces is finite and constructible. Moreover, every normal surface can be written as a positive, integer linear combination of the fundamental surfaces. Similarly, vertex surfaces can be partitioned into finitely many equivalence classes where the set of chosen representatives for these classes is constructible.

1.4. Layered and 0–efficient triangulations

Two important classes of 3–manifold triangulations, both introduced by Jaco and Rubinstein, play a central role in this thesis — *layered triangulations* and *0–efficient triangulation*. We define both classes and provide important examples of layered triangulations.

1.4.1. Layered triangulations. Layered triangulations, introduced by Jaco and Rubinstein [**JR06**] in 2006, have played a major role in the understanding of minimal triangulations [**JRT09**, **JRT13**, **JRST20a**, **JRST20b**, **RST24**] and the construction of triangulation censuses [**Bur07**, **Bur11b**].

The primary focus of Jaco and Rubinstein's paper was the *layered solid torus*, together with a classification of all normal surfaces and almost normal surfaces contained therein. Layered solid tori are interesting in their own right and provide a layered construction of all lens spaces. More interestingly, they commonly appear as subcomplexes in many minimal triangulations (in particular, all cited works above classify infinite families of minimal triangulations which contain layered solid tori as embedded subcomplexes). Layered solid tori have also proven useful in the construction of triangulations of 3–manifolds obtained via Dehn filling (see, for example, recent work of Thompson [**Tho25**] and work of Guéritaud and Schleimer [**GS10**]).

We define layered triangulations under the assumption that $\mathscr{T}$ is a material triangulation of M. However, it should be noted that the construction for ideal triangulations is the same.

Definition 1.14 Suppose that $\partial M \neq \emptyset$ and denote by $\mathscr{T}_\partial$ the restriction of $\mathscr{T}$ to ∂M. Let e be an edge in $\mathscr{T}_\partial$ which is incident to two pairwise distinct faces. A tetrahedron Δ is said to be **layered along** e if a pair of adjacent faces in Δ are identified to the two faces incident with e "without a twist", see Figure 1.6. ◇

The resulting triangulation $\mathscr{T} \cup_e \Delta$ is homeomorphic to M with e now an interior edge. If all tetrahedra in the triangulation are attached via layering, then we call $\mathscr{T}$ a **layered triangulation of M**. We describe two important layered constructions of the solid torus.

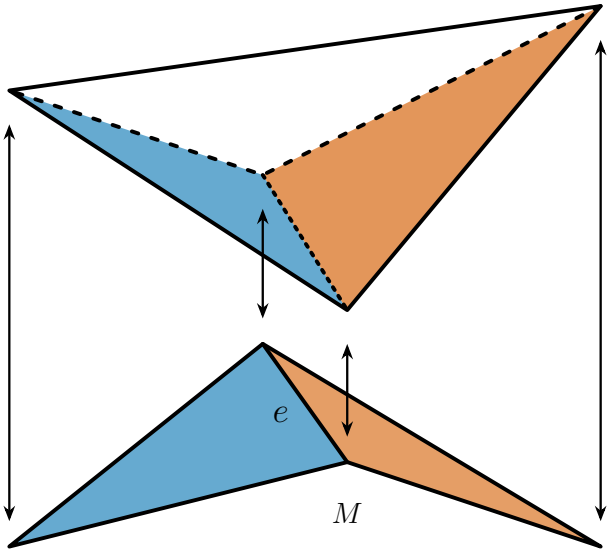

FIGURE 1.6. Layering along an edge e in the boundary of M. The blue faces are identified and the orange faces are identified.

1.4.2. Layered solid tori. A **layered solid torus** is a layered triangulation of the solid torus constructed as follows. Start with the triangulation of the Möbius band consisting of a single triangle, considered as a degenerate solid torus, and layer a tetrahedron along the interior edge (see Δ_{-1} and Δ_0 in Figure 1.7). The result of this is the standard one tetrahedron triangulation of the solid torus. This triangulation contains one vertex, three edges, and three faces. Layering along one of the boundary edges yields a layered solid torus consisting of two tetrahedra. Inductively, a layered solid torus consisting of k tetrahedra is obtained by layering along a boundary edge of a layered solid torus consisting of $k-1$ tetrahedra with each layering introducing a single new edge. A layered solid torus consisting of k tetrahedra thus has one vertex, $k+2$ edges, and $2k+1$ faces. Two faces, three edges, and the vertex are contained in the boundary and form the standard one vertex triangulation of the torus.

Starting from Δ_0, there is a unique first edge which is layered along. This edge is termed the **base edge**. There is also unique boundary edge with degree one and we term this the **unital edge**.

The geometric intersection of the meridional slope with the three boundary edges can be written as an unordered triple $\{p,q,p+q\}$, where p and q are positive, coprime integers and the **slope** of the boundary torus is p/q. Two layered triangulations of the solid torus with triples $\{p,q,p+q\}$ and $\{p',q',p'+q'\}$ are combinatorially equivalent if and only if the two sets of numbers are the same. Hence each layered solid torus can be characterised by its relevant triple

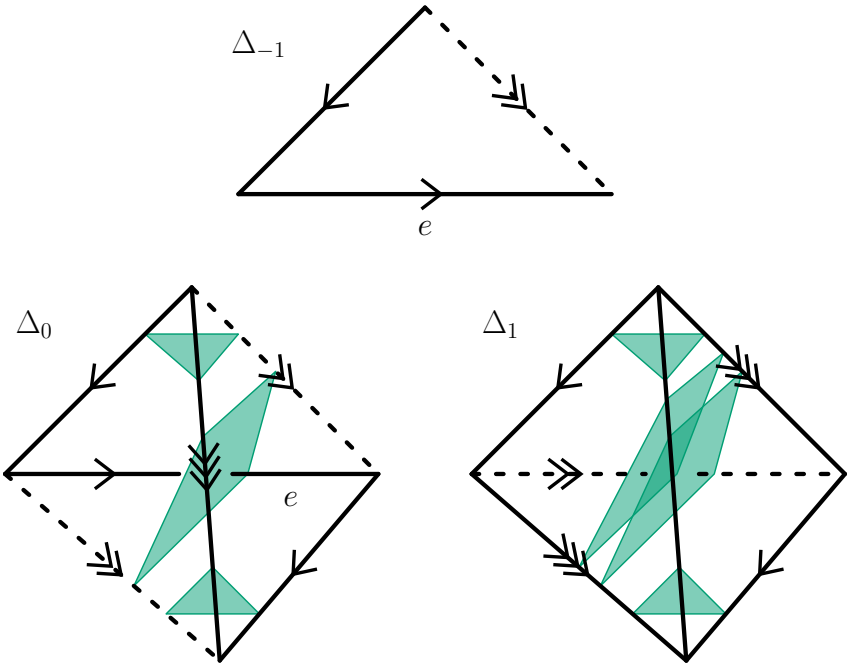

FIGURE 1.7. The construction of LST$(1,3,4)$. Δ_0 is layered along the interior edge e of the Möbius band Δ_{-1} to first obtain LST$(1,2,3)$ with Δ_1 then layered along the dashed edge to obtain LST$(1,3,4)$. The meridional disc is shown as a normal surface in Δ_0 and Δ_1.

and is denoted LST$(p,q,p+q)$. Figure 1.7 illustrates the layered triangulation of LST$(1,2,3)$ and LST$(1,3,4)$.

Given a layered solid torus LST$(p,q,p+q)$ we can determine the layered solid torus arising from each of the three possible layerings as follows. First, label the three boundary edges with the parameters p, q, and $p+q$ based on their geometric intersection with the meridional disc. Layering along the edge labelled p changes the slope of the boundary torus from p/q to $q/(p+q)$. The geometric intersection of the new unital edge with the meridional disc is given by $q+(p+q)=p+2q$ and we obtain LST$(q,p+q,p+2q)$. Similarly, layering along the edge labelled q produces LST$(p,p+q,2p+q)$. Without loss of generality, suppose that $p>q$. Layering along the edge $p+q$ changes the boundary slope to $(p-q)/q$ and we obtain LST$(p-q,q,p)$. It follows from the Euclidean algorithm that this process terminates in LST$(1,1,2)$.

1.4.3. Layered chains. The **layered chain** of length n, denoted C_n, was introduced by Burton [**Bur03**] and is one of the core components of many triangulations in the closed, orientable `Regina` census. The starting point for this triangulation is the two triangle triangulation of the annulus illustrated in Figure 1.8. The edges t, for 'top', and b, for 'bottom', form the boundary edges of the annulus and are oriented so that the correspond to the same element of the fundamental group. The remaining two edges, e_1 and e_2, are oriented from t to b. This annulus forms the layered chain C_0.

To form C_1 we layer a tetrahedron along e_1. The new edge is e_3 and is oriented from t to b. Inductively, C_n is formed by layering a tetrahedron along e_n with the new edge, e_{n+2}, oriented from t to b as depicted in Figure 1.8. The result is a triangulation of the solid torus consisting of n tetrahedra, $n+4$ edges, 4 boundary triangles, and two vertices. Both vertices are contained in the boundary.

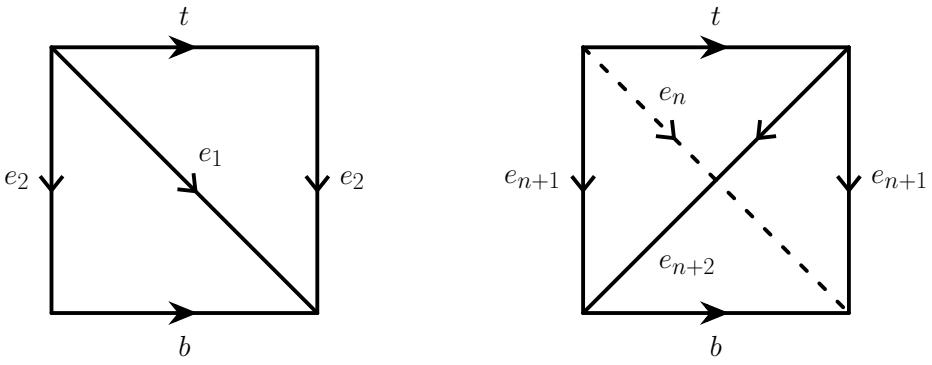

FIGURE 1.8. The construction of the chain C_n. The left illustration shows the triangulated annulus, considered as the layered chain of length 0, with boundary edges marked t and b. The n-th tetrahedron is layered along edge e_n, with the edges t and b always remaining in the boundary.

1.4.4. 0–efficient triangulations. 0–efficient triangulations were introduced by Jaco and Rubinstein [JR03] in 2003. These triangulations are particularly important when constructing minimal triangulations of closed, orientable, irreducible 3–manifolds.

Definition 1.15 A triangulation of a closed, orientable, connected 3–manifold M is **0–efficient** if the only embedded, normal 2–spheres are vertex linking.

The following two results will be heavily used throughout Chapters 3 and 4 and act as a powerful framework for studying minimal triangulations. The first result connects 0–efficient triangulations and irreducible 3–manifolds. Moreover, it controls the number of vertices which greatly simplifies Euler characteristic arguments.

Proposition 1.16 [JR03, Proposition 5.1] *Suppose M is a closed, orientable 3–manifold. If M has a 0–efficient triangulation, then M is irreducible and $M \neq \mathbb{R}P^3$. Furthermore, either the triangulation has one vertex or M is S^3 and the triangulation has precisely two vertices.*

The second result connects minimal triangulations and 0–efficient triangulations and establishes precisely when a minimal triangulation is not 0–efficient.

Theorem 1.17 [JR03, Theorem 6.1] *Let M be a closed, orientable, irreducible 3–manifold with minimal triangulation $\mathscr{T}$. If M is not homeomorphic with either $\mathbb{R}P^3$ or $L(3,1)$, then $\mathscr{T}$ is 0–efficient. Hence $\mathscr{T}$ has exactly one vertex unless M is one of S^3, $\mathbb{R}P^3$, or $L(3,1)$.*

1.5. Geometric triangulations

In Chapter 2 we study ideal triangulations of the complements of hyperbolic 2–bridge links. In this section we describe the hyperbolic geometry required in a more general setting. More details can be found in, for example, [**Pur20**] or [**Mil82**].

The main objects for this section are **geometric (ideal) triangulations**. These play a central role in Chapter 2 and allow us to use the hyperbolic geometry of the 3–manifold to study its topology. Despite a beautiful and rich theory surrounding this topic, it is still not known if every cusped hyperbolic 3-manifold admits a geometric triangulation [**LST08, FHH22, HP23, Nim23**]. Epstein and Penner [**EP88**] devised a method for decomposing a cusped hyperbolic 3–manifold of finite volume into convex ideal polyhedra. Further subdividing these polyhedra may result in degenerate tetrahedra (topological ideal tetrahedra that are 'flat' with respect to the hyperbolic structure).

1.5.1. Topological ideal triangulations. A 3–manifold M is **hyperbolic** if it admits a complete metric with all sectional curvatures equal to -1. Under the additional assumption that M is closed, it has finite volume. Our attention will be on cusped hyperbolic 3–manifolds.

Definition 1.18 A **cusped hyperbolic 3–manifold** is an orientable non-compact hyperbolic 3–manifold M of finite volume. Such a manifold is the interior of an orientable, compact, irreducible and ∂-irreducible, atoroidal, anannular 3–manifold $\overline{M}$ with boundary a finite union of tori. If $\overline{M}$ has n boundary components, then we say that M is **n–cusped**.

Cusped hyperbolic 3–manifolds always admit a triangulation consisting of only (topological) ideal triangulations. The following result, implicit from Matveev [**Mat07**], was proven in generality by Tillmann.

Theorem 1.19 ([**Til08**], Proposition 1.2) *Let M be the interior of a compact 3–manifold $\overline{M}$ with non–empty boundary. Then M admits a (topological) ideal triangulation in which the ideal vertices are in one-to-one correspondence with the boundary components of $\overline{M}$.*

1.5.2. Hyperbolic structures on ideal triangulations. Our direction now is towards endowing a topological ideal triangulation with a hyperbolic structure. We work in the upper half space model of hyperbolic 3–space, $\mathbb{H}^3$, defined as

$$\mathbb{H}^3 = \{(x+iy,t) \in \mathbb{C}\times\mathbb{R} \mid t > 0\}$$

with Riemannian metric given by the first fundamental form

$$ds^2 = \frac{dx^2+dy^2+dt^2}{t^2}$$

A topological ideal tetrahedron Δ embedded in $\mathbb{H}^3$ has each of its six ideal edges forming geodesics and its ideal vertices located on the boundary at infinity, $\partial\mathbb{H}^3 = \mathbb{C}\cup\{\infty\}$. There exists an orientation preserving isometry $\psi \in \mathrm{PSL}(2,\mathbb{C})$ taking three of these four ideal vertices to the points 0, 1, and ∞ with the fourth being sent to some $z \in \mathbb{C}$ with positive imaginary part. A topological ideal tetrahedron embedded in $\mathbb{H}^3$ this way is a **hyperbolic ideal tetrahedron** and is illustrated in Figure 1.9. Letting e be the edge with vertices at 0 and ∞, the **edge parameter** $z(e)$ of e is the complex number z at which the fourth vertex of the tetrahedron is located.

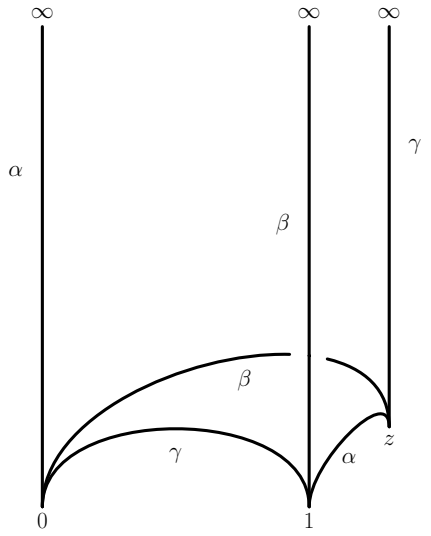

FIGURE 1.9. A hyperbolic ideal tetrahedron. The four vertices are at 0, 1, ∞, and z, where z has positive argument. The (internal) dihedral angles are labelled α, β, and γ on each pair of opposite edges.

The shape of a hyperbolic ideal tetrahedron is determined entirely by the edge parameter $z(e)$ and is preserved under any orientation preserving isometry which permutes the vertices of the tetrahedron. For a given hyperbolic ideal tetrahedron, its intersection with a Euclidean plane[§] parallel to $\mathbb{C}$ forms a Euclidean triangle with internal angles α, β, and γ. A each vertex of this triangle, label the corresponding vertical edge of the tetrahedron with the angle. The angles α, β, and γ are the **(internal) dihedral angles** of the tetrahedron. It is known that opposite pairs of edges of a hyperbolic ideal tetrahedron have the same dihedral angles and these angles determine the shape of the tetrahedron, up to isometry [**Thu80**], see also [**FG11**].

Thurston [**Thu80**] devised two sets of edge gluing equations, determining when a set of hyperbolic ideal tetrahedron will glue together and induce a hyperbolic structure (not necessarily complete) on the resulting triangulation. For each edge e of the triangulation, we obtain a polynomial equation in terms of the edge parameters of all edges gluing to e. In this thesis we will avoid this set of equations entirely. The second set of equations states that the sum of dihedral angles around each (internal) edge of the triangulation must add to 2π. Working with this set

[§]Such a plane is called a *horosphere about* ∞ and it admits a genuine Euclidean structure.

of equations we may determine not only when there is a hyperbolic structure on $\mathscr{T}$, but also when this structure is complete.

Definition 1.20 A **geometric ideal triangulation** is a topological ideal triangulation of a cusped hyperbolic 3–manifold M for which the induced hyperbolic structure is complete. The complete hyperbolic metric on $\mathscr{T}$ agrees with the complete hyperbolic metric on M.

It remains an open question as to whether every cusped hyperbolic 3–manifold admits a geometric triangulation. Those which do form a very important class of manifolds, see for instance [**Mah10**].

1.5.3. Angle structures and hyperbolic volume. Our connection between hyperbolic geometry and triangulations will be through angle structures. As alluded to above, we may avoid the complex polynomial component of Thurston's gluing equations and determine a complete hyperbolic metric of finite volume on a given triangulation $\mathscr{T}$ by considering the dihedral angles surrounding each (internal) edge.

Definition 1.21 Let M be a 3–manifold with ideal triangulation $\mathscr{T}$ consisting of n ideal tetrahedra $\{\Delta_1,\dots,\Delta_n\}$. An **angle structure** $\Theta = (\theta_1,\dots,\theta_{3n})$ on $\mathscr{T}$ is an assignment of (internal) dihedral angles $\theta_{3i-2},\theta_{3i-1},\theta_{3i}$ on each pair of opposite edges of each ideal tetrahedron Δ_i in $\mathscr{T}$ such that the following hold:

(i) $\theta_{3i-2},\theta_{3i-1},\theta_{3i} \in (0,\pi)$ for each $1 \leq i \leq n$,

(ii) For each ideal tetrahedron Δ_i we have $\theta_{3i-2}+\theta_{3i-1}+\theta_{3i} = \pi$,

(iii) The sum of dihedral angles around every (interior) ideal edge in $\mathscr{T}$ is 2π.

The set of all angle structures on a triangulation is denoted $\mathscr{A}(\mathscr{T})$. The assignment of dihedral angles to the i–th ideal tetrahedron is notated as $\Theta^{(i)} = (\theta_{3i-2},\theta_{3i-1},\theta_{3i})$. The hyperbolic ideal tetrahedron with dihedral angles $\{\theta_{3i-2},\theta_{3i-1},\theta_{3i}\}$ is denoted $\Delta(\theta_{3i-2},\theta_{3i-1},\theta_{3i})$. ◇

Condition (iii) in the above definition is precisely Thurston's edge gluing equation for dihedral angles. Our definition is sometimes referred to as a *strict* or *positive* angle structure in the literature. There is no reason why $\mathscr{A}(\mathscr{T})$ should be non–empty, however if it is non–empty, then it is the interior of a convex, compact polytope in $[0,\pi]^{3n} \subset \mathbb{R}^{3n}$.

The assignment of (internal) dihedral angles to a hyperbolic ideal tetrahedron allows the computation of its hyperbolic volume. The following result, attributed to Milnor, provides this calculation.

Theorem 1.22 ([**Mil82**], Lemma 2) *Suppose* $\theta_{3i-2},\theta_{3i-1},\theta_{3i} \in (0,\pi)$ *and* $\theta_{3i-2}+\theta_{3i-1}+\theta_{3i} = \pi$. *Then these angles determine a hyperbolic ideal tetrahedron* $\Delta(\theta_{3i-2},\theta_{3i-1},\theta_{3i})$ *with*

volume

$$\mathrm{Vol}(\Delta(\theta_{3i-2},\theta_{3i-1},\theta_{3i})) = \Lambda(\theta_{3i-2})+\Lambda(\theta_{3i-1})+\Lambda(\theta_{3i}),$$

where $\Lambda:\mathbb{R}\to\mathbb{R}$ *is the Lobachevsky function*

$$\Lambda(\theta) = \int_0^\theta \log|2\sin u|du.$$

The volume of a hyperbolic ideal tetrahedron is maximised when each of its dihedral angles are equal to $\pi/3$. Such an ideal tetrahedron is called a **regular ideal tetrahedron** and its volume is

$$v_3 = \mathrm{Vol}(\Delta(\pi/6,\pi/6,\pi/6)) \approx 1.0149\ldots \tag{1.5.1}$$

Given an angle structure $\Theta\in\mathscr{A}(\mathscr{T})$, we obtain a volume of each ideal tetrahedron in $\mathscr{T}$. The volume of the triangulation is obtained by summing the volumes of the tetrahedra. By varying Θ in $\mathscr{A}(\mathscr{T})$, we vary the volumes of the tetrahedra and hence the volume of $\mathscr{T}$.

Definition 1.23 Let M be a 3-manifold with ideal triangulation $\mathscr{T}$ consisting of n ideal tetrahedra. The **volume functional** $\mathscr{V}:\mathscr{A}(\mathscr{T})\to\mathbb{R}$ is defined by

$$\mathscr{V}(\Theta) = \sum_{i=1}^{n}\mathrm{Vol}(\Delta(\theta_{3i-2},\theta_{3i-1},\theta_{3i})).$$

The volume functional is a concave function on $\mathscr{A}(\mathscr{T})$ [**Riv94**, Theorem 2.1], and it is a continuous function on $\overline{\mathscr{A}(\mathscr{T})}$, with image contained in $[0,3n\Lambda(\frac{\pi}{3})]$. That means it either takes its maximum on the interior of the space $\mathscr{A}(\mathscr{T})$ and this maximum is unique, or there is no maximum in $\mathscr{A}(\mathscr{T})$, and $\mathscr{V}$ is maximised on the boundary of the closure $\overline{\mathscr{A}(\mathscr{T})}$.

The following theorem, proved independently by Casson and Rivin, allows us to use angle structures to obtain a geometric triangulation in the case that the maximum occurs in the interior of the space $\mathscr{A}(\mathscr{T})$.

Theorem 1.24 (Casson, Rivin) *Let M be the interior of a compact orientable 3–manifold with torus boundary, and let $\mathscr{T}$ be an ideal triangulation of M. Then a point $p\in\mathscr{A}(\mathscr{T})$ determines a complete hyperbolic structure on the interior of M if and only if the volume functional $\mathscr{V}:\mathscr{A}(\mathscr{T})\to\mathbb{R}$ has a maximum at p.*

The proof of Theorem 1.24 follows from work in [**Riv94**]. This version is found in [**GS10**, Theorem 5]. An alternative proof which includes a nice exposition is given by Futer and Guéritaud [**FG11**].

Corollary 1.25 *Let M be a hyperbolic 3-manifold with ideal triangulation $\mathscr{T}$. Suppose $\mathscr{A}(\mathscr{T})$ is non–empty. For each $\Theta\in\mathscr{A}(\mathscr{T})$,*

$$\mathscr{V}(\Theta)\leq\mathrm{Vol}(M).$$

CHAPTER 2

Complexity bounds on hyperbolic 2–bridge links

In this chapter we establish new results on the complexity of 2-bridge link complements through a detailed study of the Sakuma-Weeks triangulations [SW95]. The manifolds we consider are cusped hyperbolic 3–manifolds (Theorem 1.18) and the triangulations examined are geometric ideal triangulations (Theorem 1.20). The approach we take utilises the connection between angle structures and hyperbolic volume.

Thurston [Thu80] established a one-sided inequality connecting the hyperbolic volume of a hyperbolic 3–manifold (cusped or closed) and its complexity:

$$c(M) \geq \frac{\mathrm{Vol}(M)}{v_3} \tag{2.0.1}$$

The moral of this inequality is that a minimal triangulation of M requires at least the maximal number of the 'largest' possible pieces and, importantly, any geometric triangulation involving only regular ideal tetrahedra is minimal. Manifolds admitting such minimal triangulations are referred to as **tetrahedral** in the literature, see [FGG+16] for a census of examples. Thurston's bound remains one of very few lower bounds on the complexity of 3-manifolds.

In an idealised setting, we aim to maximise the number of regular ideal tetrahedra in a triangulation and then fill in the remaining volume with the minimal number of smaller volume hyperbolic ideal tetrahedra. This approach has already been realised in the case of 2–bridge links by Ishikawa and Nemoto [IN16]. Using bounds on the hyperbolic volume they successfully classified an infinite family of 2–bridge links whose Sakuma-Weeks triangulation is minimal. The minimal triangulations identified have only four tetrahedra which are *not* regular ideal.

The Sakuma-Weeks triangulations of hyperbolic 2–bridge links have been studied in detail by Futer in the appendices to [Gué06] and Purcell in [Pur20]. Work of Akiyoshi, Sakuma, Wada, and Yamashita [ASWY00] gave an affirmative answer to a conjecture of Sakuma and Weeks [SW95], showing that the Sakuma-Weeks triangulations were geometrically canonical[†]. A method to compute their volumes exactly is due to Tsvietkova [Tsv14], however we are unable to infer explicit volume or complexity bounds for infinite families of 2-bridge links from these calculations.

[†]We will not need the assumption that the triangulations are canonical. The interested reader is directed to [Pur20].

Bounds on their complexity are contained in work by Ishikawa and Nemoto [IN16], where they observe that many of the Sakuma-Weeks triangulations are not minimal by constructing a smaller upper bound on the complexity of some 2-bridge link complements by realising the triangulations as spines. In more recent work, Aribi, Guéritaud and Piguet-Nakazawa describe triangulations of twist knots, a family of 2–bridge links, which are roughly half the size of the improved Ishikawa and Nemoto bound – and conjectured to be minimal [BAGPN23, Conjecture 3.3].

The chapter proceeds as follows. In Section 2.1 we describe the construction of 2–bridge links, closely following the construction used by Futer [Gué06], and connect this to the standard continued fraction expansion. The construction and anatomy of the Sakuma-Weeks triangulations are described in Section 2.2 with a focus on providing a visual construction with which we can discern the combinatorics easily. Utilising this anatomy we provide a necessary condition for the Sakuma-Weeks triangulations to be minimal in Section 2.3. Our proof provides a fundamental, but alternative, argument of the Ishikawa and Nemoto non-minimality result. The heart of this chapter is presented in Section 2.4 in which we apply (2.0.1) to give lower bounds for the complexity of 2-bridge link complements. Our proof goes by explicitly describing strict angle structures on the canonical triangulations of all of these 2-bridge link triangulations, alongside an evaluation of the volume functional on those angle structures. We conjecture that all of the triangulations satisfying the hypotheses of these results are minimal. We conclude this chapter with a comparison of our complexity bounds to existing volume bounds in the literature.

2.1. Constructing 2–bridge links

We follow the setup from Appendix A in [Gué06]. Let S denote a sphere with four marked points, which we refer to as a **pillowcase**. A four-string braid between two pillowcases, one interior and one exterior, is an embedding of four disjoint arcs into the **product region** $S \times I$, where $I = [a,b]$, such that each arc connects a marked point on the exterior pillowcase $S \times \{b\}$ to a marked point on the interior pillowcase $S \times \{a\}$. Such an embedding is described by a word

$$\Omega = \begin{cases} R^{a_1}L^{a_2}\cdots R^{a_n} \quad \text{or} \quad L^{a_1}R^{a_2}\cdots L^{a_n}, & \text{if } n \text{ is odd,} \\ R^{a_1}L^{a_2}\cdots L^{a_n} \quad \text{or} \quad L^{a_1}R^{a_2}\cdots R^{a_n}, & \text{if } n \text{ is even} \end{cases}$$

where $a_i \in \mathbb{Z}$. We fix the projection of the braid onto a plane such that each R encodes a twist between the top two strands and each L encodes a twist between the right two strands, shown in Figure 2.1. We refer to these as **vertical** and **horizontal** crossings, respectively, and note that the word Ω encodes a sequence of twists from the outside in; we start at $S \times \{b\}$ and work in towards $S \times \{a\}$. A **syllable** is a maximal subword in L or R. For example, R^aR^b will occur as the single syllable R^{a+b}. The word Ω consists of n syllables. The sign of each a_i determines whether a crossing is positive or negative and $|a_i|$ determines the number of

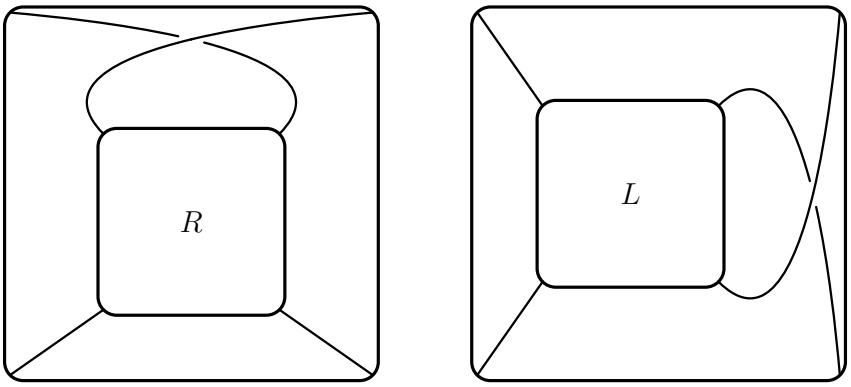

FIGURE 2.1. Crossings of the four arcs encoded by R and L. A crossing encoded by R is called **vertical** and a crossing encoded by L is called **horizontal**.

crossings in the syllable. The crossings associated to a syllable form a **twist region** which is homeomorphic to $S \times I$. A **2-bridge link** $K(\Omega)$ is obtained by adding two arcs with a single crossing connecting the opposite pairs of marked points on the exterior pillowcase and two arcs with a single crossing connecting opposite pairs of marked points on the interior pillowcase. This is shown in Figure 2.2. Note that every 2-bridge link can be obtained this way.

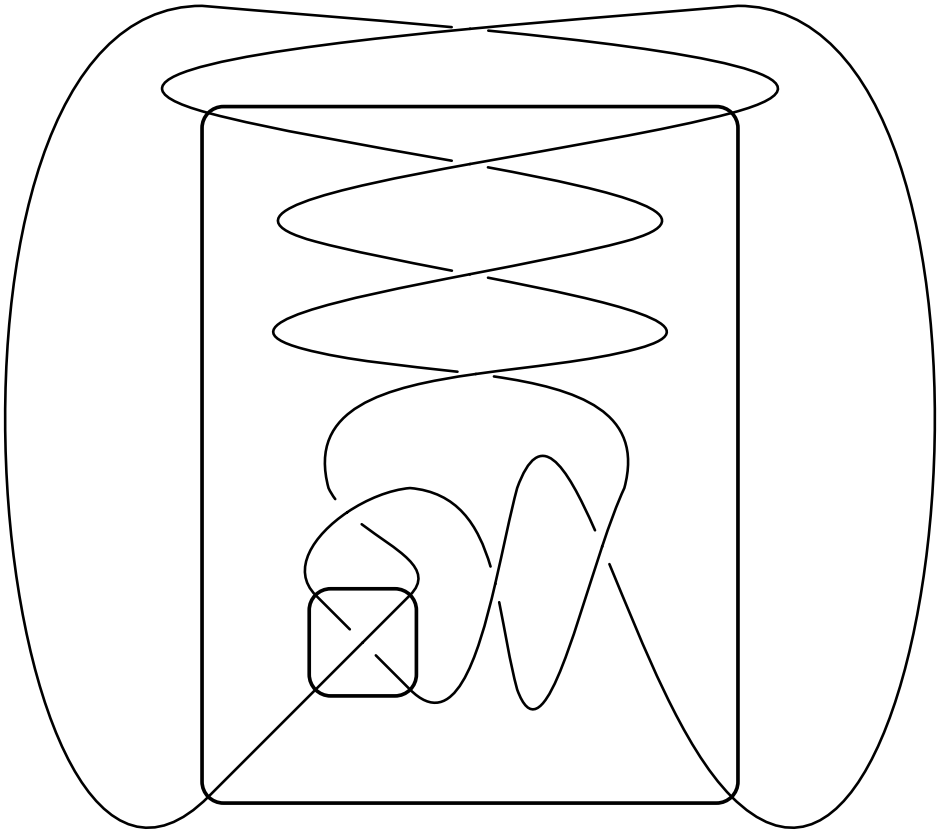

FIGURE 2.2. The 2-bridge link $K(\Omega)$ with $\Omega = R^3L^2R$. Removing the outermost and innermost crossings returns the four-string braid corresponding to Ω.

The presentation of a 2-bridge link by a word Ω is connected to continued fraction expansions

of rational tangles, see [Con70, Pur20]. Hence we make the following simplifying assumptions:

- Given any word Ω describing a 2-bridge link $K(\Omega)$ there is another word Ω' with either all $a_i > 0$ or all $a_i < 0$ for $1 \leq i \leq n$ such that $K(\Omega')$ is ambient isotopic to $K(\Omega)$;
- The first syllable of Ω is R^{a_1}; and
- $|a_1| \geq 1$ and $|a_n| \geq 1$.

Throughout we assume that $a_i > 0$ for all $1 \leq i \leq n$. The case where all $a_i < 0$ is similar.

For the purposes of this thesis we concern ourselves only with hyperbolic 2-bridge links; those whose complements admit a complete hyperbolic metric of finite volume. For each word Ω the associated 2-bridge link $K(\Omega)$ is non-split, in the sense that the complement is irreducible, and the chosen projection is alternating. In particular, $K(\Omega)$ is a torus link when Ω contains exactly one syllable. This imposes the following condition on Ω due to Menasco.

Theorem 2.1 ([Men84], Corollary 2) *A 2-bridge link $K(\Omega)$ is hyperbolic if and only if the associated word Ω has at least two syllables.*

2.2. Sakuma-Weeks triangulations of 2–bridge link complements

We now outline the construction of the Sakuma-Weeks triangulations for the complements of 2-bridge links and detail the combinatorics needed for our results. We follow the setup described in Section 2.1. Further details of this construction can be found in [Gué06, Pur20, SW95]. Throughout this section we define $\Omega = R^{a_1}L^{a_2}\cdots(R^{a_n} \mid L^{a_n})$ with $K(\Omega)$ denoting the associated 2-bridge link, where $(R^{a_n} \mid L^{a_n})$ denotes the regular expression determining either the string R^{a_n} or L^{a_n} which we assume is done appropriately. We assume that $a_i > 0$ for all $1 \leq i \leq n$ and that $a_1, a_n \geq 1$. We set $\ell = \sum_{i=1}^{n} a_i$. Let $M = S^3 \backslash K(\Omega)$ denote the link complement. It is vital to first note that we consider a 2–bridge link as being embedded in S^3; we suppress this for most of what follows.

2.2.1. Construction of the Sakuma-Weeks triangulations. Each crossing of the four-string braid determined by Ω occurs inside a product region homeomorphic to $S \times I$. We denote the complement of these regions as $S_i \times I$ for $1 \leq i \leq \ell$, where S_i is a four-punctured sphere and $I = [0,1]$. The Sakuma-Weeks triangulation is constructed by first creating isotopic ideal triangulations of $S_i \times \{1\}$ and $S_i \times \{0\}$ for each i. Each such triangulation contains three pairs of edges - vertical, horizontal and diagonal which follow the perspective shown in Figure 2.3.

By gluing $S_i \times \{0\}$ and $S_{i+1} \times \{1\}$ along their horizontal and vertical edges we obtain two regions, each bounded by four ideal vertices, six ideal edges, and four triangular faces. This forms a pair of ideal tetrahedra for each $1 \leq i \leq \ell - 1$. We call each such pair of tetrahedra a

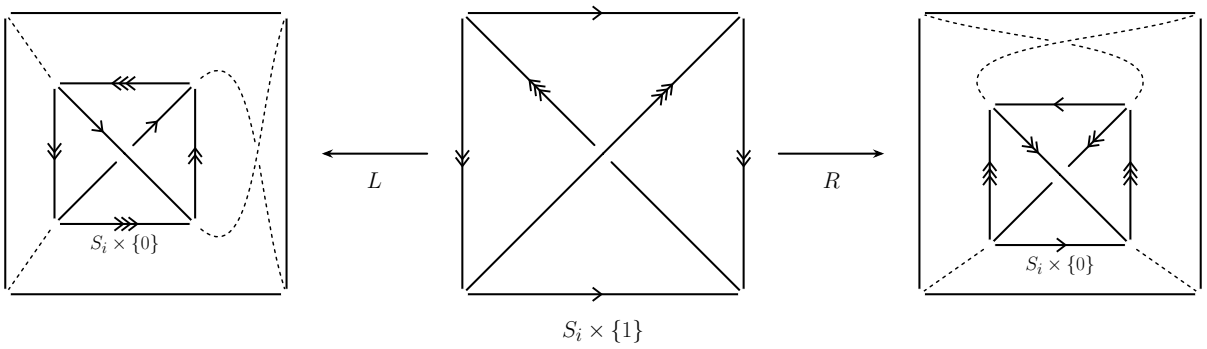

FIGURE 2.3. Ideal triangulation of $S_i \times \{1\}$ (outside) and $S_i \times \{0\}$ (inside) with orientations marked on each pair of edges. The complements of the four arcs define an isotopy between the ideal triangulations. Going from $S_i \times \{1\}$ to $S_i \times \{0\}$, a vertical twist R exchanges vertical and diagonal edges and a horizontal twist L exchanges horizontal and diagonal edges, as indicated by the braid arcs (dashed lines).

layer and denote this by $\widetilde{\Delta}_i$. These layers are glued together by identifying the diagonal edges in $S_{i+1} \times \{1\}$ to either the horizontal or vertical edges in $S_{i+1} \times \{0\}$ for $1 \leq i \leq \ell - 2$. This process is shown in Figure 2.4. There remains four unidentified faces in $\widetilde{\Delta}_1$ and four unidentified faces in $\widetilde{\Delta}_{\ell-1}$ coming from $S_1 \times \{0\}$ and $S_\ell \times \{1\}$, respectively. In order to complete the triangulation of the complement of the 2-bridge link $K(\Omega)$ we identify the four remaining ideal triangles on $S_1 \times \{0\}$ in pairs following the isotopy defined by the crossing in S_1 and the added exterior crossing. Similarly, for the four remaining faces on $S_\ell \times \{1\}$, we follow the isotopy defined by the crossing in S_ℓ and the added interior crossing. The identification on $S_{\ell-1} \times \{0\}$ is shown in Figure 2.5. Since we assume that the Ω starts with R^{a_1} we can note that the ideal triangles on $S_1 \times \{1\}$ are identified similarly to those on $S_{\ell-1} \times \{0\}$ in the case where Ω ends with R^{a_n}. The resulting triangulation $\mathscr{T} = \mathscr{T}(M)$ consists of layers $\widetilde{\Delta}_1, \ldots, \widetilde{\Delta}_{\ell-1}$, each consisting of two ideal tetrahedra Δ_{2i-1} and Δ_{2i} for $1 \leq i \leq \ell - 1$. This gives the size of the Sakuma-Weeks triangulation as $|\mathscr{T}| = 2(\ell - 1) = 2\sum_{i=1}^{n} a_i - 2$.

As a final note on the construction of the Sakuma-Weeks triangulation, we can observe that the gluing of two layers together forms, in essence, a layered triangulation. In Figure 2.4 we layer the blue and red diagonal edges in $\widetilde{\Delta}_i$ over opposite pairs of horizontal or vertical edges in $\widetilde{\Delta}_{i+1}$ for horizontal (L) and vertical (R) twists, respectively.

2.2.2. Edge Degrees. The Sakuma-Weeks triangulations of 2-bridge link complements possess many attractive properties; the construction can be read directly from the link diagram or done algorithmically by reading the word Ω. Our interest lies in computing the degree of each edge class in the triangulation $\mathscr{T} = \mathscr{T}(M)$.

The isotopy defined by the crossing between $S_i \times \{1\}$ and $S_i \times \{0\}$ combined with the gluing of $S_i \times \{0\}$ and $S_{i+1} \times \{1\}$ along vertical and horizontal edges allows us to determine each edge class of $\mathscr{T}$ explicitly and hence compute their degrees. Figure 2.4 shows the tracking of edges

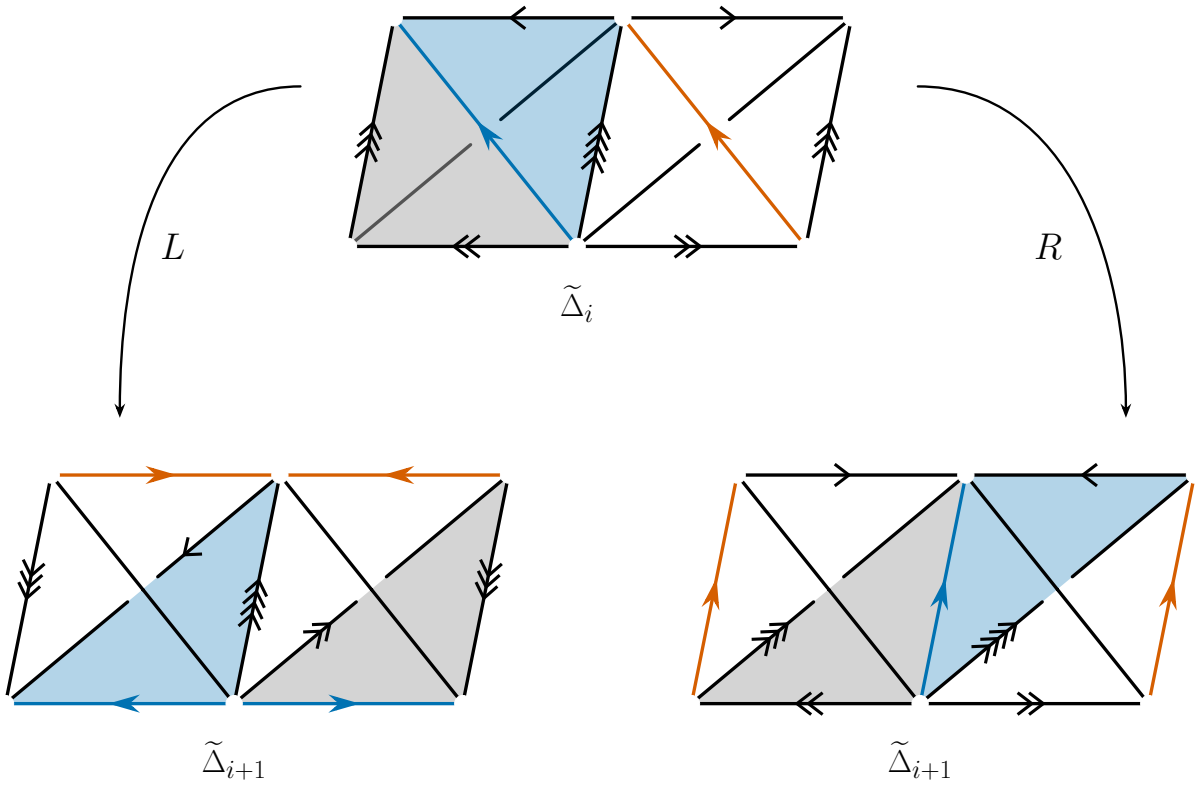

FIGURE 2.4. The process of gluing the layers of the Sakuma-Weeks triangulation together. Each layer consists of two ideal tetrahedra glued along their horizontal and vertical edges. The four faces on the back of $\widetilde{\Delta}_i$ lie on $S_i \times \{0\}$ and the four faces on the front lie on $S_{i+1} \times \{1\}$ and similarly for $\widetilde{\Delta_{i+1}}$. We have highlighted two faces on $S_{i+1} \times \{1\}$ and the faces they glue to in $S_{i+1} \times \{0\}$.

through the triangulation with Figure 2.5 showing the edge identifications coming from the gluing of faces on $S_1 \times \{0\}$ (Figure 2.5a) and $S_\ell \times \{1\}$ (Figure 2.5b). We make two immediate observations from these figures.

First, there are no edges of degree 1 or 2 in $\mathscr{T}$. Each layer $\widetilde{\Delta}_i$ consists of two ideal tetrahedra glued along four edges. The corresponding edge classes must have degree of at least 2. Each such edge class also includes at least one diagonal edge. Hence the minimum edge degree is 3. Second, opposite edges in any layer (e.g. horizontal) belong to edge classes of the same degree. This follows since the isotopies are the same on opposite pairs of edges, up to preserving orientation.

The following lemma provides the number of edges in $\mathscr{T}$. This result is not new and can be found, for example, in [**FG11**].

Lemma 2.2 *Let M be the interior of a compact 3-manifold $\widehat{M}$ with $\partial \widehat{M} \neq \emptyset$ consisting only of a finite number of tori. Let $\mathscr{T}$ be a topologically ideal triangulation of M. Then $|\mathscr{T}^{(1)}| = |\mathscr{T}|$, where $\mathscr{T}^{(1)}$ denotes the one-skeleton of $\mathscr{T}$.*

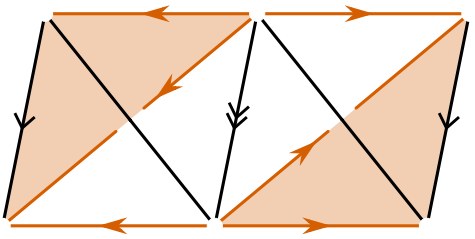

$\widetilde{\Delta}_1$

(a) Identifications of ideal triangles on $S_1 \times \{0\}$. The shaded faces are identified and the unshaded faces are identified.

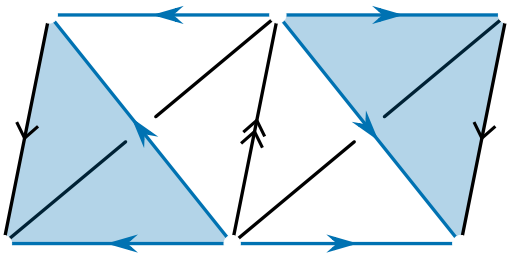

$\widetilde{\Delta}_{\ell-1}$ (n odd)

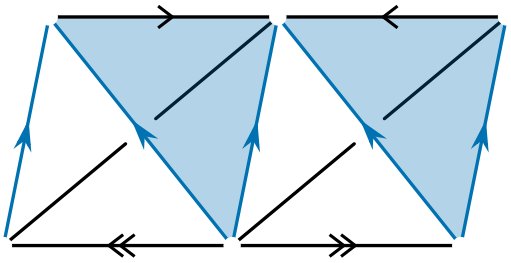

$\widetilde{\Delta}_{i+1}$ (n even)

(b) Identifications of ideal triangles on $S_\ell \times \{1\}$ when Ω ends with R (left) and L (right). For each case, the shaded faces are identified and the unshaded faces are identified.

FIGURE 2.5. Identifications of remaining ideal triangles in $\widetilde{\Delta}_1$ and $\widetilde{\Delta}_2$. For each layer shown, the back faces belong to $S_i \times \{0\}$ and the front faces belong to $S_i \times \{1\}$. Note that no two faces of a single ideal tetrahedron are identified.

Proof The triangulation of the boundary tori is obtained by truncating the ideal tetrahedra in M, giving $4|\mathscr{T}|$ triangles along with $12|\mathscr{T}|$ edges identified in pairs for a total of $6|\mathscr{T}|$ edges. From the Euler characteristic we have

$$0 = \chi(\partial \widehat{M}) = v - 6|\mathscr{T}| + 4|\mathscr{T}|$$

giving $2|\mathscr{T}|$ vertices. Since each pair of vertices corresponds to a single edge in $\mathscr{T}$ we obtain the desired equality. □

Minimal triangulations of 3-manifolds often place restrictions on the possible anatomy of the triangulation. One key restriction is the presence of low-degree edges [**JRT09**, **JRT13**, **JRST20a**, **JRST20b**]. We conclude this section with necessary and sufficient conditions for the Sakuma-Weeks triangulation to possess edges of degree 3 or 4.

Lemma 2.3 *Let $K(\Omega)$ be the 2-bridge link generated by the word $\Omega = R^{a_1}L^{a_2}\cdots(R^{a_n} \mid L^{a_n})$. Let $\mathscr{T} = \mathscr{T}(M)$ be the Sakuma-Weeks triangulation of the complement $M = S^3 \backslash K(\Omega)$. $\mathscr{T}$ contains an edge of degree 3 if and only if $a_1 > 1$ or $a_n > 1$.*

Proof Any edge class containing two diagonal edges must have even degree. This can be determined from Figures 2.4 and 2.5. Hence any edge class with odd degree must contain either the vertical edges from Δ_1 or the horizontal or vertical edges from $\widetilde{\Delta}_{\ell-1}$ if the last syllable of Ω is L^{a_n} or R^{a_n}, respectively.

If $a_1 = 1$, then the first two letters of Ω are RL and we see that the vertical edges in $\widetilde{\Delta}_1$ are glued to vertical edges in $\widetilde{\Delta}_2$. If $a_1 > 1$, however, then the vertical edges in $\widetilde{\Delta}_1$ are glued to distinct diagonal edges in $\widetilde{\Delta}_2$ giving edge classes of degree 3. The argument for $a_n > 1$ is analogous, noting that the last letter of Ω only determines how the remaining four faces are identified on the last layer. □

Lemma 2.4 *Let $K(\Omega)$ be the 2-bridge link generated by the word $\Omega = R^{a_1}L^{a_2}\cdots(R^{a_n} \mid L^{a_n})$. Let $\mathscr{T} = \mathscr{T}(M)$ be the Sakuma-Weeks triangulation of the complement $M = S^3\backslash K(\Omega)$. $\mathscr{T}$ contains an edge of degree 4 if and only if $a_i \geq 2$ for some $1 < i < n$ or $a_i \geq 3$ for $i \in \{1, n\}$.*

Proof From Figures 2.4 and 2.5 we observe the only way to form an edge class of degree 4 is to glue edges in the sequence diagonal–vertical/horizontal–diagonal. This sequence is only obtainable by performing the same crossing at least twice in succession, with the first diagonal coming from an ideal tetrahedron in the previous layer. Hence we require $a_i \geq 2$ for some $1 < i < n$. The first letter of Ω introduces the first diagonal edges to start this sequence whilst the last letter does not introduce any new ideal tetrahedra. Hence we require that $a_1 \geq 3$ or $a_n \geq 3$ for an edge class of degree 4 to contain an edge in $\widetilde{\Delta}_1$ or $\widetilde{\Delta}_{\ell-1}$. □

2.3. Non-minimality via elementary moves

Utilising the combinatorics from the previous section we now provide a necessary condition for the Sakuma-Weeks triangulation to be minimal.

2.3.1. A necessary condition for minimality. In order to show that a triangulation is non-minimal one could simply find a different triangulation possessing fewer tetrahedra. This is often hard. A common approach is to locally change the given triangulation in such a way that we decrease the number of tetrahedra whilst simultaneously preserving the manifold. We use the 3–2 move and the 4–4 move, defined in Section 1.2.2. We remind the reader of these moves below.

For the 3–2 move consider a triangulation of a triangular bipyramid consisting of three distinct tetrahedra glued along an internal edge of degree 3. The 3–2 move replaces this triangulation with one consisting of two distinct tetrahedra glued along an internal triangle (Figure 1.2). For the 4–4 move, consider an octahedron triangulated with four distinct tetrahedra glued along an internal edge of degree 4. This edge is realised as a main diagonal of the octahedron which can

occur in three distinct ways giving rise to three distinct triangulations of the octahedron. The 4–4 move replaces one of these triangulations with one of the other two [**Bur13**]. Crucially, the 4–4 move adjusts the edge degrees of each edge class incident to the tetrahedra by either ± 1 or 0. The edges whose degree decreases are indicated in Figure 1.3.

Theorem 2.5 *Let $K(\Omega)$ be the 2-bridge link generated by the word $\Omega = R^{a_1}L^{a_2}\cdots(R^{a_n} \mid L^{a_n})$. Let $\mathscr{T} = \mathscr{T}(M)$ be the Sakuma-Weeks triangulation of the complement $S^3\backslash K(\Omega)$. $\mathscr{T}$ is minimal only if $a_1 = a_n = 1$ and $a_i \in \{1,2\}$ for $1 < i < n$ with $n \geq 2$.*

Ishikawa and Nemoto [**IN16**] provide an upper bound on the complexity of the complements of hyperbolic 2-bridge links as

$$c(M) \leq \sum_{i=1}^{n} a_i + 2(n-1) - \#\{a_i = 1\}$$

where we have adjusted the formula for our notation of Ω. This result agrees with Theorem 2.5 and quantifies a lower bound on the amount of ideal tetrahedra that can be removed.

Proof If $a_1 > 1$ or $a_n > 1$, then there is a degree 3 edge by Theorem 2.3. By the construction of the Sakuma-Weeks triangulation we know that no two faces of a single ideal tetrahedron are identified and there must be three distinct ideal tetrahedra glued around this edge. Applying a Pachner 3–2 move reduces the size of the triangulation by one and thus $\mathscr{T}$ is not minimal.

Suppose now that $a_i \geq 3$ for some $1 \leq i \leq n$ and that the corresponding syllable in Ω is R^{a_i}. There are two degree 4 edges, $\mathfrak{e}$ and $\mathfrak{e}'$, incident to each other. Figure 2.6 shows the four layers of $\mathscr{T}$ containing $\mathfrak{e}$ (shown in red) and $\mathfrak{e}'$ (shown in blue) with the four ideal tetrahedra glued around $\mathfrak{e}$ shaded. We see that $\mathfrak{e}'$ is contained in this octahedron. Applying a 4–4 move replacing $\mathfrak{e}$ with $\widehat{\mathfrak{e}}$ in the octahedron so that $\widehat{\mathfrak{e}}$ and $\mathfrak{e}'$ are not incident reduces the degree of $\mathfrak{e}'$ by one giving $\deg(\mathfrak{e}') = 3$. Observe that the two faces incident to $\mathfrak{e}'$ now belong to the same ideal tetrahedron and, as we can deduce from Figure 2.6, there are two ideal tetrahedra glued around $\mathfrak{e}'$ not contained in the octahedron. Hence there are three distinct tetrahedra glued around $\mathfrak{e}'$ after performing the 4–4 move and we can apply a Pachner 3–2 move to reduce the size of the triangulation by one and thus $\mathscr{T}$ is not minimal.

Finally, we note that if $a_i \in \{1,2\}$ for all $1 \leq i \leq n$ then no two degree 4 edges will be incident to each other in the triangulation and thus we cannot perform a sequence of 4–4 moves to create a degree 3 edge in order to simplify the triangulation. □

Combining our combinatorial analysis with Ishikawa and Nemoto's upper bound on complexity [**IN16**], leads us to the following conjecture.

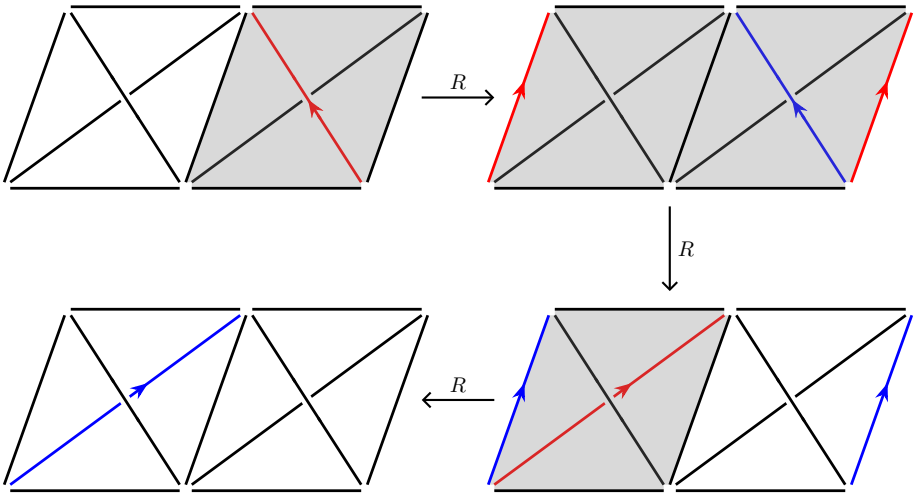

FIGURE 2.6. The four layers of $\mathscr{T}$ containing incident degree 4 edges corresponding to R^3 in Ω. The four shaded ideal tetrahedra are glued around the red edge $\mathfrak{e}$ to form an octahedron which contains the blue edge $\mathfrak{e}'$.

Conjecture 2.6 Let $K(\Omega)$ be the 2-bridge link generated by the word $\Omega = R^{a_1}L^{a_2}\cdots(R^{a_n} \mid L^{a_n})$. Let $\mathscr{T} = \mathscr{T}(M)$ be the Sakuma-Weeks triangulation of the complements $S^3\backslash K(\Omega)$. $\mathscr{T}$ is minimal if and only if $a_1 = a_n = 1$ and $a_i \in \{1,2\}$ for $1 < i < n$ with $n \geq 2$.

2.3.2. Example of a simplification. We conclude this section with two examples of a 2-bridge links whose Sakuma-Weeks triangulation is non-minimal, demonstrating the use of 4–4 and Pachner 3–2 moves to simplify this using `Regina` [**BBP+23**].

Consider $K(\Omega)$ generated by the word $\Omega = R^2LR$. The Sakuma-Weeks triangulation contains 6 ideal tetrahedra with gluings described by Table 2.1. All numbers referenced in this section are given with respect to the numbering provided by Regina given this gluing table.

The triangulation contains two edges of degree 3, listed as Edge 1 and Edge 3. Performing a Pachner 3–2 move along Edge 1 returns a triangulation with 5 ideal tetrahedra. The isomorphism signature of the simplified triangulation is `fLLQcbcdeeetsfxxh`.

Now consider $K(\Omega')$ generated by the word $\Omega' = RL^3R$. The Sakuma-Weeks triangulation contains 8 ideal tetrahedra with gluings described by Table 2.2. To perform the 4–4 move we use Edge 4 and perform the 4–4 move along Axis 0 to ensure the new edge is not incident to the edge whose degree we want to decrease. The new triangulation obtained has isomorphism signature `iLLMLQcbcdefhghhmvftgafqa`. This triangulation contains one degree 3 edge with 3 distinct ideal tetrahedra glued around it. Selecting this and performing a Pachner 3–2 move produces a triangulation with 7 ideal tetrahedra and isomorphism signature `hLLMPkbcdfggfgmvfafwkf`.

Tetrahedron	Face 012	Face 013	Face 023	Face 123
0	3 (102)	1 (213)	1 (021)	2 (023)
1	0 (032)	2 (103)	3 (123)	0 (103)
2	4 (032)	1 (103)	0 (123)	5 (321)
3	0 (102)	4 (031)	5 (021)	1 (023)
4	5 (032)	3 (031)	2 (021)	5 (103)
5	3 (032)	4 (213)	4 (021)	2 (321)

TABLE 2.1. `Regina` gluing table for the Sakuma-Weeks triangulation of $K(\Omega)$ generated by $\Omega = R^2LR$.

Tetrahedron	Face 012	Face 013	Face 023	Face 123
0	2 (032)	1 (213)	1 (021)	3 (321)
1	0 (032)	2 (031)	3 (021)	0 (103)
2	4 (032)	1 (031)	0 (021)	5 (321)
3	1 (032)	4 (031)	5 (021)	0 (321)
4	6 (032)	3 (031)	2 (021)	7 (321)
5	3 (032)	6 (031)	7 (021)	2 (321)
6	7 (032)	5 (031)	4 (021)	7 (103)
7	5 (032)	6 (213)	6 (021)	4 (321)

TABLE 2.2. `Regina` gluing table for the Sakuma-Weeks triangulation of $K(\Omega')$ generated by $\Omega' = RL^3R$.

2.4. Complexity bounds via angle structures

In the previous section we provide necessary conditions for the Sakuma-Weeks triangulations of 2-bridge link complements to be minimal. In this section we provide complexity bounds on the remaining triangulations.

Our argument is centred on a two–sided version of Thurston's lower bound (2.0.1). Given a triangulation $\mathscr{T}$ of a hyperbolic 3-manifold M, we obtain the two–sided bound on complexity

$$\frac{\mathrm{Vol}(M)}{v_3} \leq c(M) \leq |\mathscr{T}| \tag{2.4.1}$$

where $v_3 \approx 1.0149\ldots$ is the volume of a regular ideal tetrahedron.

The construction of the Sakuma-Weeks triangulations is symmetric. The layerings used when adding the two ideal tetrahedra from the next layer are the same with the only difference being that we layer each tetrahedron on opposite edges. It is also known that these triangulations have a non-empty space of angle structures. Combining these leads to the following result.

Lemma 2.7 ([Pur20], Lemma 10.24) *Let $\mathscr{T}$ be a Sakuma-Weeks triangulation of a 2-bridge link complement with $2n$ tetrahedra. Let Δ_{2i-1} and Δ_{2i} be the two tetrahedra in the i-th layer $\widetilde{\Delta}_i$ with angles $(\theta^1_{3i-2}, \theta^1_{3i-1}, \theta^1_{3i})$ and $(\theta^2_{3i-2}, \theta^2_{3i-1}, \theta^2_{3i})$, respectively. The volume function $\mathscr{V} : \mathscr{A}(\mathscr{T}) \to \mathbb{R}$ obtains a maximum when the angles for Δ_{2i-i} agree with those for Δ_{2i} for all $1 \leq i \leq n$.*

We utilise this lemma to simplify the construction of explicit angle structures. For the remainder of this chapter, in an abuse of notation, we refer to both the i-th layer and the tetrahedra it contains as Δ_i. Throughout this section we assume the conditions from Theorem 2.5.

2.4.1. Block decomposition of 2–bridge links. Let Ω' denote the subword of Ω obtained by removing the first and last letters. Then for $n \geq 1$,

$$\Omega' := \begin{cases} L^{a_1}R^{a_2}\cdots L^{a_n}, & \text{for odd } n, \\ L^{a_1}R^{a_2}\cdots R^{a_n}, & \text{for even } n \end{cases} \tag{2.4.2}$$

We define a decomposition of Ω' via regular expressions to characterise subwords through the use of two operations:

- $(\omega)^m$ determines m copies of the string ω,
- $(\alpha|\omega)$ determines either the string α or the string ω.

These operations allow us, for instance, to write (2.4.2) simply as $\Omega' = L^{a_1}R^{a_2}\cdots(L^{a_n}|R^{a_n})$.

Definition 2.8 A **block** is a collection of consecutive syllables matching one of the following types:

(B1) $(L^p(RL)^m \mid R^p(LR)^m)$ for $m \geq 0$ and $p \in \{0,1\}$;

(B2) $((L^2)^p(R^2L^2)^m \mid (R^2)^p(L^2R^2)^m)$ for $m \geq 0$ and $p \in \{0,1\}$;

(B3) A sequence of $(k+1)$ blocks of type (B1) of length one separated by k blocks of type (B2).

The **length** of a block is the number of syllables it contains. ◇

The above blocks can be described simply. (B1) describes strings of alternating L's and R's and (B2) describes strings of alternating L^2's and R^2's. A (B3) block may look like $R(L^2)R(L^2R^2L^2R^2)L(R^2L^2)R$.

The length of a block is not defined in terms of the number of letters the block contains since we aim to decompose words by their syllables. This means that no syllable is split between two different blocks. By our definition we can see that (B1) and (B2) blocks have length $2m+p$ and a (B3) block consisting of k (B2) blocks has length $(k+1)+\sum_{i=1}^{k}(2m_i+p_i)$ where $2m_i+p_i$ is the length of the i-th (B2) block. Given a fixed word Ω', we call a block of Ω' *maximal* if it cannot be extended to a larger block (possibly of a different type).

Lemma 2.9 *Let $\Omega' = L^{a_1}R^{a_2}\cdots(R^{a_n} \mid L^{a_n})$ with $a_i \in \{1,2\}$ for all $1 \leq i \leq n$. Then Ω' can be decomposed into maximal sequences of (B3) blocks, possibly separated by (B1) blocks, and such that (B2) blocks occur at most at the start or end of Ω'.*

Proof If $a_1 = 2$ or $a_n = 2$, then the decomposition consists of a (B2) block at the start or end Ω', respectively. Assume this is not the case and that $a_1 = a_n = 1$. We show that the decomposition of Ω' consists only of (B1) and (B3) blocks.

Let $(a_i, \dots, a_{i+k})$ be a maximal sequence of exponents such that $a_j = 1$ for $i \leq j \leq i+k$ with $k \geq 0$. This sequence has length $k+1$. If $n = k+1$, then $i = 1$ and the sequence corresponds to a (B1) block. Hence let $n > k+1$. If $i = 1$, then $a_{i+k+1} = 2$ and the (possibly empty) subsequence $(a_1, \dots, a_{i+k-1})$ corresponds to a (B1) block with (a_{i+k}, a_{i+k+1}) corresponding to the start of a (B3) block. Similarly, if $i+k = n$, then $a_{i-1} = 2$ and (a_{i-1}, a_i) corresponds to the end of a (B3) block followed by a (possibly empty) (B1) block. Otherwise $a_{i-1} = a_{i+k+1} = 2$. If $k = 0$, then the sequence is contained in a (B3) block; if $k \geqq 1$, then the sequence corresponds to the end of a (B3) block followed by a (possibly empty) (B1) block followed by the start of another (B3) block.

From this, the maximal sequences of exponents equal to one determine the decomposition of Ω' with (B2) blocks occurring only at the start or end of Ω'. □

2.4.2. Angle structures on blocks. We show that a decomposition of the Sakuma-Weeks triangulation $\mathscr{T}$ associated to a word Ω can be endowed with an angle structure $\Theta \in \mathscr{A}(\mathscr{T})$ which can be computed directly from the decomposition of Ω' into blocks of types (B1), (B2) and (B3). Given a block of Ω' corresponding to one of the types in Theorem 2.8 we can find the corresponding subcomplex $\mathscr{S} \subseteq \mathscr{T}$. The edge classes which glue to adjacent subcomplexes are incomplete. From condition (2) of Theorem 1.21, the angle sum around any edge class in $\mathscr{T}$ adds to 2π. We define the **angle deficit** as the remaining angle required to achieve 2π on such incomplete edge classes. An edge is **interior** if its edge class is entirely contained in a single block, otherwise we call it a **boundary** edge. Each block has three boundary edge classes at both the start and end of the corresponding subcomplex, each with an angle deficit. We call the triple of angle deficits at the start or end of a block a δ- or ε-**boundary deficit**, respectively. Recall from Theorem 1.21 that $\Theta = (\theta_1, \dots, \theta_{3\ell}) \in \mathscr{A}(\mathscr{T})$ where $\ell = |\Omega| - 1$ and the angles assigned to the i-th tetrahedron are $\Theta^{(i)} = (\theta_{3i-2}, \theta_{3i-1}, \theta_{3i})$. We define the boundary deficits on a block $\delta = (\delta_0, \delta_1, \delta_2)$ and $\varepsilon = (\varepsilon_0, \varepsilon_1, \varepsilon_2)$ in the same way (Figure 2.7).

Ishikawa and Nemoto [**IN16**] prove that the Sakuma-Weeks triangulation of the 2-bridge link complement $S^3 \backslash L(\Omega)$ is minimal when the word Ω can be decomposed as a single (B1) block. Their proof shows that the volume of the link complement in this case is almost $|\mathscr{T}| \cdot v_3$, with a deficit of approximately 0.66 in total. We generalise their work by assigning a dihedral angle of $\pi/3$ to each edge in a (B1) block ensuring these tetrahedra are regular ideal.

Lemma 2.10 *Let $\mathscr{T}$ be the Sakuma-Weeks triangulation of a 2-bridge link complement. A subcomplex $\mathscr{S} \subset \mathscr{T}$ corresponding to a (B1) block can be constructed from only regular ideal*

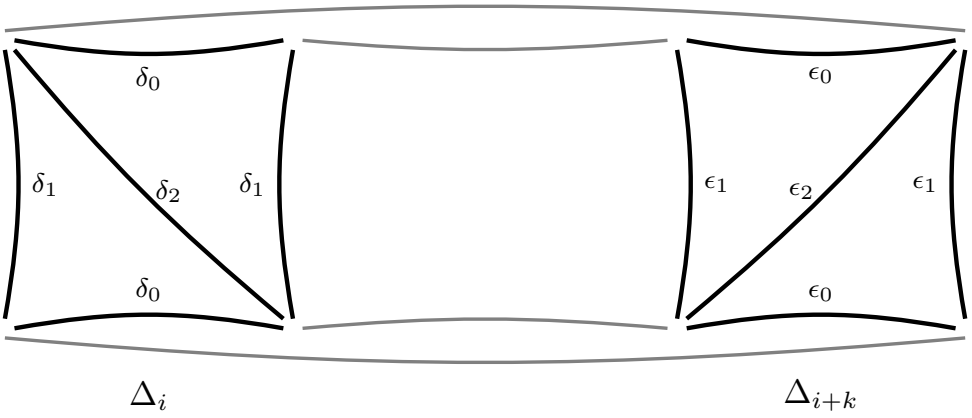

FIGURE 2.7. Assignment of $\delta = (\delta_0, \delta_1, \delta_2)$ and $\varepsilon = (\varepsilon_0, \varepsilon_1, \varepsilon_2)$ boundary deficits on a block containing $k+1$ layers, starting from layer Δ_i and containing all layers up to (and including) Δ_{i+k}.

tetrahedra. The first and last letter of the block determine the $\delta-$ and $\varepsilon-$boundary deficits, respectively as

- *L at start: $\delta = (\pi/3,\ \pi,\ 5\pi/3)$; L at end: $\varepsilon = (\pi,\ \pi/3,\ 5\pi/3)$*
- *R at start: $\delta = (\pi,\ \pi/3,\ 5\pi/3)$; R at end: $\varepsilon = (\pi/3,\ \pi,\ 5\pi/3)$*

Proof Let $\Omega' = L^p(RL)^m$ be the (B1) block. When $m = 0, p = 1$ we have the following angle equations associated with the boundary edges of $\mathscr{S}$,

$$\begin{aligned} \delta_0 + 2\theta_{3i-2} + \varepsilon_0 &= 2\pi \\ \delta_1 + 2\theta_{3i-1} + \varepsilon_1 &= 2\pi \\ \delta_2 + \theta_{3i} &= 2\pi \\ \theta_{3i} + \varepsilon_2 &= 2\pi \end{aligned}$$

where δ_i and ε_i denote the boundary deficits at the start and end of the block, respectively. Setting $\theta_j = \pi/3$ for each $3i-2 \le j \le 3i$ gives,

$$\delta_0 + \varepsilon_0 = \delta_1 + \varepsilon_1 = \frac{4\pi}{3} \qquad \text{and} \qquad \delta_2 = \varepsilon_2 = \frac{5\pi}{3}$$

This satisfies the claimed boundary deficits. When $m = 1, p = 0$ we obtain the following angle equations associated with the boundary edges of $\mathscr{S}$,

$$\begin{aligned} \delta_0 + 2\theta_{3i-2} + \theta_{3(i+1)} &= 2\pi \\ \delta_1 + 2\theta_{3i-1} + 2\theta_{3(i+1)-1} + \varepsilon_1 &= 2\pi \\ \delta_2 + \theta_{3i} &= 2\pi \\ \theta_{3i} + 2\theta_{3(i+1)-2} + \varepsilon_0 &= 2\pi \\ \theta_{3(i+1)} + \varepsilon_2 &= 2\pi \end{aligned}$$

Setting $\theta_j = \pi/3$ for each $3i-2 \leq j \leq 3(i+1)$ gives

$$\delta_0 = \varepsilon_0 = \pi \qquad \delta_1 + \varepsilon_1 = \frac{2\pi}{3} \qquad \text{and} \qquad \delta_2 = \varepsilon_2 = \frac{5\pi}{3}$$

Setting $\delta_1 = \varepsilon_1 = \pi/3$ gives the desired boundary deficit.

Suppose that for Ω' we achieve the desired boundary deficits with each tetrahedron being regular ideal for some $m \geq 1$ and $p \in \{0,1\}$. The angle equation an interior edge of the block first appearing in Δ_{i+k}, $k \geq 0$, is either

$$\theta_{3(i+k)} + 2\theta_{3(i+k+1)-2} + 2\theta_{3(i+k+2)-2} + \theta_{3(i+k+3)} = 2\pi \qquad \text{or}$$
$$\theta_{3(i+k)} + 2\theta_{3(i+k+1)-1} + 2\theta_{3(i+k+2)-1} + \theta_{3(i+k+3)} = 2\pi$$

In each case, setting each angle to be $\pi/3$ satisfies these equations. The angle equations for boundary edge classes at the start of the block are,

$$\begin{aligned} \delta_0 + 2\theta_{3i-2} + 2\theta_{3(i+1)-2} + \theta_{3(i+2)} &= 2\pi & \qquad \delta_0 + 2\theta_{3i-2} + \theta_{3(i+1)} &= 2\pi \\ \delta_1 + 2\theta_{3i-1} + \theta_{3(i+1)} &= 2\pi \qquad \text{or} \qquad & \delta_1 + 2\theta_{3i-1} + 2\theta_{3(i+1)-1} + \theta_{3(i+2)} &= 2\pi \\ \delta_2 + \theta_{3i} &= 2\pi & \delta_2 + \theta_{3i} &= 2\pi \end{aligned}$$

for $p = 1$ and $p = 0$, respectively. Setting $\theta_j = \pi/3$ for each $3i-2 \leq j \leq 3(i+1)$ gives the desired boundary deficit. The angle equations for the boundary edge classes at the end of the block are then,

$$\begin{aligned} \theta_{3(i+m-1)} + 2\theta_{3(i+m)-2} + \varepsilon_0 &= 2\pi \\ \theta_{3(i+m-2)} + 2\theta_{3(i+m-1)-1} + 2\theta_{3(i+m)-1} + \varepsilon_1 &= 2\pi \\ \theta_{3(i+m)} + \varepsilon_2 &= 2\pi \end{aligned}$$

Setting $\theta_j = \pi/3$ for each $3(i+m-2) \leq j \leq 3(i+m)$ gives the desired boundary deficit with $\varepsilon_0 = \pi$, $\varepsilon_1 = \pi/3$ and $\varepsilon_2 = 5\pi/3$.

The proof follows similarly if we assume instead that $\Omega' = R^p(LR)^m$. □

It remains to show that we can assign angles to the remaining block types which are compatible with the boundary deficits on the (B1) blocks. As there are many ways to achieve this, we endeavour to assign angles which achieve a larger volume for the block. We restrict to the

following shapes of ideal tetrahedra,

(0) $\Delta(\pi/3, \pi/3, \pi/3)$	(V) $\Delta(\pi/6,\ \pi/2,\ \pi/3)$
(I) $\Delta(\pi/3,\ 3\pi/8,\ 7\pi/24)$	(VI) $\Delta(\pi/6,\ \pi/4,\ 7\pi/12)$
(II) $\Delta(\pi/3,\ \pi/4,\ 5\pi/12)$	(VII) $\Delta(\pi/8, 3\pi/8, \pi/2)$
(III) $\Delta(\pi/4,\ \pi/4,\ \pi/2)$	(VIII) $\Delta(\pi/8,\ \pi/4,\ 5\pi/8)$
(IV) $\Delta(5\pi/24,\ 7\pi/24,\ \pi/2)$	(IX) $\Delta(\pi/12,\ 7\pi/12,\ \pi/3)$

Remark 2.11 The above shapes can be refined further to obtain slightly better volume estimates for our main result. However, such a refinement introduces more shapes and more complicated arguments decreasing the overall readability of the remainder of this section. At the same time the increase in volume estimates is not sufficient to sharpen our main result significantly enough to justify the extra burden put on the reader.

Lemma 2.12 *Let $\mathscr{T}$ be the Sakuma-Weeks triangulation of a 2-bridge link complement. A subcomplex $\mathscr{S} \subset \mathscr{T}$ corresponding to a (B3) block can be constructed using only ideal tetrahedra of shape types (I), (II), (III), (IV), (VI) and (VIII) assigned depending on the number of (B2) blocks as:*

- *a single (B2) block of length k*
$$(I) \longrightarrow (VI) \longrightarrow \big[\,(III)\big]^{\,2(k-1)} \longrightarrow (IV) \longrightarrow (II)$$
- *k (B2) blocks of length 1,*
$$(I) \longrightarrow (VI) \longrightarrow \Big[\,(III) \longrightarrow (III) \longrightarrow (VIII)\Big]^{\,k-1} \longrightarrow (IV) \longrightarrow (II)$$
- *k (B2) blocks of arbitrary lengths combines the above two by adding more layers of shape (III).*

The first and last letter of the block determines the $\delta-$ and $\varepsilon-$boundary deficits, respectively as

- *L at start: $\delta = (\pi/3,\ \pi,\ 5\pi/3)$; L at end: $\varepsilon = (\pi,\ \pi/3,\ 5\pi/3)$*
- *R at start: $\delta = (\pi,\ \pi/3,\ 5\pi/3)$; R at end: $\varepsilon = (\pi/3,\ \pi,\ 5\pi/3)$*

Proof Recall that a (B3) block consists of at least two (B1) blocks of length one separated by nonempty (B2) blocks. The shapes which appear are determined by both the number of (B1) blocks, and the lengths of the (B2) blocks. We assume throughout that our block starts with L,

however all of the following arguments still hold if it instead starts with R by switching θ_{3j-2} and θ_{3j-1} in each Δ_j.

One (B2) block – Let $\Omega' = L(R^2L^2)^m(R^2L)^pR^{1-p}$ with $m \geq 0,\ p \in \{0,1\}$. When $m = 0,\ p = 1$ we have $\Omega' = LR^2L$ giving the following angle equations,

$$\begin{aligned}
\delta_0 + 2\theta_{3i-2} + 2\theta_{3(i+1)-2} + 2\theta_{3(i+2)-2} + \theta_{3(i+3)} &= 2\pi \\
\delta_1 + 2\theta_{3i-1} + \theta_{3(i+1)} &= 2\pi \\
\delta_2 + \theta_{3i} &= 2\pi \\
\theta_{3i} + 2\theta_{3(i+1)-1} + \theta_{3(i+2)} &= 2\pi \\
\theta_{3(i+1)} + 2\theta_{3(i+2)-1} + 2\theta_{3(i+3)-1} + \varepsilon_1 &= 2\pi \\
\theta_{3(i+2)} + 2\theta_{3(i+3)-2} + \varepsilon_0 &= 2\pi \\
\theta_{3(i+3)} + \varepsilon_2 &= 2\pi
\end{aligned} \tag{2.4.3}$$

where δ_j and ε_j denote the boundary deficits at the start and end of the block, respectively. We obtain tetrahedra of types (I), (II), (IV) and (VI) by setting,

$$\begin{aligned}
&\text{(I)} \quad \Theta^{(i)} = \left(\frac{7\pi}{24}, \frac{3\pi}{8}, \frac{\pi}{3}\right) \qquad \text{(VI)} \quad \Theta^{(i+1)} = \left(\frac{\pi}{6}, \frac{7\pi}{12}, \frac{\pi}{4}\right) \\
&\text{(IV)} \quad \Theta^{(i+2)} = \left(\frac{5\pi}{24}, \frac{7\pi}{24}, \frac{\pi}{2}\right) \qquad \text{(II)} \quad \Theta^{(i+3)} = \left(\frac{\pi}{4}, \frac{5\pi}{12}, \frac{\pi}{3}\right)
\end{aligned} \tag{2.4.4}$$

Substituting these values into (2.4.3) results in the following boundary deficits,

$$\delta_0 = \varepsilon_1 = \frac{\pi}{3} \qquad \delta_1 = \varepsilon_0 = \pi \qquad \text{and} \qquad \delta_2 = \varepsilon_2 = \frac{5\pi}{3}.$$

Proceeding to the case when $m = 1,\ p = 0$ so that $\Omega' = LR^2L^2R$, we can note that the first four angle equations of (2.4.3) remain the same and are solved by the same values as above, also preserving the δ-boundary deficit. The remaining angle equations are as follows,

$$\begin{aligned}
\theta_{3(i+1)} + 2\theta_{3(i+2)-1} + 2\theta_{3(i+3)-1} + 2\theta_{3(i+4)-1} + \theta_{3(i+5)} &= 2\pi \\
\theta_{3(i+2)} + 2\theta_{3(i+3)-2} + \theta_{3(i+4)} &= 2\pi \\
\theta_{3(i+3)} + 2\theta_{3(i+4)-2} + 2\theta_{3(i+5)-2} + \varepsilon_0 &= 2\pi \\
\theta_{3(i+4)} + 2\theta_{3(i+5)-1} + \varepsilon_1 &= 2\pi \\
\theta_{3(i+5)} + \varepsilon_2 &= 2\pi
\end{aligned}$$

We set $\Theta^{(i)}$ and $\Theta^{(i+1)}$ as in (2.4.4). To obtain tetrahedra of shapes (IV) and (II) we set,

$$\text{(IV)} \quad \Theta^{(i+4)} = \left(\frac{7\pi}{24}, \frac{5\pi}{24}, \frac{\pi}{2}\right) \qquad \text{(II)} \quad \Theta^{(i+5)} = \left(\frac{5\pi}{12}, \frac{\pi}{4}, \frac{\pi}{3}\right) \tag{2.4.5}$$

This assignment of angles yields $\varepsilon_1 = \pi$ and $\varepsilon_2 = 5\pi/3$. To satisfy the remaining equations, we choose Δ_{i+2} and Δ_{i+3} to be have shape (III) as,

$$\Theta^{(i+2)} = \left(\frac{\pi}{4}, \frac{\pi}{4}, \frac{\pi}{2}\right) \qquad \text{and} \qquad \Theta^{(i+3)} = \left(\frac{\pi}{2}, \frac{\pi}{4}, \frac{\pi}{4}\right) \tag{2.4.6}$$

yielding $\varepsilon_0 = \pi/3$. Observe that in the preceding two cases the first two angle vectors are the same and the last two angle vectors are the same with the first two angles swapped. The order in which these angles are assigned can be determined by the last letter of the block. If Ω' ends on L, then we assign these angles as in (2.4.4), otherwise we set them as in (2.4.5). For this assignment of angles we always obtain the desired boundary deficits. Similarly, when increasing m, if the added pair of syllables is L^2R^2 we repeat the assignment of angles in (2.4.6) with the first two angles swapped in each vector.

Suppose now that $m \geq 2$ and $p \in \{0,1\}$. We only need to verify the claim that all tetrahedra not in the first or last two layers are of type (III). The angle equations for the interior edge classes alternate between,

$$\begin{aligned} \theta_{3(i+k)} + 2\theta_{3(i+k+1)-1} + 2\theta_{3(i+k+2)-1} + 2\theta_{3(i+k+3)-1} + \theta_{3(i+k+4)} &= 2\pi \\ \theta_{3(i+k+1)} + 2\theta_{3(i+k+2)-2} + \theta_{3(i+k+3)} &= 2\pi \end{aligned} \tag{2.4.7}$$

and

$$\begin{aligned} \theta_{3(i+k)} + 2\theta_{3(i+k+1)-2} + 2\theta_{3(i+k+2)-2} + 2\theta_{3(i+k+3)-2} + \theta_{3(i+k+4)} &= 2\pi \\ \theta_{3(i+k+1)} + 2\theta_{3(i+k+2)-1} + \theta_{3(i+k+3)} &= 2\pi \end{aligned} \tag{2.4.8}$$

for $k \geq 1$. In the case that (2.4.7) is followed by (2.4.8), obtained by replacing $(i+k)$ in the latter equation with $(i+k+2)$, we can solve the equations by setting the relevant tetrahedra to have shape (III) as

$$\Theta^{(i+k+1)} = \left(\frac{\pi}{4}, \frac{\pi}{4}, \frac{\pi}{2}\right) \qquad \Theta^{(i+k+2)} = \left(\frac{\pi}{2}, \frac{\pi}{4}, \frac{\pi}{4}\right)$$
$$\Theta^{(i+k+3)} = \left(\frac{\pi}{4}, \frac{\pi}{4}, \frac{\pi}{2}\right) \qquad \Theta^{(i+k+4)} = \left(\frac{\pi}{4}, \frac{\pi}{2}, \frac{\pi}{4}\right)$$

where this sequence of angle vectors is repeated as necessary. If instead (2.4.8) is followed by (2.4.7) we simply swap $\Theta^{(i+k+2)}$ and $\Theta^{(i+k+4)}$ above.

Multiple (B2) blocks of length one – Let $\Omega' = L(R^2L)^m$. When $m = 2$ we have $\Omega' = LR^2LR^2L$ giving the following angle equations,

$$\begin{aligned}
\delta_0 + 2\theta_{3i-2} + 2\theta_{3(i+1)-2} + 2\theta_{3(i+2)-2} + \theta_{3(i+3)} &= 2\pi \\
\delta_1 + 2\theta_{3i-1} + \theta_{3(i+1)} &= 2\pi \\
\delta_2 + \theta_{3i} &= 2\pi \\
\theta_{3i} + 2\theta_{3(i+1)-1} + \theta_{3(i+2)} &= 2\pi \\
\theta_{3(i+1)} + 2\theta_{3(i+2)-1} + 2\theta_{3(i+3)-1} + \theta_{3(i+4)} &= 2\pi \\
\theta_{3(i+2)} + 2\theta_{3(i+3)-2} + 2\theta_{3(i+4)-2} + 2\theta_{3(i+5)-2} + \theta_{3(i+6)} &= 2\pi \\
\theta_{3(i+3)} + 2\theta_{3(i+4)-1} + \theta_{3(i+5)} &= 2\pi \\
\theta_{3(i+4)} + 2\theta_{3(i+5)-1} + 2\theta_{3(i+6)-1} + \varepsilon_1 &= 2\pi \\
\theta_{3(i+5)} + 2\theta_{3(i+6)-2} + \varepsilon_0 &= 2\pi \\
\theta_{3(i+6)} + \varepsilon_2 &= 2\pi
\end{aligned} \tag{2.4.9}$$

Noting that Ω' ends on L, we set $\Theta^{(i)}$, $\Theta^{(i+1)}$, $\Theta^{(i+5)}$ and $\Theta^{(i+6)}$ as in (2.4.4) in order to obtain tetrahedra of types (I), (VI), (IV) and (II), respectively. To obtain tetrahedra of type (III) we set,

$$\Theta^{(i+2)} = \left(\frac{\pi}{4}, \frac{\pi}{4}, \frac{\pi}{2}\right) \qquad \text{and} \qquad \Theta^{(i+3)} = \left(\frac{\pi}{4}, \frac{\pi}{2}, \frac{\pi}{4}\right) \tag{2.4.10}$$

Note that the part of Ω' these angles are associated to is the first R^2L and hence the $\pi/2$ appears as the second angle in $\Theta^{(i+3)}$, rather than as the first angle. Solving the remaining equations gives us a layer of shape (VIII) as

$$\Theta^{(i+4)} = \left(\frac{\pi}{8}, \frac{5\pi}{8}, \frac{\pi}{4}\right) \tag{2.4.11}$$

Substituting these angles into (2.4.9) results in the following boundary deficits,

$$\delta_0 = \varepsilon_1 = \frac{\pi}{3} \qquad \delta_1 = \varepsilon_0 = \pi \qquad \text{and} \qquad \delta_2 = \varepsilon_2 = \frac{5\pi}{3}$$

Suppose that for some $m \geq 2$ we can assign angles as above with tetrahedra shapes (I) and (VI) appearing at the start of the block, shapes (IV) and (II) appearing at the end of the block and all other tetrahedra having shapes (III) and (VIII) following the pattern of $\Theta^{(i+2)}, \Theta^{(i+3)}$ and $\Theta^{(i+4)}$ above. Consider $\Omega' = L(R^2L)^{m+1}$. The modified and new angle equations are

$$\begin{aligned}
\theta_{3(i+3m-2)} + 2\theta_{3(i+3m-1)-1} + 2\theta_{3(i+3m)-1} + \theta_{3(i+3m+1)} &= 2\pi \\
\theta_{3(i+3m-1)} + 2\theta_{3(i+3m)-2} + 2\theta_{3(i+3m+1)-2} + 2\theta_{3(i+3m+2)-2} + \theta_{3(i+3m+3)} &= 2\pi \\
\theta_{3(i+3m)} + 2\theta_{3(i+3m+1)-1} + \theta_{3(i+3m+2)} &= 2\pi \\
\theta_{3(i+3m+1)} + 2\theta_{3(i+3m+2)-1} + 2\theta_{3(i+3m+3)-1} + \varepsilon_1 &= 2\pi \\
\theta_{3(i+3m+2)} + 2\theta_{3(i+3m+3)-2} + \varepsilon_0 &= 2\pi \\
\theta_{3(i+3m+3)} + \varepsilon_2 &= 2\pi
\end{aligned} \tag{2.4.12}$$

By our assumption Δ_{i+3m-2} has shape (VIII). We set Δ_{i+3m+2} and Δ_{i+3m+3} to have shapes (IV) and (II), respectively, as in (2.4.4). Substituting these values into the above equations we find

$$\text{(III)} \quad \Theta^{(i+3m-1)} = \left(\frac{\pi}{4}, \frac{\pi}{4}, \frac{\pi}{2}\right) \qquad \text{(III)} \quad \Theta^{(i+3m)} = \left(\frac{\pi}{4}, \frac{\pi}{2}, \frac{\pi}{4}\right)$$
$$\text{(VIII)} \quad \Theta^{(i+3m+1)} = \left(\frac{\pi}{8}, \frac{5\pi}{8}, \frac{\pi}{4}\right)$$

This assignment of angles gives the desired ε-boundary deficit of $\varepsilon_0 = \pi$, $\varepsilon_1 = \pi/3$ and $\varepsilon_2 = 5\pi/3$.

At least two (B2) blocks with arbitrary length – The final case combines the previous two cases. Starting from the second case, we claim that increasing the length of any (B2) block adds additional tetrahedra of shape (III) whilst preserving the shapes of the remaining tetrahedra. Note that it follows from the preceding arguments that if there are at least two (B2) blocks, then increasing the length of the first or last (B2) block does not affect the equations containing the first or last boundary deficit, respectively, up to permuting the first two angles.

Suppose $\Omega' = L(R^2L)^m$ with $m \geq 2$ with shapes described above. Consider the subword $\Omega'' = LR^2$ consisting of the first two syllables of Ω' and the relevant subcomplex $\mathscr{S}'' \subset \mathscr{S}$. Then $\mathscr{S}''$ has boundary deficits along the edges which glue to $\mathscr{S} \setminus \mathscr{S}''$. We show that these deficits are preserved up to permutation of the first two angles if we extend the (B2) block in Ω''.

By assumption Δ_i, Δ_{i+1} and Δ_{i+2} have shapes (I), (VI) and (III), respectively, assigned as in the previous case. Substituting into lines 1, 5 and 6 of (2.4.9), which are the angle equations containing the deficits in $\mathscr{S}''$, we have

$$\begin{aligned} \delta_0 + \frac{14\pi}{24} + \frac{2\pi}{6} + \frac{\pi}{2} + \mu_0 &= 2\pi \\ \frac{\pi}{4} + \frac{2\pi}{4} + \mu_1 &= 2\pi \\ \frac{\pi}{2} + \mu_2 &= 2\pi \end{aligned}$$

where μ_0, μ_1, μ_2 denote the angle deficits on $\mathscr{S}''$, replacing the angles from $\Theta^{(k)}$ for $k \geq i+3$ in (2.4.9). Since $\delta_0 = \pi/3$ we solve the above equations as

$$\mu_0 = \frac{\pi}{4} \qquad \mu_1 = \frac{5\pi}{4} \qquad \text{and} \qquad \mu_2 = \frac{3\pi}{2}$$

Suppose we now extend the length of the (B2) block in Ω'' by one. This corresponds to a subword of $\Omega' = (LR^2L^2)(RL^2)^qR$ with $q = m-1$. By assumption we have $\Theta^{(i)}$ and $\Theta^{(i+1)}$ as above and further that $\Theta^{(i+2)}, \Theta^{(i+3)}$ and $\Theta^{(i+4)}$ have shape (III) assigned as

$$\Theta^{(i+2)} = \left(\frac{\pi}{4}, \frac{\pi}{4}, \frac{\pi}{2}\right) \quad \Theta^{(i+3)} = \left(\frac{\pi}{2}, \frac{\pi}{4}, \frac{\pi}{4}\right) \quad \text{and} \quad \Theta^{(i+4)} = \left(\frac{\pi}{4}, \frac{\pi}{4}, \frac{\pi}{2}\right).$$

The relevant equations containing the new deficits of $\mathscr{S}''$ are

$$\begin{aligned}\theta_{3(i+1)} + 2\theta_{3(i+2)-1} + 2\theta_{3(i+3)-1} + 2\theta_{3(i+4)-1} + \eta_0 &= 2\pi\\ \theta_{3(i+3)} + 2\theta_{3(i+4)-2} + \eta_1 &= 2\pi\\ \theta_{3(i+4)} + \eta_2 &= 2\pi\end{aligned}$$

where η_0, η_1, η_2 denote the new deficits on $\mathscr{S}''$. Substituting the angles in we have

$$\begin{aligned}\frac{\pi}{4} + \frac{2\pi}{4} + \frac{2\pi}{4} + \frac{2\pi}{4} + \eta_0 &= 2\pi\\ \frac{\pi}{4} + \frac{2\pi}{4} + \eta_1 &= 2\pi\\ \frac{\pi}{2} + \eta_2 &= 2\pi\end{aligned}$$

Solving the above equations we see that

$$\eta_0 = \frac{\pi}{4} \qquad \eta_1 = \frac{5\pi}{4} \qquad \text{and} \qquad \eta_2 = \frac{3\pi}{2}$$

Since $\mu_i = \eta_i$ for each $i = 0,1,2$, extending any (B2) block in Ω' must introduce ideal tetrahedra with shape (III). The remaining shapes of the tetrahedra in both instances remain the same. However, after we extend the (B2) block we must swap the first two angles in each remaining $\Theta^{(j)}$ as described in Cases 1 and 2 above. We also observe that the angle deficits seen here are the same if we follow this procedure at the end of any (B2) block in Ω'. □

Given the angle structures on (B1) and (B3) blocks we now check that these angle structures are valid when we glue a (B1) block to a (B3) block.

Lemma 2.13 *The angle structures on (B1) and (B3) blocks are compatible. More precisely, a (B1) block can always be glued to either the start or the end of a (B3) block.*

Proof Denote the first and last letters of a (B1) and (B3) block by $\alpha_{(B1)}$, $\alpha_{(B3)}$, and $\omega_{(B1)}$, $\omega_{(B3)}$, respectively. Let ε_0, ε_1 and ε_2 denote the boundary deficits at the end of the (B1) block as in Figure 2.7. Similarly, let δ_0, δ_1 and δ_2 be the boundary deficits at the start of the (B3) block. One key take away from Theorems 2.10 and 2.12 is that the ε-boundary deficit of a (B1) block equals the δ-boundary deficit of a block of (B3) as long as $\omega_{(B1)} \neq \alpha_{(B3)}$. In particular, we have $\delta_i = \varepsilon_i$, $0 \leq i \leq 2$ whenever $\omega_{(B1)} \neq \alpha_{(B3)}$. The same is true for the end of a (B3) block and the start of a (B1) block.

For the angle structures from the blocks to extend to a valid angle structure after gluing, the boundary angles of the identified edges must sum to 2π. If $\omega_{(B1)} = L$ and $\alpha_{(B3)} = R$ we have identifications leading to $\varepsilon_0 + \delta_0 = \varepsilon_2 + \delta_1 = \varepsilon_1 + \delta_2 = 2\pi$. To see this note that, since $\alpha_{(B3)} = R$, this layering swaps vertical and diagonal edges (indices 1 and 2). Since, following Theorems 2.10 and 2.12 we have $\varepsilon_0 = \delta_0 = \pi$, $\varepsilon_1 = \delta_1 = \pi/3$, and $\varepsilon_2 = \delta_2 = 5\pi/3$, these identities

hold. If instead we have $\omega_{(B1)} = R$ and $\alpha_{(B3)} = L$, we have $\varepsilon_0 + \delta_2 = \varepsilon_1 + \delta_1 = \varepsilon_2 + \delta_0 = 2\pi$. Again, following Theorems 2.10 and 2.12, we have $\varepsilon_0 = \delta_0 = \pi/3$, $\varepsilon_1 = \delta_1 = \pi$, $\varepsilon_2 = \delta_2 = 5\pi/3$, and the equations are satisfied.

An analogous argument shows that the angle structures are compatible when gluing the end of a (B3) block to the start of a (B1) block. □

Lemma 2.14 *Let $\Omega = RL^{a_1}\cdots(R^{a_n}L \mid L^{a_n}R)$ with $n \geq 1$ be a word such that $\Omega' = L^{a_1}\cdots(R^{a_n} \mid L^{a_n})$ can be decomposed into only (B1) and (B3) blocks. Let $\mathscr{T}$ be the Sakuma-Weeks triangulation of the associated 2-bridge link complement consisting of $\Sigma = 1 + \sum a_i$ layers. There is an angle structure on $\mathscr{T}$ such that each block has the angles assigned as in Theorem 2.10 and Theorem 2.12 and Δ_1 has shape (V). If the last block in Ω' is of type (B1), then Δ_Σ has shape (V). If the last block of Ω' is of type (B3), then $\Delta_{\Sigma-1}$ has shape (III) and Δ_Σ has shape (VIII). In both cases, Δ_Σ replaces the last tetrahedron in the final block.*

Proof From Theorems 2.10 and 2.12 we have the δ-boundary deficit at the start of the first block

$$\delta_0 = \frac{\pi}{3} \qquad \delta_1 = \pi \quad \text{and} \quad \delta_2 = \frac{5\pi}{3}$$

From Figure 2.5a we equate this boundary deficit to edges in Δ_1 as,

$$\delta_0 = \theta_{3(1)} \qquad \delta_1 = 2\theta_{3(1)-1} \qquad \text{and} \qquad \delta_2 = 4\theta_{3(1)-2} + 2\theta_{3(1)} + \theta_{3(2)}$$

As Δ_2 is the first layer in a (B1) or (B3) block, we have $\theta_{3(2)} = \pi/3$ (see (2.4.4) for the case of (B3)). Assigning shape (V) to Δ_1 as

$$\Theta^{(1)} = (\theta_1, \theta_2, \theta_3) = \left(\frac{\pi}{6}, \frac{\pi}{2}, \frac{\pi}{3}\right)$$

solves the boundary angle equations. Note that extending the length of the block in the case of (B1) replaces the δ-boundary deficit with multiples of $\pi/3$ leaving the above assignment of $\Theta^{(1)}$ to satisfy the equations.

We now consider the shape of Δ_Σ. Suppose that $\Omega = R\cdots R^{a_{n-1}}L^{a_n}R$ so that n is odd. From Figures 2.4 and 2.5b (using the case of n odd), the angle equations for edges in Δ_Σ are

$$\begin{aligned} 4\theta_{3\Sigma-2} + 2\theta_{3\Sigma} + 2\theta_{3(\Sigma-1)} &= 2\pi \\ x + 2\theta_{3\Sigma-1} &= 2\pi \end{aligned} \tag{2.4.13}$$

where x denotes the angle deficit on the vertical edge class of Δ_Σ. To verify this, we note that the four horizontal edges and two diagonal edges in Δ_Σ are identified and, given Ω, must also include both diagonal edges from the previous layer. This gives the first equation. To obtain the second equation, note that we have two distinct edge classes for the four vertical edges in Δ_Σ which also include some edges from previous layers. We consider two cases for the values of a_{n-1} and a_n.

Case 1: Suppose that $a_n = a_{n-1} = 1$ so that Ω' ends on a (B1) block. Note that $R^{a_{n-1}}$ either corresponds to a part of the same (B1) block or to the last syllable of a (B3) block. From Theorems 2.10 and 2.12 we know that we have $\theta_{3(\Sigma-1)} = \pi/3$ in both of these cases. Using this, the first line of (2.4.13) above is satisfied by $\theta_{3\Sigma-2} = \pi/6$ and $\theta_{3\Sigma} = \pi/3$.

We now verify that $\theta_{3\Sigma-1} = \pi/2$. This angle corresponds to the vertical edge class of Δ_Σ. Remove L^{a_n} from Ω' and consider it as a (B1) block of length one. Then $R^{a_{n-1}}$ is the end of either a (B1) or (B3) block. We know that the vertical edge class of Δ_Σ glues to the vertical edge class of $\Delta_{\Sigma-1}$ and hence it suffices to check that the angle deficit in $\Delta_{\Sigma-1}$ is π. It follows from Theorems 2.10 and 2.12 that the angle deficit of the vertical edge class for a (B1) or (B3) block ending on R is indeed π, and hence $\Theta^{(\Sigma)}$ has shape (V).

Case 2: Suppose now that Ω has the same form as above with $a_{n-1} = 2$ and $a_n = 1$ so that Ω' ends on a (B3) block. The angles in the first equation from (2.4.13) remain the same, however we can determine x explicitly from Figure 2.4 as

$$x = \theta_{3(\Sigma-2)} + 2\theta_{3(\Sigma-1)-1}$$

It must be that $\Delta_{\Sigma-2}$ has shape (VI) or (VIII). From (2.4.4) and (2.4.11) we must have that $\theta_{3(\Sigma-2)} = \pi/4$. Substituting in the second line of (2.4.13) yields

$$2\theta_{3(\Sigma-1)-1} + 2\theta_{3\Sigma-1} = \frac{7\pi}{4}$$

This is solved by setting $\theta_{3(\Sigma-1)-1} = \pi/4$ and $\theta_{3\Sigma-1} = 5\pi/8$. Solving the remaining equation gives $\theta_{3\Sigma-2} = \pi/8$, $\theta_{3\Sigma} = \pi/4$ and $\theta_{3(\Sigma-1)} = \pi/2$. This gives shapes (III) and (VIII) as

$$\Theta^{(\Sigma-1)} = \left(\frac{\pi}{4}, \frac{\pi}{4}, \frac{\pi}{2}\right) \quad \text{and} \quad \Theta^{(\Sigma)} = \left(\frac{\pi}{8}, \frac{5\pi}{8}, \frac{\pi}{4}\right)$$

To check compatibility we consider the one remaining angle equation which interacts with these shapes,

$$\theta_{3(\Sigma-3)} + 2\theta_{3(\Sigma-2)-1} + \theta_{3(\Sigma-1)} = 2\pi$$

For these shapes to be compatible we require $\theta_{3(\Sigma-3)} + 2\theta_{3(\Sigma-2)-1} = 7\pi/4$. If $\Delta_{\Sigma-2}$ has shape (VI), then (2.4.4) gives us $\theta_{3(\Sigma-2)-1} = 7\pi/12$ and $\theta_{3(\Sigma-3)} = \pi/3$. Otherwise both $\Delta_{\Sigma-2}$ and $\Delta_{\Sigma-3}$ have shape (III) and we have $\theta_{3(\Sigma-2)-1} = \pi/2$ and $\theta_{3(\Sigma-3)} = \pi/2$ and conclude that the shapes are compatible. □

We now have valid angle structures for the Sakuma-Weeks triangulation of any 2-bridge link described by a word $\Omega = RLR^{a_2}\cdots(LR \mid RL)$ such that $a_2, \ldots, a_{n-1} \in \{1,2\}$ – that is, the subword obtained by removing the first and last letter can be decomposed into only (B1) and (B3) blocks.

We now examine the angle structures on (B2) blocks. Recall from Theorem 2.9 that a (B2) block must occur as the first or last block in the word. We find an angle structure on these

blocks which is compatible with (B1) and (B3) blocks on one boundary and satisfies the face identifications corresponding to the first or last letter of Ω on the other boundary. For reference, we record the $\delta-$ and $\varepsilon-$boundary deficits of (B1) and (B3) blocks here.

δ_0	δ_1	δ_2		ε_0	ε_1	ε_2
$\pi/3$	π	$5\pi/3$	L	π	$\pi/3$	$5\pi/3$
π	$\pi/3$	$5\pi/3$	R	$\pi/3$	π	$5\pi/3$

Lemma 2.15 *Let $\mathscr{T}$ be the Sakuma-Weeks triangulation of a 2-bridge link complement associated to the word $\Omega = RL^{a_1}\cdots(L^{a_n}R \mid R^{a_n}L)$ with $a_i = 2$ for $1 \le i \le k$. The subcomplex $\mathscr{S} \subset \mathscr{T}$ corresponding to the (B2) block at the start of Ω' can be constructed using only ideal tetrahedra of shape types (I), (III) and (VI) arranged as*

$$\big[(III)\big]^{2(k-1)} \longrightarrow (VI) \longrightarrow (I)$$

The block is compatible with Δ_1 having shape (VII) and the end of the block is compatible with (B1) and (B3) blocks.

Proof Let $\Omega' = (L^2R^2)^{m-1}L^2$ for $m \ge 1$ be the (B2) block. Denote the layers of this block as $\Delta_2, \ldots, \Delta_{4m-1}$. The angle equations for the edges of Δ_{4m-2} and Δ_{4m-1} are,

$$\begin{aligned}
x_0 + 2\theta_{3(4m-2)-2} + \theta_{3(4m-1)} &= 2\pi \\
x_1 + 2\theta_{3(4m-2)-1} + 2\theta_{3(4m-1)-1} + \varepsilon_1 &= 2\pi \\
x_2 + \theta_{3(4m-2)} &= 2\pi \\
\theta_{3(4m-2)} + 2\theta_{3(4m-1)-2} + \varepsilon_0 &= 2\pi \\
\theta_{3(4m-1)} + \varepsilon_2 &= 2\pi
\end{aligned} \tag{2.4.14}$$

where x_0, x_1 and x_2 denote angle deficits on the respective edge classes. For any angle structure on this block to be compatible with a (B1) or (B3) block we require that the ε-boundary deficit on Δ_{4m-1} agrees with the δ-boundary deficit of the (B1) or (B3) blocks - which must start on R. That is $\varepsilon_i = \delta_i$ for $0 \le i \le 2$. Hence $\varepsilon_0 = \pi$, $\varepsilon_1 = \pi/3$ and $\varepsilon_2 = 5\pi/3$.

Setting

$$\text{(VI)}\quad \Theta^{(4m-2)} = \left(\frac{7\pi}{12}, \frac{\pi}{6}, \frac{\pi}{4}\right) \qquad \text{and} \qquad \text{(I)}\quad \Theta^{(4m-1)} = \left(\frac{3\pi}{8}, \frac{7\pi}{24}, \frac{\pi}{3}\right)$$

solves the last two equations and determines the angle deficits as

$$x_0 = \frac{\pi}{2} \qquad x_1 = \frac{3\pi}{4} \quad \text{and} \quad x_2 = \frac{7\pi}{4} \tag{2.4.15}$$

Suppose that $m = 1$ so that the (B2) block is of length one. The angle deficits above must be satisfied by the angle equations from Δ_1. From Figures 2.4 and 2.5a we have,

$$\begin{aligned} x_0 &= \theta_{3(1)} \\ x_1 &= 2\theta_{3(1)-1} \\ x_2 &= 4\theta_{3(1)-2} + 2\theta_{3(1)} + \theta_{3(2)} \end{aligned} \tag{2.4.16}$$

Setting $\Theta^{(1)} = (\pi/8, 3\pi/8, \pi/2)$ gives Δ_1 shape (VII) and satisfies the deficits in (2.4.15).

Suppose now that $m > 1$. We claim that the additional layers between Δ_1 and Δ_{4m-2} all have shape (III). The angle equations are the same as those seen in the proof of Theorem 2.12 and so it suffices to check that this assignment is compatible with (2.4.15) and assigning shape (VII) to Δ_1.

We first expand the angle deficits above as,

$$\begin{aligned} x_0 &= \theta_{3(4m-3)} \\ x_1 &= \theta_{3(4m-4)} + 2\theta_{3(4m-3)-1} \\ x_2 &= y + 2\theta_{3(4m-4)-2} + 2\theta_{3(4m-3)-2} \end{aligned}$$

We have $\pi/2 = x_0 = \theta_{3(4m-3)}$ and assume Δ_{4m-3} has shape (III), hence we assign $\Theta^{(4m-3)} = (\pi/4, \pi/4, \pi/2)$. By construction, y must correspond to the horizontal edge class of the previous layer. Observe that Ω' repeats strings of (L^2R^2). This corresponds to (2.4.8) followed by (2.4.7) and hence, from the reasoning following these equations, we have $\Theta^{(4m-4)} = (\pi/4, \pi/2, \pi/4)$. This forces $y = 3\pi/4$. From the proof of Theorem 2.12 (the case of one (B2) block) we know that $y = 2\pi/4 + \pi/4$ and thus conclude that Δ_{4m-4} and Δ_{4m-3} have shape (III).

To check that this assignment is compatible with Δ_1 having shape (VII), we consider the following angle equations from Δ_2 and Δ_3, assuming $m > 1$,

$$\begin{aligned} x_0 + 2\theta_{3(2)-2} + \theta_{3(3)} &= 2\pi \\ x_1 + 2\theta_{3(2)-1} + 2\theta_{3(3)-1} + z &= 2\pi \\ x_2 + \theta_{3(2)} &= 2\pi \end{aligned}$$

where the deficits x_i are as in (2.4.16). Assigning shape (III) as $\Theta^{(2)} = (\pi/2, \pi/4, \pi/4)$ and $\Theta^{(3)} = (\pi/4, \pi/4, \pi/2)$ gives Δ_1 shape (VII) as above if $z = \pi/4$. Note that Δ_4 must have either shape (III) or shape (VI) and z must correspond to the diagonal edge class. In either case, we have $\theta_{3(4)} = \pi/4$ and thus the shape assignment is compatible.

An analogous argument applies if $\Omega' = (L^2R^2)^m$ for $m \geq 1$. Here, the first two angles in each layer are swapped. □

Lemma 2.16 *Let $\mathscr{T}$ be the Sakuma-Weeks triangulation of a 2-bridge link complement associated to the word $\Omega = RL^{a_1} \cdots (L^{a_n}R \mid R^{a_n}L)$ with $a_i = 2$ for $n-k < i \leq n$, $k \geq 2$, and let*

$\Sigma = 1 + \sum a_i$. The subcomplex $\mathscr{S} \subset \mathscr{T}$ corresponding to the (B2) block at the end of Ω can be constructed using only ideal tetrahedra of shape types (III), (V) and (IX) arranged as

$$(IX) \longrightarrow \big[(V)\big]^{\,3}$$

for $k = 2$ and,

$$(IX) \longrightarrow \big[(III)\big]^{\,2k-5} \longrightarrow \big[(V)\big]^{\,4}$$

for $k \geq 3$. The start of the block is compatible with blocks of types (B1) and (B3) and the end of the block is compatible with the face identifications on Δ_Σ.

Proof Assume the last letter of Ω is R. Suppose that $k = 2$ and the (B2) block is given by R^2L^2. The block contains the layers $\Delta_{\Sigma-3}$ to Δ_Σ, inclusive. The angle equations of this block are now,

$$\begin{aligned}
\delta_0 + 2\theta_{3(\Sigma-3)-2} + 2\theta_{3(\Sigma-2)-2} + \theta_{3(\Sigma-1)} &= 2\pi \\
\delta_1 + 2\theta_{3(\Sigma-3)-1} + \theta_{3(\Sigma-2)} &= 2\pi \\
\delta_2 + \theta_{3(\Sigma-3)} &= 2\pi \\
\theta_{3(\Sigma-3)} + 2\theta_{3(\Sigma-2)-1} + 2\theta_{3(\Sigma-1)-1} + 2\theta_{3\Sigma-1} &= 2\pi \\
\theta_{3(\Sigma-2)} + 2\theta_{3(\Sigma-1)-2} + \theta_{3\Sigma} &= 2\pi \\
2\theta_{3(\Sigma-1)} + 4\theta_{3\Sigma-2} + 2\theta_{3\Sigma} &= 2\pi
\end{aligned}$$

The block starts on R hence the δ-boundary deficit is given by $\delta_0 = \pi$, $\delta_1 = \pi/3$ and $\delta_2 = 5\pi/3$. We assign shape (IX) to $\Delta_{\Sigma-3}$ as

$$\Theta^{(\Sigma-3)} = \left(\frac{\pi}{12}, \frac{7\pi}{12}, \frac{\pi}{3}\right)$$

We then assign shape (V) to the remaining shapes as,

$$\Theta^{(\Sigma-2)} = \left(\frac{\pi}{3}, \frac{\pi}{6}, \frac{\pi}{2}\right) \qquad \Theta^{(\Sigma-1)} = \left(\frac{\pi}{2}, \frac{\pi}{3}, \frac{\pi}{6}\right) \quad \text{and} \quad \Theta^{(\Sigma)} = \left(\frac{\pi}{6}, \frac{\pi}{3}, \frac{\pi}{2}\right)$$

Increasing to $k = 3$ the (B2) block is now given by $L^2R^2L^2$. We can observe that the last three angle equations above remain the same. The three boundary angle equations are the same as above, however the angles assigned to vertical and horizontal edges are swapped. From this we assign shape (IX) to $\Delta_{\Sigma-5}$ as was done for $\Delta_{\Sigma-3}$ above but swapping the first two angles, and shape (V) to layers $\Delta_{\Sigma-2}$, $\Delta_{\Sigma-1}$ and Δ_Σ exactly as above. The angle equations involving layers

$\Delta_{\Sigma-4}$ and $\Delta_{\Sigma-3}$ are,

$$\begin{aligned}
\delta_0 + 2\theta_{3(\Sigma-5)-2} + \theta_{3(\Sigma-4)} &= 2\pi \\
\delta_1 + 2\theta_{3(\Sigma-5)-1} + 2\theta_{3(\Sigma-4)-1} + \theta_{3(\Sigma-3)} &= 2\pi \\
\theta_{3(\Sigma-5)} + 2\theta_{3(\Sigma-4)-2} + 2\theta_{3(\Sigma-3)-2} + 2\theta_{3(\Sigma-2)-2} + \theta_{3(\Sigma-1)} &= 2\pi \\
\theta_{3(\Sigma-4)} + 2\theta_{3(\Sigma-3)-1} + \theta_{3(\Sigma-2)} &= 2\pi \\
\theta_{3(\Sigma-3)} + 2\theta_{3(\Sigma-2)-1} + 2\theta_{3(\Sigma-1)-1} + 2\theta_{3\Sigma-1} &= 2\pi
\end{aligned}$$

Substituting in $\delta_0 = \pi/3$, $\delta_1 = \pi$ and the angles from the shape assignments to $\Delta_{\Sigma-5}, \Delta_{\Sigma-2}, \Delta_{\Sigma-1}$ and Δ_Σ allows us to assign shape (III) to $\Delta_{\Sigma-4}$ and (V) to $\Delta_{\Sigma-3}$ as,

$$\Theta^{(\Sigma-4)} = \left(\frac{\pi}{4}, \frac{\pi}{4}, \frac{\pi}{2}\right) \qquad \text{and} \qquad \Theta^{(\Sigma-3)} = \left(\frac{\pi}{6}, \frac{\pi}{2}, \frac{\pi}{3}\right)$$

Extending the block to $k > 3$ adds angle equations as in (2.4.7) and (2.4.8) and can be solved by adding additional layers of shape (III).

An analogous argument shows that this assignment of shapes is valid if the (B2) block ends on R^2 (giving the last letter of Ω to be L) or starts on L^2 with the first two angles of each shape vector swapped. □

We now address the case of $a_{n-1} = 1$ and $a_n = 2$, which is neglected in the above lemma. Extending this block to contain the final letter of Ω we obtain a (B3) block in which the final (B2) block contained within it has length one. In this situation it is more convenient to treat the subcomplex corresponding to this block as an 'unfinished' (B3) block.

Lemma 2.17 *Let $\mathscr{T}$ be the Sakuma-Weeks triangulation of a 2-bridge link complement associated to the word $\Omega = RL^{a_1}\cdots(L^{a_n}R \mid R^{a_n}L)$ with $a_{n-1} = 1$, $a_n = 2$, $n \geq 2$, and $\Sigma = 1 + \sum a_i$. The subcomplex $\mathscr{S} \subset \mathscr{T}$ corresponding to an unfinished (B3) block at the end of Ω containing the layers $\Delta_{\Sigma-2}$, $\Delta_{\Sigma-1}$ and Δ_Σ can be constructed as in Theorem 2.12 with the two layers containing ideal tetrahedra of shapes (IV) and (II) replaced with a single layer containing ideal tetrahedra of shape (VII) or (III) if the block contains one or more (B2) blocks, respectively.*

Proof Suppose that $\Omega' = LR^2(L)$ so that $\mathscr{S}$ contains only three layers, with (L) denoting the final letter of Ω. The corresponding angle equations are,

$$\begin{aligned}
\delta_0 + 2\theta_{3(\Sigma-2)-2} + 2\theta_{3(\Sigma-1)-2} + 2\theta_{3\Sigma-2} &= 2\pi \\
\delta_1 + 2\theta_{3(\Sigma-2)-1} + \theta_{3(\Sigma-1)} &= 2\pi \\
\delta_2 + \theta_{3(\Sigma-2)} &= 2\pi \\
\theta_{3(\Sigma-2)} + 2\theta_{3(\Sigma-1)-1} + \theta_{3\Sigma} &= 2\pi \\
2\theta_{3(\Sigma-1)} + 4\theta_{3\Sigma-1} + 2\theta_{3\Sigma} &= 2\pi
\end{aligned}$$

The block starts on L hence the δ-boundary deficit is given by $\delta_0 = \pi/3$, $\delta_1 = \pi$ and $\delta_2 = 5\pi/3$. We obtain shapes (I), (VI) and (VII) by assigning the angles,

$$\Theta^{(\Sigma-2)} = \left(\frac{7\pi}{24}, \frac{3\pi}{8}, \frac{\pi}{3}\right) \quad \Theta^{(\Sigma-1)} = \left(\frac{\pi}{6}, \frac{7\pi}{12}, \frac{\pi}{4}\right) \quad \text{and} \quad \Theta^{(\Sigma)} = \left(\frac{3\pi}{8}, \frac{\pi}{8}, \frac{\pi}{2}\right)$$

If instead the (B3) block is longer, then we only need to consider an additional two layers preceding $\Delta_{\Sigma-2}$. Suppose that the tail of Ω' has the form $R^2LR^2(L)$, where (L) denotes the final letter of Ω. The corresponding angle equations are,

$$\begin{aligned}
\theta_{3(\Sigma-4)} + 2\theta_{3(\Sigma-3)-1} + 2\theta_{3(\Sigma-2)-1} + \theta_{3(\Sigma-1)} &= 2\pi \\
\theta_{3(\Sigma-3)} + 2\theta_{3(\Sigma-2)-2} + 2\theta_{3(\Sigma-1)-2} + 2\theta_{3\Sigma-2} &= 2\pi \\
\theta_{3(\Sigma-2)} + 2\theta_{3(\Sigma-1)-1} + \theta_{3\Sigma} &= 2\pi \\
2\theta_{3(\Sigma-1)} + 4\theta_{3\Sigma-1} + 2\theta_{3\Sigma} &= 2\pi
\end{aligned}$$

Following Theorem 2.12 we assign shape (VIII) as

$$\Theta^{(\Sigma-1)} = \left(\frac{\pi}{8}, \frac{5\pi}{8}, \frac{\pi}{4}\right)$$

and shape (III) as

$$\Theta^{(\Sigma-2)} = \left(\frac{\pi}{4}, \frac{\pi}{4}, \frac{\pi}{2}\right) \quad \text{and} \quad \Theta^{(\Sigma-3)} = \left(\frac{\pi}{4}, \frac{\pi}{2}, \frac{\pi}{4}\right)$$

This assignment yields Δ_Σ having shape (III) as $\Theta^{(\Sigma)} = (\pi/2, \pi/4, \pi/4)$. Finally, we require $\theta_{3(\Sigma-4)} = \pi/4$. We must have the ideal tetrahedra in $\Delta_{\Sigma-4}$ having either shape (VI) or shape (III). In both cases we can set $\theta_{3(\Sigma-4)} = \pi/4$. All solutions to any remaining angle equations can be set as in Theorem 2.12. □

Lemma 2.18 *Let $\mathscr{T}$ be the Sakuma-Weeks triangulation of a 2-bridge link complement associated to the word $\Omega = RL^{a_1} \cdots (L^{a_n}R \mid R^{a_n}L)$ with $a_i = 2$ for all $1 \leq i \leq n$. That is, the subword $\Omega' = L^{a_1}R^{a_2} \cdots (L^{a_n} \mid R^{a_n})$ consists of a single (B2) block. Then $\mathscr{T}$ admits an angle structure consisting only of shapes (III) and (VII) arranged as*

$$\textit{(VII)} \longrightarrow \big[\textit{(III)}\big]^{\,2n-1} \longrightarrow \textit{(VII)}$$

Proof Suppose $n = 1$ so that $\Omega = RL^2R$. The angle equations describing $\mathscr{T}$ are,

$$\begin{aligned}
4\theta_{3(1)-2} + 2\theta_{3(1)} + 2\theta_{3(2)} &= 2\pi \\
2\theta_{3(1)-1} + 2\theta_{3(2)-1} + 2\theta_{3(3)-1} &= 2\pi \\
\theta_{3(1)} + 2\theta_{3(2)-2} + \theta_{3(3)} &= 2\pi \\
2\theta_{3(2)} + 4\theta_{3(3)-2} + 2\theta_{3(3)} &= 2\pi
\end{aligned}$$

We assign shape (VII) to Δ_1 and Δ_3 as,

$$\Theta^{(1)} = \Theta^{(3)} = \left(\frac{\pi}{8}, \frac{3\pi}{8}, \frac{\pi}{2}\right)$$

The remaining equations are solved by assigning shape (III) to Δ_2 as

$$\Theta^{(2)} = \left(\frac{\pi}{2}, \frac{\pi}{4}, \frac{\pi}{4}\right)$$

Adding additional syllables with $a_i = 2$ adds angle equations that are solved by assigning shape (III) to the added layers in the following (cyclic) order starting from Δ_2,

$$\left(\frac{\pi}{2}, \frac{\pi}{4}, \frac{\pi}{4}\right) \longrightarrow \left(\frac{\pi}{4}, \frac{\pi}{4}, \frac{\pi}{2}\right) \longrightarrow \left(\frac{\pi}{4}, \frac{\pi}{2}, \frac{\pi}{4}\right) \longrightarrow \left(\frac{\pi}{4}, \frac{\pi}{4}, \frac{\pi}{2}\right)$$

The assignment of shape (VII) is as above if Ω ends with R, otherwise the first two angles are exchanged. □

2.4.3. Complexity bounds. We now prove lower bounds on the complexity of 2-bridge link complements through the angle structures established in the previous section. The first step of this proof is determining explicit formulae for the volume of a given block type in the decomposition of Ω. The approximate volume of each of the ten shapes is given below as a multiple of the volume of a regular ideal tetrahedron v_3.

$$v_3 = \mathrm{Vol}(\Delta(\pi/3, \pi/3, \pi/3)) \approx 1.0149$$

$$v_I = \mathrm{Vol}(\Delta(\pi/3,\ 3\pi/8,\ 7\pi/24)) \approx 0.9902 v_3$$

$$v_{II} = \mathrm{Vol}(\Delta(\pi/3,\ \pi/4,\ 5\pi/12)) \approx 0.9604 v_3$$

$$v_{III} = \mathrm{Vol}(\Delta(\pi/4,\ \pi/4,\ \pi/2)) \approx 0.9024 v_3$$

$$v_{IV} = \mathrm{Vol}(\Delta(5\pi/24,\ 7\pi/24,\ \pi/2)) \approx 0.8855 v_3$$

$$v_V = \mathrm{Vol}(\Delta(\pi/6,\ \pi/2,\ \pi/3)) \approx 0.8333 v_3$$

$$v_{VI} = \mathrm{Vol}(\Delta(\pi/6,\ \pi/4,\ 7\pi/12)) \approx 0.7754 v_3$$

$$v_{VII} = \mathrm{Vol}(\Delta(\pi/8, 3\pi/8, \pi/2)) \approx 0.7417 v_3$$

$$v_{VIII} = \mathrm{Vol}(\Delta(\pi/8,\ \pi/4,\ 5\pi/8)) \approx 0.6768 v_3$$

$$v_{IX} = \mathrm{Vol}(\Delta(\pi/12,\ 7\pi/12,\ \pi/3)) \approx 0.5833 v_3$$

Recall that the length of a block is the number of syllables it contains - that is, the number of maximal subwords R^{a_i} or L^{a_i}.

Using the lemmas in the Section 5.2, we can determine the number of layers containing ideal tetrahedra of each shape type in each given block. This also provides the volume of each block type in terms of its length and is collected in Table 2.3. To prove our main result we first

	# layers	(0)	(I)	(II)	(III)	(IV)	(V)	(VI)	(VII)	(VIII)	(IX)
(B1)	k	$k^\star$	0	0	0	0	Δ_1, Δ_Σ	0	0	0	0
(B2), at start	$2k$	0	1	0	$2(k-1)$	0	0	1	Δ_1	0	0
(B2), at end ($k=2$)	4	0	0	0	0	0	3	0	0	0	1
(B2), at end ($k \geq 3$)	$2k$	0	0	0	$2k-5$	0	4	0	0	0	1
(B3)	$2\ell+m+1$	0	1	1	$2(\ell-1)$	1	Δ_1	1	0	$m-1$	0
(B3), at end	$2\ell+m+1$	0	1	0	$2\ell-1$	0	Δ_1	1	0	m	0
Unfinished (B3) ($m=1$)	3	0	1	0	0	0	Δ_1	1	1	0	0
Unfinished (B3) ($m>1$)	$2\ell+m$	0	1	0	$2\ell-1$	0	Δ_1	1	0	$m-1$	0
All (B2)	$2k$	0	0	0	$2k-1$	0	0	0	2	0	0

TABLE 2.3. Number of layers containing ideal tetrahedra of each shape in each block type. The length of a block is denoted k (length does not include Δ_1) and the number of (B2) blocks in a (B3) block is denoted m and the total length of the (B2) blocks is denoted ℓ. Values marked by $\star$ contain one less layer of this shape if the block occurs at the end of the word Ω, with the final layer replaced with the shape marked by Δ_Σ. The entry marked by Δ_1 indicates the shape of the initial layer of $\mathscr{T}$ if the block occurs at the start of Ω. Recall that the unfinished (B3) block occurs only when $a_{n-1}=1$ and $a_n=2$ and is always at the end of Ω.

show that the above prescription of angle structures, combined with Thurston's lower bound on complexity (2.4.1), determine that the Sakuma-Weeks triangulation is minimal if $a_i = 1$ for all $1 \leq i \leq n$.

Lemma 2.19 ([IN16], Corollary 1.1) *Let $K = K(\Omega)$ be the 2-bridge link associated to the word $\Omega = RL^{a_1}\cdots(L^{a_n}R \mid R^{a_n}L)$ with $a_i = 1$ for all $1 \leq i \leq n$, $n \geq 1$. Let $M = S^3\backslash K$ and $\mathscr{T} = \mathscr{T}(M)$ be the Sakuma-Weeks triangulation of M, Moreover, let $c(M)$ denote the complexity of M. Then $\mathscr{T}$ is minimal; that is*

$$c(M) = |\mathscr{T}| = 2(n+1)$$

Proof The subword $\Omega' = L^{a_1}\cdots(L^{a_n}R \mid R^{a_n}L)$ decomposes into a single (B1) block consisting of n layers. Using Table 2.3, we note that the ideal tetrahedra in Δ_1 and Δ_Σ, where $\Sigma = n+1$, have shape (V) whilst the ideal tetrahedra in the remaining $n-1$ layers are regular ideal. Denote the corresponding angle structure $\Theta^\star$. Combining (2.4.1) with Theorem 1.25 we obtain

$$\frac{\mathscr{V}(\Theta^\star)}{v_3} \leq c(M) \leq |\mathscr{T}| \tag{2.4.17}$$

This gives us a lower bound on the complexity as

$$\frac{2(2v_V + (n-1)v_3)}{v_3} = 2n + 1.3332 \tag{2.4.18}$$

Combining with the upper bound on complexity we have,

$$2n + 1.3332 \leq c(M) \leq 2n + 2,$$

and conclude that $\mathscr{T}$ is minimal. □

Theorem 2.20 *Let $L = L(\Omega)$ be the 2-bridge link associated to the word $\Omega = RL^{a_1} \cdots (L^{a_n}R \mid R^{a_n}L)$ where $a_i \in \{1,2\}$ for all $1 \leq i \leq n$ and $n \geq 1$. Let $M = S^3 \backslash L$ and $\mathscr{T} = \mathscr{T}(M)$ be the Sakuma-Weeks triangulation of M and let $c(M)$ denote the complexity of M. Then,*

$$0.8|\mathscr{T}| \leq c(M) \leq |\mathscr{T}|$$

Before we provide a proof we remark that the lower bound we find is conservative. For example, if Ω is such that $a_i = 2$ for all $1 \leq i \leq n$, then the angle structure we find gives a lower bound of approximately $0.85|\mathscr{T}| \leq c(M)$ for $n = 3$ and this converges to approximately $0.9|\mathscr{T}| \leq c(M)$ as $n \to \infty$. Moreover, we show below that the greatest volume deficits are attained by (B3) blocks with all (B2) blocks having "small length". Provided that the total length of such blocks is finite, we typically see an asymptotic lower bound of approximately $0.9|\mathscr{T}| \leq c(M)$. The choice of conservative bound was made as providing a complete list of constraints decreased the readability of the proof more than what was justifiable.

Proof Using (2.4.17) it suffices to show that there is some angle structure $\Theta^\star$ on $\mathscr{T}$ such that

$$0.8 \leq \frac{\mathscr{V}(\Theta^\star)}{|\mathscr{T}|v_3}$$

Consider a decomposition of $\mathscr{T}$ into three subcomplexes $\mathscr{S}_1$, $\mathscr{S}_2$, and $\mathscr{S}_3$ where $\mathscr{S}_1$ contains Δ_1 and the ideal tetrahedra associated to the first block in the decomposition of Ω, $\mathscr{S}_3$ contains Δ_Σ and the ideal tetrahedra associated to the last block of the decomposition of Ω, and $\mathscr{S}_2$ contains all remaining ideal tetrahedra. Denote the angle structure on $\mathscr{S}_i$ by $\Theta_i^\star$ so that $\Theta^\star$ is the concatenation of these three angle structures.

We proceed by computing the volume for each $\mathscr{S}_i$ in terms of the length of the block(s) it contains different from (B1). Refer to Table 2.3 for all shapes used in what follows.

The first observation we make is that the volume of a (B3) block is smallest when it contains m (B2) blocks of length 1. This follows since each (B2) block after the first replaces two ideal tetrahedra of shape (III) with two ideal tetrahedra of shape (VIII), which have a smaller volume. To minimise the volume for a fixed length of the block we maximise the number of ideal tetrahedra of shape (VIII) which is done by giving each (B2) block length 1. Consequently, we only consider (B3) blocks of this form.

Consider first $\mathscr{S}_1$. A single (B2) block consists of $2k_1$ layers plus Δ_1 giving $|\mathscr{S}_1| = 2(2k_1+1)$ ideal tetrahedra. Assigning the appropriate angle structures we compute

$$\frac{\mathscr{V}(\Theta_1^{(B2)})}{2(2k_1+1)v_3} = \frac{2\left(v_{VII}+v_I+v_{VI}+2(k_1-1)v_{III}\right)}{2(2k_1+1)v_3} = \frac{3.6096k_1+1.405}{2(2k_1+1)}$$

This evaluates to 0.8357 for $k_1 = 1$ and increases with k_1. A single (B3) block with m_1 (B2) blocks of length 1 consists of $3m_1+1$ layers plus Δ_1 giving $|\mathscr{S}_1| = 2(3m_1+2)$ ideal tetrahedra. As above we find

$$\begin{aligned}\frac{\mathscr{V}(\Theta_1^{(B3)})}{2(3m_1+2)v_3} &= \frac{2\left(v_V+v_I+v_{II}+v_{IV}+v_{VI}+2(m_1-1)v_{III}+(m_1-1)v_{VIII}\right)}{2(3m_1+2)v_3} \\ &= \frac{4.9632m_1+3.9264}{2(3m_1+2)}\end{aligned}$$

This evaluates to 0.8889 for $m_1 = 1$ and decreases with m_1, approaching 0.8272 as $m_1 \to \infty$.

For $\mathscr{S}_2$, observe that the largest deficit for the subcomplex $\mathscr{S}_2$ must occur with a single (B3) block with m_2 (B2) blocks of length 1. Adding multiple (B3) blocks – or even (B1) blocks in between (B3) blocks – introduces tetrahedra of shapes (0), (I), (II), (IV) and (VI), which have a larger volume than an ideal tetrahedra of shape (VIII). Hence, using the calculations above without the ideal tetrahedra of shape (V),

$$\frac{\mathscr{V}(\Theta_2^{\star})}{2(3m_2+1)v_3} = \frac{4.9632m_2+2.2598}{2(3m_2+1)}$$

This evaluates to 0.9028 for $m_2 = 1$ and, as above, decreases with m_2, approaching 0.8272 as $m_2 \to \infty$.

Consider now $\mathscr{S}_3$. A single (B2) block consists of $2k_3$ layers for $k_3 \geq 2$ giving $4k_3$ ideal tetrahedra. We compute

$$\frac{\mathscr{V}(\Theta_3^{(B2)})}{4k_3v_3} = \begin{cases} \frac{2(3v_V+v_{IX})}{8v_3} = 0.7708, & k_3 = 2 \\ \frac{2(4v_V+v_{IX}+(2k_3-5)v_{III})}{4k_3v_3} = \frac{3.6096k_3-1.191}{4k_3}, & k_3 \geq 3 \end{cases}$$

This evaluates to 0.8031 for $k_3 = 3$ and increases with k_3. However, we need to ensure that the deficit when $k_3 = 2$ is balanced by the other subcomplexes. We need only check two cases. First, if $\mathscr{T} = \mathscr{S}_1 \cup \mathscr{S}_3$ with $\mathscr{S}_1$ a (B3) block with m_1 (B2) blocks of length 1 then,

$$\frac{\mathscr{V}(\Theta^{\star})}{2(3m_1+6)v_3} = \frac{4.9632m_1+0.0928}{2(3m_1+6)}$$

This evaluates to 0.8364 when $m_1 = 1$ and decreases with m_1 as above. If instead $\mathscr{T} = \mathscr{S}_1 \cup \mathscr{S}_2 \cup \mathscr{S}_3$ with $\mathscr{S}_1$ a (B2) block of length k_1 and $\mathscr{S}_2$ a (B3) block with m_2 (B2) blocks of length 1, then we obtain

$$\frac{\mathscr{V}(\Theta^{\star})}{2(2k_1+3m_2+6)v_3} = \frac{3.6096k_1+4.9632m_2+9.8312}{2(2k_1+3m_2+6)}$$

This evaluates to 0.8365 for $k_1 = m_2 = 1$ and increases with k_1 and decreases with m_2, approaching 0.8272 as $m_2 \to \infty$.

Returning to $\mathscr{S}_3$, we consider now when $\mathscr{S}_3$ is a single unfinished (B3) block with m_3 (B2) blocks of length 1. This gives $3m_3$ layers and hence $|\mathscr{S}_3| = 6m_3$. We compute

$$\frac{\mathscr{V}(\Theta^\star)}{6m_3v_3} = \begin{cases} \frac{2(v_I+v_{VI}+v_{VII})}{6v_3} = 0.8357, & m_3 = 1 \\ \frac{2(v_I+v_{VI}+(2m_3-1)v_{III}+(m_3-1)v_{VIII})}{6m_3v_3} = \frac{4.9632m+0.3728}{6m_3}, & m_3 \geq 2 \end{cases}$$

This evaluates to 0.8582 for $m_3 = 2$ and decreases with m_3, approaching 0.8272 as $m_3 \to \infty$.

For all of the above computations we have $0.8 \leq \mathscr{V}(\Theta_i^\star)/|\mathscr{S}_i|v_3$ for each $1 \leq i \leq 3$. Combining these subcomplexes together ensures that the inequality is true for $|\mathscr{T}|$. Note that we have omitted the case when $\mathscr{T}$ is a single (B3) block or a single unfinished (B3) block. Whilst this will reduce the ratios computed above, we still compute a value above 0.8 which decreases to 0.8272 as the number of (B2) blocks increases.

Finally, we consider when $\mathscr{T}$ decomposes as a single (B2) block of length k. We have $|\mathscr{T}| = 2(2k+1)$ and compute

$$\frac{\mathscr{V}(\Theta^{(B2)})}{2(2k+1)v_3} = \frac{2((2k-1)v_{III}+2v_{VII})}{2(2k+1)v_3} = \frac{3.6096k+1.162}{2(2k+1)}$$

This evaluates to 0.8381 for $k = 2$ and increases with k and satisfies our desired result. However, when $k = 1$ this evaluates to 0.7952. In this case we assign a different angle structure to the triangulation. We solve the angle equations, obtained from Figures 2.4 and 2.5a, by assigning

$$(II) \quad \Theta^{(1)} = \Theta^{(3)} = \left(\frac{\pi}{4}, \frac{5\pi}{12}, \frac{\pi}{3}\right) \quad \text{and} \quad \Theta^{(2)} = \left(\frac{2\pi}{3}, \frac{\pi}{6}, \frac{\pi}{6}\right)$$

The volume of the new shape here is computed as $\mathrm{Vol}(\Delta(2\pi/3, \pi/6, \pi/6)) = 0.6666v_3$. Hence we have,

$$\frac{\mathscr{V}(\Theta^\star)}{|\mathscr{T}|v_3} = \frac{2(0.9604)+0.6666}{3} = 0.8720$$

It follows that the Sakuma-Weeks triangulation of a 2-bridge link associated to the word $\Omega = RL^{a_1}\cdots(L^{a_n}R \mid R^{a_n}L)$ with $a_i \in \{1,2\}$ for all $1 \leq i \leq n$ satisfies $0.8|\mathscr{T}| \leq c(M) \leq |\mathscr{T}|$. □

The minimal volume for each subcomplex in the preceding proof occurs with a (B3) block containing m blocks of type (B2) of length one. This provides a linear relationship between m, the number of $a_i = 2$, and the gap between certifying minimality of the Sakuma-Weeks triangulation.

Corollary 2.21 *Let* $W = \{\Omega = RL^{a_1}\cdots(L^{a_n}R \mid R^{a_n}L) \mid a_i \in \{1,2\} \text{ for } 1 \leq i \leq n\}$ *and for each* $C \in \mathbb{N}$ *set*

$$W_C = \{\Omega \in W \mid a_1 + \cdots + a_n = n + C,\ n \in \mathbb{N}, n \geq C\}$$

For $\Omega \in W_C$ let $K = K(\Omega)$ be the associated 2-bridge link. Let $M = S^3\backslash K$ and $\mathscr{T} = \mathscr{T}(M)$ be the Sakuma-Weeks triangulation of M with $|\mathscr{T}| = 2(n+1+C)$. Let $c(M)$ denote the complexity of M. Then,

$$2n+1+(0.9632C+0.393) \leq c(M) \leq 2n+1+(2C+1)$$

Proof It follows from the proof of Theorem 2.20 that the only case we need to consider is when Ω decomposes as a single (B1) block of length $3C+1$. Let Φ^* denote the associated angle structure. The largest deficit is obtained when Ω decomposes as a single (B3) block of length $3C+1$ consisting of C (B2) blocks of length 1. Let Θ^* denote the associated angle structure. We compute the volume functional for Θ^* as

$$\mathscr{V}(\Theta^*) = 2\left(v_V + v_I + v_{VI} + (C-1)(2v_{III}+v_{VIII}) + v_{III} + v_{VIII}\right) \approx (4.9632C+3.3930)v_3$$

The largest deficit obtained from $\Omega \in W_C$ is then

$$\frac{\mathscr{V}(\Phi^\star) - \mathscr{V}(\Theta^\star)}{v_3} \approx \frac{2(2v_V+3Cv_3) - (4.9632C+3.3930)v_3}{v_3} \approx 1.0368C - 0.0598$$

This gives the lower bound on the complexity as,

$$\begin{aligned}\frac{\mathrm{Vol}(S^3\backslash K)}{v_3} \geq \frac{\mathscr{V}(\Theta^\star)}{v_3} &\geq \frac{\mathscr{V}(\Phi^\star)}{v_3} - (1.0369C - 0.0597) \\ &= 2\left(n+C-1+\frac{2v_V}{v_3}\right) - (1.0369C-0.0597) \\ &\geq 2n+1+(0.9632C+0.393)\end{aligned}$$

□

In Theorem 2.20 we have determined the complexity of infinitely many hyperbolic 2-bridge links up to a multiplicative constant of 0.8. In the proof of this theorem we have also certified that the Sakuma-Weeks triangulation of the complement of the 2-bridge link associated to $\Omega = RL^2R$ is minimal.

We now analyse when the general lower bound in Theorem 2.20 is better than that in Theorem 2.21. For this, consider a word $\Omega \in W_C$ giving $|\mathscr{T}| = 2(n+C+1)$. This gives us

$$\begin{aligned}2n+1+(0.9632C+0.393) &\leq 0.8|\mathscr{T}| \\ &\leq 1.6(n+C+1)\end{aligned}$$

and hence

$$C \geq 0.628n - 0.325 \tag{2.4.19}$$

We conclude that our additive bound is more suitable when C is small relative to n. This aligns with the fact that Theorem 2.21 is meant to provide the complexity of infinitely many 2-bridge link complements up to a fixed additive constant, only depending on the number C of syllables

of length two. Theorem 2.20, on the other hand, is meant to work in the general setting, where we can capitalise on the fact that syllables of length two must become adjacent once they are numerous enough.

2.4.4. Comparison using existing volume bounds. Lower bounds for volumes of alternating links have been established by Lackenby [**Lac04**] and refined by Agol, Storm and Thurston [**AST07**]. Work by Futer [**Gué06**, Appendix B] improves this lower bound multiplicatively, establishing $2v_3 n - 2.7066 < \mathrm{Vol}(S^3 \backslash K(\Omega))$ for all hyperbolic 2-bridge links constructed from a word Ω with n syllables. Petronio and Vesnin [**PV09**] prove a further refinement of this as

$$v_3 \cdot \max\{2, 2n - 2.6667\} \leq \mathrm{Vol}(S^3 \backslash K(\Omega))$$

To the best of the author's knowledge, this bound provides the best estimate of the volume for infinite families of hyperbolic 2-bridge links as

$$\max\{2, 2n - 2.6667\} \leq c(M)$$

In particular, this bound readily provides a lower bound for the complexity of $S^3 \backslash K(\Omega)$. We conclude this chapter by comparing our results to this lower bound on complexity.

For convenience we work in the setting of Theorem 2.21. Consider $\Omega \in W_C$ for $C \geq 0$ and let $\mathscr{T}$ be the Sakuma-Weeks triangulation of the complement of $K(\Omega)$. We write $|\mathscr{T}| = 2(n + C + 1)$. An immediate observation is that for all $n \geq 1$ and $0 \leq C \leq n$ we have

$$\max\{2, 2n - 2.6667\} \leq 2n + 1 + (0.9632C + 0.393)$$

That is to say incorporating the number of syllables and length of syllables in Theorem 2.21 provides a better lower bound on the complexity for the 2–bridge links we are considering.

We compare the lower bound in Theorem 2.20 in two cases. First, if $n = 1, 2$ then the Petronio-Vesnin bound gives $2 \leq c(M)$. The smallest triangulation we consider occurs when $n = 1$ and $C = 0$ with $0.8|\mathscr{T}| = 3.2$. Hence our lower bound is better in this case. For $n \geq 3$ we consider $2n - 2.6667 \leq 0.8|\mathscr{T}|$. This is satisfied when

$$C \geq 0.25n - 2.6666$$

Again, we can see that the bound from Theorem 2.20 works better in the case of C being sufficiently large, with the case of relatively small C covered by the bound from Theorem 2.21.

CHAPTER 3

The anatomy of minimal triangulations via the $\mathbb{Z}_2$–Thurston norm

Commencing in 2009, a series of papers by Jaco, Rubinstein, Spreer, and Tillmann [**JRT09**, **JRT13**, **JRST20a**, **JRST20b**, **JRST25**] develops a theory of minimal triangulations via a $\mathbb{Z}_2$ analogue of Thurston's norm on homology [**Thu86**]. This framework has been used to classify several infinite families of minimal triangulations of 3–manifolds, both material and ideal. In this chapter, we build on this framework in the setting of closed, orientable, irreducible, connected 3–manifolds.

Our main contribution to this theory is the following technical result:

Theorem 3.1 *Let M be a closed, orientable, irreducible, connected 3–manifold with minimal triangulation $\mathscr{T}$. Suppose that all edge loops are coloured by the rank–2 subgroup H of $H^1(M;\mathbb{Z}_2)$, $\mathscr{T}$ is $(\Delta_{qq},4)$–free with respect to the colouring and that $|\mathscr{T}| = (2+k) + \sum_{\varphi\in H}\|\varphi\|$. Letting $\mathfrak{e}_d$ denote the number of H–even edges of degree d, we have:*

$$\mathfrak{e}_3 \leq k + 2\sum_{i=1}^{3} d_{\varphi_i} + \sum_{d=5}^{\infty}(d-4)\mathfrak{e}_d. \tag{3.0.1}$$

Providing a concrete bound for the number of degree 3 edges present in a rank–2 coloured minimal triangulations plays a central role in this work. A bound under the additional assumption that M is atoroidal was established by Jaco, Rubinstein, and Tillmann [**JRT13**]. As we demonstrate in Section 3.3.3, dropping this assumption requires a drastically finer analysis.

Using this result, we provide the following corollary.

Corollary 3.2 *Let M be a closed, orientable, irreducible, connected 3–manifold with minimal triangulation $\mathscr{T}$. Suppose that all edge loops are coloured by the rank–2 subgroup H of $H^1(M;\mathbb{Z}_2)$ and that $\mathscr{T}$ is $(\Delta_{qq},4)$–free with respect to the colouring with $|\mathscr{T}| = (2+k) + \sum_{i=1}^{3}\|\varphi_i\|$. Then $n_{tt} + n_{qtt} \leq 3k$.*

This bound provides the main tool for determining the types of tetrahedra present in a rank–2 coloured minimal triangulation. In particular, we use this to provide a complete list of profiles when $k = 1$.

Using this theory, we characterise central subcomplexes in minimal rank–2 coloured triangulations in which $k = 1$ and classify two new infinite families of 3–manifolds achieving such a complexity.

The chapter is organised as follows. In Sections 3.1 and 3.2 we provide the background for the new results. We omit all proofs in Section 3.1 and only include those in Section 3.2 which offer insight into the techniques used to carry out our analysis. Section 3.3 marks the start of our contribution to this theory. In this section, we provide the proofs to Theorem 3.1 and Corollary 3.2. We turn our attention to the aforementioned case of $k = 1$ in Section 3.4 and analyse the anatomy of minimal triangulations satisfying this assumption. We conclude the chapter with Section 3.5 in which we classify two new infinite families of minimal triangulations.

3.1. Preliminaries

The main results used throughout this chapter concern 0–efficient triangulations (see Theorem 1.15) and layered solid tori (see Definition 3.3). In this section we summarise the definitions and results from [**JR03**, **JRT09**, **JRT13**] used to carry out the new proofs. Unless otherwise stated, we assume M is a closed, orientable, irreducible, connected 3–manifold.

3.1.1. Intersections of maximal layered solid tori. Throughout our analysis, we will be interested in the subcomplexes contained within a triangulation $\mathscr{T}$. Of the possible subcomplexes that arise, our focus will often be on those which are combinatorially equivalent to a layered solid torus.

Definition 3.3 A **layered solid torus with respect to** $\mathscr{T}$ is a subcomplex $\mathbf{T}$ of $\mathscr{T}$ which is combinatorially equivalent to a layered solid torus $\mathrm{LST}(p,q,p+q)$ where p and q are positive, co-prime integers. The boundary of $\mathbf{T}$ is a triangulation of the torus with two triangles. If an edge e is in the boundary of $\mathbf{T}$, then we refer to it as a **boundary edge** of $\mathbf{T}$, otherwise we refer to it as an **interior edge** of $\mathbf{T}$. ◇

It is sometimes useful to distinguish between the degree of an edge e with respect to the triangulation and the degree of e with respect to a layered solid torus subcomplex $\mathbf{T}$. We refer to the former as the M–degree of e, denoted $\deg(e)$, and the latter as the $\mathbf{T}$–degree of e, denoted $\deg_{\mathbf{T}}(e)$, as needed. From this definition, the $\mathbf{T}$–degree of any edge not contained in $\mathbf{T}$ is 0 and the M–degree agrees with the $\mathbf{T}$–degree for any interior edge of $\mathbf{T}$. The unique boundary edge of $\mathbf{T}$ with $\mathbf{T}$–degree equal to one is the **unital edge**.

Definition 3.4 A layered solid torus $\mathbf{T}$ with respect to $\mathscr{T}$ is **maximal** if there is no other layered solid torus $\mathbf{T}'$ with respect to $\mathscr{T}$ such that $\mathbf{T} \subset \mathbf{T}'$. ◇

Often times there may be more than one maximal layered solid torus in a minimal triangulation of M. Their intersections, however, are small.

Lemma 3.5 [JR03, JRT09] *Assume that the triangulation $\mathscr{T}$ is minimal and 0–efficient. If M is not a lens space with layered triangulation, then the intersection of two distinct maximal layered solid tori in M consists of at most a single edge.*

Lemma 3.6 [JR03, JRT09] *Assume that the triangulation $\mathscr{T}$ is minimal and 0–efficient and suppose that M contains a layered solid torus $\mathbf{T}$ made up of at least two tetrahedra and having boundary edge e of M–degree 4. Then either*

(i) $\mathbf{T}$ *is not a maximal layered solid torus in M; or*

(ii) e *is the unital edge for* $\mathbf{T}$ *and it is contained in four pairwise distinct tetrahedra in M; or*

(iii) M *is a lens space with minimal triangulation.*

3.1.2. Edges of low degree in minimal triangulations. Let M be a closed 3–manifold with one–vertex triangulation $\mathscr{T}$. Let $E = |\mathscr{T}^{(1)}|$ denote the number of edges in $\mathscr{T}$ and E_d the number of edges of degree d. As M is closed, $\chi(M) = 0$ and, as $\mathscr{T}$ has a single vertex, $|\mathscr{T}| = E - 1$. Since $E = \sum_{d=1}^{\infty} E_d$ we observe

$$\sum_{d=1}^{\infty} dE_d = 6|\mathscr{T}| = 6(E-1) = 6\sum_{d=1}^{\infty} E_d - 6$$

and hence obtain $6 = \sum_{d=1}^{\infty}(6-d)E_d$. It follows that $\mathscr{T}$ must have at least two edges of degrees at most five. The following two lemmas strengthen this observation.

Lemma 3.7 (Edges of degree 1 or 2, [JR03, JRT09]) *A minimal and 0–efficient triangulation $\mathscr{T}$ of the closed, orientable, irreducible, connected 3–manifold M has:*

(i) no edge of degree 1 unless $M = S^3$; and

(ii) no edge of degree 2 unless $M = L(3,1)$ or $L(4,1)$.

Lemma 3.8 (Edges of degree 3, [JR03, JRT09]) *A minimal and 0–efficient triangulation $\mathscr{T}$ of the closed, orientable, irreducible, connected 3–manifold M has no edge of degree 3 unless either:*

(3a) $\mathscr{T}$ contains a single tetrahedron and $M = L(5,2)$; or

(3b) $\mathscr{T}$ contains two tetrahedra and $M = L(5,1)$ or $L(7,2)$; or

(3c) $\mathscr{T}$ contains a two tetrahedron subcomplex combinatorially equivalent to the layered solid torus $\mathrm{LST}(1,3,4)$. Moreover, $\mathscr{T}$ contains at least three tetrahedra and every edge of degree 3 is contained in such a subcomplex.

3.1.3. Neighbourhoods of low degree edges. Jaco, Rubinstein, and Tillmann completely describe the maximal complexes containing degree 4 and degree 5 edges in minimal and 0–efficient triangulations of closed orientable 3–manifolds [**JRT09**]. Together with Lemmas 3.7 and 3.8, this provides a complete classification of the neighbourhoods of low degree edges.

Let M be a closed, orientable, irreducible, connected 3–manifold with minimal and 0–efficient triangulation $\mathscr{T} = (\widetilde{\Delta}, \Phi, p)$. Suppose $\overline{e}$ is a degree d edge contained in k pairwise distinct simplices $\sigma_1, \dots, \sigma_k \in \widetilde{\Delta}$, with $1 \leq k \leq n$. There exists triangulated complex $X = X_{d;k}$ consisting of k tetrahedra with an interior edge e of degree d, and a well defined map $p_e : X \to M$ with $p_e(e) = \overline{(e)}$ such that the restriction of p to $\{\sigma_1, \dots, \sigma_k\}$ factors through X. The complex X is **maximal** if there is no other complex X' such that this restriction of p first factors through X'. If $X_{d;k}$ is maximal, then we say that $(X_{d;k}, e)$ is a **model** for $\overline{e}$.

Theorem 3.9 [**JRT09**, Proposition 10] *Let M be a closed, orientable, irreducible, connected 3–manifold with minimal triangulation $\mathscr{T}$ containing a degree 4 edge $\overline{e}$. The model $(X_{4;k}, e)$ for $\overline{e}$ is one of the following.*

(i) If $j = 1$, then $X_{4;1} \cong S^3$ or $L(4,1)$. In each case we have $\mathscr{T} = X_{4;1}$ and $M = S^3$ or $L(4,1)$. See Figures 3.1a and 3.1b, respectively.

(ii) If $j = 2$, then $X_{4;2} \cong L(8,3)$, S^3/Q_8, or $\mathrm{LST}(2,3,5)$. When $X_{4;2} \cong L(8,3)$ it is a two tetrahedron triangulation of $L(8,3)$ where e is the unique edge having degree 2 with respect to each tetrahedron and $M = L(8,3)$. When $X_{4;2} \cong S^3/Q_8$ it is a two tetrahedron triangulation of the generalised quarternionic space S_3/Q_8 where e is any of its three degree 4 edges and $M = S^3/Q_8$. When $X_{4;2} \cong \mathrm{LST}(2,3,5)$ is a two tetrahedron layered solid torus where e is the base edge. See Figures 3.1c to 3.1e, respectively.

(iii) If $j = 3$, then $X_{4;3}$ is one of two solid tori. The first is formed by attaching two tetrahedra to the boundary faces of the layered solid torus $\mathrm{LST}(1,2,3)$ so that the degree 2 boundary edge becomes an interior edge e of degree 4. The second is formed by first identifying a pair of opposite edges of a tetrahedron and then layering two tetrahedra along the resulting degree 2 edge making it an interior edge e of degree 4. See Figures 3.1f and 3.1g, respectively.

(iv) If $j = 4$, then $X_{4;4}$ is an octahedron consisting of four tetrahedra glued around a common edge e. See Figure 3.1h.

Theorem 3.10 [**JRT09**, Proposition 11] *Let M be a closed, orientable, irreducible, connected 3–manifold with minimal triangulation $\mathscr{T}$ containing a degree 5 edge $\overline{e}$. The model $(X_{5;k}, e)$ for $\overline{e}$ is one of the following.*

(i) If $j = 1$, then $X_{5;1}$ is a one tetrahedron triangulation of S^3 and $M = S^3$. See Figure 3.2a.

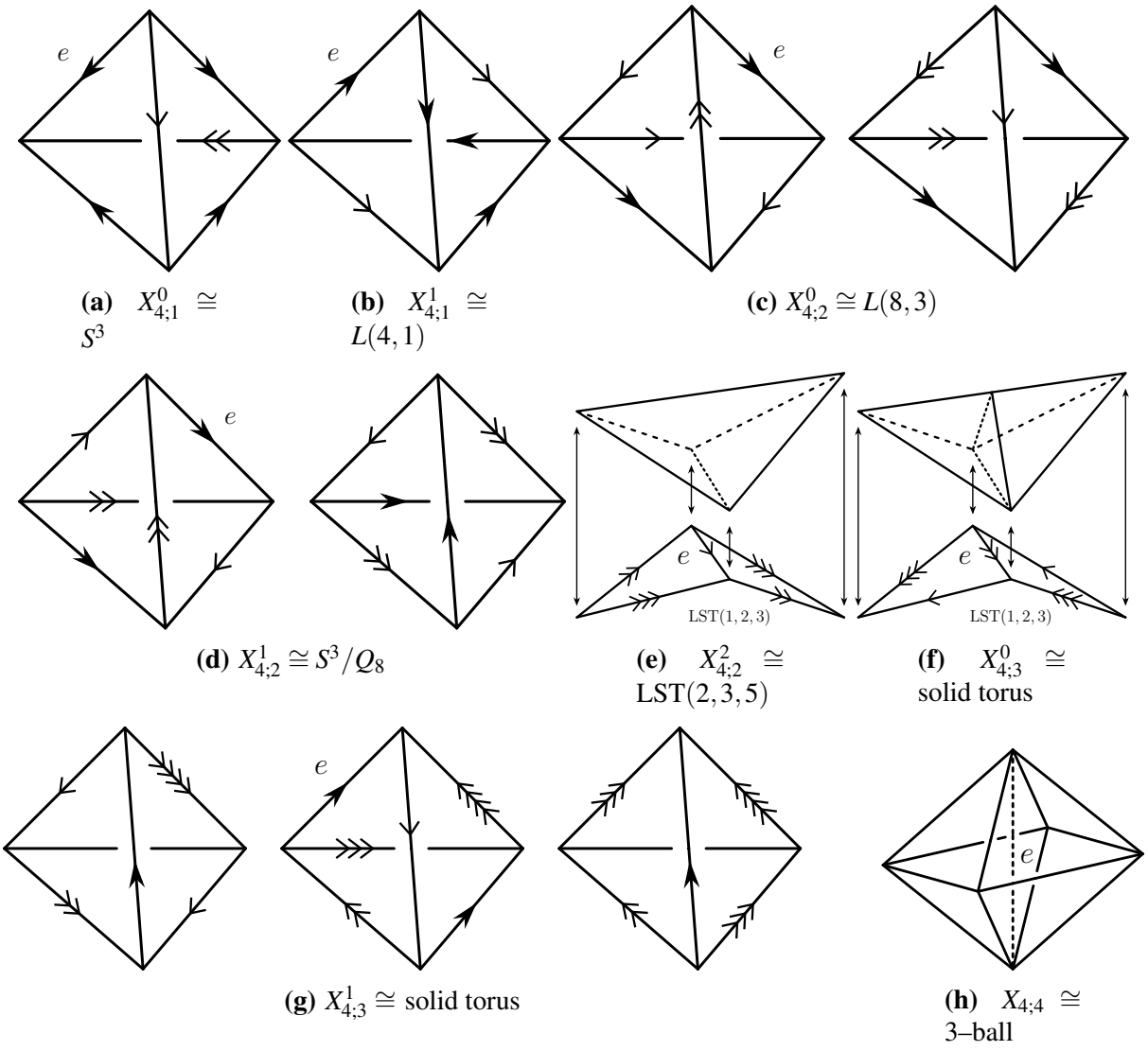

(a) $X^0_{4;1} \cong S^3$

(b) $X^1_{4;1} \cong L(4,1)$

(c) $X^0_{4;2} \cong L(8,3)$

(d) $X^1_{4;2} \cong S^3/Q_8$

(e) $X^2_{4;2} \cong \mathrm{LST}(2,3,5)$

(f) $X^0_{4;3} \cong$ solid torus

(g) $X^1_{4;3} \cong$ solid torus

(h) $X_{4;4} \cong$ 3–ball

FIGURE 3.1. The models $(X_{4;k}, e)$ for the degree 4 edge $\bar{e}$ in the closed, orientable, irreducible 3–manifold M. Edges in layered solid tori are marked to correspond with the edges in Figure 1.7.

(ii) *If $j = 2$, then $X_{5;2} \cong L(3,1)$ or $L(7,2)$. When $X_{5;2} \cong L(3,1)$ it is a two tetrahedron triangulation of $L(3,1)$ where e is either of the two degree 5 edges and $M = L(3,1)$. When $X_{5;2} \cong L(7,2)$ it is a two tetrahedron triangulation of $L(7,2)$ where e is the unique degree 5 edge and $M = L(7,2)$. See Figures 3.2b and 3.2c, respectively.*

(iii) *If $j = 3$, then $X_{5;3}$ is one of three solid tori. The first is formed by layering a tetrahedron along the unique degree 4 boundary edge of $\mathrm{LST}(2,3,5)$ resulting in an interior edge e of degree 5 and $X_{5;3} \cong \mathrm{LST}(3,5,8)$. The second is formed by attaching two tetrahedra to the boundary faces of $\mathrm{LST}(1,2,3)$ so that the degree 3 boundary edge becomes an interior edge e of degree 5. The third is formed by identifying two boundary squares of a three tetrahedron triangular prism resulting in a unique interior edge e of degree 5. See Figures 3.2d to 3.2f, respectively.*

(iv) If $j=4$, then $X_{5;4}$ is one of two solid tori. The first is formed by attaching three tetrahedra to the boundary faces of $\mathrm{LST}(1,2,3)$ so that the degree 2 boundary edge becomes an interior edge e of degree 5. The second is formed by identifying a pair of opposite edges of a tetrahedron, then layered one tetrahedron along this edge, and then attaching two tetrahedra to the remaining boundary faces to create a unique interior edge of degree 5. See Figures 3.2g and 3.2h.

(v) If $j=5$, then $X_{5;5}$ is a triangulated 3 ball with five tetrahedra such that their common intersection is a unique interior edge e of degree 5. See Figure 3.2i.

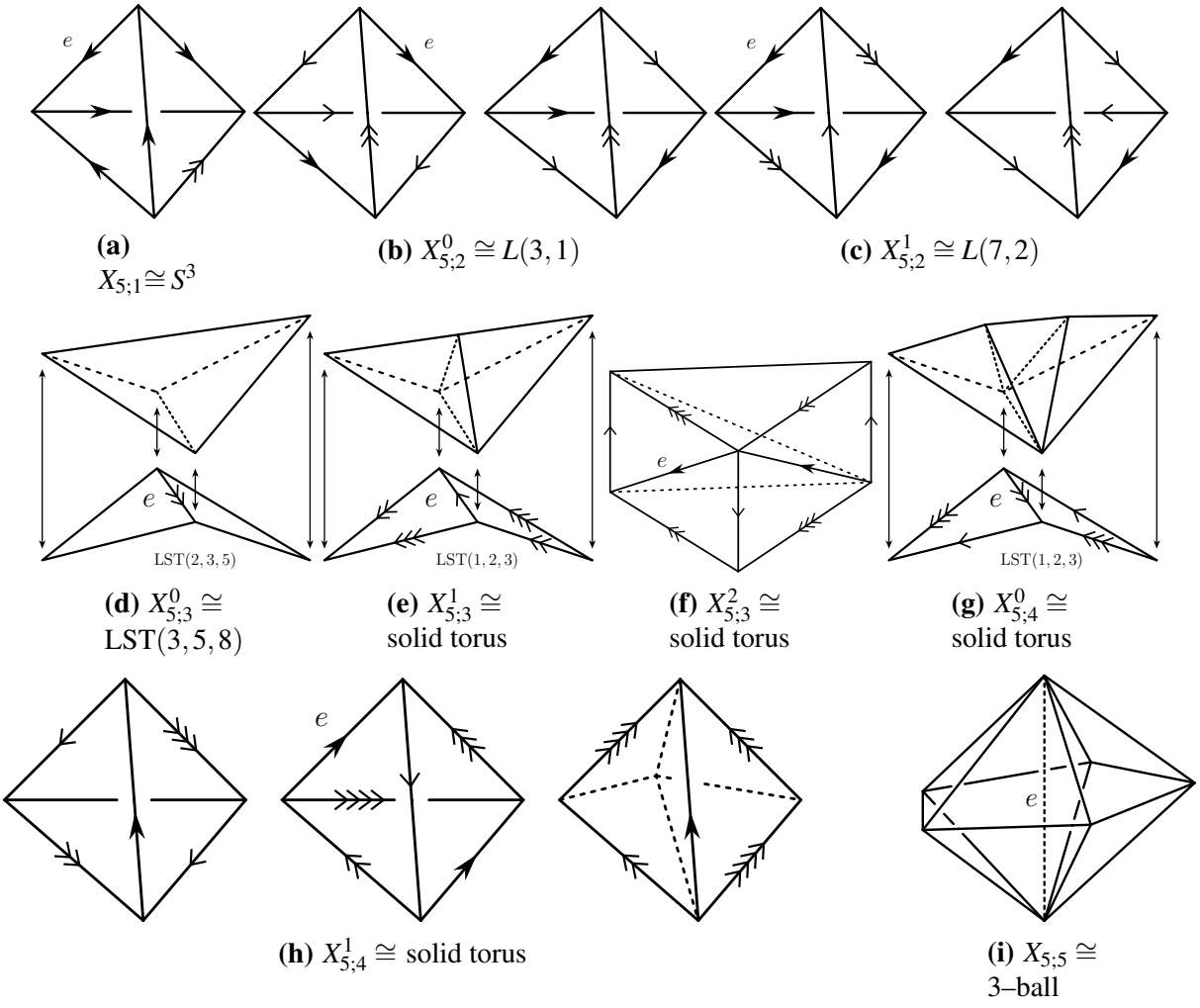

(a) $X_{5;1} \cong S^3$ **(b)** $X^0_{5;2} \cong L(3,1)$ **(c)** $X^1_{5;2} \cong L(7,2)$

(d) $X^0_{5;3} \cong \mathrm{LST}(3,5,8)$ **(e)** $X^1_{5;3} \cong$ solid torus **(f)** $X^2_{5;3} \cong$ solid torus **(g)** $X^0_{5;4} \cong$ solid torus

(h) $X^1_{5;4} \cong$ solid torus **(i)** $X_{5;5} \cong$ 3–ball

FIGURE 3.2. The models $(X_{5;k}, e)$ for the degree 5 edge $\bar{e}$ in the closed, orientable, irreducible 3–manifold M. Edges in layered solid tori are marked to correspond with the edges in Figure 1.7.

3.1.4. The Q–matching equations. Recall that a properly embedded surface S in $\mathscr{T}$ is a **normal surface** if the intersection of S with any tetrahedron is comprised of a collection of pairwise disjoint triangles and quadrilaterals as depicted in Figure 1.5. A normal surface contains finitely many quadrilateral discs which determine the surface uniquely, up to normal isotopy. A

normal isotopy of M is an isotopy which preserves the triangulation. This sets up an algebraic framework for normal surfaces as follows. Note that equivalent algebraic frameworks for more restricted classes of 3–manifolds have been established by, for example, Tollefson [**Tol98**].

Let $\square$ denote the set of normal isotopy classes of normal quadrilaterals in $\mathscr{T}$. As $|\mathscr{T}| = t$ it follows that $|\square| = 3t$, where each class is a **quadrilateral type**. Identifying $\mathbb{R}^{\square}$ with $\mathbb{R}^{3t}$, the **normal Q–coordinate** of a normal surface S is the integer vector $x(S) = (x_1, \ldots, x_{3t}) \in \mathbb{R}^{3t}$, where x_i records the number of normal quadrilaterals in S of type q_i. For simplicity, we assume q_{3i-2}, q_{3i-1}, and q_{3i} are the three normal quadrilateral types in the i-th tetrahedron.

The normal Q–coordinate satisfies two algebraic conditions. First, $x(S)$ is admissible. A vector $x \in \mathbb{R}^{3t}$ is **admissible** if $x_i \geq 0$ for all $1 \leq i \leq 3t$ and, for each $1 \leq j \leq t$, at most one of x_{3j-2}, x_{3j-1}, and x_{3j} is non-zero. This is to say that the intersection of S and a tetrahedron Δ contains at most one normal quadrilateral type.

Second, $x(S)$ satisfies a linear equation for each edge e in $\mathscr{T}$ called a **Q–matching equation**. Intuitively, these equations state that as one circumnavigates the globe the number of times the equator is crossed from north to south must equal the number of times the equator is crossed from south to north. We give a more precise, but brief definition of these equations below and direct the reader to [**Til08**, Sections 2.3–2.9] for more details.

Assume M is oriented and all tetrahedra in $\mathscr{T}$ are given the induced orientation. Let e be a degree d edge in $\mathscr{T}$ and define $\widetilde{B(e)}$ to be the collection of all tetrahedra incident with e up to multiplicity. That is, if a tetrahedron meets e a total of k times, then we include k copies of this tetrahedron in $\widetilde{B(e)}$. The **abstract neighbourhood** $B(e)$ of e is a triangulated 3–ball formed by pairwise identifying the faces of tetrahedra in $\widetilde{B(e)}$ such that there is a well defined quotient map $p_e : B(e) \to \widetilde{\Delta}/\Phi$ taking $B(e)$ to a neighbourhood of e in $\mathscr{T}$. This is illustrated in Figure 3.3a.

Following the circumnavigation analogy, we refer to the endpoints of the edge e as the **poles** of $\partial B(e)$ and to the edges disjoint from the poles as the **equatorial edges**.

Let Δ be a tetrahedron in $\widetilde{B(e)}$ and q a normal quadrilateral in Δ. The boundary of q has a vertex on e if and only if it has a vertex on an equatorial edge of $\partial B(e)$. The boundary of such a quadrilateral has an induced orientation from Δ and thus a slope of ± 1, where the sign is well–defined and independent of the orientation of e. Figure 3.3b illustrates quadrilaterals with **negative** and **positive slopes**.

For a quadrilateral type $q_i \in \square$, define the **weight** of q_i at e, $\mathrm{wt}_e(q_i)$, to be the sum of all the slopes of q_i in $B(e)$. By taking the sum we account for instances where q_i has multiple vertices on e. If q_i has no vertices on e, then we set $\mathrm{wt}_e(q) = 0$.

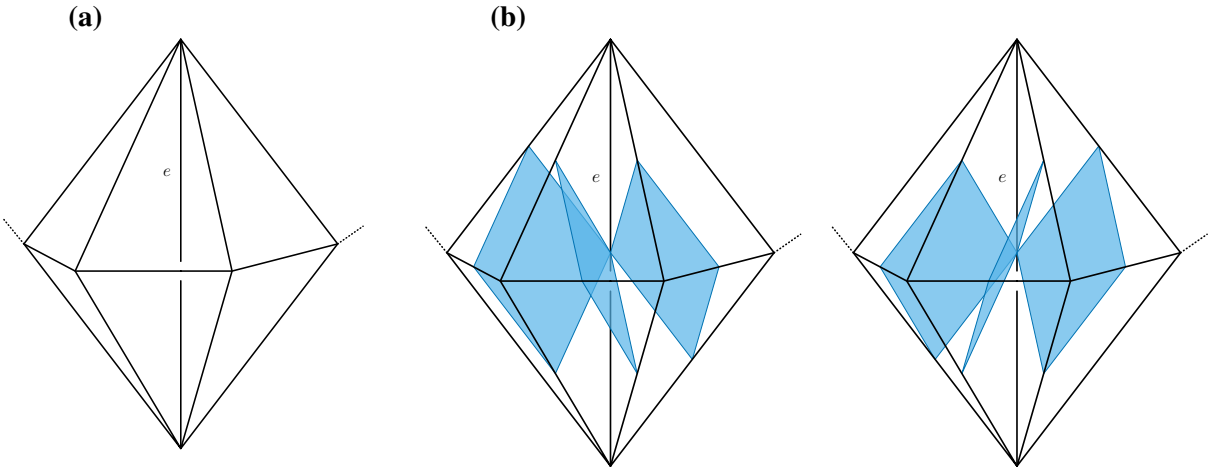

FIGURE 3.3. (a) The abstract neighbourhood $B(e)$ of the edge e. (b) Normal quadrilaterals of negative slope (left) and positive slope (right) in the abstract neighbourhood $B(e)$.

For a normal surface S in $\mathscr{T}$ with normal Q–coordinate $x(S)$, the **Q–matching equation** for e is defined as

$$0 = \sum_{i=1}^{3t} \mathrm{wt}_e(q_i)x_i$$

3.2. Rank–1 and –2 colourings of minimal triangulations and the $\mathbb{Z}_2$–Thurston norm

We now present a definition of the $\mathbb{Z}_2$–Thurston norm together with the key theorem statements from [**JRST20b**, **Nak17**]. Given these, we describe rank–1 and rank–2 colourings of minimal triangulations together with their combinatorics. We assume throughout that M is a closed, orientable, irreducible, connected 3–manifold different from $\mathbb{R}P^3$ unless otherwise stated.

Definition 3.11 [**JRT13**, **JRST20b**] Let M be a closed, orientable, irreducible, connected 3–manifold and let S be a closed, embedded surface dual to a given $\varphi \in H^1(M;\mathbb{Z}_2)$. If S is connected, let $\chi_- = \max\{0, -\chi(S)\}$ and otherwise let

$$\chi_-(S) = \sum_{S_i \subset S} \max\{0, -\chi(S_i)\}$$

where the sum is taken over the connected components of S, noting that S_i may not be orientable. The **$\mathbb{Z}_2$–Thurston norm** of φ is defined as

$$\|\varphi\| = \min\{\chi_-(S) \mid S \text{ dual to } \varphi\}$$

The surface S dual to $\varphi \in H^1(M;\mathbb{Z}_2)$ is said to be **$\mathbb{Z}_2$–taut** if no component of S is a sphere or a projective plane and $\chi(S) = -\|\varphi\|$. As observed in [Thu86] after possibly deleting compressible tori, every component of a $\mathbb{Z}_2$–taut surface is non-separating and geometrically incompressible. ◇

Each of the two theorems bounding the complexity were proven by Jaco, Rubinstein, Spreer, and Tillmann [JRT13, JRST20b] and, independently, Nakamura [Nak17]. The first theorem establishes a connection between the complexity of M and the $\mathbb{Z}_2$–Thurston norm for any non-trivial class $\varphi \in H^1(M;\mathbb{Z}_2)$. In particular, this provides a lower bound on the complexity of any such 3–manifold M with non-trivial $H^1(M;\mathbb{Z}_2)$.

Theorem 3.12 [JRST20b, Theorem 1] *Let M be a closed, orientable, irreducible, connected 3–manifold not homeomorphic with $\mathbb{R}P^3$, and suppose that $0 \neq \varphi \in H^1(M;\mathbb{Z}_2)$. Then*

$$c(M) \geq 1 + 2\|\varphi\|$$

Moreover, if equality holds, then M is a balanced lens space[*]*.*

When the rank of $H^1(M;\mathbb{Z}_2)$ is at least 2, we are able to present a finer analysis of a minimal triangulation by considering the interactions between multiple $H^1(M;\mathbb{Z}_2)$ classes.

Theorem 3.13 [JRST20b, Theorem 3] *Let M be a closed, orientable, irreducible, connected 3–manifold with the property that $H^1(M;\mathbb{Z}_2)$ has rank at least two. Then, for any rank two subgroup $H \leq H^1(M;\mathbb{Z}_2)$*

$$c(M) \geq 2 + \sum_{0 \neq \varphi \in H} \|\varphi\|$$

Moreover, if $H^1(M;\mathbb{Z}_2)$ has rank 2 and this is and equality, then M is a generalised quaternionic space[†]*.*

3.2.1. Rank–1 colourings and dual normal surfaces. Let M be a closed, orientable, connected 3–manifold with arbitrary one–vertex triangulation $\mathscr{T}$. For each edge $e \in \mathscr{T}^{(1)}$ we fix an orientation to obtain a representative of $[e] \in \pi_1(M)$. Consider an element $\varphi \in H^1(M;\mathbb{Z}_2)$ as a nontrivial homomorphism $\varphi : \pi_1(M) \to \mathbb{Z}_2$. If $\varphi[e] = 0$, then we say that e is **φ–even**; if $\varphi[e] = 1$, then we say that e is **φ–odd**. This construction and terminology is independent of the orientation of e.

As $\varphi \in H^1(M;\mathbb{Z}_2)$, it follows that φ partitions the tetrahedra of $\mathscr{T}$ into three distinct types:

Type $\Delta_\emptyset$: All edges of the tetrahedron are φ–even;

[*]Using the terminology in Section 3.2.1, a lens space is balanced if the number of φ–even edges equals the number of φ–odd edges in a minimal layered triangulation.

[†]The generalised quarternionic spaces S^3/Q_{4k} are the Seifert fibred spaces over S^2 with three exception fibres $S^2((2,1),(2,1)(k,-k+1))$. See [JRT11] for more details.

Type Δ_t: The three edges bounding a face of the tetrahedron are φ–even and the remaining edges are φ–odd; and

Type Δ_q: A pair of opposite edges of the tetrahedron are φ–even and the remaining edges are φ–odd.

Such a partition of the tetrahedra in $\mathscr{T}$ is termed a **rank–1 colouring by φ**. This colouring provides a natural way to construct a normal surface S_φ dual to the colouring. Such a surface is guaranteed to exist by Poincaré duality and is termed **the canonical normal surface dual to φ**. We construct this surface as follows. In each tetrahedron of type Δ_t we place a normal triangle with a single vertex on each φ–odd edge. In each tetrahedron of type Δ_q we place a normal quadrilateral with a single vertex on each φ–odd edge. The types of tetrahedra and their associated normal discs are shown in Figure 3.4.

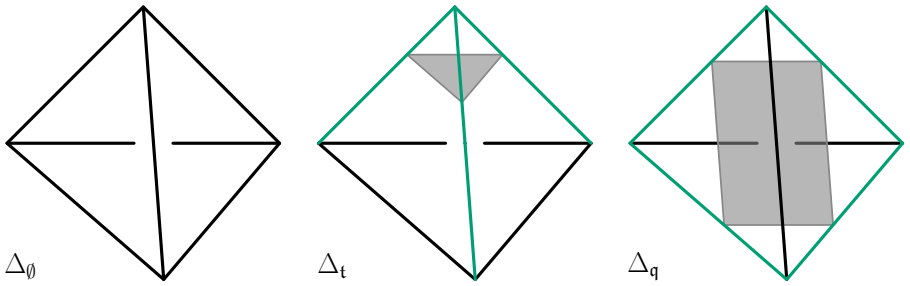

FIGURE 3.4. Rank–1 colouring by $0 \neq \varphi \in H^1(M;\mathbb{Z}_2)$ and dual normal discs.

Lemma 3.14 ([JRT13], Lemma 1) *Let M be a closed, orientable, irreducible, connected 3–manifold with one–vertex triangulation $\mathscr{T}$ and $0 \neq \varphi \in H^1(M;\mathbb{Z}_2)$. Then*

$$\|\varphi\| \leq -\chi(S_\varphi)$$

unless $M = \mathbb{R}P^3$.

3.2.2. Rank–2 colourings and dual normal surfaces. The construction of a rank–1 coloured one–vertex triangulations naturally extends to colourings by subgroups of $H^1(M;\mathbb{Z}_2)$ of arbitrary rank. We are concerned with colourings by a rank–2 subgroup.

Let $\varphi_1, \varphi_2 \in H^1(M;\mathbb{Z}_2)$ with nontrivial $\varphi_3 = \varphi_1 + \varphi_2$ and consider $\langle \varphi_1, \varphi_2 \rangle = H \leq H^1(M;\mathbb{Z}_2)$. It follows that $H \cong \mathbb{Z}_2 \oplus \mathbb{Z}_2$. Each φ_i, $1 \leq i \leq 3$, gives a rank–1 colouring of $\mathscr{T}$ and a canonical surface S_{φ_i} dual to φ_i. These three rank–1 colourings partition the edges of $\mathscr{T}$ into the following classes:

- e is **H–even** if $\varphi_i[e] = 0$ for all $1 \leq i \leq 3$; and
- e if **i–even** if $\varphi_i[e] = 0$ for a unique $1 \leq i \leq 3$.

An edge e is φ_i–even if it is i–even or H–even; we still refer to an edge as φ_i–odd if $\varphi_i[e] = 1$. To determine the partition of tetrahedra in $\mathscr{T}$ we consider the possible assignment of H–even and φ_i–even edges for a single tetrahedron. Let $\{e, e', e''\}$ be the three edges bounding a face of a tetrahedron Δ. For each $1 \leq i \leq 3$ it must hold that $\varphi_i[e] + \varphi_i[e'] + \varphi_i[e''] = 0$ as $\varphi_i \in H^1(M; \mathbb{Z}_2)$. This allows us to characterise the possible colourings of the edges bounding a face of a tetrahedron.

Let $(i, j, k) = (1, 2, 3)$. The possible colourings of the three edges bounding a face of a tetrahedron in $\mathscr{T}$ are: all three edges are H–even; two edges are φ_i–even and the third is H–even; two edges are φ_j–even and the third is H–even; two edges are φ_k–even and the third is H–even; or one edge is φ_i–even, one edge is φ_j–even, and one edge is φ_k even. Piecing these possible colourings together over the four faces of each **oriented** tetrahedron in $\mathscr{T}$ partitions the tetrahedra into five distinct types:

Type $\Delta_\emptyset$: All edges of the tetrahedron are H–even;

Type Δ_{tt}: The three edges bounding a face of the tetrahedron are H–even and the remaining edges are i–even (there are three distinct subtypes);

Type Δ_{qtt}: One edge e is H–even and the edge opposite e is k–even. The remaining two edges of one face incident with e are i–even and the remaining two edges of the other face incident with e are j–even (there are six distinct subtypes);

Type Δ_{qq}: One pair of opposite edges is H–even and the remaining edges are i–even (there are three distinct subtypes); and

Type Δ_{qqq}: One pair of opposite edges is i–even, one pair of opposite edges is j–even, and one pair of opposite edges is k–even (there are two distinct subtypes).

When two or more tetrahedra belong to the same distinct subtype we say that they are **coloured the same**.

The canonical surface S_i dual to φ_i is constructed by placing a single vertex on each j–even edge and k–even edge followed by placing the appropriate normal disc in each tetrahedron. The types of rank–2 coloured tetrahedra and their associated normal discs are shown in Figure 3.5.

The existence of a rank–2 colouring of the edges of $\mathscr{T}$ allows all layered solid tori with respect to $\mathscr{T}$ to be partitioned, broadly, into two families.

Lemma 3.15 ([JRT13], Lemma 7) *Let $\mathscr{T}$ be a one–vertex triangulation of a closed, orientable, connected 3–manifold M whose edges are coloured by a rank–2 subgroup H of $H^1(M; \mathbb{Z}_2)$. Then all tetrahedra in a layered solid torus $\mathbf{T}$ with respect to $\mathscr{T}$ are of type $\Delta_\emptyset$ or Δ_{qq}, but not both.*

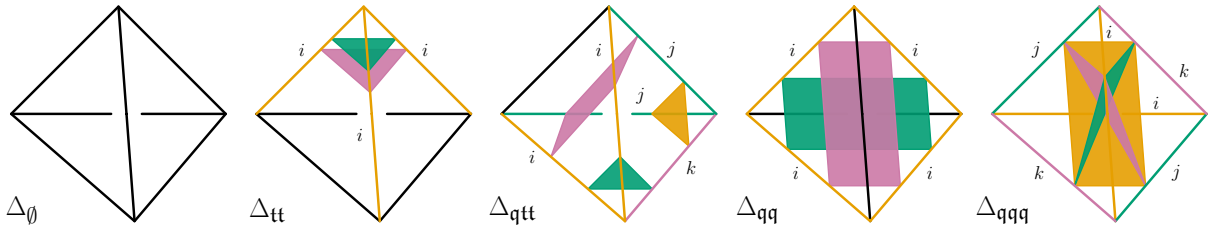

FIGURE 3.5. Rank–2 colouring by $\mathbb{Z}_2 \oplus \mathbb{Z}_2 \cong H \leq H^1(M;\mathbb{Z}_2)$ and dual normal discs. The i–even (resp. j–even and k–even) edges are coloured and indicated with the appropriate letter for $(i,j,k) = (1,2,3)$.

Proof Any layered solid torus $\mathbf{T}$ contains, as an embedded subcomplex, the one tetrahedron layered solid torus $\mathrm{LST}(1,2,3)$. This contains a degree 3 edge which does not bound a face and hence must be of type $\Delta_\emptyset$ or Δ_{qq}. It follows from the layering procedure that the type of each subsequent tetrahedron must match that of the initial tetrahedron. □

Definition 3.16 Let $\mathscr{T}$ be a one–vertex triangulation of a closed, orientable, connected 3–manifold M whose edges are coloured by a rank–2 subgroup H of $H^1(M;\mathbb{Z}_2)$. A layered solid torus $\mathbf{T}$ with respect to $\mathscr{T}$ is of type $\Delta_\emptyset$ (respectively Δ_{qq}) if all tetrahedra in $\mathbf{T}$ are of type $\Delta_\emptyset$ (respectively Δ_{qq}). ◇

3.2.3. Combinatorics of rank–2 coloured minimal triangulations. Let M be a closed, orientable, irreducible, connected 3–manifold with one–vertex minimal triangulation $\mathscr{T}$ whose edge loops are coloured by the rank–2 subgroup $H \leq H^1(M;\mathbb{Z}_2)$. Using the setup and notation of the previous section we let:

$n_\emptyset(\mathscr{T}) =$ the number of tetrahedra of type $\Delta_\emptyset$,
$n_{tt}(\mathscr{T}) =$ the number of tetrahedra of type Δ_{tt},
$n_{qtt}(\mathscr{T}) =$ the number of tetrahedra of type Δ_{qtt},
$n_{qq}(\mathscr{T}) =$ the number of tetrahedra of type Δ_{qq},
$n_{qqq}(\mathscr{T}) =$ the number of tetrahedra of type Δ_{qqq},
$\mathfrak{e}(\mathscr{T}) =$ the number of H–even edges,
$\mathfrak{e}_d(\mathscr{T}) =$ the number of H–even edges of degree d,
$\widetilde{\mathfrak{e}}(\mathscr{T}) =$ the number of pre-images of H–even edges in $\widetilde{\Delta}$.

The number of tetrahedra in $\mathscr{T}$ can be expressed as

$$|\mathscr{T}| = n_\emptyset(\mathscr{T}) + n_{tt}(\mathscr{T}) + n_{qtt}(\mathscr{T}) + n_{qq}(\mathscr{T}) + n_{qqq}(\mathscr{T})$$

When the triangulation is fixed, or there is no confusion, we will suppress the references to $\mathscr{T}$. The tuple $(n_\emptyset, n_{tt}, n_{qtt}, n_{qq}, n_{qqq})$ is termed the **profile** of $\mathscr{T}$. We stress that the profile of a triangulation does not determine the triangulation nor the manifold; it does give a streamlined

way to determine the types of tetrahedra and combinatorics of the canonical normal surfaces dual to classes in H.

Lemma 3.17 ([JRT13], Lemma 2) *Let $\mathscr{T}$ be a rank–2 coloured minimal and 0–efficient triangulation of the closed, orientable, irreducible, connected 3–manifold M. Then $n_{\mathfrak{tt}}$ and $n_{\mathfrak{qqq}}$ are even.*

Proof We pullback the colouring of $\mathscr{T}$ to $\widetilde{\Delta}$. The number of faces bounded by three H–even edges in $\widetilde{\Delta}$ is $n_{\mathfrak{tt}} + 4n_{\emptyset}$. As faces in $\widetilde{\Delta}$ are paired, with no face identified to itself, we require this quantity to be even and hence have $n_{\mathfrak{tt}}$ is even.

Let q be a quadrilateral disc in S_{φ_1}. The vertices of q must lie on 2–even and 3–even edges of $\mathscr{T}$. As M is orientable we know that adjacent vertices of q must contribute opposite slopes to the Q–matching equations. Consider the sum of the Q–matching equations for all 2–even edges. This sum must be zero and we consider the possible contributions of q.

If q is contained in a $\Delta_{\mathfrak{qtt}}$ tetrahedron, then it must have a pair of adjacent vertices on 2–even edges. As these have opposite signs, the contribution is $(+1)+(-1)=0$. If instead q is contained in a $\Delta_{\mathfrak{qq}}$ tetrahedron, then either all four vertices lie on 2–even edges or 3–even edges. In the former case the contribution is $2(+1)+2(-1)=0$ and the latter case has no contribution. Finally, if q is contained in a $\Delta_{\mathfrak{qqq}}$ tetrahedron, then a pair of opposite vertices lie on 2–even edges. The contribution is either $2(+1)$ or $2(-1)$. To balance this contribution, we must have another quadrilateral disc in S_{φ_1} contained in a distinct $\Delta_{\mathfrak{qqq}}$ tetrahedron. Hence $n_{\mathfrak{qqq}}$ is even. □

We now consider the contribution of each normal disc to $\chi(S_{\varphi_i})$. The surface S_{φ_i} has a single vertex on each φ_i–odd edge, as in the rank–1 colouring case. Let t_i be the number of triangle discs and q_i the number of quadrilateral discs. We obtain

$$\chi(S_{\varphi_i}) = \sum_{[e]\in\mathscr{T}^{(1)}} \varphi_i[e] - \frac{3}{2}t_i - 2q_i + t_i + q_i = \sum_{[e]\in\mathscr{T}^{(1)}} \varphi_i[e] - \frac{1}{2}t_i - q_i$$

where $\varphi_i[e] \in \{0,1\}$ and the sum is taken over $\mathbb{Z}$. Each triangle contributes $-1/2$ and each quadrilateral -1. Let K be the subcomplex spanned by the H–even edges of $\mathscr{T}$. We compute its Euler characteristic as

$$\chi(K) = 1 - \mathfrak{e} + \frac{1}{2}n_{\mathfrak{tt}} + n_{\emptyset}$$

Let $N = N(K)$ a small regular neighbourhood of K. Then ∂N is a normal surface meeting tetrahedra of types $\Delta_{\mathfrak{tt}}$, $\Delta_{\mathfrak{qtt}}$, and $\Delta_{\mathfrak{qq}}$ in the same number and types of normal discs as the canonical surfaces S_{φ_i}, $1 \le i \le 3$. As $\mathscr{T}$ has a single vertex, ∂N meets each type $\Delta_{\mathfrak{qqq}}$ tetrahedron in four normal triangles – one for each vertex of the 3–simplex. It follows from the above that we

have

$$\chi(S_{\varphi_1})+\chi(S_{\varphi_2})+\chi(S_{\varphi_3})+n_{qqq}=\chi(\partial N)=2\chi(N)=2\chi(K)=2-2\mathfrak{e}+n_{tt}+2n_{\emptyset}$$

Rearranging this expression yields

$$n_{tt}+2n_{\emptyset}-n_{qqq}=2\mathfrak{e}-2+\sum_{i=1}^{3}\chi(S_{\varphi_i}) \tag{3.2.1}$$

Lemma 3.18 ([JRT13], Lemma 4) *Let M be a closed, orientable, irreducible 3–manifold, and suppose that $\varphi_1,\varphi_2\in H^1(M;\mathbb{Z}_2)$ are non-trivial with $\varphi_1+\varphi_2=\varphi_3\neq 0$. Let $\mathscr{T}$ be a minimal triangulation with $|\mathscr{T}|$ tetrahedra and let S_{φ_i} be the canonical surface dual to φ_i. Letting $\mathfrak{e}_d$ denote the number of H–even edges of degree d, we have:*

$$\mathfrak{e}_3=4+n_{tt}+n_{qtt}-2\left(|\mathscr{T}|+\sum_{i=1}^{3}\chi(S_{\varphi_i})\right)+\sum_{d=5}^{\infty}(d-4)\mathfrak{e}_d \tag{3.2.2}$$

Proof The existence of a rank–2 subgroup of $H^1(M;\mathbb{Z}_2)$ implies that M is not one of S^3, $\mathbb{R}P^3$, $L(3,1)$, or $L(4,1)$. From [JR03] we have that $\mathscr{T}$ is 0–efficient and hence has a single vertex. Moreover the smallest degree of any edge in $\mathscr{T}$ is three from Lemma 3.7. Using (3.2.1) we have

$$\begin{aligned}\widetilde{\mathfrak{e}}&=6n_{\emptyset}+3n_{tt}+n_{qtt}+2n_{qq}\\&=2|\mathscr{T}|+4n_{\emptyset}+n_{tt}-n_{qtt}-2n_{qqq}\\&=2|\mathscr{T}|-n_{tt}-n_{qtt}+4\mathfrak{e}-4+2\sum_{i=1}^{3}\chi(S_{\varphi_i})\end{aligned}$$

Note that we have

$$\widetilde{\mathfrak{e}}=\sum_{d=3}^{\infty}d\mathfrak{e}_d \quad\text{and}\quad \mathfrak{e}=\sum_{d=3}^{\infty}\mathfrak{e}_d$$

Combining these equations we obtain

$$\sum_{d=3}^{\infty}d\mathfrak{e}_d=2|\mathscr{T}|-n_{tt}-n_{qtt}+4\sum_{d=3}^{\infty}\mathfrak{e}_d-4+2\sum_{i=1}^{3}\chi(S_{\varphi_i})$$

Rearranging this equality yields the desired result. □

Definition 3.19 Let M be a closed, orientable, irreducible, connected 3–manifold with minimal triangulation $\mathscr{T}$ whose edges are coloured by the rank–2 subgroup $H\leq H^(M;\mathbb{Z}_2)$. The **H–thickness**, $t_H(M)$, of M is the quantity

$$t_H(M)=c(M)-2-\sum_{i=1}^{3}\|\varphi_i\|$$

where $0\neq\varphi_i\in H$ for each $i\in\{1,2,3\}$.The **2–thickness** of M is the minimum $t_H(M)$ taken over all rank–2 subgroups of $H^1(M;\mathbb{Z}_2)$. ◇

The H–thickness allows the bound in Theorem 3.13 to be written as an equality instead and we observe that $t_H(M) \geq 0$.

For each nontrivial class $\varphi_i \in H,\ 1 \leq i \leq 3,$ we have from Lemma 3.14 that $\|\varphi_i\| \leq -\chi(S_{\varphi_i})$ and can instead write

$$\|\varphi_i\| = -\chi(S_{\varphi_i}) - d_{\varphi_i} \tag{3.2.3}$$

where $d_{\varphi_i} \geq 0$. The quantity d_{φ_i} is called the **defect**. It is zero if and only if S_{φ_i} is $\mathbb{Z}_2$–taut. Letting $t_H(M) = k \geq 0$, for a minimal triangulation $\mathscr{T}$, we have

$$|\mathscr{T}| = (2+k) + \sum_{i=1}^{3} \|\varphi_i\| = (2+k) - \sum_{i=1}^{3} \chi(S_{\varphi_i}) - \sum_{i=1}^{3} d_{\varphi_i}$$

where $k \geq 0$. Rearranging and substituting into (3.2.2) we obtain

$$\mathfrak{e}_3 + 2k = n_{\mathrm{tt}} + n_{\mathrm{qtt}} + 2\sum_{i=1}^{3} d_{\varphi_i} + \sum_{d=5}^{\infty} (d-4)\mathfrak{e}_d \tag{3.2.4}$$

3.3. Rank–2 coloured minimal triangulations

Throughout this section let M be a closed, orientable, irreducible, connected 3–manifold with minimal triangulation $\mathscr{T}$. Suppose $H \leq H^1(M;\mathbb{Z}_2)$ is a rank–2 subgroup containing nontrivial classes φ_1, φ_2, and $\varphi_3 = \varphi_1 + \varphi_2$. Then for $k \geq 0$ we can write

$$|\mathscr{T}| = (2+k) + \sum_{i=1}^{3} \|\varphi_i\| \tag{3.3.1}$$

The main goal of this section is to understand the arrangement of maximal layered solid tori in $\mathscr{T}$. A consequence of this will be to generalise Lemma 13 in [**JRT13**] to provide an upper bound on the number of degree three edges and extend this to bound the number of Δ_{tt} and Δ_{qtt} tetrahedra in a minimal triangulation.

3.3.1. Not all profiles at odd thickness. Given a rank–2 subgroup $H \leq H^1(M;\mathbb{Z}_2)$ with H–thickness $t_H(M) = k$ we establish for which profiles may be excluded when considering minimal triangulations of M.

Proposition 3.20 *Let M be a closed, orientable, irreducible, connected 3–manifold with minimal triangulation $\mathscr{T}$. Suppose all edges are coloured by the rank–2 subgroup $H \leq H^1(M;\mathbb{Z}_2)$ and that $|\mathscr{T}| = (2+k) + \sum_{i=1}^{3} \|\varphi_i\|$ where $H \cong \langle \varphi_1, \varphi_2 \rangle$. If k is odd, then the profile of $\mathscr{T}$ cannot be $(0,0,0,0,n_{\mathrm{qqq}})$*

Proof Suppose that the profile of $\mathscr{T}$ is $(0,0,0,0,n_{\mathrm{qqq}})$. Then each canonical surface S_{φ_i} dual to the colouring is a quadrilateral surface and consists of exactly one normal quadrilateral disc

in each tetrahedron. From [**JRT13**, Lemma 11], each S_{φ_i} is non-separating and

$$|\mathscr{T}| + \sum_{i=1}^{3} \chi(S_{\varphi_i}) = 2$$

As $\chi(S_{\varphi_i}) = -\|\varphi_i\| - d_{\varphi_i}$, for some $d_{\varphi_i} \geq 0$,

$$2 = |\mathscr{T}| + \sum_{i=1}^{3} \chi(S_{\varphi_i}) = |\mathscr{T}| - \sum_{i=1}^{3} \|\varphi_i\| - \sum_{i=1}^{3} d_{\varphi_i} = (2+k) - \sum_{i=1}^{3} d_{\varphi_i}$$

It follows that $\sum_{i=1}^{3} d_{\varphi_i} = k$.

Since S_{φ_i} is a quadrilateral surface, $M \backslash\backslash S_{\varphi_i}$ is a handlebody. As k is odd it follows that at least one d_{φ_i} is odd so that $\sum_{i=1}^{3} d_{\varphi_i} = k$. Without loss of generality, suppose that d_{φ_1} is odd so that $-\|\varphi_1\| = \chi(S_{\varphi_1}) + d_{\varphi_1}$. Let F be the $\mathbb{Z}_2$–taut representative dual to φ_1 so that $[F] = [S_{\varphi_1}] \in H_2(M;\mathbb{Z}_2)$ and $-\|\varphi_1\| = \chi(F) = \chi(S_{\varphi_1}) + d_{\varphi_1}$.

As S_{φ_1} is non–separating, we have a one–sided Heegaard splitting (M, S_{φ_1}) of M and the small closed regular neighbourhood $N(S_{\varphi_1})$ of S_{φ_1} is homeomorphic to the twisted I–bundle $S_{\varphi_1} \tilde{\times} I$ [**Rub78**]. Let $\Gamma_1 \subset \mathscr{T}^{(1)}$ denote the 1–even edges. It follows that $N(S_{\varphi_1}) \cap \Gamma_1 = \emptyset$ and $F \cap e$ consists of an even, non–negative number of points for each edge $e \in \Gamma_1$.

Consider a small regular neighbourhood $N(\Gamma_1)$ of Γ_1 homeomorphic to a handlebody of genus g. The surface F intersects each 1–handle of $N(\Gamma_1)$ in an even number of discs. For each such pair of discs D_1 and D_2 we perform surgery on F replacing D_1 and D_2 with an annulus A such that $\partial A = \partial D_1 \cup \partial D_2$. The result is a surface F' with $[F'] = [F] \in H_2(M;\mathbb{Z}_2)$, $F' \cap \Gamma_1 = \emptyset$ and $\chi(F') + 2m = \chi(F) = \chi(S_{\varphi_1}) + d_{\varphi_1}$ where $2m$ is the number of intersections of F with Γ_1.

We claim that $[F'] = [S_{\varphi_1}] \in H_2(S_{\varphi_1} \tilde{\times} I;\mathbb{Z}_2)$. First note that $M = N(S_{\varphi_1}) \cup (M - \mathrm{int}(N(S_{\varphi_1})))$ where $M - \mathrm{int}(N(S_{\varphi_1}))$ is a handlebody Σ of genus g satisfying $N(S_{\varphi_1}) \cap \Sigma = \partial\Sigma$. The inclusion $(\Sigma, \partial\Sigma) \hookrightarrow (M, N(S_{\varphi_1}))$ induces an isomorphism $H_n(\Sigma, \partial\Sigma;\mathbb{Z}_2) \cong H_n(M, N(S_{\varphi_1});\mathbb{Z}_2)$ for all n. We know $H_3(M;\mathbb{Z}_2) \cong H_2(N(S_{\varphi_1});\mathbb{Z}_2) \cong H_3(\Sigma, \partial\Sigma;\mathbb{Z}_2) \cong \mathbb{Z}_2$ and $H_3(N(S_{\varphi_1});\mathbb{Z}_2) = 0$. This gives the long exact sequence of the pair $(M, N(S_{\varphi_1}))$

$$\begin{array}{ccccccccc} 0 & \longrightarrow & H_3(M;\mathbb{Z}_2) & \longrightarrow & H_3(M, N(S_{\varphi_1});\mathbb{Z}_2) & \longrightarrow & H_2(N(S_{\varphi_1});\mathbb{Z}_2) & \longrightarrow & H_2(M;\mathbb{Z}_2) \longrightarrow \cdots \\ & & \| & & \| & & \| & & \\ & & \mathbb{Z}_2 & & \mathbb{Z}_2 & & \mathbb{Z}_2 & & \end{array}$$

From exactness we have $\ker(\mathbb{Z}_2 \to H_2(M;\mathbb{Z}_2))$ is trivial and hence there is an injection $\iota_* : H_2(N(S_{\varphi_1});\mathbb{Z}_2) \to H_2(M;\mathbb{Z}_2)$ with $\iota_*[F'] = \iota_*[S_{\varphi_1}] = [F] \in H_2(M;\mathbb{Z}_2)$ and thus $[F'] = [S_{\varphi_1}] \in H_2(N(S_{\varphi_1});\mathbb{Z}_2)$.

Let F'' be the surface obtained by performing all possible compressions on F' in $N(S_{\varphi_1})$, noting that we may have $F'' = F'$. Then F'' is an incompressible representative for the class $[S_{\varphi_1}]$ in $N(S_{\varphi_1})$ and it follows from [**Rub78**, Lemma 15] that S_{φ_1} and F'' are isotopic giving $\chi(S_{\varphi_1}) = \chi(F'')$. However, as F'' was obtained from F' it must be that $\chi(F'')$ and $\chi(F')$

differ by an even amount. This contradicts $\chi(S_{\varphi_1}) + d_1 = \chi(F') + 2m$ as this implies $\chi(S_{\varphi_1})$ and $\chi(F'')$ differ by an odd amount. No such surface S_{φ_1} can exist in $\mathscr{T}$ and the profile of $\mathscr{T}$ cannot be $(0,0,0,0,n_{qqq})$. □

3.3.2. Controlling Maximal Layered Solid Tori. We restate and prove Lemma 12 from [**JRT13**] with the assumption of atoroidal removed. The arguments we present closely follow those seen in [**JRT09**] (proof of Theorem 5 on pp. 173–175) and [**JRST20a, JRST20b**]. These lemmas allow us to provide a profile for the anatomy of the minimal triangulations we are considering.

Let $\mathbf{T}$ be a maximal layered solid torus containing an H–even edge e of M–degree 3. We call $\mathbf{T}$ **supportive** if it is of type Δ_{qq} and all H–even edges distinct from e have M–degree 4; we call $\mathbf{T}$ **almost supportive** if each interior H–even edge distinct from e has degree 4 and the unique H–even boundary edge has M-degree at least 5. We say that $\mathbf{T}$ is of type $(\Delta_{qq},4)$ if it is of type Δ_{qq} and the unique H–even boundary edge has M-degree equal to 4. Note that every supportive maximal layered solid torus is of type $(\Delta_{qq},4)$. If $\mathscr{T}$ contains no maximal layered solid torus of type $(\Delta_{qq},4)$, then we say that $\mathscr{T}$ is $(\Delta_{qq},4)$**–free**.

A **constellation** is a subcomplex $K \subset \mathscr{T}$ consisting of all tetrahedra in $\mathscr{T}$ incident with a specified edge. In the following lemma, we consider special constellations surrounding degree 4 H–even edges.

Lemma 3.21 ([**JRT13**], Lemma 12) *Let M be a closed, orientable, irreducible, connected 3–manifold with minimal triangulation $\mathscr{T}$. Suppose that all edge loops are coloured by the rank–2 subgroup H of $H^1(M;\mathbb{Z}_2)$. Then there is a $(\Delta_{qq},4)$–free minimal triangulation of M which is obtained from $\mathscr{T}$ by a finite number of 4–4 bistellar flips.*

Proof Suppose that $\mathbf{T}$ is of type $(\Delta_{qq},4)$ with unique H–even boundary edge e. Lemma 3.6 implies that e is the unital edge of $\mathbf{T}$ and that it is contained in four distinct tetrahedra in M. The proof proceeds by performing 4–4 bistellar flips to replace the four tetrahedra around e with a different constellation of four tetrahedra, shown in Figure 3.6. We show that there is always a flip which reduces either the number of maximal layered solid tori of type $(\Delta_{qq},4)$ or the number of maximal layered solid tori of type $\Delta_{\emptyset}$. Since both of these quantities are finite and 4–4 bistellar flips don't change the number of tetrahedra in the triangulation, this process terminates with a $(\Delta_{qq},4)$–free minimal triangulation of M.

We consider three cases determined by how we choose the appropriate 4–4 bistellar flip. In each case we list the types of the tetrahedra surrounding e in cyclic order, starting with $\mathbf{T}$. Denote the triangulation obtained from $\mathscr{T}$ after the 4–4 bistellar flip as $\mathscr{T}'$.

$(\Delta_{qq},\Delta_{qq},\Delta_{qq},\Delta_{qq}), (\Delta_{qq},\Delta_{qq},\Delta_{qtt},\Delta_{qtt}), (\Delta_{qq},\Delta_{qtt},\Delta_{qq},\Delta_{qtt}), (\Delta_{qq},\Delta_{qtt},\Delta_{qtt},\Delta_{qq}), (\Delta_{qq},\Delta_{qtt},\Delta_{qtt},\Delta_{qtt})$: In each constellation there are at most two maximal layered solid tori incident to e. Denote the

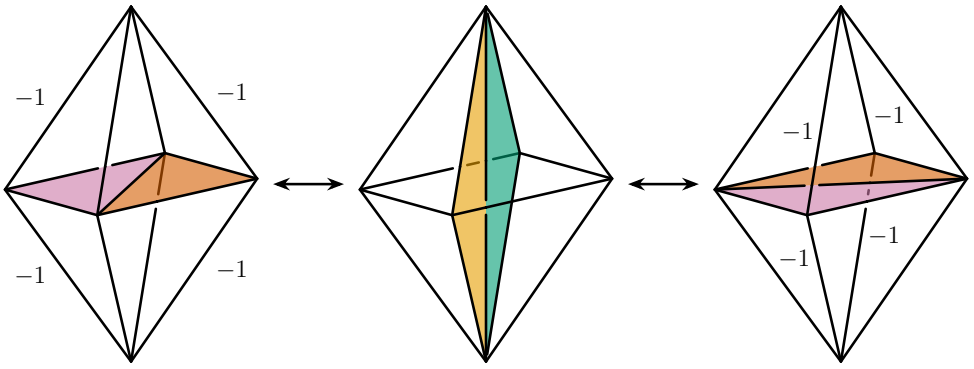

FIGURE 3.6. 4–4 bistellar flip with negative changes in degrees marked. Note that the degrees of the equatorial edges always increase by 1 regardless of which flip is chosen.

second one $\mathbf{T}_1$ and note that we may have $\mathbf{T}_1 = \mathbf{T}$. Any 4–4 bistellar flip replaces the constellation with one containing only tetrahedra of types Δ_{tt} and Δ_{qtt}. Since no maximal layered solid torus contains tetrahedra of these types we have that every maximal layered solid torus with respect to $\mathscr{T}$ is a maximal layered solid torus with respect to $\mathscr{T}'$, except possibly $\mathbf{T}$ and $\mathbf{T}_1$. In all cases the degrees of the equatorial edges of the constellation increase by one and the unique H–even boundary edges of $\mathbf{T}'$ and $\mathbf{T}'_1$ cannot be unital. The number of maximal layered solid tori of type $(\Delta_{qq}, 4)$ decreases.

$(\Delta_{qq}, \Delta_{tt}, \Delta_{tt}, \Delta_{qq}), (\Delta_{qq}, \Delta_{tt}, \Delta_{tt}, \Delta_{qtt}), (\Delta_{qq}, \Delta_{qq}, \Delta_{tt}, \Delta_{tt}), (\Delta_{qq}, \Delta_{qtt}, \Delta_{tt}, \Delta_{tt})$: In each constellation $\mathbf{T}$ is the unique maximal layered solid torus containing e. We claim that choosing the flip which preserves the degree of the non-equatorial H–even edges not contained in faces of $\mathbf{T}$ decreases the number of maximal layered solid tori of type $(\Delta_{qq}, 4)$. Such a flip replaces e with a φ_i–odd edge, for some $i \in \{1,2,3\}$. If every maximal layered solid torus with respect to $\mathscr{T}$ is also a maximal layered solid torus with respect to $\mathscr{T}'$, then $\mathbf{T}$ cannot remain of type $(\Delta_{qq}, 4)$ after the flip. Assume that some maximal layered solid torus, $\mathbf{T}'_0$, with respect to $\mathscr{T}'$ is not a maximal layered solid torus with respect to $\mathscr{T}$. Then $\mathbf{T}'_0$ is obtained from some maximal layered solid torus, $\mathbf{T}_0$, with respect to $\mathscr{T}$ by layering onto one of the tetrahedra of type Δ_{qq} in the new constellation. There cannot be two tetrahedra in the constellation contained in $\mathbf{T}'_0$ otherwise, by Lemma 3.5, $\mathbf{T}'_0$ is not maximal or it meets another maximal layered solid torus in a face, which cannot happen. The H–even boundary edge of $\mathbf{T}_0$ increases by one with this layering and so it cannot be the unital edge of $\mathbf{T}'_0$ and hence $\mathbf{T}'_0$ cannot be of type $(\Delta_{qq}, 4)$. The number of maximal layered solid tori of type $(\Delta_{qq}, 4)$ decreases.

$(\Delta_{qq}, \Delta_{tt}, \Delta_{\emptyset}, \Delta_{tt})$: Any flip produces a constellation consisting of two tetrahedra of type Δ_{qq} and two tetrahedra of type Δ_{tt} surrounding a φ_i–odd edge, for some $i \in \{1,2,3\}$. This reduces the number of tetrahedra of type $\Delta_{\emptyset}$. □

The remainder of this section is dedicated to proving Theorem 3.1. The 4–4 bistellar flips

used to produce a $(\Delta_{qq},4)$–free triangulation remove all supportive maximal layered solid tori but may leave behind some almost supportive maximal layered solid tori. Our approach for bounding the number of degree 3 edges is to examine the subcomplexes of $\mathscr{T}$ in which the almost supportive solid tori are contained.

3.3.3. Proof of Theorem 3.1.

Theorem 3.1 Let M be a closed, orientable, irreducible, connected 3–manifold with minimal triangulation $\mathscr{T}$. Suppose that all edge loops are coloured by the rank–2 subgroup H of $H^1(M;\mathbb{Z}_2)$, $\mathscr{T}$ is $(\Delta_{qq},4)$–free with respect to the colouring and that $|\mathscr{T}| = (2+k) + \sum_{\varphi\in H}\|\varphi\|$. Letting $\mathfrak{e}_d$ denote the number of H–even edges of degree d, we have:

$$\mathfrak{e}_3 \leq k + 2\sum_{i=1}^{3} d_{\varphi_i} + \sum_{d=5}^{\infty}(d-4)\mathfrak{e}_d.$$

Remark 3.22 Before we begin the proof, we remark on the perspective from which certain subcomplexes are illustrated. When it is reasonable, we shall endeavour to provide a schematic of the entire subcomplex and any normal surfaces embedded within. When a subcomplex contains too many tetrahedra, or we wish to provide an exhaustive list, we shall instead exploit certain symmetries of the subcomplex and provide a 'top–down' perspective. An example of this is shown in Figure 3.7.

We now commence the proof. Assume, for the sake of contradiction, that

$$\mathfrak{e}_3 > k + 2\sum_{i=1}^{3} d_{\varphi_i} + \sum_{d=5}^{\infty}(d-4)\mathfrak{e}_d \tag{3.3.2}$$

Every edge e of degree three is H–even and, by Lemma 3.8, is contained in a unique maximal layered solid torus $\mathbf{T}(e)$. Hence (3.3.2) states that there are at least $k+1$ maximal layered solid tori containing a degree three edge. Note that only H–even edges appear in (3.3.2).

We will construct a set of subcomplexes $\mathscr{K}$ by examining the intersections of maximal layered solid tori, together with a partition $\mathscr{E}$ of all H–even edges which satisfies the following properties:

(E1) for each $K \in \mathscr{K}$ there is a partition set $E_K \in \mathscr{E}$ such that $E_K \subset K$;

(E2) for each degree 3 edge $e \in \mathscr{T}^{(1)}$ there is a unique $K \in \mathscr{K}$ such that $e \in E_K$; and

(E3) the H–even edges not contained in $\cup_{K\in\mathscr{K}} E_K$ are in a partition set which we denote $E_\star$.

We stress that the subcomplexes in $\mathscr{K}$ will not necessarily be pairwise distinct nor will every tetrahedron in $\mathscr{T}$ be in a subcomplex. Any tetrahedron, however, will belong to at most one subcomplex in $\mathscr{K}$. Moreover, the partition set $E_\star$ need not be associated to any subcomplex $K \in \mathscr{K}$. Roughly speaking, each subcomplex $K \in \mathscr{K}$ will be contained in a maximal layered

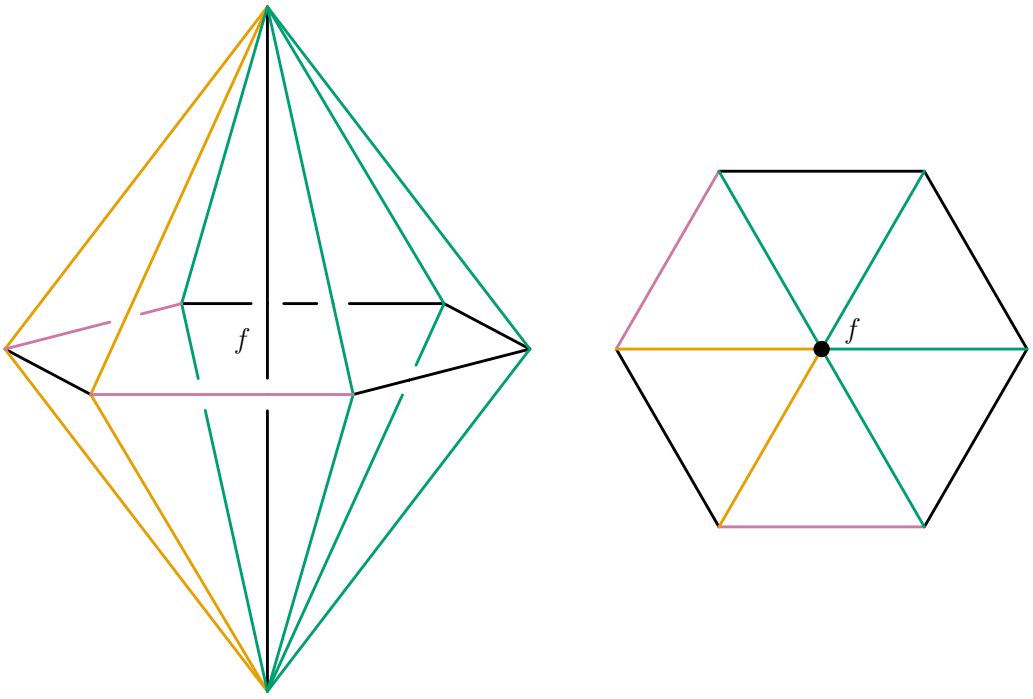

FIGURE 3.7. Example of a top–down perspective for a subcomplex containing six tetrahedra arranged around a central edge f. The left shows the subcomplex from a three–dimensional perspective with the right showing the same subcomplex viewed from one end of the edge labelled f. Each radial 'edge' in the right figure corresponds to a pair of incident edges with matching colours.

solid torus or consist of multiple layered solid tori incident to some H–even edge. The only maximal layered solid tori we will be interested in are those which contain a degree 3 edge.

For a given $K \in \mathscr{K}$ we let $\mathfrak{e}_d(K)$ denote the number of H–even edges of degree d contained in K. Observing that $\mathfrak{e}_d \geq \mathfrak{e}_d(K)$ for any $K \in \mathscr{K}$ and $d \geq 3$, we may rewrite (3.3.2) as

$$\sum_{K\in\mathscr{K}} \mathfrak{e}_3(K) = \mathfrak{e}_3 > k + 2\sum_{i=1}^{3} d_{\varphi_i} + \sum_{d=5}^{\infty}(d-4)\mathfrak{e}_d \geq k + 2\sum_{i=1}^{3} d_{\varphi_i} + \sum_{K\in\mathscr{K}}\sum_{d=5}^{\infty}(d-4)\mathfrak{e}_d(K)$$

Rearranging this further we obtain

$$\sum_{K\in\mathscr{K}} \left(\mathfrak{e}_3(K) - \sum_{d=5}^{\infty}(d-4)\mathfrak{e}_d(K) \right) - 2\sum_{i=1}^{3} d_{\varphi_i} > k \geq 0 \tag{3.3.3}$$

We also distribute some of d_{φ_i} over some of the subcomplexes by analysing compressions in a neighbourhood of K. We let $d_{\varphi_i}(K)$ denote the allocation of d_{φ_i} to K. This will give

$$2\sum_{K\in\mathscr{K}}\sum_{i=1}^{3} d_{\varphi_i}(K) \leq 2\sum_{i=1}^{3} d_{\varphi_i}$$

We proceed by constructing subcomplexes K and their associated partition sets E_K and calculating their contribution to the left side of (3.3.3). Denote this contribution by

$$\delta(K) = \mathfrak{e}_3(K) - \sum_{d=5}^{\infty}(d-4)\mathfrak{e}_d(K) - 2\sum_{i=1}^{3} d_{\varphi_i}(K)$$

As $k \geq 0$ it is sufficient to determine whether $\delta(K) \leq 0$ or $\delta(K) > 0$. We term the former a **deficit** and the latter a **gain**.

The first subcomplexes we consider are those that consist of at most one maximal layered solid torus. Let $\mathbf{T}(e)$ be a maximal layered solid torus with degree 3 edge e. Since H has rank two, M is not a lens space. Since $\mathscr{T}$ is minimal, each edge incident with $\mathbf{T}(e)$, except for e, has degree at least four. We claim that for $K \subset \mathbf{T}(e)$, $\delta(K)$ is a gain only when $\mathbf{T}(e)$ is almost supportive and the unique H–even boundary edge is unital.

Claim 1: If any interior H–even edge of $\mathbf{T}(e)$ has degree at least 5, then $\delta(K)$ is a deficit.

Proof of Claim 1: Suppose that $\mathbf{T}(e)$ contains an interior H–even edge f with $\deg(f) \geq 5$. Let K be the subcomplex $\mathbf{T}(e)\backslash\partial\mathbf{T}(e)$ and $E_K = \{e, f\}$. Then $\mathfrak{e}_3(K) = 1$ and, for some $d \geq 5$, $\mathfrak{e}_d(K) \geq 1$ giving $\delta(K) \leq 0$. This proves the claim. □

Currently, for any $K \in \mathscr{K}$ we have that K is the interior of a maximal layered solid torus $\mathbf{T}(e)$ which contains at least one H–even edge of degree at least 5. The associated partition set E_K consists of the degree 3 edge e and one H–even edge of degree at least 5. We add the remaining interior H–even edges of $\mathbf{T}(e)$ to $E_\star$. The boundary edges of such a subcomplex are contained in $\mathscr{T}\backslash\mathscr{K}$.

Claim 2: If $\mathbf{T}(e)$ is of type $\Delta_\emptyset$, then $\delta(K)$ is a deficit.

Proof of Claim 2: Assume $\mathbf{T}(e)$ is of type $\Delta_\emptyset$. All of its interior edges distinct from e are H–even and, from Claim 1, it remains to assume they all have degree four. Since $\mathbf{T}(e)$ contains a degree three edge it must contain, as an embedded subcomplex, $\mathbf{T}_1 \cong \mathrm{LST}(1,3,4)$ by Lemma 3.8. We claim that $\mathbf{T}(e)$ always has a boundary edge with $\mathbf{T}$-degree at least five.

The subcomplex $\mathbf{T}_1$ has unital boundary edge h and non–unital boundary edges f and g with $\deg_{\mathbf{T}_1}(f) = 5$ and $\deg_{\mathbf{T}_1}(g) = 3$. If $\mathbf{T}(e) = \mathbf{T}_1$, then we are done. Otherwise we construct $\mathbf{T}(e)$ by first layering a tetrahedron onto one of the non–unital boundary edges. Layering onto f yields an interior H–even edge of degree six, contradicting the assumption that all interior edges distinct from e have degree 4 and so we must layer on g. Then f and h are non–unital boundary edges with $\deg_{\mathbf{T}}(f) = 7$ and $\deg_{\mathbf{T}}(h) = 3$. Repeating this argument we must always layer on the boundary edge with $\mathbf{T}$-degree three and conclude that $\mathbf{T}(e)$ must have a non–unital boundary edge f with $\deg_{\mathbf{T}}(f) \geq 5$.

Suppose that $m-1$ additional maximal layered solid tori containing a degree three edge and with all other interior H–even edges of degree 4 are incident with f. Let K be the union of these solid tori and let E_K be the collection of the degree 3 edges in K together with the common boundary edge f. Then $\mathfrak{e}_3(K) = m$, $\deg(f) \geq 2m+4$, and $\sum_{d=5}^{\infty}(\mathfrak{e}_d(K)-4) \geq 2m > m$. This gives the deficit $\delta(K) < 0$. □

For each K arising in Claim 2 we add all remaining H–even edges in $K \backslash E_K$ to $E_\star$. Claims 1 and 2 verify that any $\mathbf{T}(e)$ in $\mathscr{T}\backslash\mathscr{K}$ must be almost supportive. It remains to check that the unique H–even boundary edge in each of these remaining maximal layered solid tori is unital.

Claim 3: If $\mathbf{T}(e)$ is almost supportive and the unique H–even boundary edge is non–unital, then $\delta(K)$ is a deficit.

Proof of Claim 3: As $\mathbf{T}(e)$ is almost supportive it is of type $\Delta_{\mathfrak{qq}}$ with unique H–even boundary edge f. Suppose that f is non–unital. Then $\deg_{\mathbf{T}}(f) \geq 3$ as $\mathbf{T}(e)$ contains $\mathrm{LST}(1,3,4)$ as an embedded subcomplex.

Suppose an additional $m-1$ almost supportive maximal layered solid tori are incident with f. Let K be the union of these solid tori and E_K the union of the m degree 3 edges and f. Then $\mathfrak{e}_3(K) = m$, $\deg(f) \geq 2m+2$, and $\sum_{d=5}^{\infty}\mathfrak{e}_d(K)-4 \geq 2m-2$. This yields $\delta(K) \leq 2-m$. When $m \geq 2$ we observe $\delta(K)$ is a deficit. If $m = 1$, then we claim that $\deg(f) \geq 5$ and thus $\delta(K)$ is a deficit. Suppose this is not the case. Then $\deg(f) = 4$, contradicting the fact that $\mathscr{T}$ is $(\Delta_{\mathfrak{qq}},4)$–free. Hence $\deg(f) \geq 5$ and $\delta(K) \leq 0$ is a deficit. □

For each K arising in Claim 3 we add all H–even edges in $K\backslash E_K$ to $E_\star$. Reviewing the subcomplexes in $\mathscr{K}$ we observe that each K obtained from Claims 1–3 satisfies

$$\mathfrak{e}_3(K) \leq \sum_{d=5}^{\infty}(d-4)\mathfrak{e}_d(K)$$

From Claims 1–3 we conclude that if K consists only of the union of $m \geq 1$ maximal layered solid tori, then $\delta(K)$ is a gain only when these tori are almost supportive and each unique H–even boundary edge is unital. In particular, the only maximal layered solid tori left in $\mathscr{T}\backslash\mathscr{K}$ are precisely those satisfying this restriction. We will build our remaining subcomplexes from these solid tori and show that the total possible gain cannot exceed k, giving the desired contradiction.

Suppose $m \geq 1$ almost supportive maximal layered solid tori are incident to the H–even edge f, which is necessarily unital in each of them and not yet contained in any partition set of $\mathscr{E}$. Let K be the union of these solid tori. Then $\mathfrak{e}_3(K) = m$, $\deg(f) \geq 2m$, and $\sum_{d=5}^{\infty}(d-4)\mathfrak{e}_d(K) \geq 2m-4$. We observe a deficit $\delta(K) = 4-m < 0$ if $m > 4$ or $m = 4$ and $\deg(f) > 8$. Furthermore, we obtain the deficit $\delta(K) = 0$ when

$$(m, \deg(f)) \in \{(4,8),(3,7),(2,6),(1,5)\}$$

We call these subcomplexes **balanced** and we assign to E_K the degree 3 edges together with f. The remaining H–even edges in K are placed into $E_\star$. It remains that a gain of $\delta(K) = 1$ can be obtained when

$$(m, \deg(f)) \in \{(3,6),(2,5)\}$$

We call these subcomplexes **unbalanced** and say that f is the **central** edge. Note that we need not consider any configuration in which $\deg(f) = 4$ as $\mathscr{T}$ is $(\Delta_{\mathfrak{qq}}, 4)$–free. We proceed by analysing the cases where $\delta(K) = 1$.

Claim 4: If $(m, \deg(f)) \in \{(3,6),(2,5)\}$, then the edge f is incident to $\deg(f)$ pairwise distinct tetrahedra.

Proof of Claim 4: Writing $d = \deg(f)$, let $\Delta_1, \ldots \Delta_d$ denote the (not necessarily distinct) tetrahedra meeting around f in cyclic order such that Δ_i and Δ_{i+1} share a face for $1 \leq i \leq d$ where it is understood that $\Delta_{d+1} = \Delta_1$. Without loss of generality we assume that the tetrahedra which belong to the maximal layered solid tori in this arrangement are Δ_{2i} for $1 \leq i \leq m$. Each of these tetrahedra is of type $\Delta_{\mathfrak{qq}}$.

There are no tetrahedra of type $\Delta_{\mathfrak{qqq}}$ incident with f and any tetrahedron of type $\Delta_{\mathfrak{qtt}}$ can only occur only once around f as it possesses exactly one H–even edge. The minimum arrangement for a tetrahedron Δ_i to be of type $\Delta_\emptyset$ requires Δ_{i-1} and Δ_{i+1} to be of type $\Delta_{\mathfrak{tt}}$. When $(m,d) = (3,6)$ we have Δ_2, Δ_4, and Δ_6 of type $\Delta_{\mathfrak{qq}}$; $(m,d) = (2,5)$ gives Δ_2 and Δ_4 of type $\Delta_{\mathfrak{qq}}$. Hence this arrangement is not possible and we have no tetrahedra of type $\Delta_\emptyset$.

Suppose now that Δ_1 is of type $\Delta_{\mathfrak{qq}}$ and meets f twice. Letting f' denote the other H–even edge in Δ_1 it must be that f' is identified with f and the two faces of Δ_1 containing f' meet Δ_d in at least two edges. Hence we cannot identify these faces with a face of any tetrahedron Δ_{2i} for $1 < i \leq m$. By a symmetric argument, this shows that all tetrahedra in the $(3,6)$ case must be pairwise distinct. In the $(2,5)$ case this reasoning shows that $\Delta_1 \neq \Delta_3$. Observing that the two faces of Δ_1 containing f' meet Δ_2 in two edges, the same argument shows that $\Delta_1 \neq \Delta_5$. This leaves the possibility that $\Delta_3 = \Delta_5$, however we can note that this would mean that $\Delta_2 \cap \Delta_4$ consists of two edges, which is not possible.

It remains to check when f occurs more than once in a tetrahedron of type $\Delta_{\mathfrak{tt}}$. A tetrahedron of this type can only occur when $(m,d) = (2,5)$ and forces $\Delta = \Delta_4 = \Delta_5$ to be this tetrahedron. This configuration identifies two faces of Δ in an orientation preserving manner, giving rise to an edge of degree one, which is not possible. Hence we cannot have a tetrahedron of type $\Delta_{\mathfrak{tt}}$ meeting f more than once and all the tetrahedra in the configuration $(m,d) = (2,5)$ are pairwise distinct. □

The remaining claims require a more subtle analysis, taking into account the constant k and any compressions of the canonical surfaces. Recall that $k \geq 0$ and the minimal triangulation $\mathscr{T}$

satisfies

$$c(M) = |\mathscr{T}| = (2+k) + \sum_{i=1}^{3} \|\varphi_i\|$$

Recall further that from Lemma 3.14 we can write $-\|\varphi_i\| = \chi(S_{\varphi_i}) - d_{\varphi_i}$ for each $i \in \{1,2,3\}$, where $d_{\varphi_i} \geq 0$. A compression of the canonical surface S_{φ_i} contributes $+2$ to d_{φ_i} and hence $+4$ to $2\sum_{i=1}^{3} d_{\varphi_i}$. For the following claims we will consider this latter contribution in order to make the allocations to $2\sum_{i=1}^{3} d_{\varphi_i}(K)$ clear.

The first subcomplexes we consider are the $(2,5)$ unbalanced subcomplexes which contain two $\Delta_{\mathtt{tt}}$ tetrahedra. Following Claim 4, we assume Δ_1 and Δ_5 are the $\Delta_{\mathtt{tt}}$ tetrahedra and their shared face is bounded by three H–even edges f, g, and h (see Figure 3.8).

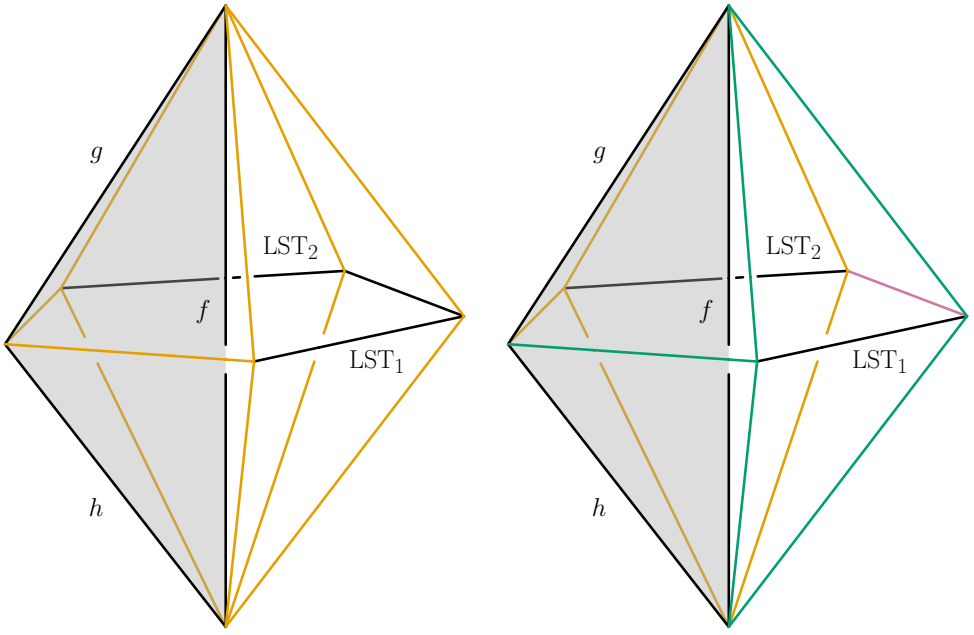

FIGURE 3.8. The two possible $(2,5)$ unbalanced subcomplexes containing two tetrahedra of type $\Delta_{\mathtt{tt}}$. The $\Delta_{\mathtt{tt}}$ tetrahedra meet in the shaded face which is bounded by H–even edges f, g, and h. The left subcomplex contains three tetrahedra of type $\Delta_{\mathtt{qq}}$. The right subcomplex contains two tetrahedra of type $\Delta_{\mathtt{qq}}$ and one of type $\Delta_{\mathtt{qtt}}$.

Claim 5: Suppose $(m, \deg(f)) = (2,5)$ and each H–even edge f, g, and h is incident to exactly two $\Delta_{\mathtt{tt}}$ tetrahedra. Then we may adjust $d_{\varphi_i}(K)$ so that $\delta(K)$ is a deficit.

Proof of Claim 5: Let Δ_1 and Δ_5 denote the tetrahedra of type $\Delta_{\mathtt{tt}}$ and label the three H–even edges bounding the face they meet along f, g, and h with $\deg(f) = 5$ (see Figure 3.8). Let m_g, m_h denote the number of almost supportive maximal layered solid tori incident with g and h, respectively. We consider the possible subcomplexes for $(m_g, \deg(g))$ as the case for $(m_h, \deg(h))$ is similar. After performing any compression in the following arguments, we do not change the types of the tetrahedra and only adjust the compressed surface(s).

The first arrangement to consider is $(m_g, \deg(g)) = (2,5)$. This subcomplex around g must be coloured the same as that around f – if three $\Delta_{\mathtt{qq}}$ tetrahedra of the same type are incident with

f, then three $\Delta_{\mathfrak{qq}}$ tetrahedra must also meet g and if one $\Delta_{\mathfrak{qtt}}$ tetrahedron is incident with f, then one $\Delta_{\mathfrak{qtt}}$ tetrahedron is incident with g. In the former arrangement, two of the canonical surface S_{φ_i}, $i \in \{1,2,3\}$, each intersect three tetrahedra incident with f and three tetrahedra incident with g in normal quadrilaterals forming an annulus linking the face bounded by f, g, and h through a triangle in each $\Delta_{\mathfrak{tt}}$ tetrahedron. We can perform a compression of each surface by cutting along these annuli and pasting in two discs, each intersecting f and g once. This is illustrated for a single surface in Figure 3.9. The resulting surface is normal with each quadrilateral replaced by two normal triangles and each triangle replaced with one triangle and one quadrilateral. Considering the latter arrangement, we obtain the same compression for only a single canonical surface.

The number of connected components in each surface is preserved under the compression since four of the quadrilaterals in each annulus meet the maximal layered solid tori and hence have their corners identified in diagonally opposite pairs. As $\mathscr{T}$ is 0–efficient, no component of the compressed surface can be a sphere as it intersects some edges of $\mathscr{T}$ only once; M being irreducible and not $\mathbb{R}P^3$ implies no component of the compressed surface is a projective plane and the Euler characteristic of each component remains non–positive.

Letting K be the union of the four maximal layered solid tori and E_K the union of degree 3 edges in K together with f and g we observe $2\sum_{i=1}^{3} d_{\varphi_i} \geq 4$ when Δ_3 is of type $\Delta_{\mathfrak{qtt}}$ and $2\sum_{i=1}^{3} d_{\varphi_i} \geq 8$ when Δ_3 is of type $\Delta_{\mathfrak{qq}}$. We allocate $+2$ to $2\sum_{i=1}^{3} d_{\varphi_i}(K)$ in each case to obtain

$$\delta(K) = \mathfrak{e}_3(K) - \sum_{d=5}^{\infty} (d-4)\mathfrak{e}_d(K) - 2\sum_{i=1}^{3} d_{\varphi_i}(K) = 4 - 2 - 2 = 0$$

Alternatively, g may be the central edge of a balanced subcomplex. If $(m_g, \deg(g)) = (3,7)$ or $(m_g, \deg(g)) = (2,6)$, then $\deg(g)$ pairwise distinct tetrahedra are incident with g, following the proof of Claim 4. If $(m_g, \deg(g)) \in \{(1,5),(0,4)\}$, then either $\deg(g)$ or $\deg(g)-1$ pairwise distinct tetrahedra are incident with g.

Suppose that $\deg(g)$ pairwise distinct tetrahedra are incident with g. Further assume that there is at most one distinct type of $\Delta_{\mathfrak{qtt}}$ tetrahedron (with both subtypes permissible) and that the only $\Delta_{\mathfrak{tt}}$ tetrahedra incident with g are Δ_1 and Δ_5. We list the possible arrangements of tetrahedra around g, up to changing symmetry, in Figure 3.10. In all arrangements, at least one canonical surface S_{φ_i}, $i \in \{1,2,3\}$, intersects three tetrahedra incident with f and $\deg(g)-2$ tetrahedra incident with g in quadrilaterals forming an annulus linking the face bounded by f, g, and h through a triangle in each $\Delta_{\mathfrak{tt}}$ tetrahedron. Following previous arguments, we can compress each such surface by cutting along the annulus and pasting two discs, each intersecting f and g once. This compression replaces each quadrilateral with two triangles and the triangles in Δ_1 and Δ_5 with a triangle and a quadrilateral. No component of the compressed surface is a sphere or projective plane and the Euler characteristic remains non-positive.

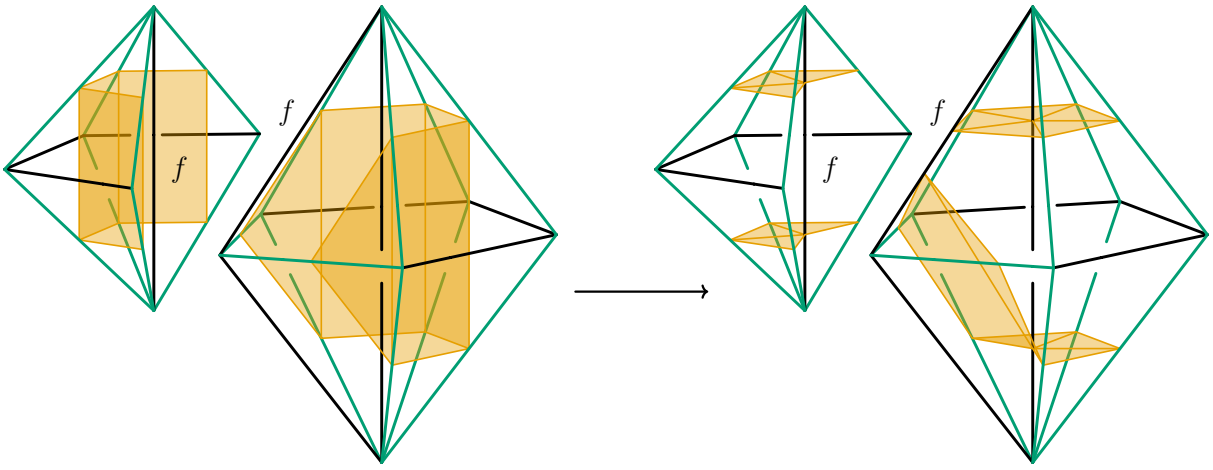

FIGURE 3.9. The single compression of the annulus linking the face bounded by H–even edges f, g, and h when $\deg(g) = 5$. The compressions when $\deg(g) = 6,7$ are the same with the only change being additional quadrilaterals around g. The compression is only shown for one canonical surface, however it is the same when there are two. Note that the back faces do not need to be coloured the same, despite this illustration.

Letting K be the union of the solid tori and E_K the union of the degree 3 edges in K together with f and g, we observe $2\sum_{i=1}^{3} d_{\varphi_i} \geq 4$ for all arrangements depicted in Figure 3.10 and $2\sum_{i=1}^{3} d_{\varphi_i} \geq 8$ when $\deg(g) - 2$ tetrahedra incident with g are of type $\Delta_{\mathfrak{qq}}$. For each case we allocate $+2$ to $2\sum_{i=1}^{3} d_{\varphi_i}(K)$ to obtain the deficit

$$\delta(K) = \mathfrak{e}_3(K) - \sum_{d=5}^{\infty} (d-4)\mathfrak{e}_d(K) - 2\sum_{i=1}^{3} d_{\varphi_i}(K) = 1 - 2 = -1$$

Consider now $\deg(g) = 5$ with 4 pairwise distinct tetrahedra incident with g. Referring to Figure 3.2, the only neighbourhood of g which is both compatible with the colouring and possesses one almost supportive layered solid torus is $X^1_{5;4}$. The colouring and edge identifications are shown in Figure 3.11 and it is noted that we require the two $\Delta_{\mathfrak{tt}}$ tetrahedra to be coloured the same. Restricting to this subcomplex, there are no compression discs for any canonical surface dual to the colouring. It can be observed by combining the position of the maximal layered solid tori in Figure 3.8 and the identifications in Figure 3.11 that if h is of degree 5, then it must meet five pairwise distinct tetrahedra and we apply the arguments above to obtain a deficit in $\delta(K)$.

The final arrangements to consider are those with $(m_g, \deg(g)) = (0,4)$. If g is incident to exactly four pairwise distinct tetrahedra, then the possible arrangements are shown in the final row of Figure 3.10. If instead g is incident to three pairwise distinct tetrahedra, then the neighbourhood must be modelled on $X^0_{4;3}$ from Figure 3.1 with edges coloured as in Figure 3.12.

In each of these arrangements at least one canonical surface S_{φ_i}, $i \in \{1,2,3\}$, intersects the three tetrahedra incident with f and two tetrahedra incident with g in quadrilaterals forming

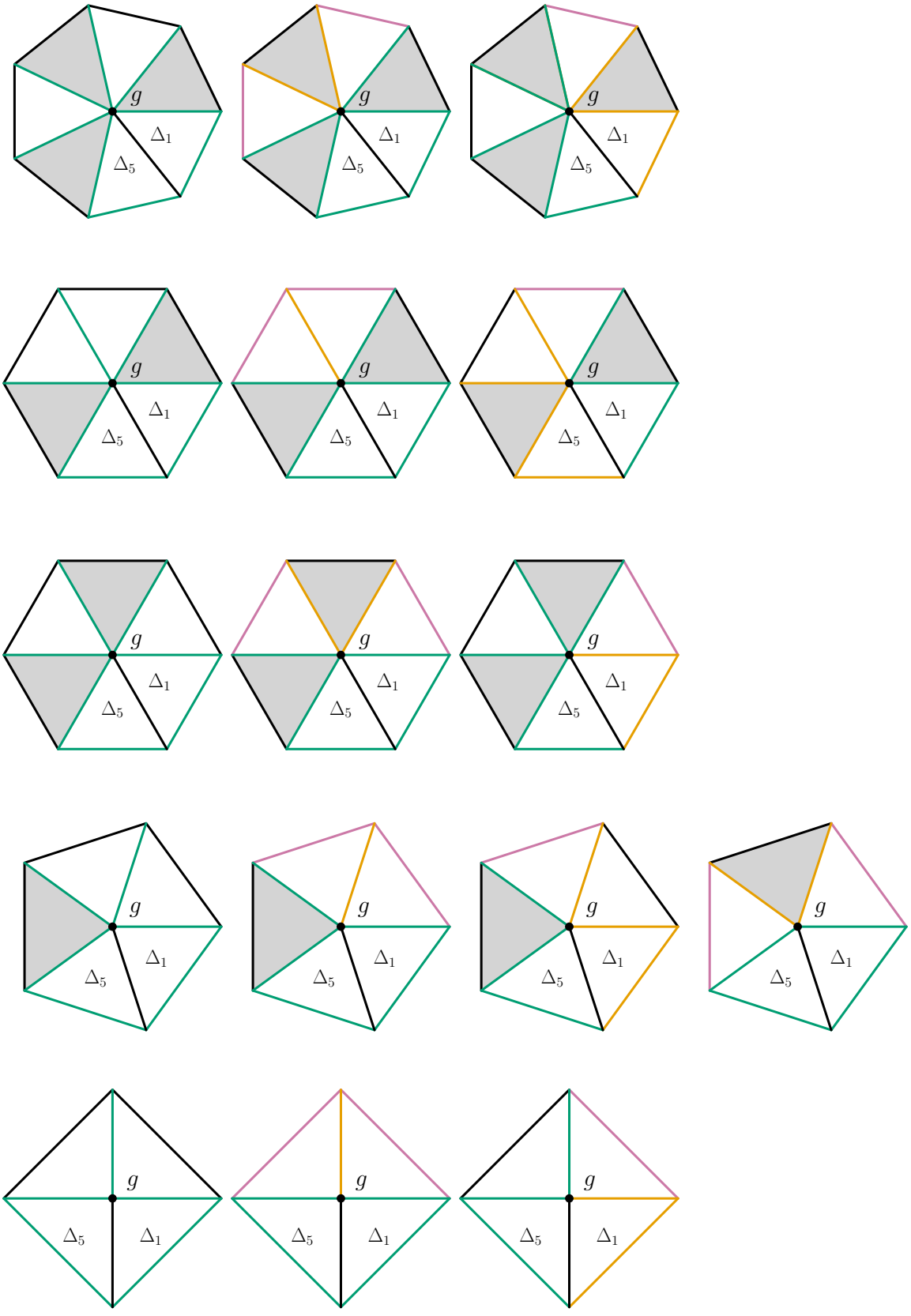

FIGURE 3.10. Arrangements of balanced subcomplexes about g from a top down perspective. We assume that at most one distinct type of Δ_{qtt} tetrahedron is incident with g and that the only Δ_{tt} tetrahedra incident with g are Δ_1 and Δ_5. Symmetric cases have not been included.

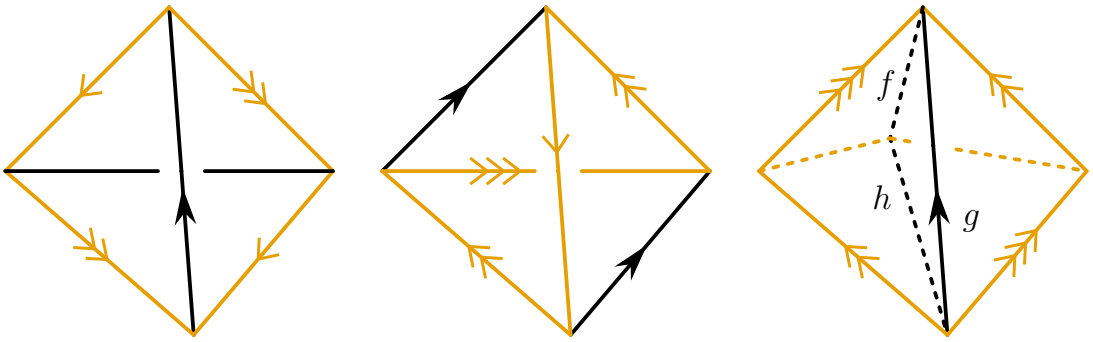

FIGURE 3.11. The neighbourhood of g modelled on $X^1_{5;4}$ with identifications adjusted so that the two tetrahedra of type Δ_{qq} belong to a maximal layered solid torus consisting of at least three tetrahedra. The solid arrows indicate identifications from the maximal layered solid tori incident with f, the single coming from one and the double coming from the other.

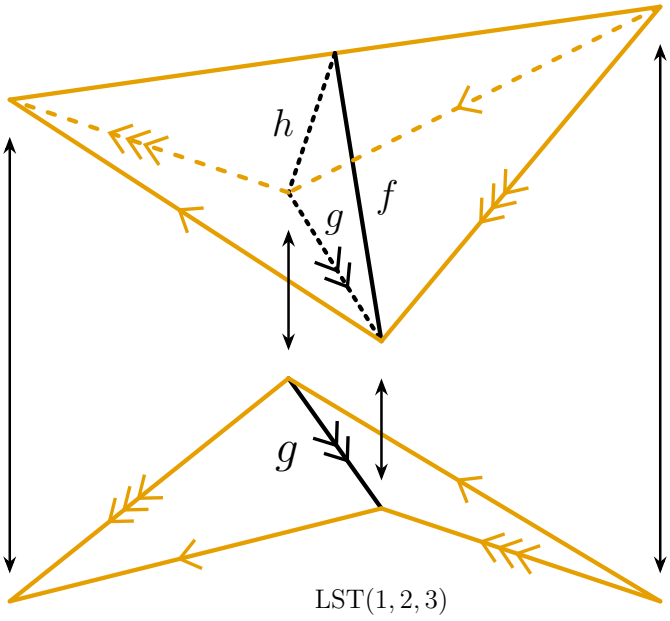

FIGURE 3.12. The neighbourhood of g modelled on $X^0_{4;3}$. The single tetrahedron of type Δ_{qq} forms the one tetrahedron layered solid torus $\mathrm{LST}(1,2,3)$.

an annulus linking the face bounded by f, g, and h through a triangle in each Δ_{tt} tetrahedron. Following previous arguments, we can compress each such surface by cutting along the annulus and pasting in two discs, each intersecting f and g once. This compression replaces each quadrilateral with two triangles and the triangles in Δ_1 and Δ_5 with a triangle and a quadrilateral. No component of the compressed surface is a sphere or projective plane and the Euler characteristic remains non–positive.

Letting K be the union of the solid tori and E_K the union of the degree 3 edges in K together with f and g, we observe $2\sum_{i=1}^{3} d_{\varphi_i} \geq 4$ when at least one Δ_{qtt} tetrahedron is incident with g and $2\sum_{i=1}^{3} d_{\varphi_i} \geq 8$ otherwise. For each case we allocate $+2$ to $2\sum_{i=1}^{3} d_{\varphi_i}(K)$ to obtain the

deficit

$$\delta(K) = \mathfrak{e}_3(K) - \sum_{d=5}^{\infty}(d-4)\mathfrak{e}_d(K) - 2\sum_{i=1}^{3} d_{\varphi_i}(K) = 1-2 = -1$$

This completes the analysis of the local neighbourhoods of the $(2,5)$ unbalanced subcomplexes satisfying the assumptions of this claim. We note that there are some extensions to consider and cover those here.

Suppose that Δ_1 and Δ_5 are coloured the same and further suppose that g is the central edge of a $(3,7)$ balanced subcomplex such that five tetrahedra of type $\Delta_{\mathfrak{qq}}$ are incident with g (this is the first arrangement shown in Figure 3.10). We observe three $\Delta_{\mathfrak{qq}}$ tetrahedra incident either f or g that are not contained in a layered solid torus. Label the H–even edges distinct from f and g in these tetrahedra a, b, and c and label the tetrahedra Δ_a, Δ_b, and Δ_c, respectively. It remains that a, b, and c may be the central edge in a balanced or an unbalanced subcomplex analysed above. Performing a compression of a canonical surface above f and g prevents any compressions of the same surface above a, b, and c and the surface will no longer form an annulus about these edges. Thus, we must consider the compressions we lose by performing one of the compressions described above.

In Figure 3.13 we extend this situation to the worst case scenario. Here, each of a, b, and c is the central edge of a $(3,7)$ balanced subcomplex containing two $\Delta_{\mathfrak{tt}}$ tetrahedra which are coloured the same. To each such subcomplex is attached a $(2,5)$ unbalanced subcomplex. By performing a compression of two canonical surfaces about f and g, we may no longer perform the same compressions to the canonical surfaces about these new subcomplexes. We extend K to include all maximal layered solid tori from these subcomplexes and extend E_K to include all degree 3 edges, the edges a, b, and c, together with the three additional degree 5 H–even edges. Using our previous deficit, we now have

$$\delta(K) = \mathfrak{e}_3(K) - \sum_{d=5}^{\infty}(d-4)\mathfrak{e}_d(K) - 2\sum_{i=1}^{3} d_{\varphi_i}(K) = 20-(5-4)\times 4-(7-4)\times 4-2 = 2$$

As the compression of two surfaces gives $2\sum_{i=1}^{3} d_{\varphi_i} \geq 8$, we give a total allocation of $+4$ to $2\sum_{i=1}^{3} d_{\varphi_i}(K)$, rather than our previous $+2$, to obtain the deficit of $\delta(K) = 0$. Note that this chain of subcomplexes may arise in different ways but the contribution from such a chain to $\delta(K)$ will not exceed the above.

As a final observation, we note that the edge h may be the central edge of a balanced or unbalanced subcomplex as above. We could perform an additional compression of the surfaces in this case (see [**JRST20b**], Figure 4). However, it is easier to note that in our set up there are only two $\Delta_{\mathfrak{tt}}$ tetrahedra meeting h and thus no performing our compression(s) about f and g will not prevent the compressions of any further subcomplexes which may be connected to h.

□

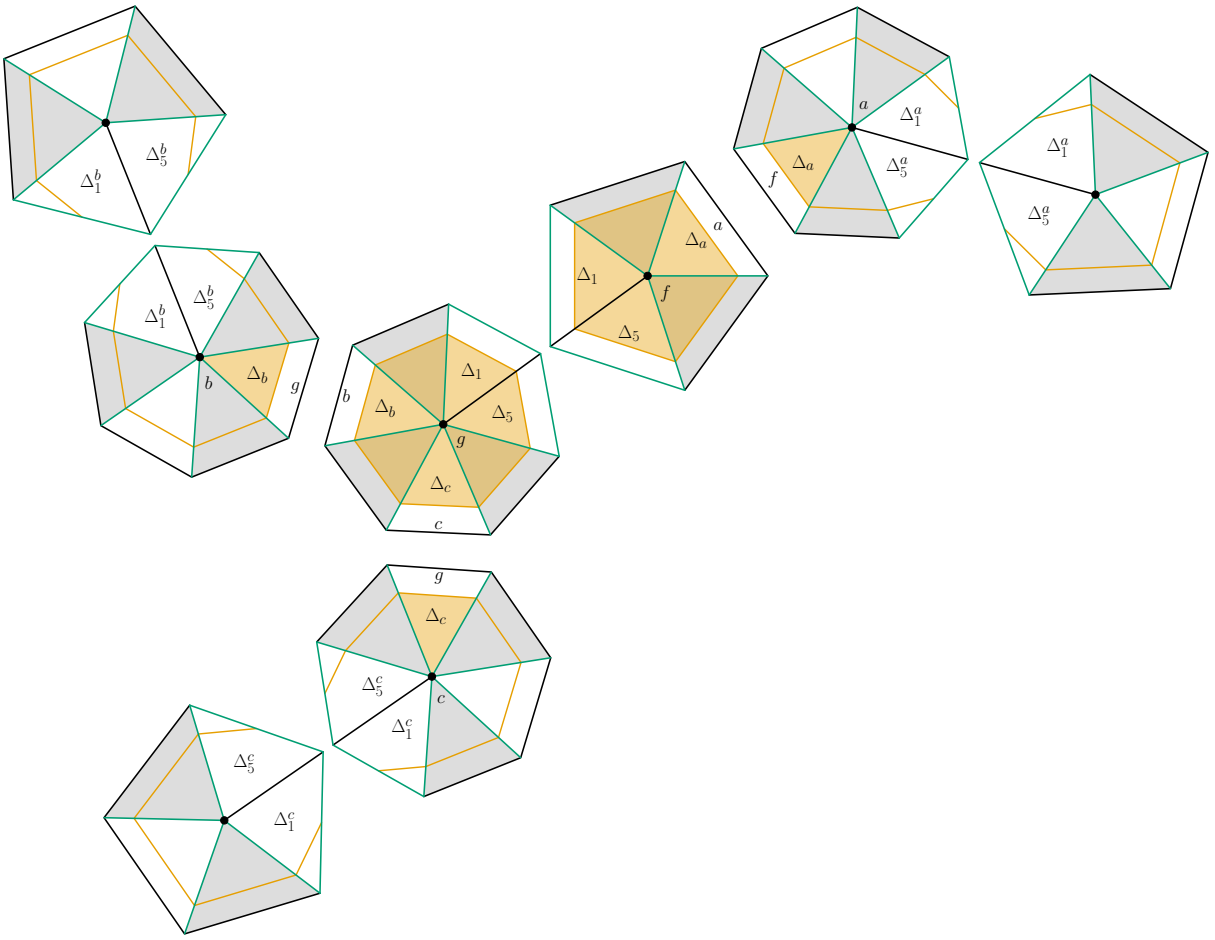

FIGURE 3.13. The maximum number of balanced and unbalanced subcomplexes which may be chained together through Δ_{qq} tetrahedra so that any compression of a canonical surface about f and g prevents a compression of the same surface in any other depicted subcomplex. The lines cutting through the tetrahedra show the intersection of normal discs in one canonical surface with the subcomplexes - quadrilaterals run parallel to the exterior edges and triangles intersect the exterior edges. The coloured shaded regions show the compressions performed in our analysis. No further compressions of the canonical surface about the central edge of a subcomplex with one of these shaded region can be performed. Grey shaded regions denote maximal layered solid tori.

There are several other arrangements in which we may perform a compression of at least one canonical surface. The following claim handles these and we leverage what we can from the previous proof in an attempt to avoid repetition.

Claim 6: If $(m, \deg(f)) \in \{(3,6),(2,5)\}$ and the intersection of a canonical surface S_{φ_i} with the $\deg(f)$ pairwise distinct tetrahedra incident with f consists only of normal of quadrilaterals, then we may adjust $d_{\varphi_i}(K)$ so that $\delta(K)$ is a deficit.

Proof of Claim 6: Using the notation from Claim 4, we assume Δ_{2i}, $1 \leq i \leq m$, belong to the almost supportive maximal layered solid tori incident with f and are of type Δ_{qq}. After

performing any compression in the following arguments, we do not change the types of the tetrahedra and only adjust the compressed surface(s).

First, suppose that $(m,\deg(f)) = (3,6)$ and that each of the maximal layered solid tori are coloured the same. Each of Δ_1, Δ_3, and Δ_5 must be of type Δ_{qq} and coloured the same. Two of the canonical surfaces S_{φ_i}, $i \in \{1,2,3\}$, each intersect these tetrahedra in six quadrilaterals forming an annulus around f. We can perform a compression of each surface by cutting along these annuli and pasting in two discs, each intersecting f once. This is illustrated for a single surface in Figure 3.14. The resulting surfaces are normal and each has two triangles intersecting f replacing the quadrilaterals.

Following arguments in Claim 5, the number of connected components in each surface is preserved under the compression, no component of the compressed surface is a sphere or projective plane, and the non–positivity of the Euler characteristic is preserved. Each compression contributed $+2$ to the corresponding d_{φ_i} term and we observe $2\sum_{i=1}^{3} d_{\varphi_i} \geq 8$. We assign $+2$ from the available $+8$ to $2\sum_{i=1}^{3} d_{\varphi_i}(K)$ and obtain a deficit

$$\delta(K) = \mathfrak{e}_3(K) - \sum_{d=5}^{\infty}(d-4)\mathfrak{e}_d(K) - 2\sum_{i=1}^{3} d_{\varphi_i}(K) = 3-2-2 = -1$$

Suppose that the H–even edge in Δ_1 opposite f is the central edge in an unbalance subcomplex. Denote this edge g. Suppose further that the intersection of at least one canonical surface S_{φ_i} with the tetrahedra incident with g consists only of normal quadrilaterals. After performing the compression around f we may not be able to perform a compression of this surface about g. To rectify this, we extend K and E_K by adding the maximal layered layered solid tori incident with g to K and adding the degree 3 edges in these tori together with g to E_K. Observe that this situation is symmetric for the remaining H–even edges in Δ_3 and Δ_5.

Assume we have three such unbalanced subcomplexes. Each such subcomplex contributes $+1$ to $\mathfrak{e}_3(K) - \sum_{d=5}^{\infty}(d-4)\mathfrak{e}_d$. We allocate an additional $+2$ from the remaining $+6$ to $2\sum_{i=1}^{3} d_{\varphi_i}(K)$ and obtain a deficit

$$\delta(K) = -1+3-2 = 0$$

By always allocating the total of $+4$ to $2\sum_{i=1}^{3} d_{\varphi_i}(K)$ we ensure that a gain is never obtained from this arrangement.

Continuing with $(m,\deg(f)) = (3,6)$, suppose instead that one of Δ_{2i}, $1 \leq i \leq 3$, is coloured differently from the other two. Without loss of generality, suppose this is Δ_2. It follows that Δ_1 and Δ_3 must be of type Δ_{qtt} corresponding to the two distinct subtypes with the edge opposite f coloured the same. Δ_5 is of type Δ_{qq} and coloured the same as Δ_4 and Δ_6. One of the canonical surfaces S_{φ_i}, $i \in \{1,2,3\}$, intersects these tetrahedra in six quadrilaterals forming an annulus around f. We may perform the same compression described above, cutting along this annulus and pasting in two discs, each intersecting f once. This contributes $+2$ to the corresponding

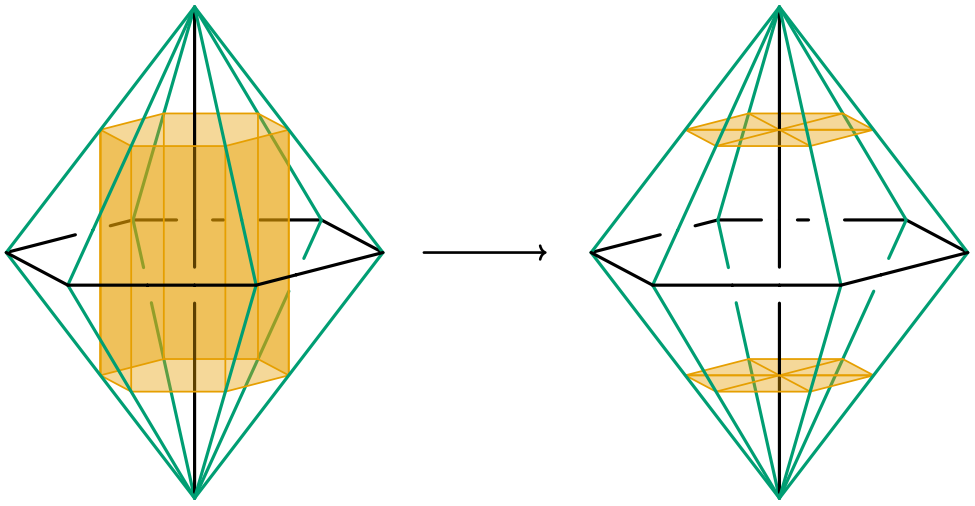

FIGURE 3.14. Compression of one canonical surface forming an annulus around the central edge of a $(3,6)$ unbalanced subcomplex. For the colourings given we may compress two canonical surfaces, however only one is drawn for clarity.

d_{φ_i}. Letting K be the union of the maximal layered solid tori and E_K the union of degree 3 edges in K and f we observe $2\sum_{i=1}^{3} d_{\varphi_i}(K) \geq 4$ and assign $+2$ of this to $2\sum_{i=1}^{3} d_{\varphi_i}(K)$, yielding the deficit $\delta(K) = -1$ as before.

We may have one additional unbalanced subcomplex intersecting K in Δ_5. We extend both K and E_K as before and note that this unbalanced subcomplex contributes $+1$ to $\delta(K)$ and the result is $\delta(K) = 0$, maintaining the deficit.

We now consider the subcomplexes arising when $(m, \deg(f)) = (2,5)$. We have Δ_2 and Δ_4 contained in maximal layered solid tori and hence are of type Δ_{qq}. To avoid repeating the arguments above we indicate the types and colourings of tetrahedra incident with f, the number of compressions and their contributions to $2\sum_{i=1}^{3} d_{\varphi_i}$, and the allocation to $2\sum_{i=1}^{3} d_{\varphi_i}(K)$. In each case, K consists of the union of the solid tori and E_K is the union of degree 3 edges in K and f. We also indicate if any additional unbalanced subcomplexes may need to be accounted for and extend both K and E_K as above.

- All five tetrahedra are of type Δ_{qq} and coloured the same. Two canonical surfaces S_{φ_i}, $i \in \{1,2,3\}$, each intersect these tetrahedra in five quadrilaterals forming an annulus around f and can be compressed by cutting along the annulus and pasting in two discs, each intersecting f once. Each compression contributes $+2$ to the corresponding d_{φ_i} and we obtain $2\sum_{i=1}^{3} d_{\varphi_i}(K) \geq 8$. Of this $+8$ we assign $+2$ to $2\sum_{i=1}^{3} d_{\varphi_i}(K)$ obtaining the deficit $\delta(K) = -1$.
  We may observe up to three additional unbalanced subcomplexes, with the possible central edges the remaining H–even edges in Δ_1, Δ_3, and Δ_5. We extend K and E_K appropriately and allocate an additional $+2$ to $2\sum_{i=1}^{3} d_{\varphi_i}(K)$ to ensure $\delta(K)$ remains a deficit.

- Δ_2, Δ_3, and Δ_4 are of type $\Delta_{\mathfrak{qq}}$ and coloured the same with Δ_1 and Δ_5 of type $\Delta_{\mathfrak{qtt}}$ corresponding to the two distinct subtypes with the edge opposite f coloured the same. One canonical surface S_{φ_i}, $i \in \{1,2,3\}$, intersects these tetrahedra in five quadrilaterals forming an annulus around f and can be compressed by cutting along the annulus and pasting in two discs, each intersecting f once. This compression contributes $+2$ to the corresponding d_{φ_i} and we obtain $2\sum_{i=1}^{3} d_{\varphi_i}(K) \geq 4$. Of this $+4$ we assign $+2$ to $2\sum_{i=1}^{3} d_{\varphi_i}(K)$ obtaining the deficit $\delta(K) = -1$.
  The only additional unbalanced subcomplex must contain Δ_3, using its remaining $H-$even edge as its central edge. This contributes an additional $+1$ to $\delta(K)$ and the deficit is maintained without any further allocations.

- Δ_2 and Δ_4 are coloured differently with Δ_1, Δ_3, and Δ_5 each of a distinct $\Delta_{\mathfrak{qtt}}$ type. One canonical surface S_{φ_i}, $i \in \{1,2,3\}$, intersects these tetrahedra in five quadrilaterals forming an annulus around f. The compression, contributions, and allocations follow the same as the previous colouring and we obtain $\delta(K) = -1$. There are no additional unbalanced subcomplexes to consider.

Hence for each unbalanced subcomplex we may allocate a sufficient amount to $2\sum_{i=1}^{3} d_{\varphi_i}(K)$ from each compression to obtain a deficit in $\delta(K)$. □

The only remaining subcomplexes to consider are the unbalanced subcomplexes in which no canonical surface is compressible. These can be loosely characterised as:

- $(3,6)$ and $(2,5)$ unbalanced subcomplexes in which each layered solid torus is coloured differently, forcing the remaining tetrahedra to correspond to different $\Delta_{\mathfrak{qtt}}$ types; and
- $(2,5)$ unbalanced subcomplexes in which two tetrahedra are of type $\Delta_{\mathfrak{tt}}$, both included in an additional balanced or unbalanced subcomplex with at least two additional $\Delta_{\mathfrak{tt}}$ tetrahedra.

In each such subcomplex, or an expanded neighbourhood of the subcomplex, we must see an increased number of tetrahedra of types $\Delta_{\mathfrak{tt}}$ and $\Delta_{\mathfrak{qtt}}$ to avoid compressions. We consider these in the context of (3.2.4), which we remind the reader is

$$\mathfrak{e}_3 + 2k = n_{\mathfrak{tt}} + n_{\mathfrak{qtt}} + 2\sum_{i=1}^{3} d_{\varphi_i} + \sum_{d=5}^{\infty} (d-4)\mathfrak{e}_d$$

Each term on the right side of the equation is non–negative and their sum may only exceed the total number of degree 3 edges when $k > 0$. For example, when $k = 0$ the contributions to both sides must be equal (as observed in [**JRST20b**]). Each remaining subcomplex K will be built using one of the $(2,5)$ or $(3,6)$ unbalanced subcomplexes described above with E_K being the union of degree 3 edges and the degree 5 or 6 edge. Let $\mathscr{P}$ denote the set of all such subcomplexes.

Claim 7: $\sum_{K\in\mathscr{P}} \delta(K) \leq k$.

Proof of Claim 7: Consider first a $(3,6)$ unbalanced subcomplex where Δ_2, Δ_4, and Δ_6 correspond to the layered solid tori and are each coloured distinctly. The remaining tetrahedra are each of type Δ_{qtt}. The contribution to the left side of (3.2.4) is $+3$ and the contribution to the right side is $+5$. For equality to hold we require $k \geq 1$. Inductively, if $k_{(3,6)}$ denotes the number of such subcomplexes K, then we require $k \geq k_{(3,6)}$.

Consider instead a $(2,5)$ unbalanced subcomplex where Δ_2 and Δ_4 correspond to the layered solid tori and are each coloured distinctly. If these tetrahedra are coloured distinctly, then Δ_3 is of type Δ_{qtt} and Δ_1 and Δ_5 are either both of type Δ_{tt} or both of type Δ_{qtt}. The contribution to the left side of (3.2.4) is $+2$ and the contribution to the right side is $+4$. For equality to hold we require $k \geq 1$. Inductively, if $k_{(2,5)}$ denotes the number of such subcomplexes K, then we require $k \geq k_{(2,5)}$.

Alternatively, suppose Δ_2 and Δ_4 are coloured the same. Then Δ_3 is of type Δ_{qq} and coloured the same and Δ_1 and Δ_5 are of type Δ_{tt} and coloured the same. The contribution to the left side of (3.2.4) is $+2$ and the contribution to the right is now $+3$. We consider the possible expanded neighbourhoods of the constellation.

Let f, g, and h denote the H–even edges incident with Δ_1 and Δ_5 as in Figure 3.8. Without loss of generality, we consider the possible $(m_g, \deg(g))$ subcomplexes surrounding g. Observe that these subcomplexes must be balanced, otherwise at least one canonical surface will be compressible. All such balanced subcomplexes, up to symmetry, about g are illustrated in Figure 3.15. We omit any arguments concerning the pairwise distinctness of the tetrahedra that have already been explained in previous claims.

In each of the illustrated subcomplexes we observe two additional tetrahedra of types Δ_{qtt} or Δ_{tt} bringing the total contribution to the right side of (3.2.4) to at least $+5$. For equality to hold we require $k > 1$. Inductively, letting $k'_{(2,5)}$ denote the number of such subcomplexes K, we require $k > k'_{(2,5)}$.

The final arrangement to consider is when $(m_g, \deg(g)) = (1,5)$ and the neighbourhood of g is modelled on $X^1_{5;4}$, as in Claim 5 (see Figure 3.11). As stated in the proof of Claim 5, the neighbourhood of h cannot also be modelled on $X^1_{5;4}$ and so we apply the above analysis to h. Note that contribution from the additional degree 3 edge coming from the maximal layered solid torus with unital edge g is cancelled out by $\deg(g) = 5$.

Letting the number of subcomplexes in $\mathscr{P}$ be $k_{(3,6)} + k_{(2,5)} + k'_{(2,5)}$ and combining the above arguments, we require $k > k_{(3,6)} + k_{(2,5)} + k'_{(2,5)}$ to ensure (3.2.4) holds. For each $K \in \mathscr{P}$ we

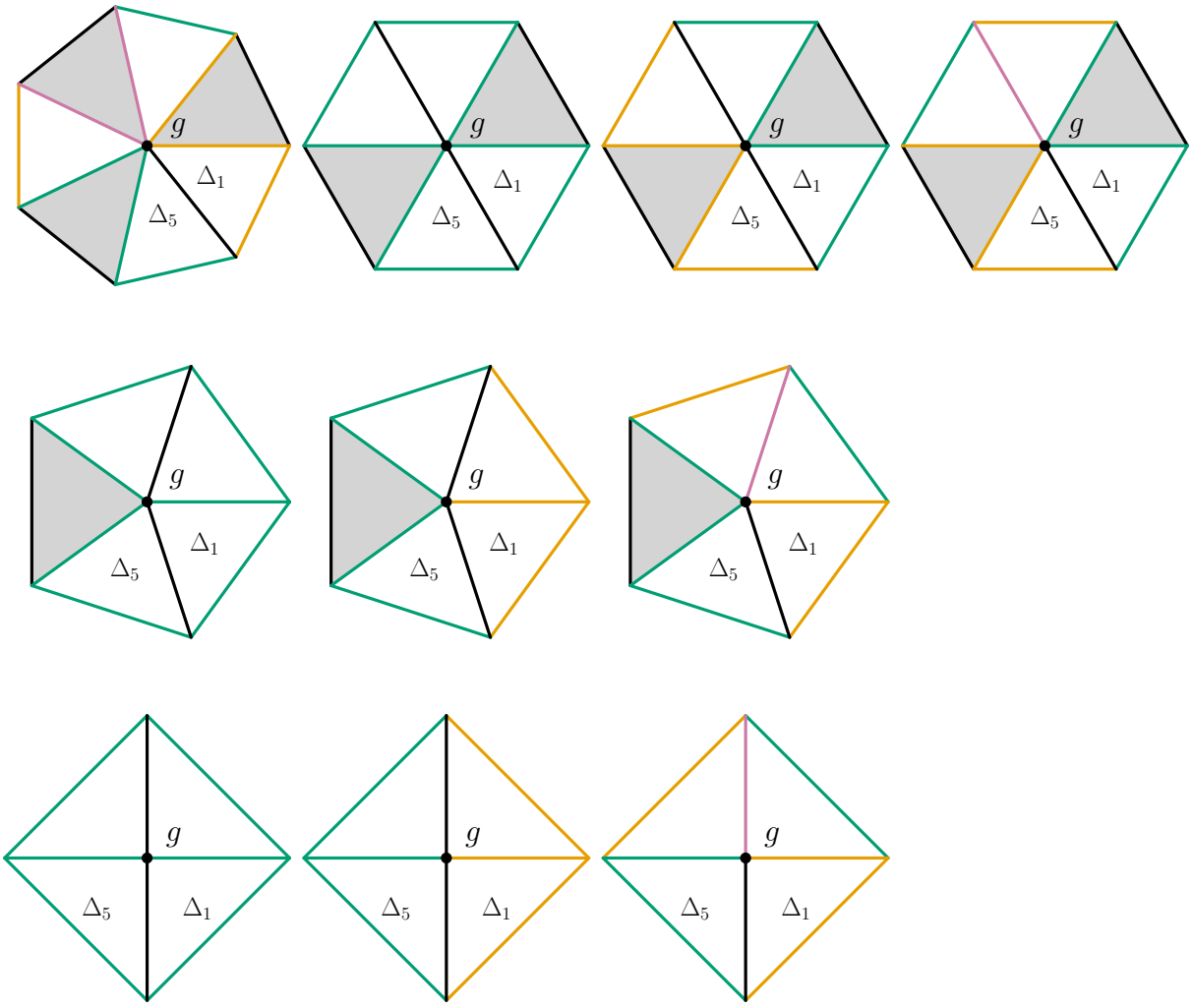

FIGURE 3.15. The balanced subcomplexes about g, up to symmetry, for which there is no compression of a canonical surface.

have $\delta(K) = 1$ and hence

$$\sum_{K \in \mathscr{P}} \delta(K) = k_{(3,6)} + k_{(2,5)} + k'_{(2,5)} < k.$$

□

Combining Claims 1–7 we obtain

$$\sum_{K \in \mathscr{K}} \delta(K) = \sum_{K \in \mathscr{K}} \left(\mathfrak{e}_3(K) - \sum_{d=5}^{\infty} (d-4)\mathfrak{e}_d(K) - 2\sum_{i=1}^{3} d_{\varphi_i} \right) \leq k,$$

and hence the desired contradiction with (3.3.2). This completes the proof of Theorem 3.1.

3.3.4. Bounding $n_{\mathrm{tt}} + n_{\mathrm{qtt}}$. The proof of Theorem 3.1 has important consequences for the rank–2 coloured minimal triangulations. It provides the main tool for determining the allowable profiles for a given H–thickness. The result is as follows.

Corollary 3.2 Let M be a closed, orientable, irreducible, connected 3–manifold with minimal triangulation $\mathscr{T}$. Suppose that all edge loops are coloured by the rank–2 subgroup H of $H^1(M;\mathbb{Z}_2)$ and that $\mathscr{T}$ is $(\Delta_{qq},4)$–free with respect to the colouring with $|\mathscr{T}| = (2+k) + \sum_{i=1}^{3} \|\varphi_i\|$. Then $n_{tt} + n_{qtt} \leq 3k$.

Proof From (3.0.1) we have,

$$\mathfrak{e}_3 \leq 4 + 3k - 2(k+2) + \sum_{i=1}^{3} d_{\varphi_i} + \sum_{d=5}^{\infty} (d-4)\mathfrak{e}_d.$$

Recall that for the canonical surface S_{φ_i} dual to $\varphi_i \in H$ we have $\|\varphi_i\| = -\chi(S_{\varphi_i}) - d_{\varphi_i}$, $d_{\varphi_i} \geq 0$. Combining this with $|\mathscr{T}|$ the inequality becomes

$$\mathfrak{e}_3 \leq 4 + 3k - 2\left(|\mathscr{T}| + \sum_{i=1}^{3} \chi(S_{\varphi_i})\right) + \sum_{d=5}^{\infty} (d-4)\mathfrak{e}_d.$$

Combining this with (3.2.2) gives the desired result. □

3.4. Rank–2 coloured minimal triangulations with H–thickness 1

The results of the previous section set up a general framework in which we can determine profiles of minimal triangulations for a given H–thickness. In this section we take the H–thickness equal to one and consider minimal triangulations $\mathscr{T}$ satisfying

$$|\mathscr{T}| = 3 + \sum_{i=1}^{3} \|\varphi_i\|.$$

3.4.1. Profiles of rank–2 colourings. Given a rank–2 coloured minimal triangulation $\mathscr{T}$ of the closed, orientable, irreducible, connected 3–manifold M, where the rank–2 colouring is by the subgroup $H \leq H^1(M;\mathbb{Z}_2)$, recall that the profile of $\mathscr{T}$ is the tuple $(n_\emptyset, n_{tt}, n_{qtt}, n_{qq}, n_{qqq})$ so that the number of a tetrahedra in $\mathscr{T}$ can be expressed as

$$|\mathscr{T}| = n_\emptyset + n_{tt} + n_{qtt} + n_{qq} + n_{qqq}.$$

Using Proposition 3.20 and Corollary 3.2 we provide a strengthened version of Lemma 3 from [**JRT13**], classifying the allowable profiles of minimal triangulations when $t_H(M) = 1$.

Proposition 3.23 *Let M be a closed, orientable, irreducible, connected 3–manifold with minimal triangulation $\mathscr{T}$. Suppose all edges are coloured by the rank–2 subgroup H of $H^1(M;\mathbb{Z}_2)$ and that $|\mathscr{T}| = 3 + \sum_{i=1}^{3} \|\varphi_i\|$. Suppose further that $\mathscr{T}$ is $(\Delta_{qq},4)$–free with respect to the colouring. Then $n_{tt} + n_{qtt} \leq 3$ and the profile of $\mathscr{T}$ is one of the following forms:*

$$(0,0,2,n_{qq},n_{qqq}), \quad (0,0,3,n_{qq},n_{qqq}), \quad (0,0,3,n_{qq},0)$$

where $n_{qq}, n_{qqq} > 0$. Moreover, there is a unique H–even edge incident with all tetrahedra of type Δ_{qtt}.

Proof As $t_H(M) = 1$ we have $n_{tt} + n_{qtt} \leq 3$ by Corollary 3.2. We first show that $n_{qtt} \neq 0$ and use this to show that $n_{tt} = 0$.

For a contradiction, suppose that $n_{qtt} = 0$.

If $n_{qqq} > 0$, then $n_\emptyset = n_{tt} = n_{qq} = 0$ as each face of a tetrahedron of type $\Delta_\emptyset$, Δ_{tt}, or Δ_{qq} contains at least one H–even edge and M is connected. This forces the profile of $\mathscr{T}$ to be $(0,0,0,0,n_{qqq})$. As $t_H(M)$ is odd, this is impossible from Proposition 3.20. Hence $n_{qqq} = 0$.

If $n_{tt} = 0$, then either all tetrahedra are of type $\Delta_\emptyset$ or all tetrahedra are of type Δ_{qq}. In either case, this contradicts the fact that $H^1(M;\mathbb{Z}_2)$ has rank at least two. Hence $n_{tt} \neq 0$ and we must have $n_{tt} = 2$ from Lemma 3.17. Both tetrahedra of type Δ_{tt} must be of distinct subtypes lest $H^1(M;\mathbb{Z}_2)$ has rank one; suppose one has three i–even edges and the other has three j–even edges for $i, j \in \{1,2,3\}$ and $i \neq j$. Pulling back the colouring to $\widetilde{\Delta}$ we observe an odd number of faces with one H–even edge and two i–even edges, contradicting the fact that M is closed. Since all possibilities lead to a contradiction, we have $n_{qtt} \neq 0$.

We now show that $n_{tt} = 0$.

Suppose, to the contrary, that $n_{tt} = 2$. As $n_{qtt} \neq 0$ it must be that $n_{qtt} = 1$. Let Δ_0 denote the tetrahedron of type Δ_{qtt} with Δ_1 and Δ_2 of type Δ_{tt}. There is an H–even edge e incident to Δ_0, Δ_1, and Δ_2. Let f and g denote the two remaining H–even edges in Δ_1, oriented so that $e + f + g$ homologically is the boundary of a face. As $M \neq S^3$, we have from [**JR03**, Corollary 5.4] and [**JRT09**, Lemma 7] that this face is neither a cone nor dunce hat. As $\mathscr{T}$ has only one vertex, it follows that either $e = f = g$ or $e \neq f = g$. Let $B(f)$ denote the abstract neighbourhood of f, considered with an orientation, and denote the quotient map $\rho_f : B(f) \to \mathscr{T}$. As $f = g$ there exist two tetrahedra in $B(f)$ whose image under ρ_f is Δ_1. Moreover, the images of these tetrahedra induce opposite orientations on Δ_1, contradicting the orientability of M. This completes the proof that $n_{tt} = 0$ and $n_{qtt} \neq 0$.

We have shown that $n_{qtt} \in \{1,2,3\}$ and $n_{tt} = 0$. An immediate observation is that $n_\emptyset = 0$ as M is connected. Hence the remaining profiles are of the form $(0,0,n_{qtt},n_{qq},n_{qqq})$. If $n_{qtt} = 1$, then the H–even edge e incident with the single Δ_{qtt} tetrahedron is incident with a face containing two i–even edges and a face containing two j–even edges, $i, j \in \{1,2,3\}$ with $i \neq j$. As this contradicts M being closed, we have $n_{qtt} \neq 1$.

The remaining profiles are of the form $(0,0,2,n_{qq},n_{qqq})$ and $(0,0,3,n_{qq},n_{qqq})$. For each profile there is a unique H–even edge, e, incident with all tetrahedra of type Δ_{qtt}. Moreover $\deg(e) > 3$ since otherwise it would be contained in a maximal layered solid torus by Lemma 3.8 and all tetrahedra incident to it would be of type $\Delta_\emptyset$ or Δ_{qq}.

Our final consideration is the profile $(0,0,2,n_{\mathfrak{qq}},n_{\mathfrak{qqq}})$ as we will show that $n_{\mathfrak{qqq}} \neq 0$ in this case. Observe that the two $\Delta_{\mathfrak{qtt}}$ tetrahedra must be of the same subtype. Each of these tetrahedra must have two i–even, two j–even, and one k–even edge for $i,j,k \in \{1,2,3\}$ with $i \neq j \neq k$. If $n_{\mathfrak{qqq}} = 0$, then the two k–even edges must be identified to form a degree 2 edge, which is impossible from Lemma 3.7. Hence if $n_{\mathfrak{qtt}} = 2$, then $n_{\mathfrak{qqq}} > 0$. □

3.4.2. H–thin layered solid tori and central subcomplexes. Let $\mathbf{T} = \mathbf{T}(e)$ be a maximal layered solid torus in $\mathscr{T}$ containing a degree 3 edge e. As we are assuming $t_H(M) = 1$ we have $n_{\emptyset} = 0$ and thus $\mathbf{T}$ is of type $\Delta_{\mathfrak{qq}}$. We define a H–thin layered solid torus as follows.

Let f be the first H–even edge in $\mathbf{T}$ with $\deg(f) \geq 5$. We consider the order of the H–even edges in $\mathbf{T}$ to be the order they are introduced via the layering procedure. The **H–thin layered solid torus** $\mathbf{T}_{th} \subset \mathbf{T}$ is the layered solid torus subcomplex in $\mathbf{T}$ such that f is the unique H–even boundary edge. Moreover, this means that $\deg_{\mathbf{T}_{th}}(f) = 1$. If f is the unique H–even boundary edge of $\mathbf{T}$, then we set $\mathbf{T}_{th} = \mathbf{T}$. By this definition, a thin layered solid torus may not be maximal.

We use the concept of a thin layered solid torus to provide a modified version of (3.2.4). Let $\mathfrak{e}_{d,x}$ denote the number of H–even edges of degree d incident with exactly x pairwise distinct H–thin layered solid tori, where $x \geq 0$. In particular, such an edge must be the unique H–even boundary edge of all x layered solid tori when $x \geq 2$. With this notation, we may write

$$\mathfrak{e}_d = \sum_{x \geq 0} \mathfrak{e}_{d,x} \tag{3.4.1}$$

Moreover, the number of degree 3 edges is equal to the number of H–thin layered solid torus. By noting that no H–even edge of degree d is counted by more than one $e_{d,x}$, we write

$$\mathfrak{e}_3 = \sum_{d=4}^{\infty} \sum_{x \geq 0} x\mathfrak{e}_{d,x} \tag{3.4.2}$$

Using $t_H(M) = 1$ and $n_{\mathfrak{tt}} = 0$ from Proposition 3.23, we rewrite (3.2.4) as

$$0 = (n_{\mathfrak{qtt}} - 2) + 2\sum_{i=1}^{3} d_{\varphi_i} - \mathfrak{e}_3 + \sum_{d=4}^{\infty} (d-4)\mathfrak{e}_d$$

noting the change of the starting index $d = 4$ in the final sum. Substituting in (3.4.1) and (3.4.2) we obtain

$$0 = (n_{\mathfrak{qtt}} - 2) + 2\sum_{i=1}^{3} d_{\varphi_i} + \sum_{d=4}^{\infty} \sum_{x \geq 0} (d-4-x)\mathfrak{e}_{d,x} \tag{3.4.3}$$

Define the **central subcomplex** of $\mathscr{T}$ to be the union of all tetrahedra incident with the unique H–even edge along which the tetrahedra of type $\Delta_{\mathfrak{qtt}}$ meet. We determine the possible central subcomplexes when $n_{\mathfrak{qtt}} = 2$.

Remark 3.24 In many of arguments that follow we will encounter the same, or similar arrangements to those analysed in the proof of Theorem 3.1. In particular, these arguments will involve having two maximal layered solid tori intersecting in more than one edge. When these are encountered we will not repeat the arguments and instead note that they have been explained previously.

3.4.3. Central subcomplexes for $(0,0,2,n_{\mathrm{qq}},n_{\mathrm{qqq}})$. Substituting $n_{\mathrm{qtt}}=2$ into (3.4.3) yields

$$0=2\sum_{i=1}^{3}d_{\varphi_i}+\sum_{d=4}^{\infty}\sum_{x\geq 0}(d-4-x)\mathfrak{e}_{d,x} \tag{3.4.4}$$

Observe that since $d_{\varphi_i}\geq 0$ for all $i\in\{1,2,3\}$, any positive contribution to this equation must be cancelled by a some collection of summands in the second sum. We check the possible contributions.

Consider an H–even edge e of degree d meeting exactly x pairwise distinct H–thin layered solid tori. From Lemma 3.5, at most $d/2$ maximal layered solid tori may meet along e and thus

$$d-4-x\geq d-4-\frac{d}{2}=\frac{1}{2}(d-8)$$

Hence, $(d-4-x)\mathfrak{e}_{d,x}>0$ for all $x\geq 0$ when $d\geq 9$. The remaining values of d require a finer analysis of the cases when $d-4-x=0$.

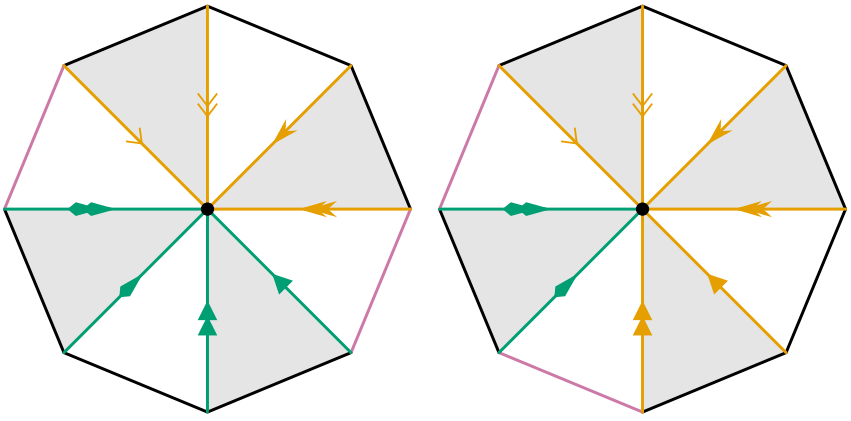

FIGURE 3.16. Arrangements of tetrahedra around an H–even edge of degree 8 meeting exactly four H–thin layered solid tori. Two of the tetrahedra are of type Δ_{qtt}. A top-down perspective is used.

Suppose that $d=8$. Then $x\leq 4$ and $d-4-x>0$ when $x\leq 3$. If $x=4$, then four pairwise distinct maximal layered solid tori of type Δ_{qq} meet along an H–even edge of degree 8. Using previous arguments, if all tetrahedra meeting this edge are of type Δ_{qq}, then they are pairwise distinct and two of the canonical normal surfaces dual to the colouring admit compression discs, each giving $+2$ to the corresponding d_{φ_i} terms. If the two tetrahedra of type Δ_{qtt} meet this edge, then the remaining tetrahedra are pairwise distinct and one of the canonical normal

surfaces dual to the colouring admits a compression disc (these arrangements are illustrated in Figure 3.16). Both cases yield a positive contribution to (3.4.4).

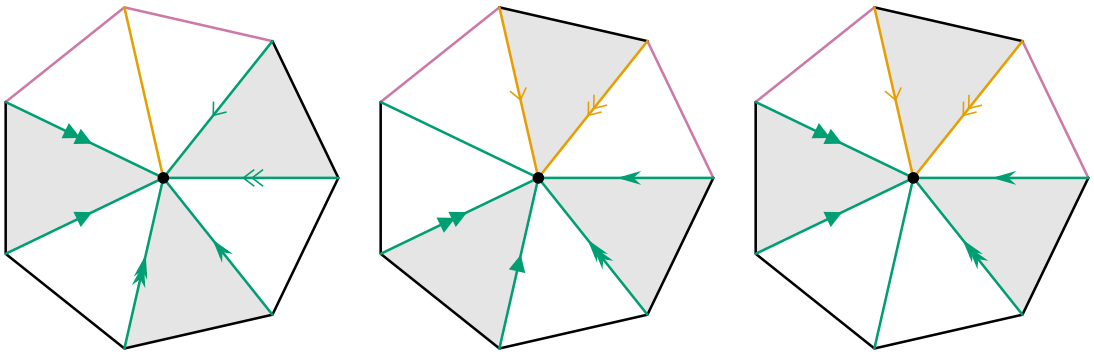

FIGURE 3.17. Arrangements of tetrahedra around an H–even edge of degree 7 meeting exactly three H–thin layered solid tori. The shaded tetrahedra belong to the layered solid tori. Two of the tetrahedra are of type Δ_{qtt}. A top-down perspective is used.

Suppose that $d = 7$. Then $x \leq 3$ and $d - 4 - x > 0$ when $x \leq 2$. We consider the possible arrangements for $x = 3$. Let f denote the H–even edge of degree 7. If all tetrahedra meeting f are of type Δ_{qq}, then seven pairwise distinct tetrahedra meet f and two of the canonical normal surfaces dual to the colouring admit compression discs. Instead, consider the situation in which the two tetrahedra of type Δ_{qtt} meet f. As the tetrahedra of type Δ_{qtt} partition the tetrahedra of type Δ_{qq} meeting in f into two subcomplexes there are, up to symmetry, three partitions to consider. These are illustrated in Figure 3.17. Applying the same arguments, f must meet seven pairwise distinct tetrahedra lest two maximal layered solid tori meet in more than one edge. Hence one of the canonical normal surfaces admits a compression disc. In all cases, a positive contribution to (3.4.4) is obtained.

Suppose now that $d = 6$. Then $x \leq 3$ and $d - 4 - x > 0$ when $x \leq 1$. The arrangements when $x = 3$ are analogous to the above, and at least one of the canonical normal surfaces admits a compression disc. We consider $x = 2$ and enumerate the possible arrangements, up to symmetry, in Figure 3.18. We examine these cases individually, using the notation from the figure.

(i) Observe that $\Delta_0 \neq \Delta_2$, $\Delta_0 \neq \Delta_4$, and $\Delta_2 \neq \Delta_4$ as this would result in the two maximal layered solid tori intersecting in more than one edge. We also must have $\Delta_0 \neq \Delta_3$ as this would leave Δ_2 and Δ_4 each with a cone face. As $\mathscr{T}$ is 0–efficient and not S^2, this cannot happen.

Suppose that $\Delta_2 = \Delta_3$. The induced identifications are illustrated in Figure 3.19. Observe that the tetrahedron Δ_2 forms the one tetrahedron layered solid torus $\mathrm{LST}(1,2,3)$. In particular, this is maximal and intersects another maximal layered solid torus in a face. Hence $\Delta_2 \neq \Delta_3$. Hence we have six pairwise distinct tetrahedra meeting in a degree 6 H–even edge. Two of the canonical normal surfaces dual to the colouring admit compression discs and we obtain a contribution of $+2$ to each of the corresponding d_{φ_i}'s.

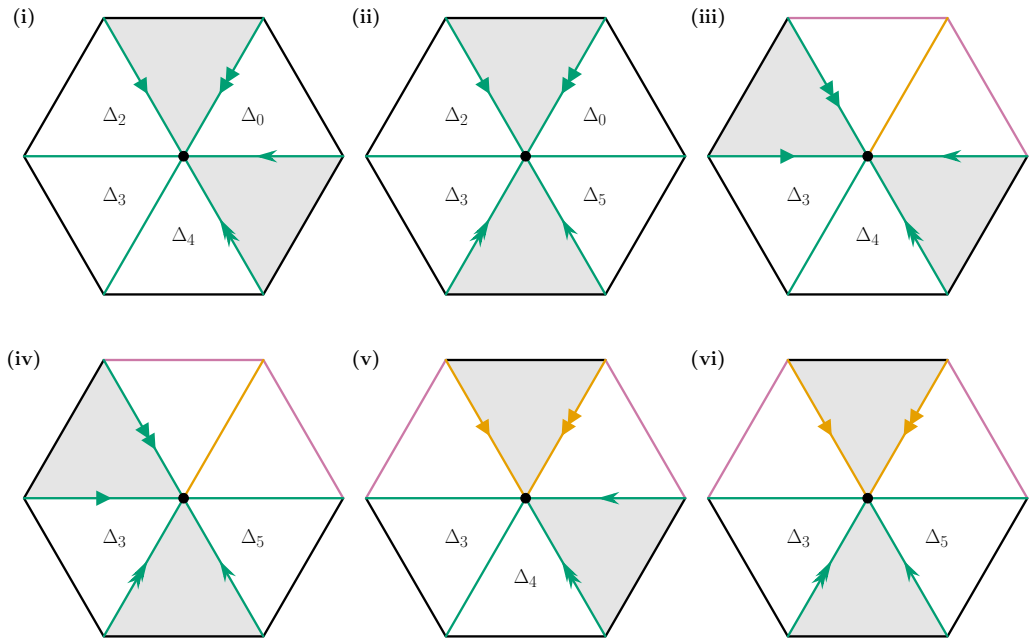

FIGURE 3.18. Arrangements of tetrahedra around an H–even edge of degree 6 meeting exactly two H–thin layered solid tori. The shaded tetrahedra belong to the H–thin layered solid tori and labelled tetrahedra are of type $\Delta_{\mathtt{qq}}$. The unshaded, unlabelled tetrahedra are of type $\Delta_{\mathtt{qtt}}$. A top down perspective is used.

(ii) Following the reasoning in (i), we must have $\Delta_0 \neq \Delta_3$, $\Delta_2 \neq \Delta_3$, and $\Delta_0 \neq \Delta_5$. The only identifications that we need to check are $\Delta_0 = \Delta_2$ and $\Delta_3 = \Delta_5$. As these are symmetric, we only check the former. The induced identifications are illustrated in Figure 3.20. The resulting boundary of this subcomplex is a pinched torus consisting of four faces. If, in addition, $\Delta_3 = \Delta_5$, then we obtain two layered solid tori meeting in two faces and conclude that M is a lens space. As we assume $\mathscr{T}$ admits a rank–2 colouring, this is not possible. Hence this arrangement is possible with exactly one of $\Delta_0 = \Delta_2$ or $\Delta_3 = \Delta_5$. In either case, we obtain a contribution of 0.

(iii) If $\Delta_3 = \Delta_4$, then the two maximal layered solid tori meet in more than one edge. This is not possible and we have six pairwise distinct tetrahedra. One of the canonical normal surfaces dual to the colouring admits a compression disc and we obtain a contribution of $+2$ to the corresponding d_{φ_i}.

(iv) If $\Delta_3 = \Delta_5$, then the two maximal layered solid tori meet in more than one edge. This is not possible and we have six pairwise distinct tetrahedra. One of the canonical normal surfaces dual to the colouring admits a compression disc and we obtain a contribution of $+2$ to the corresponding d_{φ_i}.

(v) Setting $\Delta_3 = \Delta_4$ is analogous to (i) and we obtain a maximal $\mathrm{LST}(1,2,3)$ which meets another maximal layered solid torus in a face. Hence the tetrahedra are pairwise distinct and we obtain a positive contribution as above.

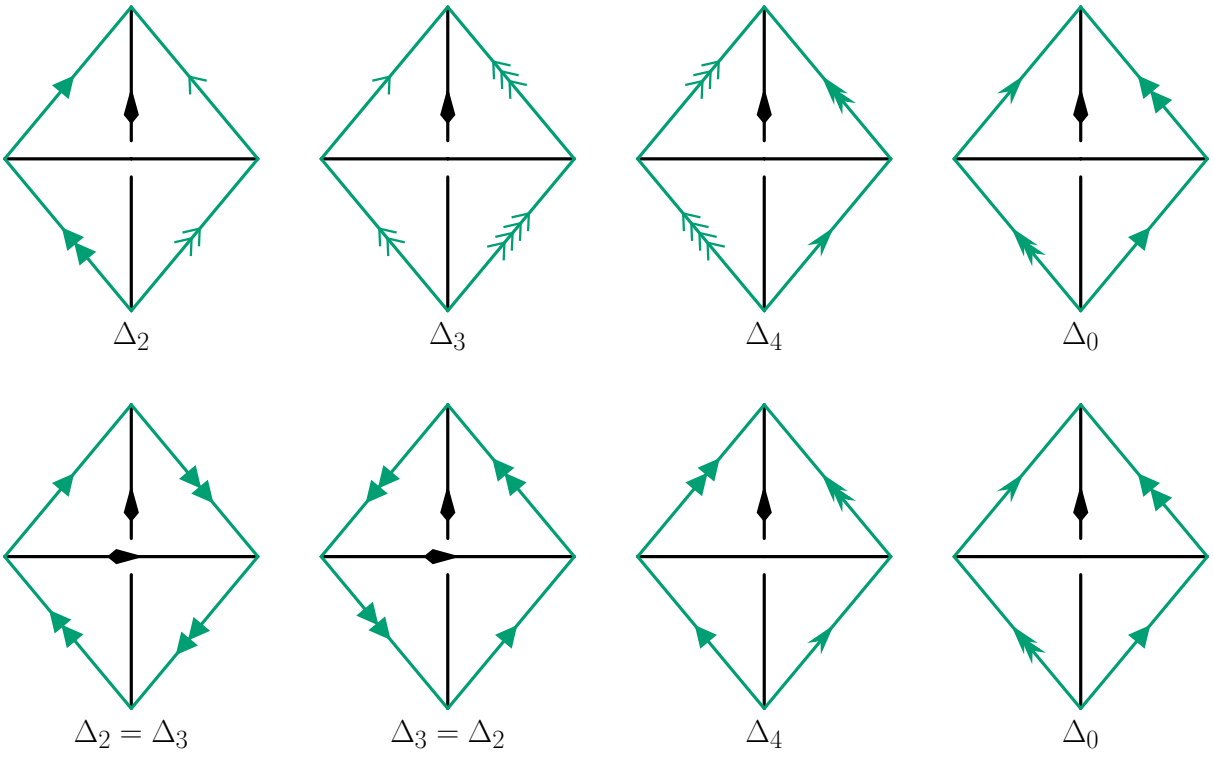

FIGURE 3.19. Induced identifications on Δ_2, Δ_3, Δ_4, and Δ_0 when $\Delta_2 = \Delta_3$ for arrangement (i) in Figure 3.18. The H–even edge at the back is the edge of degree 6. The first row shows the tetrahedra before the identification $\Delta_2 = \Delta_3$. The second row shows the tetrahedra after this identification.

(vi) Setting $\Delta_3 = \Delta_5$ extends the layered solid torus by one tetrahedron. This configuration is valid and contributes 0.

Combining all of the above cases, only (ii) and (vi) give a contribution of 0 to (3.4.3).

As the second last collection of cases, suppose $d = 5$. Then $x \leq 2$ and $d - 4 - x > 0$ only if $x = 0$. When $x = 2$, we must have five pairwise distinct tetrahedra meeting around the H–even edge of degree 5. To see this, note that if two of the tetrahedra are of type Δ_{qtt} then we can only have one tetrahedron of type Δ_{qq} which is not contained in the layered solid tori. Otherwise if all tetrahedra are of type Δ_{qq}, then the case is analogous to identifying Δ_2 and Δ_3 in Figure 3.18, (ii). Hence if $x = 2$, then we obtain a positive contribution to (3.4.3) taking the compression discs into account.

It remains to check $x = 1$. First suppose that all tetrahedra in the subcomplex are of type Δ_{qq}. We examine the neighbourhoods of the degree 5 edge by considering the subcomplexes listed in Figure 3.2. We can immediately rule out $X_{5;1}$, $X^0_{5;2}$, and $X^1_{5;2}$ as these do not admit a colouring by a non-trivial $\mathbb{Z}_2$ class. We may also rule out $X^0_{5;3}$ as this forms $\mathrm{LST}(3,5,8)$ which does not contain a degree 3 edge, and $X^1_{5;3}$ as this would result in two maximal layered solid tori meeting in a face. The neighbourhood $X^2_{5;3}$, from the identification of the edge e, would require a tetrahedron of type Δ_{tt} and we may rule it out. If the neighbourhood is modelled on

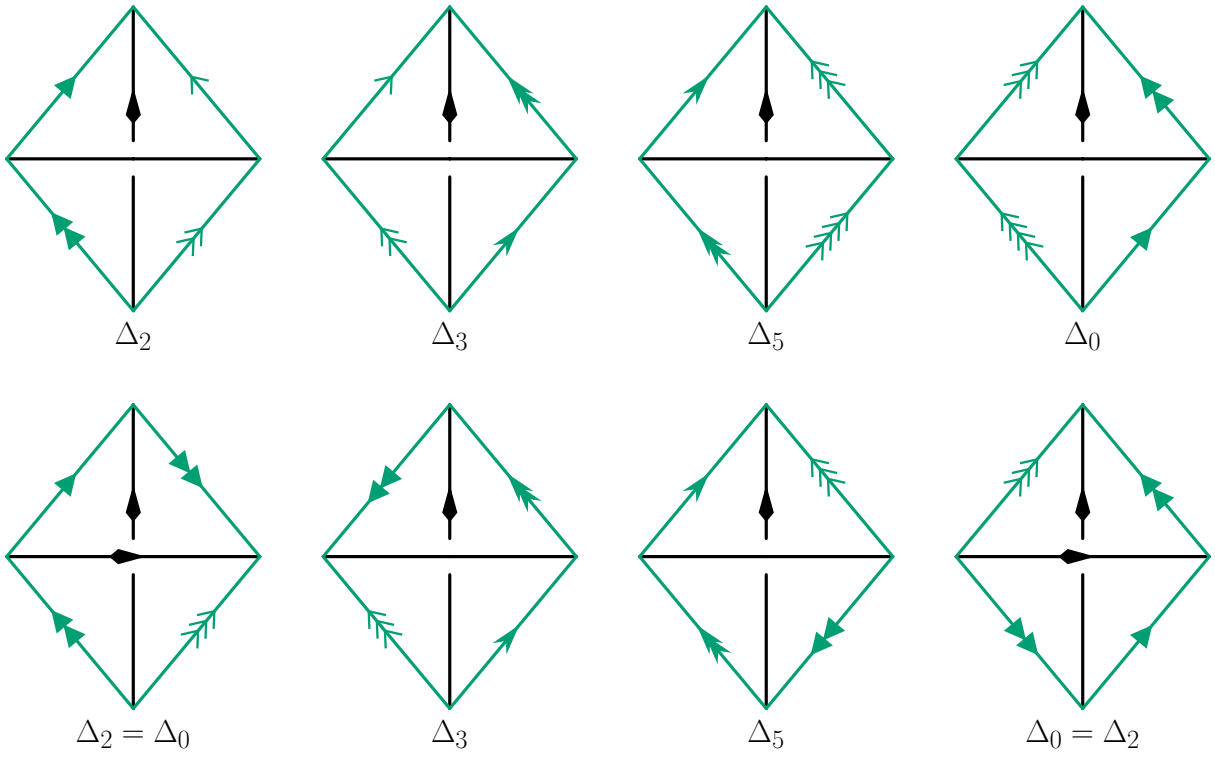

FIGURE 3.20. Induced identifications on Δ_2, Δ_3, Δ_4, and Δ_0 when $\Delta_0 = \Delta_2$ for arrangement (ii) in Figure 3.18. The H–even edge at the back is the edge of degree 6. The first row shows the tetrahedra before the identification $\Delta_0 = $. The second row shows the tetrahedra after this identification.

$X_{5;5}$, then there are five pairwise distinct tetrahedra and we find the aforementioned compression discs.

The only remaining neighbourhoods are $X^0_{5;4}$ and $X^1_{5;4}$. We illustrate these with the induced identifications in Figure 3.21. We observe a contribution of 0 to (3.4.3) from either of these subcomplexes.

Assume instead that the two tetrahedra of type Δ_{qtt} meet in the H–even edge f of degree 5. If there are two distinct types of Δ_{qq} tetrahedra meeting f, then f must meet five pairwise distinct tetrahedra. Hence the tetrahedra of type Δ_{qtt} meet in a face. The two possible arrangements are illustrated in Figure 3.22. For arrangement (i), this is analogous to arrangement (v) in Figure 3.18 and we obtain two maximal layered solid tori meeting in a face. Hence (i) contains five pairwise distinct tetrahedra. For arrangement (ii), this is analogous to arrangement (vi) in Figure 3.18. We identify $\Delta_2 = \Delta_4$ which extends the layered solid torus by one tetrahedron. Note that in this case, we obtain no contribution to (3.4.3).

For the final analysis, take $d = 4$. Then $d - 4 - x \leq 0$ and $x \leq 2$. Note that $x > 0$ contradicts our assumption that $\mathscr{T}$ is $(\Delta_{qq}, 4)$–free and thus the only possibility here is $x = 0$. Using the neighbourhoods illustrated in Figure 3.1, the only subcomplexes which admit a rank–2 colouring are $X^0_{4;3}$ and $X^1_{4;3}$. The former attaches one $\mathrm{LST}(1,2,3)$ of type Δ_{qq} to two tetrahedra

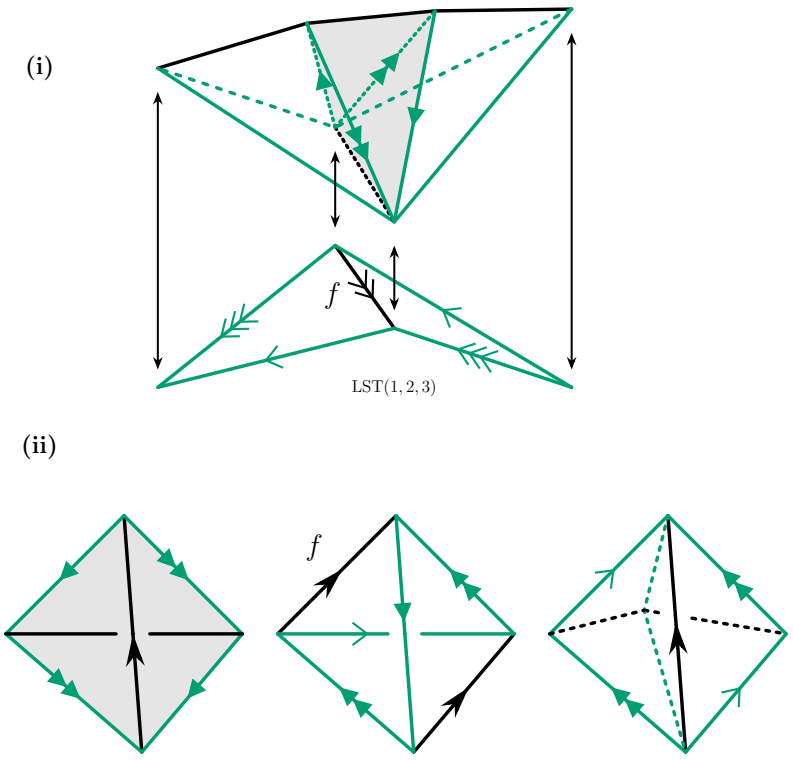

FIGURE 3.21. The neighbourhoods of (i) $X^0_{5;4}$; and (ii) $X^1_{5;4}$. The identifications from the H–thin layered solid torus are drawn as solid arrows and the H–thin layered solid torus is shaded in each case.

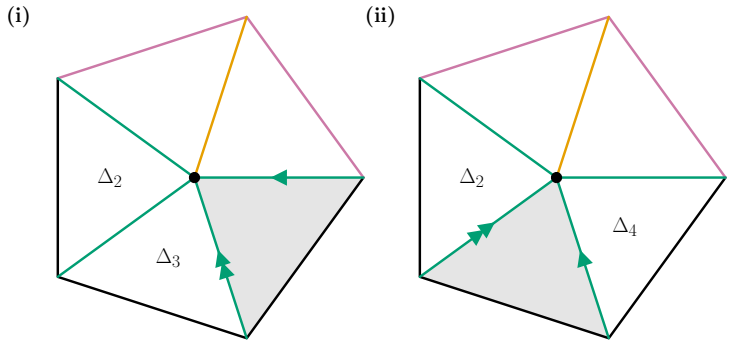

FIGURE 3.22. Neighbourhoods of an H–even edge of degree 5 which meets two tetrahedra of type Δ_{qtt} and exactly one H–thin layered solid torus. The shaded tetrahedra belong to the H–thin layered solid tori and labelled tetrahedra are of type Δ_{qq}. The unshaded, unlabelled tetrahedra are of type Δ_{qtt}. A top down perspective is used.

either both of type Δ_{qq} or both of type Δ_{qtt}, whilst the latter must contain three tetrahedra of type Δ_{qq}.

In all of the above configurations, we obtain a non-negative contribution to (3.4.3). The subcomplexes in which we obtain a contribution of 0 are illustrated in Figure 3.23.

Theorem 3.25 *Let M be a closed, orientable, irreducible, connected 3–manifold with minimal triangulation $\mathscr{T}$. Suppose further that $\mathscr{T}$ is coloured by the rank two subgroup $H \leq H^1(M;\mathbb{Z}_2)$*

and is $(\Delta_{qq},4)$–free with respect to the colouring. If $t_H(M)=1$ and the profile of $\mathscr{T}$ is $(0,0,2,n_{qq},n_{qqq})$, then all canonical normal surfaces dual to the colouring are $\mathbb{Z}_2$–taut and $\mathscr{T}$ falls into one of the following combinatorial types:

(i) the central subcomplex is (6.1) and $\mathscr{T}$ contains exactly two edges of degree 3. Moreover, the interior of the subcomplex consisting of the tetrahedra of type Δ_{qtt} and Δ_{qq} is a Seifert fibred space over D^2 with two exceptional fibres;

(ii) the central subcomplex is (5.1) and $\mathscr{T}$ contains a single edge of degree 3. Moreover, the subcomplex consisting of the tetrahedra of type Δ_{qtt} and Δ_{qq} is a solid torus; or

(iii) the central subcomplex is (4.1) and $\mathscr{T}$ contains no degree 3 edges. Moreover, the subcomplex consisting of the tetrahedra of type Δ_{qtt} and Δ_{qq} is a solid torus.

Proof Suppose that the profile of $\mathscr{T}$ is $(0,0,2,n_{qq},n_{qqq})$. As $n_{qtt}\neq 0$ there is at least one H–even edge in $\mathscr{T}$. From the previous discussion, the maximum degree of any H–even edge in $\mathscr{T}$ is 6. As $n_{qtt}=2$, this forces the central subcomplex to be of type (6.1), (5.1), or (4.1). The four boundary faces of such a central subcomplex, not contained in a layered solid torus, are each bounded by exactly one 1–even, one 2–even, and one 3–even edge. Hence, the tetrahedra glued to these faces must be of type Δ_{qqq}. The subcomplexes (6.2), (5.2), (5.3), (4.2), and (4.3) in Figure 3.23 possess no such faces in their boundaries and hence cannot glue to the central subcomplex nor a tetrahedron of type Δ_{qqq}.

Suppose the central subcomplex is (6.1). We can build a triangulation of a 3–manifold containing this subcomplex in `Regina` by attaching a layered chain of even length to the four tri coloured boundary faces. An isomorphism signature of such a triangulation consisting of 13 tetrahedra and having profile $(0,0,2,5,6)$ is `nLAvPMzAMkbcbgfhijkilmmmhxjqxqhqqsqqfo`. This triangulation can be simplified and the manifold is recognised by `Regina` as the Seifert fibred space $S^2((1,-1),(4,1),(4,-1),(6,1))$. Drilling out the exceptional fibre formed by the layered chain results in a Seifert fibred space over the disc with exactly two exceptional fibres.

The statements for the cases where the central subcomplex is (5.1) or (4.1) follow from the identification of the models $X^1_{5;4}$ and $X^0_{4;3}$, respectively. The number of degree 3 edges in each of the three cases is determined directly from the preceding analysis. □

A similar analysis can be done for profiles of the form $(0,0,3,n_{qq},n_{qqq})$ and will appear in [**MT**].

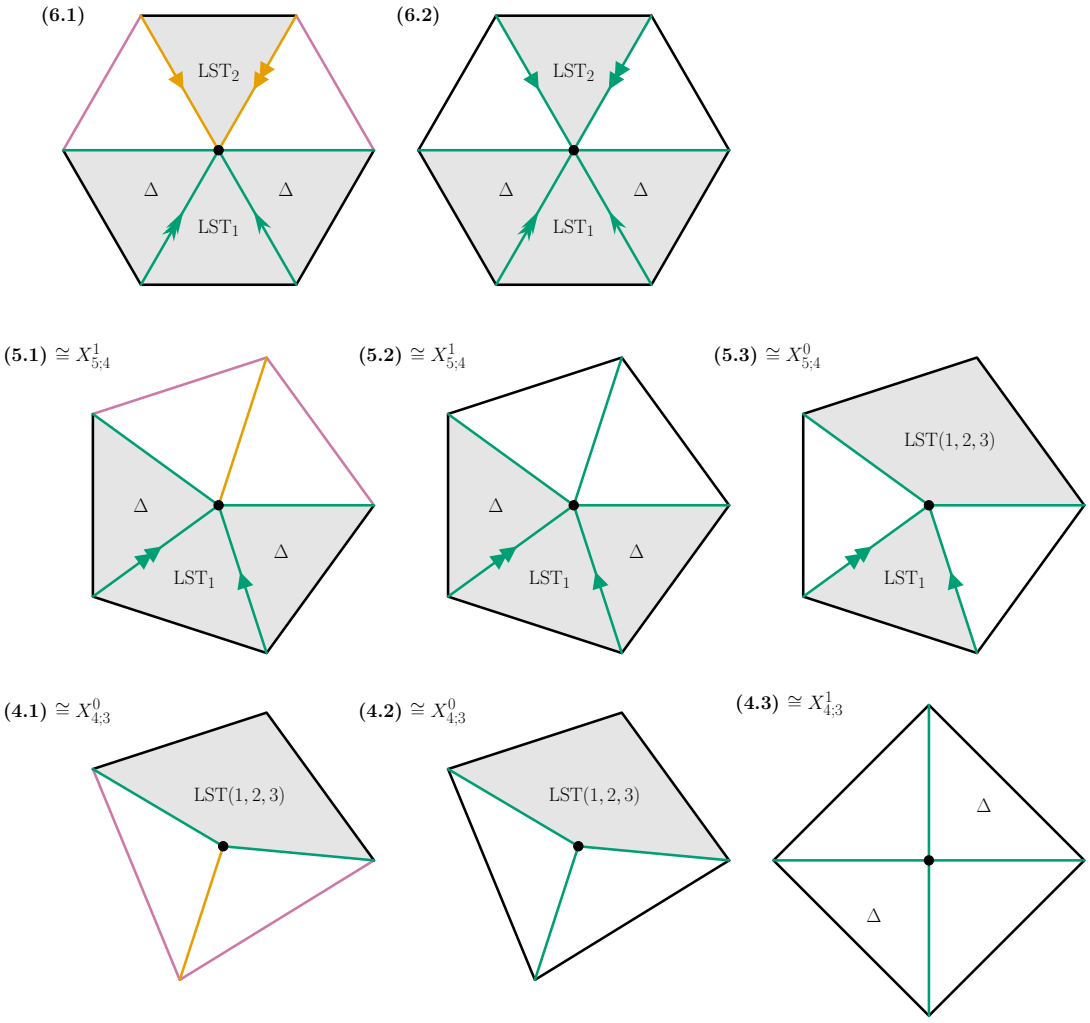

FIGURE 3.23. The central subcomplexes, numbered (x.1), and neighbourhoods of H–even edges of degree at least 4 in $\mathscr{T}$ when $n_{\text{qtt}} = 2$. The degree of the shared H–even edge is 6 in the first row, five in the second, and four in the third. Shaded tetrahedra belong to a layered solid torus. Tetrahedra marked with Δ are the same for the given subcomplex. The boundary faces are unshaded.

3.5. Examples of 3–manifolds with 2–thickness one

In this section we provide new infinite families of 3–manifolds with 2–thickness $t_2(M) = 1$ and hence have complexities satisfying

$$c(M) = 3 + \sum_{i=1}^{3} \|\varphi_i\|$$

for some rank–2 subgroup $H \leq H^1(M;\mathbb{Z}_2)$. All examples provided are small Seifert fibred spaces with base orbifold S^2 and three exceptional fibres. Hence $H^1(M;\mathbb{Z}_2)$ has rank–2. The triangulations we provide follow the notation of [**Bur03**].

3.5.1. A note on computing the non-orientable genus of one-sided vertical surfaces. Work of Du [Du22] provides an algorithm for computing the $\mathbb{Z}_2$–Thurston norm of an orientable Seifert fibred space with orientable base orbifold. This is done by providing a method for detecting one-sided horizontal surfaces and computing both their $\mathbb{Z}_2$–homology class and their genus.

The main tool used in the computations is the recursive function of Bredon and Wood [BW69]. Let $k \geq 0$ and $q > 0$ be integers such that $2k > q > 0$ and q is odd. The function $N(2k,q)$ is defined recursively as

$$N(2k,1) = k, \quad \text{and} \quad N(2k,q) = N(2(k-Q),q-2m)+1 \tag{3.5.1}$$

where Q and m satisfy $2km - Qq = \pm 1$ and $0 < Q < k$. We may extend $N(2k,q)$ to be defined for all integers k and all odd integers q by the following properties:

(i) $N(-2k,-q) = N(2k,q)$ (normalising for $k > 0$);

(ii) for $k > 0$, $N(2k,2k+q) = N(2k,q)$ (normalising for $0 < q < 2k$);

(iii) for $0 < q < 2k$, $N(2k,2k-q) = N(2k,q)$ (normalising for $0 < q < k$);

(iv) for $0 < q < k$, $N(2k,q) = 1 + N(2(k-q),q)$.

The proofs of these properties, together with additional formulations of $N(2k,q)$, can be found in [BW69, Sections 6,7,8]. An important consequence of (ii) and (iii) that we will use is $N(2k,-1) = N(2k,1) = k$. Our use of this function comes from the following lemma (which we specialise to our case)

Lemma 3.26 [Du22, Lemma 2.11] *The Seifert fibred space $S^2((\alpha_1,\beta_1),(\alpha_2,\beta_2),(\alpha_3,\beta_3))$ contain a one-sided vertical surface $S_{i,j}$ formed by connecting the fibred solid tori with parameters (α_i,β_i) and (α_j,β_j) if and only if α_i and α_j are even. Moreover, the non-orientable genus of $S_{i,j}$ is*

$$g(S_{i,j}) = N(\alpha_i,\beta_i) + N(\alpha_j,\beta_j)$$

3.5.2. An infinite family with no edges of degree 3.

Proposition 3.27 *Let $M_k = S^2((1,-1),(2,1),(4,3),(2k+2,1))$ for $k \geq 1$. Then $t_2(M_k) = 1$ and M_k has a $(\Delta_{qq},4)$–free minimal triangulation $\mathscr{T}_k$ with profile $(0,0,2,1,2k+2)$ and $c(M_k) = 2k+5$.*

Proof Standard calculations of Seifert invariants allow us to re-normalise the parameters of M_k and write $M_k = S^2((2,1),(4,-1),(2k+2,1))$. This Seifert fibred space can be triangulated by the chained triangular solid torus of major type $J(2k+1 \mid 3,-1)$ [Bur03, Definition 3.3.19 and Theorem 3.3.21]. This triangulation consists of $3+2k+1+1 = 2k+5$ tetrahedra.

By Lemma 3.26, there are three one-sided vertical surfaces and each is dual to a distinct $0 \neq \varphi \in H^1(M_k;\mathbb{Z}_2)$. Computing the non-orientable genus of each we obtain

$$\begin{aligned} g(S_{1,2}) &= N(2,1)+N(4,-1) = 3 \\ g(S_{1,3}) &= N(2,1)+N(2k+2,1) = k+2 \\ g(S_{2,3}) &= N(4,-1)+N(2k+2,1) = k+3 \end{aligned}$$

Following the algorithm in [**Du22**], all one-sided horizontal surfaces have a non-orientable genus at least as large as that of the one-sided vertical surface in the same class. Hence, the one-sided vertical surfaces are $\mathbb{Z}_2$–taut and we compute their Euler characteristics as

$$\begin{aligned} \chi(S_{1,2}) &= 2-g(S_{1,2}) = -1 \\ \chi(S_{1,3}) &= 2-g(S_{1,3}) = -k \\ \chi(S_{2,3}) &= 2-g(S_{2,3}) = -k-1 \end{aligned}$$

Hence we calculate for $0 \neq \varphi_i \in H^1(M;\mathbb{Z}_2)$

$$\sum_{i=1}^{3} \|\varphi_i\| = -\chi(S_{1,2})-\chi(S_{1,3})-\chi(S_{2,3}) = 2k+2$$

From Theorem 3.13, we thus have

$$2k+4 \leq 2k+4+t_2(M) \leq 2k+5$$

Note that M_k is not a generalised quarternionic space and thus $t_2(M) \neq 0$. This forces $t_2(M) = 1$ and we are done. □

3.5.3. An infinite family with exactly one edge of degree 3.

Proposition 3.28 *Let $M_{k,n} = S^2((1,-1),(2,1),(2k,1),(2n,2n-1))$ for $k \geq 1$ and $n \geq 2$. Then $t_2(M_k) = 1$ and $M_{k,n}$ has a $(\Delta_{qq},4)$–free minimal triangulation $\mathcal{T}_{k,n}$ with profile $(0,0,2,2n-3,2k)$ and $c(M_{k,n}) = 2k+2n-1$.*

Proof Standard calculations of Seifert invariants allow us to re-normalise the parameters of $M_{k,n}$ and write $M_k = S^2((2,1),(2k,1),(2n,-1))$. This Seifert fibred space can be triangulated by the chained triangular solid torus of major type $J(2k-1 \mid 2n-1,-1)$ [**Bur03**, Definition 3.3.19 and Theorem 3.3.21]. This triangulation consists of $3+2k-1+2n-3 = 2k+2n-1$ tetrahedra.

By Lemma 3.26, there are three one-sided vertical surfaces and each is dual to a distinct $0 \neq \varphi \in H^1(M_{k,n};\mathbb{Z}_2)$. Computing the non-orientable genus of each we obtain

$$\begin{aligned} g(S_{1,2}) &= N(2,1)+N(2k,1) = k+1 \\ g(S_{1,3}) &= N(2,1)+N(2n,-1) = n+1 \\ g(S_{2,3}) &= N(2k,1)+N(2n,-1) = k+n \end{aligned}$$

Following the algorithm in [**Du22**], all one-sided horizontal surfaces have a non-orientable genus at least as large as that of the one-sided vertical surface in the same class. Hence, the one-sided vertical surfaces are $\mathbb{Z}_2$–taut and we compute their Euler characteristics as

$$\begin{aligned} \chi(S_{1,2}) &= 2-g(S_{1,2}) = 1-k \\ \chi(S_{1,3}) &= 2-g(S_{1,3}) = 1-n \\ \chi(S_{2,3}) &= 2-g(S_{2,3}) = 2-k-n \end{aligned}$$

Hence we calculate for $0 \neq \varphi_i \in H^1(M;\mathbb{Z}_2)$

$$\sum_{i=1}^{3} \|\varphi_i\| = -\chi(S_{1,2})-\chi(S_{1,3})-\chi(S_{2,3}) = 2k+2n-4$$

From Theorem 3.13, we thus have

$$2k+2n-2 \leq 2k+2n-2+t_2(M) \leq 2k+2n-1$$

Note that $M_{k,n}$ is not a generalised quarternionic space and thus $t_2(M) \neq 0$. This forces $t_2(M) = 1$ and we are done. □

CHAPTER 4

Computing the $\mathbb{Z}_2$–Thurston norm for closed 3–manifolds

The final chapter of this thesis presents a continuation of Chapter 3 in which we describe an algorithm for computing the $\mathbb{Z}_2$–Thurston norm for any non-trivial $\varphi \in H^1(M;\mathbb{Z}_2)$. This algorithm, as previously alluded to, has played a significant role in classifying examples of 3–manifolds with rank–2 coloured minimal triangulations.

Throughout this chapter M denotes a closed, orientable, irreducible, connected 3–manifold distinct from S^3 and $\mathbb{R}P^3$ and $\mathscr{T}$ denotes a 0–efficient triangulation of M. Hence, by Proposition 1.16, $\mathscr{T}$ contains exactly one vertex. We let T denote the number of tetrahedra in $\mathscr{T}$ and $r = \operatorname{rank} H^1(M;\mathbb{Z}_2)$.

Our algorithm constructs two main objects – the compatibility complex of $\mathscr{T}$ and the φ–Euler characteristic table. The compatibility complex is the clique complex of the compatibility graph of the fundamental normal surfaces in $\mathscr{T}$. Each vertex of the compatibility graph corresponds to a normal surface in $\mathscr{T}$ and two vertices are connected by an edge if and only if the corresponding normal surfaces are compatible. The maximal cliques are termed compatibility cones. The φ–Euler characteristic table contains one column for each non-trivial class φ in $H^1(M;\mathbb{Z}_2)$ where the i-th entry of this column is the set of all compatibility cones which contain a normal surface dual to φ with Euler characteristic equal to i.

The fundamental result for correctness of our algorithm (Lemma 4.7) shows that for any $0 \neq \varphi \in H^1(M;\mathbb{Z}_2)$ the surface S dual to φ with maximal Euler characteristic can be expressed as a sum of bounded length

$$S = \sum_{i=1}^{2^r-1} \lambda_i F_i$$

where $\lambda_i \in \mathbb{Z}_2$ and F_i is a fundamental surface dual to $0 \neq \varphi_i \in H^1(M;\mathbb{Z}_2)$ for all $1 \leq i \leq 2^r-1$.

Algorithm 4.1 *Input:* a 0–efficient triangulation $\mathscr{T}$ of the closed, orientable, irreducible, connected 3–manifold M, which is different from S^3 and $\mathbb{R}P^3$.

Output: a vector $\mathbf{v} \in \mathbb{N}_0^{2^r-1}$ containing the $\mathbb{Z}_2$–Thurston norm for all 2^r-1 non-trivial classes in $H^1(M;\mathbb{Z}_2)$.

(i) If $H^1(M;\mathbb{Z}_2) = \{0\}$, return $\emptyset$.

(ii) Enumerate all non-trivial classes in $H^1(M;\mathbb{Z}_2)$ as edge weight vectors in $\mathbb{Z}_2^{T+1}$, where $T+1$ is the number of edges in $\mathscr{T}$;

(iii) Enumerate fundamental surfaces dual to non-trivial classes in $H^1(M;\mathbb{Z}_2)$. Compute their edge weight vectors. Group the surfaces by cohomology classes using their edge weight vectors;

(iv) Form the compatibility complex for the fundamental surfaces in (iii);

(v) Enumerate the φ–Euler characteristic table and return the maximal Euler characteristics ranging over all normal surface representatives in each $H^1(M;\mathbb{Z}_2)$ class. This can be done in finite time by Lemma 4.7.

Sections 4.1 to 4.4 each describe one of the four steps of Algorithm 4.1 and provide a complexity analysis of the respective step. In Section 4.5 we provide a proof that the φ–Euler characteristic table is finite and that our algorithm is correct.

4.1. Enumerating non-trivial classes

Let $0 \neq \varphi \in H^1(M;\mathbb{Z}_2)$ considered as a non-trivial homomorphism $\varphi : \pi_1(M) \to \mathbb{Z}_2$ and recall that an edge $e \in \mathscr{T}^{(1)}$ is **φ–even** if $\varphi[e] = 0$ and **φ–odd** if $\varphi[e] = 1$. For a given face $f \in \mathscr{T}^{(2)}$ bounded by edges e_i, e_j, and e_k, which may not be pairwise distinct, the class φ must satisfy

$$\varphi[e_i] + \varphi[e_j] + \varphi[e_k] = 0$$

Label the edges of $\mathscr{T}$ as $e_1, \ldots, e_{T+1}$ and the faces of $\mathscr{T}$ as $f_1, \ldots, f_{2T}$. We construct a matrix $A \in \mathbb{Z}_2^{2T\times(T+1)}$ such that the m-th row contains a 1 in the i-th column if and only if e_i bounds f_m an odd number of times. That is, $a_{m,i}$ counts the number of times e_i appears as a boundary edge of f_m modulo 2.

Lemma 4.2 *The nullspace of A is isomorphic, as a vector space, to $H^1(M;\mathbb{Z}_2)$.*

Proof Let $\mathscr{N}(A) \subseteq \mathbb{Z}_2^{T+1}$ denote the nullspace of A. By construction, each row of A corresponds to some $\varphi[e_i] + \varphi[e_j] + \varphi[e_k]$, where e_i, e_j, and e_k a face $f \in \mathscr{T}^{(2)}$. Hence each non-trivial element of $\mathscr{N}(A)$ corresponds to some $\varphi \in H^1(M;\mathbb{Z}_2)$. For the converse, we note that as $\mathscr{T}$ is a 1–vertex triangulation every cycle is a generator of $H^1(M;\mathbb{Z}_2)$. □

Using Gaussian elimination, a basis for $\mathscr{N}(A)$ can be found in $O(T^3)$ time. Given $r = \operatorname{rank}(H^1(M;\mathbb{Z}_2))$ basis vectors, the enumeration of all vectors in $\mathscr{N}(A)$ can be done in $O(r2^r)$ time by taking all 2^r $\mathbb{Z}_2$–linear combinations of the r basis vectors. To optimise later lookups, we sort the non-trivial vectors in lexicographical order which can be done in $O(2^r \log(2^r)) = O(r2^r)$ time. This allows for $O(r)$ run time when searching the lookup table via, for example, a binary search operation.

Enumerating the non-trivial cohomology classes occurs as a preprocessing step. We are left with an ordered list of non-trivial classes, represented as vectors in $\mathbb{Z}_2^{T+1}$. For the remainder

of this chapter, we assume that the non-trivial elements of $H^1(M;\mathbb{Z}_2)$ follow this order, with the understanding that for any $0 \neq \varphi_i, \varphi_j \in H^1(M;\mathbb{Z}_2)$ we have $\varphi_i < \varphi_j$ in the lexicographical order if $i < j$.

4.2. Enumeration of fundamental surfaces dual to non-trivial classes

Recall that a normal surface F is fundamental if it cannot be obtained as the sum $F = F_1 + F_2$, where F_1 and F_2 are non-empty normal surfaces (Definition 1.13). Hass, Lagarias, and Pippenger [**HLP99**] bound the number of fundamental normal surfaces N at $N \leq T^{7T}\, 2^{49T^2+14T}$, with the maximal coordinate of a given coordinate vector $\mathbf{v} = (v_1, v-2, \ldots, v_{7T})$ bounded by $\max_{1\leq i\leq 7T}(v_i) \leq T \cdot 2^{7T+2}$. Work of Burton [**Bur14b**] establishes enumeration methods which are effective in practice but may still suffer from combinatorial explosion. Because of this, we omit the complexity analysis of this step and instead direct the reader to the previously cited paper. We are, however, only interested in those fundamental surfaces dual to a non-trivial class in $H^1(M;\mathbb{Z}_2)$. Let $\mathscr{F}$ denote the set of such fundamental surfaces in $\mathscr{T}$.

For a normal surface $S \subset \mathscr{T}$ and an edge $e_i \in \mathscr{T}^{(1)}$, denote the **edge weight**, $w_i(S)$, of S as the number of times S intersects e_i. This number is finite, non-negative, and equal to the number of vertices of S which lie on e_i. Let the **total weight** of S, $\mathrm{wt}(S)$, be the vector in $\mathbb{Z}^{T+1}$ whose i-th entry is $w_i(S)$. Let $\varphi \in H^1(M;\mathbb{Z}_2)$ be dual to S. If $\varphi[e_i] = 1$, then any surface dual to φ must intersect e_i an odd number of times. Hence, reducing $\mathrm{wt}(S)$ modulo 2 returns $\mathrm{wt}_2(S) \in \mathbb{Z}_2^{T+1}$ equal to the corresponding $\varphi \in H^1(M;\mathbb{Z}_2)$ dual to S.

For each $F_i \in \mathscr{F}$ we compute $\mathrm{wt}(F_i)$ and $\mathrm{wt}_2(F_i)$. If F_i is dual to one of the nontrivial classes $\varphi \in H^1(M;\mathbb{Z}_2)$, then we keep F_i and compute its Euler characteristic using $\mathrm{wt}(F_i)$, otherwise we delete both. To compute the Euler characteristic we note that the sum of the components of $\mathrm{wt}(F_i)$ is the number of vertices in F_i. Letting t_i and q_i denote the number of triangles and quadrilaterals in F_i, respectively, and w_j the j-th component of $\mathrm{wt}(F_i)$, we compute

$$\chi(F_i) = \sum_{j=1}^{T+1} w_j - \frac{3t_i + 4q_i}{2} + (t_i + q_i)$$

After this step we are left with the set $\mathscr{F} = \{F_1, \ldots, F_n\}$, $n \in O(N)$, of fundamental surfaces together with the corresponding non-trivial classes in $H^1(M;\mathbb{Z})$ each is dual to. We also store the Euler characteristic of each F_i together with the minimum Euler characteristic $\chi_{\min}$

To calculate $\mathrm{wt}(F_i)$ we must determine the number of normal disc types intersecting each of the $T+1$ edges. Using $\max(v_i) \leq T \cdot 2^{7T+2}$, this count requires $O(T\log(\max(v_i))) = O(T^2)$ operations. Reducing $\mathrm{wt}(F_i)$ modulo 2 to obtain $\mathrm{wt}_2(F_i)$ requires a further $O(T)$ operations. Searching for $\mathrm{wt}_2(F_i)$ in the list of non-trivial classes requires $O(r)$ operations, if we use a binary search function. The total complexity of this component of the algorithm, not including

the enumeration of fundamental solutions, is $O(N(T^2+r))$. Note that, in practice, the values of N and $\max(v_i)$ are usually much smaller than the bounds provided above.

4.3. Construction of the compatibility complex

Given the collection of fundamental normal surfaces $\mathscr{F}$ we must compute the compatibility complex of the constituent surfaces.

Definition 4.3 Let $S_1,\dots,S_n$ be a collection of normal surfaces in $\mathscr{T}$. The **compatibility matrix** $C=(c_{ij})$ is the $n\times n$ matrix where, for $i\neq j$, $c_{ij}=1$ if S_i and S_j are compatible, and 0 otherwise. ◇

Note that we set $c_{ii}=0$, since our goal is to consider the Haken sums of the normal surfaces in $\mathscr{F}$. For any $F_i\in\mathscr{F}$ we have $[F_i+F_i]=[F_i]+[F_i]=0$ with F_i+F_i having no components a sphere as $\mathscr{T}$ is 0–efficient. Hence, these sums do not need to be considered as is shown in Lemma 4.7. The compatibility matrix forms the adjacency matrix of a simple graph, where the vertices are normal surfaces and two vertices are connected by an edge if and only if they are compatible. This motivates the definition of the compatibility complex.

Definition 4.4 Let $C=(c_{ij})$ be the compatibility matrix for a collection of normal surfaces $S_1,\dots,S_n$. The **compatibility complex** $\mathscr{C}$ is the collection of maximal cliques $\mathscr{C}_1,\dots,\mathscr{C}_m$ in the graph whose adjacency matrix is C. We call each $\mathscr{C}_i$ a **compatibility cone**. ◇

The compatibility complex plays a central role in our algorithm. Its construction reduces to the problem of enumerating maximal cliques, which may be done in $O(3^{n/3})$ time [**BK73**]. In practice, however, more naive approaches are effective. Moreover, the number of fundamental surfaces we work with is much smaller than the bound given by Hass, Lagarias, and Pippenger, rendering this computation practical despite its prohibitive running time.

The compatibility of two surfaces can be determined in $O(T)$ operations as we only need to check the normal quadrilateral types in each tetrahedron. The construction of the compatibility matrix thus requires $O(Tn^2)$ operations, with a further $O(3^{n/3})$ operations to construct the compatibility complex.

4.4. Enumerating the φ–Euler characteristic table

Following the construction of the compatibility complex $\mathscr{C}$, we move to determine the maximal Euler characteristic for each non-trivial class in $H^1(M;\mathbb{Z}_2)$. We do this by enumerating the **φ–Euler characteristic table** $\mathfrak{T}$ of $\mathscr{T}$ for $H^1(M;\mathbb{Z}_2)$ as follows.

The table $\mathfrak{T}$ contains $|\chi_{\min}|+1$ rows labelled $0,-1,\ldots,\chi_{\min}$ and 2^r-1 columns labelled $\varphi_1,\ldots,\varphi_{2^r-1}$, where $r=\operatorname{rank}(H^1(M;\mathbb{Z}_2))$. The entry $\mathfrak{t}_{i,j}$ is the set of all $1\leq k\leq m$ such that the compatibility cone $\mathscr{C}_k$ contains a surface $F\in\mathscr{F}$ dual to φ_j with $\chi(F)=i$.

To ensure that $\chi_{\min}$ is not exponential in T, which may be the case given the previous bound on $\max(v_i)$, we compute it as follows. Recall that for each $0\neq\varphi\in H^1(M;\mathbb{Z}_2)$ the canonical normal surface dual to φ, S_φ, is formed by placing at most one normal disc in each tetrahedron. For a given $0\neq\varphi\in H^1(M;\mathbb{Z}_2)$, we can construct S_φ by using the edge weight representative of φ to mark the vertices on each edge and then adding the appropriate normal disc to each tetrahedron. The number of normal triangles and quadrilaterals in S_φ can be determined in $O(T)$ operations, resulting in $-\chi_{\min}\in O(T)$. The computation of $\chi(S_\varphi)$ is as previously described. We set

$$\chi_{\min}=\min_{0\neq\varphi\in H^1(M;\mathbb{Z}_2)}(\chi(S_\varphi))$$

For any S_φ constructed, if $\chi(S_\varphi)\geq\chi(F)$ for each $F\in\mathscr{F}$ dual to φ, then we append S_φ to the relevant compatibility cone.

We first claim that the range of Euler characteristics used in $\mathfrak{T}$ is sufficient. Since we want to compute the maximal Euler characteristic for each φ_j, it suffices to check that the Euler characteristics of all surfaces in $\mathscr{F}$ are non–positive.

Lemma 4.5 *For each $F\in\mathscr{F}$, $\chi(F)\leq 0$.*

Proof Since F is a fundamental normal surface in $\mathscr{T}$ it must be connected. To see why this is true, note that each component of F must be a normal surface in $\mathscr{T}$. If F was not connected, then it could be written as the sum of its components, contradicting it being a fundamental surface.

Since F is a closed surface, it suffices to check that F is neither an S^2 nor an $\mathbb{R}P^2$. As $\mathscr{T}$ is 0–efficient and has a single vertex, all normal spheres are vertex linking and thus must intersect each edge an even number of times. Thus F is not a sphere. Since M is 0–efficient, it cannot contain any properly embedded projective planes and hence F cannot be $\mathbb{R}P^2$. □

To update the table, we make the following observation. Let $\varphi_i,\varphi_j,\varphi_k\in H^1(M;\mathbb{Z}_2)$ be such that $\varphi_i+\varphi_j=\varphi_k$. If there exist surfaces S_i dual to φ_i and S_j dual to φ_j in the same compatibility cone, then the surface S_i+S_j is dual to φ_k and also in the same compatibility cone. To modify the table, we utilise the additivity of the Euler characteristic under the Haken sum of normal surfaces.

Lemma 4.6 (Additivity of Euler characteristic under the Haken sum) *Let S_1 and S_2 be compatible normal surfaces. Then $\chi(S_1+S_2)=\chi(S_1)+\chi(S_2)$.*

Proof Let v_i, t_i, and q_i denote the number of vertices, normal triangles, and normal quadrilaterals in S_i, respectively, for $i = 1,2$. The Euler characteristic of S_i is

$$\chi(S_i) = v_i - \left(\frac{3t_i}{2} + 2q_i\right) + (t_i + q_i)$$

The surface $S = S_1 + S_2$ has vector representation $\mathbf{v} = \mathbf{v}_1 + \mathbf{v}_2$, where $\mathbf{v}_i$ is the vector representation of S_i for $i = 1,2$. Hence S contains $v = v_1 + v_2$ vertices, $t = t_1 + t_2$ normal triangles, and $q = q_1 + q_2$ normal quadrilaterals. Its Euler characteristic is

$$\chi(S) = (v_1 + v_2) - \left(\frac{3(t_1 + t_2)}{2} + 2(q_1 + q_2)\right) + ((t_1 + t_2) + (q_1 + q_2)) = \chi(S_1) + \chi(S_2)$$

□

The enumeration of $\mathfrak{T}$ proceeds as follows. For each surface $F_i \in \mathscr{F}$ we check its membership in each of the compatibility cones $\mathscr{C}_1, \ldots, \mathscr{C}_m$ and record the index of each cone returning the affirmative. Suppose $F_i \in \mathscr{C}_k$ for some $1 \leq k \leq m$. As we have already computed and stored the class φ_j dual to F_i and the Euler characteristic $\chi(F_i)$, we check whether $k \in \mathfrak{t}_{\ell,j} \in \mathfrak{T}$ for $0 \leq \ell < \chi(F_i)$. If it isn't, we append k to $t_{\chi(F_i),j}$ and remove k from all cells below.

By this construction, each $1 \leq k \leq m$ will appear at most once in each column of $\mathfrak{T}$. In particular, if $k \in \mathfrak{t}_{x,j}$, then x is the maximal Euler characteristic for all surfaces dual to φ_j in $\mathscr{C}_k$. Hence the table contains at most $m(2^r - 1)$ entries after construction. We preserve this property throughout the full enumeration.

To update the table, let $j_1 \in \{1, \ldots, 2^r - 2\}$ and $j_2 \in \{j_1 + 1, \ldots, 2^r - 1\}$ and set j_3 to be the index such that $\varphi_{j_1} + \varphi_{j_2} = \varphi_{j_3}$. For each $(x_1, x_2) \in \{0, \ldots, \chi_{\min}\}^2$ we check to see if $\mathfrak{t}_{x_1,j_1} \cap \mathfrak{t}_{x_2,j_2}$ is empty or not.

Let $k \in \mathfrak{t}_{x_1,j_1} \cap \mathfrak{t}_{x_2,j_2}$. Then there exist surfaces $F_{i_1}, F_{i_2} \in \mathscr{C}_k$ such that F_{i_1} is dual to φ_{j_1} and F_{i_2} is dual to φ_{j_2} with Euler characteristics x_1 and x_2, respectively. The surface $F_{i_3} = F_{i_1} + F_{i_2}$ is also in $\mathscr{C}_k$, is dual to φ_{j_3}, and has Euler characteristic $x_1 + x_2$. The update to the column corresponding to φ_{j_3} is one of the following cases.

- if $x_1 + x_2 < \chi_{\min}$ and the column corresponding to φ_{j_3} is not empty, then we discard this surface and move to the next iteration; else
- If $k \in \mathfrak{t}_{z,j_3}$ for some $x_1 + x_2 < z \leq 0$, then we discard this surface move to the next iteration. Otherwise we append k to $\mathfrak{t}_{x_1+x_2,j_3}$ and delete k from any t_{z,j_3}, $\chi_{\min} \leq k < x_1 + x_2$ it occurs in.

To understand the update procedure, consider the column corresponding to some φ_j. After the initial construction the information in this columns is determined by all normal surfaces dual to φ_j which can be written as a single fundamental surface. After the second update, we add information about surfaces $S = F + F'$, where F, F' are fundamental surfaces. Each update

increases the number of fundamental surface summands. Running this 2^r-2 times yields information about all surfaces which can be written as the sum of a fundamental surface from each class $\varphi_1,\dots,\varphi_{2^r-1}$ (see Lemma 4.7).

To analyse the complexity, we compare the construction and update separately. In the construction phase, for each surface we check membership in the compatibility cones, done in $O(m\log(m))$ operations, and then check whether the found indices occur in a given column. This second check requires $O(|\chi_{\min}|m)$ operations. Iterating over all surfaces, the construction has complexity $O(N\cdot m(\log(m)+|\chi_{\min}|))$.

For the update procedure, we consider $\binom{2^r-1}{2}$ pairs of classes and hence perform $O(4^r)$ iterations to add classes together. In each iteration we consider all $\chi_{\min}^2$ pairs of Euler characteristics and check the intersection of the appropriate table entries. As each table entry contains at most m entries, this check has complexity $O(m)$. Finally, for each element of the intersection we check all entries in the appropriate column which, as before, has complexity $O(|\chi_{\min}|m)$. Running the update procedure $O(2^r)$ times, the total complexity is $O(8^r\cdot|\chi_{\min}|^3\cdot m^2)$.

4.5. Correctness of the algorithm

It remains to prove that Algorithm 4.1 terminates and correctly computes the $\mathbb{Z}_2$–Thurston norm of each non-trivial $\varphi\in H^1(M;\mathbb{Z}_2)$. Parts (i)–(iii) involve a finite number of iterations, checks, and calculations and thus must terminate. It remains to show that the enumeration of the φ–Euler characteristic table is complete. To do this, we show that the maximal Euler characteristic surface dual to any non-trivial class $\varphi\in H^1(M;\mathbb{Z}_2)$ can be written as a sum of at most 2^r-1 normal surfaces.

Lemma 4.7 *Suppose* $\operatorname{rank}(H^1(M;\mathbb{Z}_2))=r$ *and let* $0\neq\varphi\in H^1(M;\mathbb{Z}_2)$. *The maximal Euler characteristic surface* S *dual to* φ *is realised as the sum of at most* 2^r-1 *distinct fundamental normal surfaces, each dual to a distinct non-trivial class in* $H^1(M;\mathbb{Z}_2)$. *That is,*

$$S=\sum_{i=1}^{2^r-1}\lambda_i F_i \tag{4.5.1}$$

where $\lambda_i\in\mathbb{Z}_2$ *and* $F_i\in\mathscr{F}$ *is a normal surface dual to* φ_i.

Proof List the non-trivial classes in $H^1(M;\mathbb{Z}_2)$ as $\varphi_1,\varphi_2,\dots,\varphi_{2^r-1}$ and suppose that we can write $S=S_1+S_2+\cdots+S_\ell$ for some $\ell\geq 1$ where the S_i's are non-empty, compatible normal surfaces. Note that $\chi(S_j)\leq 0$ for all j by Lemma 4.5. Grouping these surfaces by the cohomology classes they are dual to, we may express S as

$$S=\sum_{i=1}^{2^r-1}\sum_{\substack{S_j \text{ dual}\\ \text{to } \varphi_i}} S_j \tag{4.5.2}$$

For any φ_i, if the second sum contains an even number of terms, then the summand corresponds to the trivial class in $H_2(M;\mathbb{Z}_2)$ and hence its removal does not affect $[S]$. Moreover, using Lemmas 4.5 and 4.6, we observe

$$\sum_{\substack{S_j \text{ dual} \\ \text{to } \varphi_i}} \chi(S_j) \leq 0$$

If this sum of Euler characteristics is negative, then removing the corresponding summand in (4.5.2) results in a positive change to $\chi(S)$. This contradicts S having maximal Euler characteristic amongst the surfaces dual to φ. Hence these surfaces have a combined Euler characteristic of 0 and we remove them from the sum, preserving both $[S]$ and $\chi(S)$.

If the second sum contains an odd number of normal surfaces dual to φ_i, then let F_i denote the normal surface summand with the maximal Euler characteristic. Using this, we split the sum as

$$\sum_{\substack{S_j \text{ dual} \\ \text{to } \varphi_i}} S_j = F_i + \sum_{\substack{S_j \neq F_i \text{ dual} \\ \text{to } \varphi_i}} S_j$$

Note that the new sum on the right-hand side contains an even number of normal surfaces and hence is trivial in homology. From the previous arguments, the surfaces in this sum must have a combined Euler characteristic of 0 and we may remove them whilst preserving $[S]$ and $\chi(S)$. This leaves us with exactly one normal surface dual to φ_i in (4.5.2).

Hence S can be written as the sum of at most $2^r - 1$ fundamental normal surfaces, each dual to a distinct φ_i. □

Given that Algorithm 4.1 terminates, we now verify that it indeed computes the $\mathbb{Z}_2$–Thurston norm for each non-trivial $\varphi \in H^1(M;\mathbb{Z}_2)$.

Proposition 4.8 *Upon termination, Algorithm 4.1 returns the correct $\mathbb{Z}_2$–Thurston norm for each non-trivial $\varphi \in H^1(M;\mathbb{Z}_2)$.*

Proof First note that, since every class $\varphi \in H^1(M;\mathbb{Z}_2)$ has a normal surface representing its Poincaré dual, Lemma 4.7 ensures that, upon termination, no column of the φ–Euler characteristic table is empty.

It remains to show that, upon termination, the first non-empty entry in each column must occur at the maximal Euler characteristic for the corresponding class.

When updating $\mathfrak{T}$ we do not explicitly construct new surfaces as we only use the additivity of the Euler characteristic under the Haken sum. The update procedure of our algorithm iteratively considers the sums of cohomology classes. In the dual setting, this is the same as considering

surfaces S of the form

$$S = \sum_{\varphi} \sum_{\substack{F \text{ dual} \\ \text{to } \varphi}} F$$

where $F \in \mathscr{F}$. We claim that the maximal Euler characteristic surface S dual to some φ_j is realised as above, where the second sum contains at most a single summand for each φ in the first sum.

From Lemma 4.7, a maximal Euler characteristic surface dual to a non-trivial class must necessarily be realisable in this form. In the update procedure we only update an entry of $\mathfrak{T}$ with the compatibility class of S if it is not already realised with a larger Euler characteristic in the appropriate column. The k-th update considers normal surfaces which can be written as the sum of $k+1$ fundamental surfaces and we thus consider all combinations of Euler characteristics. Hence, a column is only updated if either: a surface dual to φ is found where previously no surface representative was known; or we find a normal surface dual to φ with larger Euler characteristic than those previously found.

After all updates are completed, the first entry of each column is thus the maximal Euler characteristic surface dual to the corresponding class $0 \neq \varphi \in H^1(M;\mathbb{Z}_2)$. The negative Euler characteristic of this surface is the $\mathbb{Z}_2$–Thurston norm of φ. □

4.6. Summary of results from Regina census

We conclude this chapter (and thus the thesis) with data obtained by an implementation of our algorithm. We calculated the $\mathbb{Z}_2$–Thurston norms of all rank 1 and 2 subgroups of $H^1(M;\mathbb{Z}_2)$ for every triangulation in the `Regina` closed orientable census up to 11 tetrahedra [**Bur11a**, **Bur**]. The manifolds we present data for in this section satisfy $\operatorname{rank}(H^1(M;\mathbb{Z}_2)) \geq 2$.

In Table 4.1 we list all triangulations in the census for which the 2–thickness of the corresponding 3–manifold is 1. Similarly, in Table 4.2 we list all triangulations in the census for which the 2–thickness of the corresponding 3–manifold is 2. In all tables we list the size of the triangulation, the $\mathbb{Z}_2$–Thurston norm for each non-trivial class in $H^1(M;\mathbb{Z}_2)$, the number of degree 3 edges, and the profile. The order in which the $\mathbb{Z}_2$–Thurston norms are reported is based on the ordered basis of $H^1(M;\mathbb{Z}_2)$ computed by our algorithm. As in Chapter 3, the profiles are ordered $(n_\emptyset, n_{\mathrm{tt}}, n_{\mathrm{qtt}}, n_{\mathrm{qq}}, n_{\mathrm{qqq}})$.

The main observation we make from this data is that all triangulations found are Seifert fibred spaces (or a graph manifold constructed from two Seifert fibred spaces). When the base orbifold is S^2 the manifold has 3 exceptional fibres. The first Seifert fibred space with four exceptional fibres and base orbifold S^2 found in the census has 2–thickness equal to 4 and is `SFS [S2: (2,1) (2,1) (2,1) (2,-1)] : #1`.

When the 2–thickness is 3, we observe orientable Seifert fibred spaces over $\mathbb{R}P^2$ with two exceptional fibres, together with 2-piece graph manifolds obtained from two Seifert fibred spaces with 2 exceptional fibres and base orbifold D^2.

The final table of data we list is Table 4.3. In this table we list all closed hyperbolic 3–manifolds in the census in which $\text{rank}(H^1(M;\mathbb{Z}_2)) \geq 2$ and calculate their 2–thickness. The smallest observed 2–thickness is 3. Based on other experimentation, and running our algorithm on the Hodgson-Weeks census data, we form the following conjecture.

Conjecture 4.9 Let M be a closed, orientable, irreducible, connected 3–manifold such that $\text{rank}(H^1(M;\mathbb{Z}_2)) \geq 2$. If $t_2(M) < 3$, then M is not hyperbolic.

Census triangulation	Size	$\mathbb{Z}_2$–norms	$\mathfrak{e}_3$	Profile
SFS [S2: (2,1) (2,1) (4,-1)] : #2	5	(1, 0, 1)	0	(0,0,2,1,2)
SFS [S2: (2,1) (2,1) (6,-1)] : #2	7	(2, 0, 2)	1	(0,0,2,3,2)
SFS [S2: (2,1) (2,1) (10,-7)] : #2	7	(2, 0, 2)	1	(0,0,2,3,2)
SFS [S2: (2,1) (2,1) (10,-7)] : #4	7	(2, 0, 2)	0	(0,0,2,1,4)
SFS [S2: (2,1) (2,1) (10,-3)] : #2	7	(2, 0, 2)	1	(0,0,2,3,2)
SFS [S2: (2,1) (4,1) (4,-1)] : #1	7	(2, 1, 1)	2	(0,0,3,4,0)
SFS [S2: (2,1) (4,1) (4,-1)] : #2	7	(2, 1, 1)	0	(0,0,2,1,4)
SFS [S2: (2,1) (4,3) (4,-1)] : #1	7	(2, 1, 1)	2	(0,0,3,4,0)
SFS [S2: (2,1) (2,1) (8,-1)] : #2	9	(3, 0, 3)	1	(0,0,2,5,2)
SFS [S2: (2,1) (2,1) (16,-13)] : #2	9	(3, 0, 3)	1	(0,0,2,5,2)
SFS [S2: (2,1) (2,1) (16,-13)] : #4	9	(3, 0, 3)	1	(0,0,2,3,4)
SFS [S2: (2,1) (2,1) (16,-13)] : #6	9	(3, 0, 3)	0	(0,0,2,1,6)
SFS [S2: (2,1) (2,1) (16,-11)] : #2	9	(3, 0, 3)	1	(0,0,2,5,2)
SFS [S2: (2,1) (2,1) (16,-11)] : #4	9	(3, 0, 3)	1	(0,0,2,3,4)
SFS [S2: (2,1) (2,1) (16,-5)] : #2	9	(3, 0, 3)	1	(0,0,2,5,2)
SFS [S2: (2,1) (2,1) (16,-3)] : #2	9	(3, 0, 3)	1	(0,0,2,5,2)
SFS [S2: (2,1) (2,1) (24,-17)] : #2	9	(3, 0, 3)	1	(0,0,2,5,2)
SFS [S2: (2,1) (2,1) (24,-17)] : #4	9	(3, 0, 3)	1	(0,0,2,3,4)
SFS [S2: (2,1) (2,1) (24,-7)] : #2	9	(3, 0, 3)	1	(0,0,2,5,2)
SFS [S2: (2,1) (4,1) (6,-1)] : #1	9	(3, 1, 2)	2	(0,0,3,6,0)
SFS [S2: (2,1) (4,1) (6,-1)] : #2	9	(3, 1, 2)	1	(0,0,2,3,4)
SFS [S2: (2,1) (4,1) (10,-3)] : #1	9	(3, 1, 2)	2	(0,0,3,6,0)
SFS [S2: (2,1) (4,1) (10,-3)] : #2	9	(3, 1, 2)	1	(0,0,2,3,4)
SFS [S2: (2,1) (4,3) (6,-5)] : #1	9	(3, 1, 2)	2	(0,0,3,6,0)
SFS [S2: (2,1) (4,3) (6,-5)] : #2	9	(3, 2, 1)	0	(0,0,2,1,6)
SFS [S2: (2,1) (4,3) (6,-1)] : #1	9	(3, 1, 2)	2	(0,0,3,6,0)
SFS [S2: (2,1) (4,3) (10,-7)] : #1	9	(3, 1, 2)	2	(0,0,3,6,0)
SFS [S2: (2,1) (4,3) (10,-3)] : #1	9	(3, 1, 2)	2	(0,0,3,6,0)
SFS [S2: (4,1) (4,1) (4,-3)] : #1	9	(2, 2, 2)	3	(0,0,3,6,0)
SFS [S2: (4,1) (4,1) (4,-1)] : #1	9	(2, 2, 2)	3	(0,0,3,6,0)
SFS [S2: (4,1) (4,3) (4,-1)] : #1	9	(2, 2, 2)	3	(0,0,3,6,0)
SFS [S2: (4,3) (4,3) (4,-1)] : #1	9	(2, 2, 2)	3	(0,0,3,6,0)

SFS [S2: (2,1) (2,1) (10,-1)] : #2	11	(4, 0, 4)	1	(0,0,2,7,2)
SFS [S2: (2,1) (2,1) (22,-19)] : #2	11	(4, 0, 4)	1	(0,0,2,7,2)
SFS [S2: (2,1) (2,1) (22,-19)] : #4	11	(4, 0, 4)	1	(0,0,2,5,4)
SFS [S2: (2,1) (2,1) (22,-19)] : #6	11	(4, 0, 4)	1	(0,0,2,3,6)
SFS [S2: (2,1) (2,1) (22,-19)] : #8	11	(4, 0, 4)	0	(0,0,2,1,8)
SFS [S2: (2,1) (2,1) (22,-15)] : #2	11	(4, 0, 4)	1	(0,0,2,7,2)
SFS [S2: (2,1) (2,1) (22,-15)] : #4	11	(4, 0, 4)	1	(0,0,2,5,4)
SFS [S2: (2,1) (2,1) (22,-7)] : #2	11	(4, 0, 4)	1	(0,0,2,7,2)
SFS [S2: (2,1) (2,1) (22,-3)] : #2	11	(4, 0, 4)	1	(0,0,2,7,2)
SFS [S2: (2,1) (2,1) (26,-21)] : #2	11	(4, 0, 4)	1	(0,0,2,7,2)
SFS [S2: (2,1) (2,1) (26,-21)] : #4	11	(4, 0, 4)	1	(0,0,2,5,4)
SFS [S2: (2,1) (2,1) (26,-21)] : #6	11	(4, 0, 4)	1	(0,0,2,3,6)
SFS [S2: (2,1) (2,1) (26,-5)] : #2	11	(4, 0, 4)	1	(0,0,2,7,2)
SFS [S2: (2,1) (2,1) (38,-31)] : #2	11	(4, 0, 4)	1	(0,0,2,7,2)
SFS [S2: (2,1) (2,1) (38,-31)] : #4	11	(4, 0, 4)	1	(0,0,2,5,4)
SFS [S2: (2,1) (2,1) (38,-31)] : #6	11	(4, 0, 4)	1	(0,0,2,3,6)
SFS [S2: (2,1) (2,1) (38,-27)] : #2	11	(4, 0, 4)	1	(0,0,2,7,2)
SFS [S2: (2,1) (2,1) (38,-27)] : #4	11	(4, 0, 4)	1	(0,0,2,5,4)
SFS [S2: (2,1) (2,1) (38,-11)] : #2	11	(4, 0, 4)	1	(0,0,2,7,2)
SFS [S2: (2,1) (2,1) (38,-7)] : #2	11	(4, 0, 4)	1	(0,0,2,7,2)
SFS [S2: (2,1) (2,1) (42,-29)] : #2	11	(4, 0, 4)	1	(0,0,2,7,2)
SFS [S2: (2,1) (2,1) (42,-29)] : #4	11	(4, 0, 4)	1	(0,0,2,5,4)
SFS [S2: (2,1) (2,1) (42,-13)] : #2	11	(4, 0, 4)	1	(0,0,2,7,2)
SFS [S2: (2,1) (2,1) (58,-41)] : #2	11	(4, 0, 4)	1	(0,0,2,7,2)
SFS [S2: (2,1) (2,1) (58,-41)] : #4	11	(4, 0, 4)	1	(0,0,2,5,4)
SFS [S2: (2,1) (2,1) (58,-17)] : #2	11	(4, 0, 4)	1	(0,0,2,7,2)
SFS [S2: (2,1) (4,1) (8,-1)] : #1	11	(4, 1, 3)	2	(0,0,3,8,0)
SFS [S2: (2,1) (4,1) (8,-1)] : #2	11	(4, 1, 3)	1	(0,0,2,5,4)
SFS [S2: (2,1) (4,1) (16,-5)] : #1	11	(4, 1, 3)	2	(0,0,3,8,0)
SFS [S2: (2,1) (4,1) (16,-5)] : #2	11	(4, 1, 3)	1	(0,0,2,5,4)
SFS [S2: (2,1) (4,1) (16,-3)] : #1	11	(4, 1, 3)	2	(0,0,3,8,0)
SFS [S2: (2,1) (4,1) (16,-3)] : #2	11	(4, 1, 3)	1	(0,0,2,5,4)
SFS [S2: (2,1) (4,1) (24,-7)] : #1	11	(4, 1, 3)	2	(0,0,3,8,0)
SFS [S2: (2,1) (4,1) (24,-7)] : #2	11	(4, 1, 3)	1	(0,0,2,5,4)
SFS [S2: (2,1) (4,3) (8,-7)] : #1	11	(4, 1, 3)	2	(0,0,3,8,0)
SFS [S2: (2,1) (4,3) (8,-7)] : #2	11	(4, 3, 1)	0	(0,0,2,1,8)
SFS [S2: (2,1) (4,3) (8,-1)] : #1	11	(4, 1, 3)	2	(0,0,3,8,0)
SFS [S2: (2,1) (4,3) (16,-13)] : #1	11	(4, 1, 3)	2	(0,0,3,8,0)
SFS [S2: (2,1) (4,3) (16,-11)] : #1	11	(4, 1, 3)	2	(0,0,3,8,0)
SFS [S2: (2,1) (4,3) (16,-5)] : #1	11	(4, 1, 3)	2	(0,0,3,8,0)
SFS [S2: (2,1) (4,3) (16,-3)] : #1	11	(4, 1, 3)	2	(0,0,3,8,0)
SFS [S2: (2,1) (4,3) (24,-17)] : #1	11	(4, 1, 3)	2	(0,0,3,8,0)
SFS [S2: (2,1) (4,3) (24,-7)] : #1	11	(4, 1, 3)	2	(0,0,3,8,0)
SFS [S2: (2,1) (6,1) (6,-1)] : #1	11	(4, 2, 2)	2	(0,0,3,8,0)
SFS [S2: (2,1) (6,1) (6,-1)] : #2	11	(4, 2, 2)	1	(0,0,2,3,6)
SFS [S2: (2,1) (6,1) (10,-3)] : #1	11	(4, 2, 2)	2	(0,0,3,8,0)

SFS [S2: (2,1) (6,1) (10,-3)] : #2	11	(4, 2, 2)	1	(0,0,2,3,6)
SFS [S2: (2,1) (6,5) (6,-1)] : #1	11	(4, 2, 2)	2	(0,0,3,8,0)
SFS [S2: (2,1) (6,5) (10,-7)] : #1	11	(4, 2, 2)	2	(0,0,3,8,0)
SFS [S2: (2,1) (6,5) (10,-3)] : #1	11	(4, 2, 2)	2	(0,0,3,8,0)
SFS [S2: (2,1) (10,3) (10,-3)] : #1	11	(4, 2, 2)	2	(0,0,3,8,0)
SFS [S2: (2,1) (10,7) (10,-3)] : #1	11	(4, 2, 2)	2	(0,0,3,8,0)
SFS [S2: (4,1) (4,1) (6,-5)] : #1	11	(3, 2, 3)	3	(0,0,3,8,0)
SFS [S2: (4,1) (4,1) (6,-1)] : #1	11	(3, 2, 3)	3	(0,0,3,8,0)
SFS [S2: (4,1) (4,1) (10,-7)] : #1	11	(3, 2, 3)	3	(0,0,3,8,0)
SFS [S2: (4,1) (4,1) (10,-3)] : #1	11	(3, 2, 3)	3	(0,0,3,8,0)
SFS [S2: (4,1) (4,3) (6,-5)] : #1	11	(3, 2, 3)	3	(0,0,3,8,0)
SFS [S2: (4,1) (4,3) (6,-1)] : #1	11	(3, 2, 3)	3	(0,0,3,8,0)
SFS [S2: (4,1) (4,3) (10,-7)] : #1	11	(3, 2, 3)	3	(0,0,3,8,0)
SFS [S2: (4,1) (4,3) (10,-3)] : #1	11	(3, 2, 3)	3	(0,0,3,8,0)
SFS [S2: (4,3) (4,3) (6,-5)] : #1	11	(3, 2, 3)	3	(0,0,3,8,0)
SFS [S2: (4,3) (4,3) (6,-1)] : #1	11	(3, 2, 3)	3	(0,0,3,8,0)
SFS [S2: (4,3) (4,3) (10,-7)] : #1	11	(3, 2, 3)	3	(0,0,3,8,0)
SFS [S2: (4,3) (4,3) (10,-3)] : #1	11	(3, 2, 3)	3	(0,0,3,8,0)

TABLE 4.1. A complete list of all minimal triangulations of closed, orientable, irreducible, connected 3–manifolds up to 11 tetrahedra with $\operatorname{rank}(H^1(M;\mathbb{Z}_2)) \geq 2$ and complexity $c(M) = 3 + \sum_{i=1}^{3} \|\varphi_i\|$. All examples are Seifert fibred spaces with three exceptional fibres and base orbifold S^2.

Census triangulation	Size	$\mathbb{Z}_2$–norms	ϵ_3	Profile
SFS [S2: (2,1) (2,1) (2,1)] : #1	4	(0, 0, 0)	0	(0,0,3,1,0)
SFS [S2: (2,1) (2,1) (4,1)] : #1	6	(1, 0, 1)	1	(0,0,3,3,0)
SFS [S2: (2,1) (2,1) (4,1)] : #2	6	(1, 0, 1)	1	(0,0,3,3,0)
SFS [S2: (2,1) (2,1) (4,3)] : #1	6	(1, 0, 1)	1	(0,0,3,3,0)
SFS [S2: (2,1) (2,1) (4,3)] : #2	6	(1, 0, 1)	1	(0,0,3,3,0)
SFS [S2: (2,1) (2,1) (8,-5)] : #1	6	(1, 0, 1)	0	(0,0,3,3,0)
SFS [S2: (2,1) (2,1) (8,-5)] : #2	6	(1, 0, 1)	0	(0,0,2,2,2)
SFS [S2: (2,1) (2,1) (8,-5)] : #3	6	(1, 0, 1)	0	(0,0,3,1,2)
SFS [S2: (2,1) (2,1) (8,-3)] : #1	6	(1, 0, 1)	0	(0,0,3,3,0)
SFS [S2: (2,1) (2,1) (8,-3)] : #2	6	(1, 0, 1)	0	(0,0,2,2,2)
SFS [S2: (2,1) (4,1) (4,-3)] : #1	6	(1, 1, 0)	0	(0,0,4,0,2)
SFS [S2: (2,1) (4,1) (4,-3)] : #2	6	(0, 1, 1)	0	(0,0,0,0,6)
SFS [S2: (2,1) (2,1) (6,1)] : #1	8	(2, 0, 2)	1	(0,0,3,5,0)
SFS [S2: (2,1) (2,1) (6,1)] : #2	8	(2, 0, 2)	1	(0,0,3,5,0)
SFS [S2: (2,1) (2,1) (6,5)] : #1	8	(2, 0, 2)	1	(0,0,3,5,0)
SFS [S2: (2,1) (2,1) (6,5)] : #2	8	(2, 0, 2)	1	(0,0,3,5,0)
SFS [S2: (2,1) (2,1) (10,3)] : #1	8	(2, 0, 2)	1	(0,0,3,5,0)
SFS [S2: (2,1) (2,1) (10,3)] : #2	8	(2, 0, 2)	1	(0,0,3,5,0)
SFS [S2: (2,1) (2,1) (10,7)] : #1	8	(2, 0, 2)	1	(0,0,3,5,0)
SFS [S2: (2,1) (2,1) (10,7)] : #2	8	(2, 0, 2)	1	(0,0,3,5,0)

SFS [S2: (2,1) (2,1) (14,-11)] : #1	8	(2, 0, 2)	0	(0,0,3,5,0)
SFS [S2: (2,1) (2,1) (14,-11)] : #2	8	(2, 0, 2)	0	(0,0,2,4,2)
SFS [S2: (2,1) (2,1) (14,-11)] : #3	8	(2, 0, 2)	0	(0,0,3,3,2)
SFS [S2: (2,1) (2,1) (14,-11)] : #4	8	(2, 0, 2)	0	(0,0,2,2,4)
SFS [S2: (2,1) (2,1) (14,-11)] : #5	8	(2, 0, 2)	0	(0,0,3,1,4)
SFS [S2: (2,1) (2,1) (14,-9)] : #2	8	(2, 0, 2)	1	(0,0,2,4,2)
SFS [S2: (2,1) (2,1) (14,-9)] : #3	8	(2, 0, 2)	1	(0,0,3,3,2)
SFS [S2: (2,1) (2,1) (14,-5)] : #2	8	(2, 0, 2)	1	(0,0,2,4,2)
SFS [S2: (2,1) (2,1) (14,-3)] : #1	8	(2, 0, 2)	0	(0,0,3,5,0)
SFS [S2: (2,1) (2,1) (14,-3)] : #2	8	(2, 0, 2)	0	(0,0,2,4,2)
SFS [S2: (2,1) (2,1) (18,-13)] : #1	8	(2, 0, 2)	0	(0,0,3,5,0)
SFS [S2: (2,1) (2,1) (18,-13)] : #2	8	(2, 0, 2)	0	(0,0,2,4,2)
SFS [S2: (2,1) (2,1) (18,-13)] : #3	8	(2, 0, 2)	0	(0,0,3,3,2)
SFS [S2: (2,1) (2,1) (18,-13)] : #4	8	(2, 0, 2)	0	(0,0,2,2,4)
SFS [S2: (2,1) (2,1) (18,-11)] : #2	8	(2, 0, 2)	1	(0,0,2,4,2)
SFS [S2: (2,1) (2,1) (18,-11)] : #3	8	(2, 0, 2)	1	(0,0,3,3,2)
SFS [S2: (2,1) (2,1) (18,-7)] : #2	8	(2, 0, 2)	1	(0,0,2,4,2)
SFS [S2: (2,1) (2,1) (18,-5)] : #1	8	(2, 0, 2)	0	(0,0,3,5,0)
SFS [S2: (2,1) (2,1) (18,-5)] : #2	8	(2, 0, 2)	0	(0,0,2,4,2)
SFS [S2: (2,1) (4,1) (4,1)] : #1	8	(2, 1, 1)	2	(0,0,3,5,0)
SFS [S2: (2,1) (4,1) (4,1)] : #2	8	(2, 1, 1)	2	(0,0,3,5,0)
SFS [S2: (2,1) (4,1) (4,3)] : #1	8	(2, 1, 1)	2	(0,0,3,5,0)
SFS [S2: (2,1) (4,1) (4,3)] : #2	8	(2, 1, 1)	2	(0,0,3,5,0)
SFS [S2: (2,1) (4,1) (4,3)] : #3	8	(2, 1, 1)	2	(0,0,3,5,0)
SFS [S2: (2,1) (4,1) (6,-5)] : #1	8	(2, 1, 1)	0	(0,0,0,0,8)
SFS [S2: (2,1) (4,1) (6,-5)] : #2	8	(2, 1, 1)	0	(0,0,4,0,4)
SFS [S2: (2,1) (4,1) (8,-5)] : #1	8	(2, 1, 1)	1	(0,0,3,5,0)
SFS [S2: (2,1) (4,1) (8,-5)] : #2	8	(2, 1, 1)	0	(0,0,2,2,4)
SFS [S2: (2,1) (4,1) (8,-5)] : #3	8	(1, 1, 2)	0	(0,0,3,1,4)
SFS [S2: (2,1) (4,1) (8,-3)] : #1	8	(2, 1, 1)	1	(0,0,3,5,0)
SFS [S2: (2,1) (4,1) (8,-3)] : #2	8	(2, 1, 1)	0	(0,0,2,2,4)
SFS [S2: (2,1) (4,3) (4,3)] : #1	8	(2, 1, 1)	2	(0,0,3,5,0)
SFS [S2: (2,1) (4,3) (4,3)] : #2	8	(2, 1, 1)	2	(0,0,3,5,0)
SFS [S2: (2,1) (4,3) (8,-5)] : #1	8	(2, 1, 1)	1	(0,0,3,5,0)
SFS [S2: (2,1) (4,3) (8,-3)] : #1	8	(2, 1, 1)	1	(0,0,3,5,0)
SFS [RP2/n2: (3,1) (3,1)] : #1	8	(2, 0, 2)	0	(0,0,3,5,0)
SFS [RP2/n2: (3,1) (3,1)] : #2	8	(2, 0, 2)	0	(0,0,4,2,2)
SFS [D: (2,1) (2,1)] U/m SFS [D: (3,1) (3,1)], m = [0,1 — 1,0] : #1	8	(2, 0, 2)	0	(0,0,3,5,0)
SFS [S2: (2,1) (2,1) (8,1)] : #1	10	(3, 0, 3)	1	(0,0,3,7,0)
SFS [S2: (2,1) (2,1) (8,1)] : #2	10	(3, 0, 3)	1	(0,0,3,7,0)
SFS [S2: (2,1) (2,1) (8,7)] : #1	10	(3, 0, 3)	1	(0,0,3,7,0)
SFS [S2: (2,1) (2,1) (8,7)] : #2	10	(3, 0, 3)	1	(0,0,3,7,0)
SFS [S2: (2,1) (2,1) (16,3)] : #1	10	(3, 0, 3)	1	(0,0,3,7,0)
SFS [S2: (2,1) (2,1) (16,3)] : #2	10	(3, 0, 3)	1	(0,0,3,7,0)
SFS [S2: (2,1) (2,1) (16,5)] : #1	10	(3, 0, 3)	1	(0,0,3,7,0)
SFS [S2: (2,1) (2,1) (16,5)] : #2	10	(3, 0, 3)	1	(0,0,3,7,0)

SFS [S2: (2,1) (2,1) (16,11)] : #1	10	(3, 0, 3)	1	(0,0,3,7,0)
SFS [S2: (2,1) (2,1) (16,11)] : #2	10	(3, 0, 3)	1	(0,0,3,7,0)
SFS [S2: (2,1) (2,1) (16,13)] : #1	10	(3, 0, 3)	1	(0,0,3,7,0)
SFS [S2: (2,1) (2,1) (16,13)] : #2	10	(3, 0, 3)	1	(0,0,3,7,0)
SFS [S2: (2,1) (2,1) (20,-17)] : #1	10	(3, 0, 3)	0	(0,0,3,7,0)
SFS [S2: (2,1) (2,1) (20,-17)] : #2	10	(3, 0, 3)	0	(0,0,2,6,2)
SFS [S2: (2,1) (2,1) (20,-17)] : #3	10	(3, 0, 3)	0	(0,0,3,5,2)
SFS [S2: (2,1) (2,1) (20,-17)] : #4	10	(3, 0, 3)	0	(0,0,2,4,4)
SFS [S2: (2,1) (2,1) (20,-17)] : #5	10	(3, 0, 3)	0	(0,0,3,3,4)
SFS [S2: (2,1) (2,1) (20,-17)] : #6	10	(3, 0, 3)	0	(0,0,2,2,6)
SFS [S2: (2,1) (2,1) (20,-17)] : #7	10	(3, 0, 3)	0	(0,0,3,1,6)
SFS [S2: (2,1) (2,1) (20,-13)] : #2	10	(3, 0, 3)	1	(0,0,2,6,2)
SFS [S2: (2,1) (2,1) (20,-13)] : #3	10	(3, 0, 3)	1	(0,0,3,5,2)
SFS [S2: (2,1) (2,1) (20,-7)] : #2	10	(3, 0, 3)	1	(0,0,2,6,2)
SFS [S2: (2,1) (2,1) (20,-3)] : #1	10	(3, 0, 3)	0	(0,0,3,7,0)
SFS [S2: (2,1) (2,1) (20,-3)] : #2	10	(3, 0, 3)	0	(0,0,2,6,2)
SFS [S2: (2,1) (2,1) (24,-19)] : #2	10	(3, 0, 3)	1	(0,0,2,6,2)
SFS [S2: (2,1) (2,1) (24,-19)] : #4	10	(3, 0, 3)	1	(0,0,2,4,4)
SFS [S2: (2,1) (2,1) (24,-19)] : #5	10	(3, 0, 3)	1	(0,0,3,3,4)
SFS [S2: (2,1) (2,1) (24,7)] : #1	10	(3, 0, 3)	1	(0,0,3,7,0)
SFS [S2: (2,1) (2,1) (24,7)] : #2	10	(3, 0, 3)	1	(0,0,3,7,0)
SFS [S2: (2,1) (2,1) (24,17)] : #1	10	(3, 0, 3)	1	(0,0,3,7,0)
SFS [S2: (2,1) (2,1) (24,17)] : #2	10	(3, 0, 3)	1	(0,0,3,7,0)
SFS [S2: (2,1) (2,1) (24,-5)] : #2	10	(3, 0, 3)	1	(0,0,2,6,2)
SFS [S2: (2,1) (2,1) (28,-23)] : #1	10	(3, 0, 3)	0	(0,0,3,7,0)
SFS [S2: (2,1) (2,1) (28,-23)] : #2	10	(3, 0, 3)	0	(0,0,2,6,2)
SFS [S2: (2,1) (2,1) (28,-23)] : #3	10	(3, 0, 3)	0	(0,0,3,5,2)
SFS [S2: (2,1) (2,1) (28,-23)] : #4	10	(3, 0, 3)	0	(0,0,2,4,4)
SFS [S2: (2,1) (2,1) (28,-23)] : #5	10	(3, 0, 3)	0	(0,0,3,3,4)
SFS [S2: (2,1) (2,1) (28,-23)] : #6	10	(3, 0, 3)	0	(0,0,2,2,6)
SFS [S2: (2,1) (2,1) (28,-17)] : #2	10	(3, 0, 3)	1	(0,0,2,6,2)
SFS [S2: (2,1) (2,1) (28,-17)] : #3	10	(3, 0, 3)	1	(0,0,3,5,2)
SFS [S2: (2,1) (2,1) (28,-11)] : #2	10	(3, 0, 3)	1	(0,0,2,6,2)
SFS [S2: (2,1) (2,1) (28,-5)] : #1	10	(3, 0, 3)	0	(0,0,3,7,0)
SFS [S2: (2,1) (2,1) (28,-5)] : #2	10	(3, 0, 3)	0	(0,0,2,6,2)
SFS [S2: (2,1) (2,1) (32,-25)] : #2	10	(3, 0, 3)	1	(0,0,2,6,2)
SFS [S2: (2,1) (2,1) (32,-25)] : #4	10	(3, 0, 3)	1	(0,0,2,4,4)
SFS [S2: (2,1) (2,1) (32,-25)] : #5	10	(3, 0, 3)	1	(0,0,3,3,4)
SFS [S2: (2,1) (2,1) (32,-23)] : #2	10	(3, 0, 3)	1	(0,0,2,6,2)
SFS [S2: (2,1) (2,1) (32,-23)] : #4	10	(3, 0, 3)	1	(0,0,2,4,4)
SFS [S2: (2,1) (2,1) (32,-9)] : #2	10	(3, 0, 3)	1	(0,0,2,6,2)
SFS [S2: (2,1) (2,1) (32,-7)] : #2	10	(3, 0, 3)	1	(0,0,2,6,2)
SFS [S2: (2,1) (2,1) (36,-25)] : #1	10	(3, 0, 3)	0	(0,0,3,7,0)
SFS [S2: (2,1) (2,1) (36,-25)] : #2	10	(3, 0, 3)	0	(0,0,2,6,2)
SFS [S2: (2,1) (2,1) (36,-25)] : #3	10	(3, 0, 3)	0	(0,0,3,5,2)
SFS [S2: (2,1) (2,1) (36,-25)] : #4	10	(3, 0, 3)	0	(0,0,2,4,4)

SFS [S2: (2,1) (2,1) (36,-23)] : #2	10	(3, 0, 3)	1	(0,0,2,6,2)
SFS [S2: (2,1) (2,1) (36,-23)] : #3	10	(3, 0, 3)	1	(0,0,3,5,2)
SFS [S2: (2,1) (2,1) (36,-13)] : #2	10	(3, 0, 3)	1	(0,0,2,6,2)
SFS [S2: (2,1) (2,1) (36,-11)] : #1	10	(3, 0, 3)	0	(0,0,3,7,0)
SFS [S2: (2,1) (2,1) (36,-11)] : #2	10	(3, 0, 3)	0	(0,0,2,6,2)
SFS [S2: (2,1) (2,1) (40,-29)] : #2	10	(3, 0, 3)	1	(0,0,2,6,2)
SFS [S2: (2,1) (2,1) (40,-29)] : #4	10	(3, 0, 3)	1	(0,0,2,4,4)
SFS [S2: (2,1) (2,1) (40,-11)] : #2	10	(3, 0, 3)	1	(0,0,2,6,2)
SFS [S2: (2,1) (2,1) (44,-31)] : #1	10	(3, 0, 3)	0	(0,0,3,7,0)
SFS [S2: (2,1) (2,1) (44,-31)] : #2	10	(3, 0, 3)	0	(0,0,2,6,2)
SFS [S2: (2,1) (2,1) (44,-31)] : #3	10	(3, 0, 3)	0	(0,0,3,5,2)
SFS [S2: (2,1) (2,1) (44,-31)] : #4	10	(3, 0, 3)	0	(0,0,2,4,4)
SFS [S2: (2,1) (2,1) (44,-27)] : #2	10	(3, 0, 3)	1	(0,0,2,6,2)
SFS [S2: (2,1) (2,1) (44,-27)] : #3	10	(3, 0, 3)	1	(0,0,3,5,2)
SFS [S2: (2,1) (2,1) (44,-17)] : #2	10	(3, 0, 3)	1	(0,0,2,6,2)
SFS [S2: (2,1) (2,1) (44,-13)] : #1	10	(3, 0, 3)	0	(0,0,3,7,0)
SFS [S2: (2,1) (2,1) (44,-13)] : #2	10	(3, 0, 3)	0	(0,0,2,6,2)
SFS [S2: (2,1) (4,1) (6,1)] : #1	10	(3, 1, 2)	2	(0,0,3,7,0)
SFS [S2: (2,1) (4,1) (6,1)] : #2	10	(3, 1, 2)	2	(0,0,3,7,0)
SFS [S2: (2,1) (4,1) (6,1)] : #3	10	(3, 1, 2)	2	(0,0,3,7,0)
SFS [S2: (2,1) (4,1) (6,5)] : #1	10	(3, 1, 2)	2	(0,0,3,7,0)
SFS [S2: (2,1) (4,1) (6,5)] : #2	10	(3, 1, 2)	2	(0,0,3,7,0)
SFS [S2: (2,1) (4,1) (6,5)] : #3	10	(3, 1, 2)	2	(0,0,3,7,0)
SFS [S2: (2,1) (4,1) (8,-7)] : #1	10	(2, 3, 1)	0	(0,0,0,0,10)
SFS [S2: (2,1) (4,1) (8,-7)] : #2	10	(2, 3, 1)	0	(0,0,4,0,6)
SFS [S2: (2,1) (4,1) (10,3)] : #1	10	(3, 1, 2)	2	(0,0,3,7,0)
SFS [S2: (2,1) (4,1) (10,3)] : #2	10	(3, 1, 2)	2	(0,0,3,7,0)
SFS [S2: (2,1) (4,1) (10,3)] : #3	10	(3, 1, 2)	2	(0,0,3,7,0)
SFS [S2: (2,1) (4,1) (10,7)] : #1	10	(3, 1, 2)	2	(0,0,3,7,0)
SFS [S2: (2,1) (4,1) (10,7)] : #2	10	(3, 1, 2)	2	(0,0,3,7,0)
SFS [S2: (2,1) (4,1) (10,7)] : #3	10	(3, 1, 2)	2	(0,0,3,7,0)
SFS [S2: (2,1) (4,1) (14,-9)] : #1	10	(3, 1, 2)	2	(0,0,3,7,0)
SFS [S2: (2,1) (4,1) (14,-9)] : #2	10	(3, 1, 2)	1	(0,0,2,4,4)
SFS [S2: (2,1) (4,1) (14,-9)] : #3	10	(2, 1, 3)	1	(0,0,3,3,4)
SFS [S2: (2,1) (4,1) (14,-5)] : #1	10	(3, 1, 2)	2	(0,0,3,7,0)
SFS [S2: (2,1) (4,1) (14,-5)] : #2	10	(3, 1, 2)	1	(0,0,2,4,4)
SFS [S2: (2,1) (4,1) (14,-3)] : #1	10	(3, 1, 2)	1	(0,0,3,7,0)
SFS [S2: (2,1) (4,1) (14,-3)] : #2	10	(3, 1, 2)	0	(0,0,2,4,4)
SFS [S2: (2,1) (4,1) (18,-11)] : #1	10	(3, 1, 2)	2	(0,0,3,7,0)
SFS [S2: (2,1) (4,1) (18,-11)] : #2	10	(3, 1, 2)	1	(0,0,2,4,4)
SFS [S2: (2,1) (4,1) (18,-11)] : #3	10	(2, 1, 3)	1	(0,0,3,3,4)
SFS [S2: (2,1) (4,1) (18,-7)] : #1	10	(3, 1, 2)	2	(0,0,3,7,0)
SFS [S2: (2,1) (4,1) (18,-7)] : #2	10	(3, 1, 2)	1	(0,0,2,4,4)
SFS [S2: (2,1) (4,1) (18,-5)] : #1	10	(3, 1, 2)	1	(0,0,3,7,0)
SFS [S2: (2,1) (4,1) (18,-5)] : #2	10	(3, 1, 2)	0	(0,0,2,4,4)
SFS [S2: (2,1) (4,3) (6,1)] : #1	10	(3, 1, 2)	2	(0,0,3,7,0)

SFS [S2: (2,1) (4,3) (6,1)] : #2	10	(3, 1, 2)	2	(0,0,3,7,0)
SFS [S2: (2,1) (4,3) (6,1)] : #3	10	(3, 1, 2)	2	(0,0,3,7,0)
SFS [S2: (2,1) (4,3) (6,5)] : #1	10	(3, 1, 2)	2	(0,0,3,7,0)
SFS [S2: (2,1) (4,3) (6,5)] : #2	10	(3, 1, 2)	2	(0,0,3,7,0)
SFS [S2: (2,1) (4,3) (6,5)] : #3	10	(3, 1, 2)	2	(0,0,3,7,0)
SFS [S2: (2,1) (4,3) (10,3)] : #1	10	(3, 1, 2)	2	(0,0,3,7,0)
SFS [S2: (2,1) (4,3) (10,3)] : #2	10	(3, 1, 2)	2	(0,0,3,7,0)
SFS [S2: (2,1) (4,3) (10,3)] : #3	10	(3, 1, 2)	2	(0,0,3,7,0)
SFS [S2: (2,1) (4,3) (10,7)] : #1	10	(3, 1, 2)	2	(0,0,3,7,0)
SFS [S2: (2,1) (4,3) (10,7)] : #2	10	(3, 1, 2)	2	(0,0,3,7,0)
SFS [S2: (2,1) (4,3) (10,7)] : #3	10	(3, 1, 2)	2	(0,0,3,7,0)
SFS [S2: (2,1) (4,3) (14,-11)] : #1	10	(3, 1, 2)	1	(0,0,3,7,0)
SFS [S2: (2,1) (4,3) (14,-9)] : #1	10	(3, 1, 2)	2	(0,0,3,7,0)
SFS [S2: (2,1) (4,3) (14,-5)] : #1	10	(3, 1, 2)	2	(0,0,3,7,0)
SFS [S2: (2,1) (4,3) (14,-3)] : #1	10	(3, 1, 2)	1	(0,0,3,7,0)
SFS [S2: (2,1) (4,3) (18,-13)] : #1	10	(3, 1, 2)	1	(0,0,3,7,0)
SFS [S2: (2,1) (4,3) (18,-11)] : #1	10	(3, 1, 2)	2	(0,0,3,7,0)
SFS [S2: (2,1) (4,3) (18,-7)] : #1	10	(3, 1, 2)	2	(0,0,3,7,0)
SFS [S2: (2,1) (4,3) (18,-5)] : #1	10	(3, 1, 2)	1	(0,0,3,7,0)
SFS [S2: (2,1) (6,1) (6,-5)] : #1	10	(2, 2, 2)	0	(0,0,0,0,10)
SFS [S2: (2,1) (6,1) (6,-5)] : #2	10	(2, 2, 2)	0	(0,0,4,0,6)
SFS [S2: (2,1) (6,1) (8,-5)] : #1	10	(3, 1, 2)	1	(0,0,3,7,0)
SFS [S2: (2,1) (6,1) (8,-5)] : #2	10	(3, 2, 1)	0	(0,0,2,2,6)
SFS [S2: (2,1) (6,1) (8,-5)] : #3	10	(1, 2, 3)	0	(0,0,3,1,6)
SFS [S2: (2,1) (6,1) (8,-3)] : #1	10	(3, 1, 2)	1	(0,0,3,7,0)
SFS [S2: (2,1) (6,1) (8,-3)] : #2	10	(3, 2, 1)	0	(0,0,2,2,6)
SFS [S2: (2,1) (6,5) (8,-5)] : #1	10	(3, 1, 2)	1	(0,0,3,7,0)
SFS [S2: (2,1) (6,5) (8,-3)] : #1	10	(3, 1, 2)	1	(0,0,3,7,0)
SFS [S2: (2,1) (8,3) (10,-7)] : #1	10	(3, 1, 2)	1	(0,0,3,7,0)
SFS [S2: (2,1) (8,3) (10,-3)] : #1	10	(3, 1, 2)	1	(0,0,3,7,0)
SFS [S2: (2,1) (8,5) (10,-7)] : #1	10	(3, 1, 2)	1	(0,0,3,7,0)
SFS [S2: (2,1) (8,5) (10,-3)] : #1	10	(3, 1, 2)	1	(0,0,3,7,0)
SFS [S2: (4,1) (4,1) (4,1)] : #1	10	(2, 2, 2)	3	(0,0,3,7,0)
SFS [S2: (4,1) (4,1) (4,3)] : #1	10	(2, 2, 2)	3	(0,0,3,7,0)
SFS [S2: (4,1) (4,1) (4,3)] : #2	10	(2, 2, 2)	3	(0,0,3,7,0)
SFS [S2: (4,1) (4,1) (8,-5)] : #1	10	(2, 2, 2)	2	(0,0,3,7,0)
SFS [S2: (4,1) (4,1) (8,-3)] : #1	10	(2, 2, 2)	2	(0,0,3,7,0)
SFS [S2: (4,1) (4,3) (4,3)] : #1	10	(2, 2, 2)	3	(0,0,3,7,0)
SFS [S2: (4,1) (4,3) (4,3)] : #2	10	(2, 2, 2)	3	(0,0,3,7,0)
SFS [S2: (4,1) (4,3) (8,-5)] : #1	10	(2, 2, 2)	2	(0,0,3,7,0)
SFS [S2: (4,1) (4,3) (8,-3)] : #1	10	(2, 2, 2)	2	(0,0,3,7,0)
SFS [S2: (4,3) (4,3) (4,3)] : #1	10	(2, 2, 2)	3	(0,0,3,7,0)
SFS [S2: (4,3) (4,3) (8,-5)] : #1	10	(2, 2, 2)	2	(0,0,3,7,0)
SFS [S2: (4,3) (4,3) (8,-3)] : #1	10	(2, 2, 2)	2	(0,0,3,7,0)
SFS [RP2/n2: (3,1) (3,7)] : #1	10	(3, 0, 3)	0	(0,0,3,7,0)
SFS [RP2/n2: (3,1) (3,7)] : #2	10	(3, 0, 3)	0	(0,0,2,6,2)

SFS [RP2/n2: (3,1) (3,7)] : #3	10	(3, 0, 3)	0	(0,0,4,2,4)
SFS [RP2/n2: (3,1) (3,7)] : #4	10	(3, 0, 3)	0	(0,0,3,5,2)
SFS [RP2/n2: (3,1) (3,7)] : #5	10	(3, 0, 3)	0	(0,0,4,2,4)
SFS [RP2/n2: (3,1) (3,7)] : #6	10	(3, 0, 3)	0	(0,0,4,2,4)
SFS [RP2/n2: (3,1) (3,7)] : #11	10	(3, 0, 3)	1	(0,0,3,7,0)
SFS [RP2/n2: (3,1) (3,7)] : #12	10	(3, 0, 3)	1	(0,0,4,4,2)
SFS [RP2/n2: (3,1) (5,1)] : #1	10	(3, 0, 3)	1	(0,0,3,7,0)
SFS [RP2/n2: (3,1) (5,1)] : #2	10	(3, 0, 3)	1	(0,0,4,4,2)
SFS [RP2/n2: (3,1) (7,3)] : #1	10	(3, 0, 3)	1	(0,0,3,7,0)
SFS [RP2/n2: (3,1) (7,3)] : #2	10	(3, 0, 3)	1	(0,0,4,4,2)
SFS [D: (2,1) (2,1)] U/m SFS [D: (3,1) (3,1)], m = [0,1 — 1,-2] : #1	10	(3, 0, 3)	0	(0,0,2,6,2)
SFS [D: (2,1) (2,1)] U/m SFS [D: (3,1) (3,1)], m = [0,1 — 1,-2] : #2	10	(3, 0, 3)	0	(0,0,3,7,0)
SFS [D: (2,1) (2,1)] U/m SFS [D: (3,1) (3,1)], m = [0,1 — 1,-2] : #5	10	(3, 0, 3)	1	(0,0,3,7,0)
SFS [D: (2,1) (2,1)] U/m SFS [D: (3,1) (5,1)], m = [0,1 — 1,0] : #1	10	(3, 0, 3)	1	(0,0,3,7,0)
SFS [D: (2,1) (2,1)] U/m SFS [D: (3,1) (7,3)], m = [0,1 — 1,0] : #1	10	(3, 0, 3)	1	(0,0,3,7,0)
SFS [D: (2,1) (4,1)] U/m SFS [D: (3,1) (3,1)], m = [0,1 — 1,0] : #1	10	(3, 2, 1)	1	(0,0,3,7,0)
SFS [D: (2,1) (4,1)] U/m SFS [D: (3,1) (3,1)], m = [-1,1 — 1,0] : #1	10	(3, 2, 1)	1	(0,0,3,7,0)
SFS [D: (2,1) (4,3)] U/m SFS [D: (3,1) (3,1)], m = [0,1 — 1,0] : #1	10	(3, 2, 1)	1	(0,0,3,7,0)
SFS [D: (2,1) (4,3)] U/m SFS [D: (3,1) (3,1)], m = [-1,1 — 1,0] : #1	10	(3, 2, 1)	1	(0,0,3,7,0)

TABLE 4.2. A complete list of all minimal triangulations of closed, orientable, irreducible, connected 3–manifolds up to 11 tetrahedra with $\operatorname{rank}(H^1(M;\mathbb{Z}_2)) \geq 2$ and complexity $c(M) = 4 + \sum_{i=1}^{3} \|\varphi_i\|$. We still observe many Seifert fibred spaces with three exceptional fibres and base orbifold S^2, but we now see orientable Seifert fibred spaces with base orbifold $\mathbb{R}P^2$ and two exceptional fibres, and two-piece graph manifolds constructed from two Seifert fibred spaces with base orbifold D^2 and two exceptional fibres each.

Census triangulation	Size	$t_H(M)$	$\mathbb{Z}_2$–norms	ϵ_3	Profile
Hyp_2.56897060 (2 Z_8) : #1	11	3	(2, 2, 2)	0	(0,0,4,3,4)
Hyp_1.83193119 (Z_2 + Z_12) : #1	10	4	(1, 1, 2)	0	(0,0,6,2,2)
Hyp_1.83193119 (Z_2 + Z_12) : #2	10	4	(2, 1, 1)	0	(0,0,6,0,4)
Hyp_1.83193119 (Z_2 + Z_4) : #1	11	5	(2, 1, 1)	0	(0,0,6,1,4)
Hyp_1.83193119 (Z_2 + Z_4) : #2	11	5	(2, 1, 1)	0	(0,0,7,0,4)
Hyp_1.83193119 (Z_2 + Z_4) : #3	11	5	(2, 1, 1)	0	(0,0,7,0,4)
Hyp_1.83193119 (Z_2 + Z_4) : #4	11	5	(2, 1, 1)	0	(0,0,7,0,4)
Hyp_1.83193119 (Z_2 + Z_4) : #5	11	5	(2, 1, 1)	0	(0,0,4,3,4)
Hyp_1.83193119 (Z_2 + Z_4) : #6	11	5	(2, 1, 1)	0	(0,0,4,3,4)
Hyp_1.83193119 (Z_2 + Z_4) : #7	11	5	(2, 1, 1)	0	(0,0,6,3,2)
Hyp_1.83193119 (Z_2 + Z_4) : #8	11	5	(2, 1, 1)	0	(0,0,4,5,2)
Hyp_1.83193119 (Z_2 + Z_4) : #9	11	5	(2, 1, 1)	0	(0,0,7,0,4)
Hyp_1.83193119 (Z_2 + Z_4) : #10	11	5	(2, 1, 1)	0	(0,0,5,2,4)
Hyp_1.83193119 (Z_2 + Z_4) : #11	11	5	(1, 1, 2)	0	(0,0,5,4,2)
Hyp_1.83193119 (Z_2 + Z_4) : #12	11	5	(2, 1, 1)	0	(0,0,7,2,2)
Hyp_1.83193119 (Z_2 + Z_4) : #13	11	5	(2, 1, 1)	0	(0,0,7,0,4)

Hyp_1.83193119 (Z_2 + Z_4) : #14	11	5	(1, 1, 2)	0	(0,0,6,1,4)
Hyp_1.83193119 (Z_2 + Z_4) : #15	11	5	(2, 1, 1)	0	(0,0,8,3,0)
Hyp_1.83193119 (Z_2 + Z_4) : #16	11	5	(2, 1, 1)	0	(0,0,7,2,2)
Hyp_1.83193119 (Z_2 + Z_4) : #17	11	5	(2, 1, 1)	0	(0,0,7,2,2)
Hyp_1.83193119 (Z_2 + Z_4) : #18	11	5	(1, 1, 2)	0	(0,0,5,2,4)
Hyp_1.83193119 (Z_2 + Z_4) : #19	11	5	(2, 1, 1)	0	(0,0,7,2,2)
Hyp_1.83193119 (Z_2 + Z_4) : #20	11	5	(1, 1, 2)	0	(0,0,7,0,4)
Hyp_1.83193119 (Z_2 + Z_4) : #21	11	5	(2, 1, 1)	0	(0,0,8,1,2)
Hyp_1.83193119 (Z_2 + Z_4) : #22	11	5	(2, 1, 1)	0	(0,0,5,2,4)
Hyp_1.83193119 (Z_2 + Z_4) : #23	11	5	(2, 1, 1)	0	(0,0,6,1,4)
Hyp_1.83193119 (Z_2 + Z_4) : #24	11	5	(2, 1, 1)	0	(0,2,5,0,4)
Hyp_1.83193119 (Z_2 + Z_4) : #25	11	5	(2, 1, 1)	0	(0,2,5,0,4)
Hyp_1.83193119 (Z_2 + Z_4) : #26	11	5	(1, 1, 2)	0	(0,2,5,0,4)
Hyp_1.83193119 (Z_2 + Z_4) : #27	11	5	(2, 1, 1)	0	(0,0,7,0,4)
Hyp_1.83193119 (Z_2 + Z_4) : #28	11	5	(1, 1, 2)	0	(0,2,5,0,4)
Hyp_1.83193119 (Z_2 + Z_4) : #29	11	5	(1, 2, 1)	0	(0,0,7,0,4)
Hyp_1.83193119 (Z_2 + Z_4) : #30	11	5	(2, 1, 1)	0	(0,2,4,1,4)
Hyp_1.83193119 (Z_2 + Z_4) : #31	11	5	(2, 1, 1)	0	(0,2,4,1,4)
Hyp_1.83193119 (Z_2 + Z_4) : #32	11	5	(1, 1, 2)	0	(0,0,6,1,4)
Hyp_1.83193119 (Z_2 + Z_4) : #33	11	5	(1, 1, 2)	0	(0,0,8,1,2)
Hyp_1.83193119 (Z_2 + Z_4) : #34	11	5	(1, 1, 2)	0	(0,0,8,1,2)
Hyp_1.83193119 (Z_2 + Z_4) : #35	11	5	(1, 1, 2)	0	(0,0,7,0,4)
Hyp_1.83193119 (Z_2 + Z_6) : #1	11	5	(2, 1, 1)	0	(0,0,5,0,6)
Hyp_1.83193119 (Z_2 + Z_6) : #2	11	5	(2, 1, 1)	0	(0,0,6,3,2)
Hyp_1.83193119 (Z_2 + Z_6) : #3	11	5	(2, 1, 1)	0	(0,0,4,3,4)
Hyp_1.83193119 (Z_2 + Z_6) : #4	11	5	(1, 1, 2)	0	(0,0,4,3,4)
Hyp_1.83193119 (Z_2 + Z_6) : #5	11	5	(2, 1, 1)	0	(0,0,4,1,6)
Hyp_1.83193119 (Z_2 + Z_6) : #6	11	5	(2, 1, 1)	0	(0,0,5,0,6)
Hyp_1.83193119 (Z_2 + Z_6) : #7	11	5	(2, 1, 1)	0	(0,0,5,2,4)
Hyp_1.83193119 (Z_2 + Z_6) : #8	11	5	(2, 1, 1)	0	(0,0,4,1,6)
Hyp_1.83193119 (Z_2 + Z_6) : #10	11	5	(2, 1, 1)	0	(0,0,7,2,2)
Hyp_1.83193119 (Z_2 + Z_6) : #11	11	5	(2, 1, 1)	0	(0,0,8,3,0)
Hyp_1.83193119 (Z_2 + Z_6) : #12	11	5	(1, 1, 2)	0	(0,2,5,2,2)
Hyp_1.83193119 (Z_2 + Z_6) : #13	11	5	(1, 1, 2)	0	(0,2,6,1,2)
Hyp_1.83193119 (Z_2 + Z_6) : #14	11	5	(2, 1, 1)	0	(0,0,8,3,0)
Hyp_1.83193119 (Z_2 + Z_6) : #15	11	5	(2, 1, 1)	0	(0,0,7,2,2)
Hyp_1.83193119 (Z_2 + Z_6) : #16	11	5	(2, 1, 1)	0	(0,0,8,1,2)
Hyp_1.83193119 (Z_2 + Z_6) : #17	11	5	(2, 1, 1)	0	(0,0,8,1,2)
Hyp_1.83193119 (Z_2 + Z_6) : #18	11	5	(2, 1, 1)	0	(0,0,8,1,2)
Hyp_1.83193119 (Z_2 + Z_6) : #19	11	5	(2, 1, 1)	0	(0,0,8,3,0)
Hyp_1.83193119 (Z_2 + Z_6) : #20	11	5	(2, 1, 1)	0	(0,2,6,1,2)
Hyp_2.02988321 (Z_2 + Z_6) : #1	11	5	(2, 1, 1)	0	(0,0,7,0,4)
Hyp_2.02988321 (Z_2 + Z_6) : #2	11	5	(1, 1, 2)	0	(0,0,5,4,2)
Hyp_2.02988321 (Z_2 + Z_6) : #3	11	5	(2, 1, 1)	0	(0,0,5,2,4)
Hyp_2.02988321 (Z_2 + Z_6) : #4	11	5	(1, 1, 2)	0	(0,0,4,5,2)
Hyp_2.02988321 (Z_2 + Z_6) : #5	11	5	(2, 1, 1)	0	(0,0,4,3,4)

Hyp_2.02988321 (Z_2 + Z_6) : #6	11	5	(2, 1, 1)	0	(0,0,4,3,4)
Hyp_2.02988321 (Z_2 + Z_6) : #7	11	5	(2, 1, 1)	0	(0,0,7,0,4)
Hyp_2.02988321 (Z_2 + Z_6) : #8	11	5	(2, 1, 1)	0	(0,0,7,0,4)
Hyp_2.02988321 (Z_2 + Z_6) : #9	11	5	(2, 1, 1)	0	(0,0,6,1,4)
Hyp_2.02988321 (Z_2 + Z_6) : #10	11	5	(1, 2, 1)	0	(0,0,8,1,2)
Hyp_2.02988321 (Z_2 + Z_6) : #11	11	5	(1, 1, 2)	0	(0,0,5,4,2)
Hyp_2.02988321 (Z_2 + Z_6) : #12	11	5	(1, 1, 2)	0	(0,0,7,0,4)
Hyp_2.02988321 (Z_2 + Z_6) : #13	11	5	(2, 1, 1)	0	(0,0,6,3,2)
Hyp_2.02988321 (Z_2 + Z_6) : #15	11	5	(2, 1, 1)	0	(0,0,7,2,2)
Hyp_2.02988321 (Z_2 + Z_6) : #16	11	5	(2, 1, 1)	0	(0,0,8,3,0)
Hyp_2.02988321 (Z_2 + Z_6) : #17	11	5	(1, 1, 2)	0	(0,2,5,2,2)
Hyp_2.02988321 (Z_2 + Z_6) : #18	11	5	(2, 1, 1)	0	(0,0,8,3,0)
Hyp_2.02988321 (Z_2 + Z_6) : #19	11	5	(1, 1, 2)	0	(0,2,6,1,2)
Hyp_2.02988321 (Z_2 + Z_6) : #20	11	5	(2, 1, 1)	0	(0,0,7,2,2)
Hyp_2.02988321 (Z_2 + Z_6) : #21	11	5	(2, 1, 1)	0	(0,0,8,1,2)
Hyp_2.02988321 (Z_2 + Z_6) : #22	11	5	(2, 1, 1)	0	(0,0,8,1,2)
Hyp_2.02988321 (Z_2 + Z_6) : #23	11	5	(2, 1, 1)	0	(0,0,8,1,2)
Hyp_2.02988321 (Z_2 + Z_6) : #24	11	5	(2, 1, 1)	0	(0,0,8,3,0)
Hyp_2.02988321 (Z_2 + Z_6) : #25	11	5	(1, 1, 2)	0	(0,2,6,1,2)
Hyp_2.02988321 (2 Z_6) : #1	11	5	(1, 1, 2)	0	(0,0,4,3,4)
Hyp_2.20766624 (Z_2 + Z_24) : #1	11	5	(1, 1, 2)	0	(0,0,6,3,2)
Hyp_2.20766624 (Z_2 + Z_24) : #2	11	5	(2, 1, 1)	0	(0,0,4,1,6)
Hyp_2.20766624 (Z_2 + Z_24) : #3	11	5	(1, 1, 2)	0	(0,0,8,1,2)
Hyp_2.20766624 (Z_2 + Z_24) : #4	11	5	(1, 1, 2)	0	(0,0,8,1,2)
Hyp_2.20766624 (Z_2 + Z_24) : #5	11	5	(1, 1, 2)	0	(0,2,5,2,2)
Hyp_2.20766624 (Z_2 + Z_24) : #6	11	5	(1, 1, 2)	0	(0,0,5,2,4)
Hyp_2.20766624 (Z_2 + Z_24) : #7	11	5	(2, 1, 1)	0	(0,0,4,1,6)
Hyp_2.37585098 (Z_2 + Z_24) : #1	11	5	(1, 1, 2)	0	(0,0,6,3,2)

TABLE 4.3. A complete list of all minimal triangulations of closed, orientable, irreducible, connected hyperbolic 3–manifolds up to 11 tetrahedra with $\text{rank}(H^1(M;\mathbb{Z}_2)) \geq 2$ and complexity $c(M) = (2 + t_2(M)) + \sum_{i=1}^{3} \|\varphi_i\|$. The table is arranged in increasing order of the 2–thickness and we observe a minimal 2–thickness of 3.

References

[AM03] Gennaro Amendola and Bruno Martelli. Non-orientable 3-manifolds of small complexity. *Topology Appl.*, 133(2):157–178, 2003.

[AM05] Gennaro Amendola and Bruno Martelli. Non-orientable 3-manifolds of complexity up to 7. *Topology Appl.*, 150(1-3):179–195, 2005.

[Ame05] Gennaro Amendola. A calculus for ideal triangulations of three-manifolds with embedded arcs. *Math. Nachr.*, 278(9):975–994, 2005.

[AST07] Ian Agol, Peter A. Storm, and William P. Thurston. Lower bounds on volumes of hyperbolic haken 3-manifolds. *J. Amer. Math. Soc.*, 20(4):1053–1077, 2007. With an appendix by Nathan Dunfield.

[ASWY00] Hirotaka Akiyoshi, Makoto Sakuma, Masaaki Wada, and Yasushi Yamashita. Ford domains of punctured torus groups and two-bridge knot groups. In *Knot Thoery - dedicated to Professor Kunio Murasugi for his 70th birthday (University of Toronto, July 1999)*, pages 67–77. 2000.

[BAGPN23] Fathi Ben Aribi, Fran¸cois Guéritaud, and Eiichi Piguet-Nakazawa. Geometric triangulations and the Teichmüller TQFT volume conjecture for twist knots. *Quantum Topol.*, 14(2):285–406, 2023.

[BBP+23] Benjamin A. Burton, Ryan Budney, William Pettersson, et al. Regina: Software for low-dimensional topology. http://regina-normal.github.io/, 1999–2023.

[Bin54] R. H. Bing. Locally tame sets are tame. *Ann. of Math. (2)*, 59:145–158, 1954.

[BK73] Coen Bron and Joep Kerbosch. Algorithm 457: finding all cliques of an undirected graph. *Commun. ACM*, 16(9):575–577, September 1973.

[BRT12] Benjamin A. Burton, J. Hyam Rubinstein, and Stephan Tillmann. The Weber-Seifert dodecahedral space is non-Haken. *Trans. Amer. Math. Soc.*, 364(2):911–932, 2012.

[Bur] Ben Burton. All minimal triangulations of all closed orientable prime 3-manifolds $\leq$ 11 tetrahedra. Available at https://regina-normal.github.io/data.html#census (09/2025).

[Bur03] Benjamin A. Burton. *Minimal triangulations and normal surfaces*. Phd thesis, The University of Melbourne, 2003.

[Bur07] Benjamin A. Burton. Structures of small closed non-orientable 3-manifold triangulations. *J. Knot Theory Ramifications*, 16(5):545–574, 2007.

[Bur10] Benjamin A. Burton. The complexity of the normal surface solution space. In *Computational geometry (SCG'10)*, pages 201–209. ACM, New York, 2010.

[Bur11a] Benjamin A. Burton. Detecting genus in vertex links for the fast enumeration of 3-manifold triangulations. In *ISSAC 2011—Proceedings of the 36th International Symposium on Symbolic and Algebraic Computation*, pages 59–66. ACM, New York, 2011.

[Bur11b] Benjamin A. Burton. Simplification paths in the pachner graphs of closed orientable 3-manifold triangulations, 2011. arXiv:1110.6080.

[Bur13] Benjamin A. Burton. Computational topology with Regina: algorithms, heuristics and implementations. In *Geometry and topology down under*, volume 597 of *Contemp. Math.*, pages 195–224. Amer. Math. Soc., Providence, RI, 2013.

[Bur14a] Benjamin A. Burton. The cusped hyperbolic census is complete, 2014. arXiv:1405.2695.

[Bur14b] Benjamin A. Burton. Enumerating fundamental normal surfaces: Algorithms, experiments and invariants. In *2014 Proceedings of the Meeting on Algorithm Engineering and Experiments (ALENEX)*, pages 112–124, 2014.

[BW69] Glen E. Bredon and John W. Wood. Non-orientable surfaces in orientable 3-manifolds. *Invent. Math.*, 7:83–110, 1969.

[Cas65] B. G. Casler. An imbedding theorem for connected 3-manifolds with boundary. *Proc. Amer. Math. Soc.*, 16:559–566, 1965.

[CDGW] Marc Culler, Nathan M. Dunfield, Matthias Goerner, and Jeffrey R. Weeks. SnapPy, a computer program for studying the geometry and topology of 3-manifolds. Available at `http://snappy.computop.org` (01/2025).

[Cha16a] Jae Choon Cha. Complexity of surgery manifolds and Cheeger-Gromov invariants. *Int. Math. Res. Not. IMRN*, 18:5603–5615, 2016.

[Cha16b] Jae Choon Cha. A topological approach to Cheeger-Gromov universal bounds for von Neumann ρ-invariants. *Comm. Pure Appl. Math.*, 69(6):1154–1209, 2016.

[Cha18] Jae Choon Cha. Complexities of 3-manifolds from triangulations, Heegaard splittings and surgery presentations. *Q. J. Math.*, 69(2):425–442, 2018.

[CHW99] Patrick J. Callahan, Martin V. Hildebrand, and Jeffrey R. Weeks. A census of cusped hyperbolic 3-manifolds. *Math. Comp.*, 68(225):321–332, 1999. With microfiche supplement.

[Con70] J. H. Conway. An enumeration of knots and links, and some of their algebraic properties. In *Computational Problems in Abstract Algebra (Proc. Conf., Oxford, 1967)*, pages 329–358. Pergamon, Oxford-New York-Toronto, Ont., 1970.

[Du22] Xiaoming Du. On $\mathbb{Z}_2$-Thurston norms and pseudo-horizontal surfaces in orientable Seifert 3-manifolds. *Topology Appl.*, 312:Paper No. 108060, 17, 2022.

[EP88] D. B. A. Epstein and R. C. Penner. Euclidean decompositions of noncompact hyperbolic manifolds. *J. Differential Geom.*, 27(1):67–80, 1988.

[FG11] David Futer and François Guéritaud. From angled triangulations to hyperbolic structures. In *Interactions between hyperbolic geometry, quantum topology and number theory*, volume 541 of *Contemp. Math.*, pages 159–182. Amer. Math. Soc., Providence, RI, 2011.

[FGG+16] Evgeny Fominykh, Stavros Garoufalidis, Matthias Goerner, Vladimir Tarkaev, and Andrei Vesnin. A census of tetrahedral hyperbolic manifolds. *Exp. Math.*, 25(4):466–481, 2016.

[FHH22] David Futer, Emily Hamilton, and Neil R. Hoffman. Infinitely many virtual geometric triangulations. *J. Topol.*, 15(4):2352–2388, 2022.

[GS10] François Guéritaud and Saul Schleimer. Canonical triangulations of Dehn fillings. *Geom. Topol.*, 14(1):193–242, 2010.

[Gué06] François Guéritaud. On canonical triangulations of once-punctured torus bundles and two-bridge link complements. *Geom. Topol.*, 10:1239–1284, 2006. With an appendix by David Futer.

[Hak61] Wolfgang Haken. Theorie der normalflächen. *Acta Math.*, 105:245–375, 1961.

[Hak62] Wolfgang Haken. über das Homöomorphieproblem der 3-Mannigfaltigkeiten. I. *Math. Z.*, 80:89–120, 1962.

[HLP99] Joel Hass, Jeffrey C. Lagarias, and Nicholas Pippenger. The computational complexity of knot and link problems. *J. ACM*, 46(2):185–211, 1999.

[HP23] Sophie L. Ham and Jessica S. Purcell. Geometric triangulations and highly twisted links. *Algebr. Geom. Topol.*, 23(3):1399–1462, 2023.

[HW89] Martin Hildebrand and Jeffrey Weeks. A computer generated census of cusped hyperbolic 3-manifolds. In *Computers and mathematics (Cambridge, MA, 1989)*, pages 53–59. Springer, New York, 1989.

[HW94] Craig D. Hodgson and Jeffrey R. Weeks. Symmetries, isometries and length spectra of closed hyperbolic three-manifolds. *Experiment. Math.*, 3(4):261–274, 1994.

[IN16] Masaharu Ishikawa and Keisuke Nemoto. Construction of spines of two-bridge link complements and upper bounds of their Matveev complexities. *Hiroshima Math. J.*, 46(2):149–162, 2016.

[JO84] William Jaco and Ulrich Oertel. An algorithm to decide if a 3-manifold is a Haken manifold. *Topology*, 23(2):195–209, 1984.

[JR03] William Jaco and J. Hyam Rubinstein. 0-efficient triangulations of 3-manifolds. *J. Differential Geom.*, 65(1):61–168, 2003.

[JR06] William Jaco and J. Hyam Rubinstein. Layered-triangulations of 3-manifolds, 2006. arXiv:0603601.

[JRST20a] William Jaco, Hyam Rubinstein, Jonathan Spreer, and Stephan Tillmann. On minimal ideal triangulations of cusped hyperbolic 3-manifolds. *J. Topol.*, 13(1):308–342, 2020.

[JRST20b] William Jaco, J. Hyam Rubinstein, Jonathan Spreer, and Stephan Tillmann.

$\mathbb{Z}_2$-Thurston norm and complexity of 3-manifolds, II. *Algebr. Geom. Topol.*, 20(1):503–529, 2020.

[JRST25] William Jaco, Joachim Hyam Rubinstein, Jonathan Spreer, and Stephan Tillmann. Complexity of 3-manifolds obtained by Dehn filling. *Algebr. Geom. Topol.*, 25(1):301–327, 2025.

[JRT09] William Jaco, Hyam Rubinstein, and Stephan Tillmann. Minimal triangulations for an infinite family of lens spaces. *J. Topol.*, 2(1):157–180, 2009.

[JRT11] William Jaco, J. Hyam Rubinstein, and Stephan Tillmann. Coverings and minimal triangulations of 3-manifolds. *Algebr. Geom. Topol.*, 11(3):1257–1265, 2011.

[JRT13] William Jaco, J. Hyam Rubinstein, and Stephan Tillmann. $\mathbb{Z}_2$-Thurston norm and complexity of 3-manifolds. *Math. Ann.*, 356(1):1–22, 2013.

[Kne29] Hellmuth Kneser. Geschlossene flächen in dreidimensionalen mannigfaltigkeiten. *Jahresber. Deut. Math. Ver.*, 38:248–260, 1929.

[Lac04] Marc Lackenby. The volume of hyperbolic alternating link complements. *Proc. London Math. Soc.*, 88(1):204–224, 2004. With an appendix by Ian Agol and Dylan Thurston.

[LST08] Feng Luo, Saul Schleimer, and Stephan Tillmann. Geodesic ideal triangulations exist virtually. *Proc. Amer. Math. Soc.*, 136(7):2625–2630, 2008.

[Mah10] Joseph Maher. Random Heegaard splittings. *J. Topol.*, 3(4):997–1025, 2010.

[Mat88] S. V. Matveev. The complexity of three-dimensional manifolds and their enumeration in the order of increasing complexity increase. *Dokl. Akad. Nauk SSSR*, 301(2):280–283, 1988.

[Mat90] Sergei V. Matveev. Complexity theory of three-dimensional manifolds. *Acta Appl. Math.*, 19(2):101–130, 1990.

[Mat07] Sergei Matveev. *Algorithmic Toplogy and Classification of 3–Manifolds*, volume 9 of *Algorithms and Computation in Mathematics*. Springer Berlin, Heidelberg, 2 edition, [2007] ©2007.

[Men84] W. Menasco. Closed incompressible surfaces in alternating knot and link complements. *Topology*, 23(1):37–44, 1984.

[Mil82] John Milnor. Hyperbolic geometry: the first 150 years. *Bull. Amer. Math. Soc. (N.S.)*, 6(1):9–24, 1982.

[Moi52] Edwin E. Moise. Affine structures in 3-manifolds. V. The triangulation theorem and Hauptvermutung. *Ann. of Math. (2)*, 56:96–114, 1952.

[Moi54] Edwin E. Moise. Affine structures in 3-manifolds. VIII. Invariance of the knot-types; local tame imbedding. *Ann. of Math. (2)*, 59:159–170, 1954.

[Mos68] G. D. Mostow. Quasi-conformal mappings in n-space and the rigidity of hyperbolic space forms. *Inst. Hautes Études Sci. Publ. Math.*, (34):53–104, 1968.

[MP01] Bruno Martelli and Carlo Petronio. Three-manifolds having complexity at most 9. *Experiment. Math.*, 10(2):207–236, 2001.

[MS74] S. V. Matveev and V. V. Savvateev. Three-dimensional manifolds having simple special spines. *Colloq. Math.*, 32:83–97, 1974.

[MS25] James Morgan and Jonathan Spreer. On the complexity of 2-bridge link complements, 2025. arXiv:2406.09629.

[MT] James Morgan and Stephan Tillmann. A combinatorial thick-thin decomposition of closed irreducible 3–manifolds with non-trivial $\mathbb{Z}_2$–cohomology. (In preparation).

[MT20] S. V. Matveev and V. V. Tarkaev. Recognition and tabulation of 3-manifolds up to complexity 13. *Chebyshevskiĭ Sb.*, 21(2):290–300, 2020.

[Nak17] Kei Nakamura. The complexity of prime 3-manifolds and the first $\mathbb{Z}_{/2\mathbb{Z}}$-cohomology of small rank, 2017. arXiv:1712.02607.

[Nim23] Barbara Nimershiem. Geometric triangulations of a family of hyperbolic 3-braids. *Algebr. Geom. Topol.*, 23(9):4309–4348, 2023.

[Pac91] Udo Pachner. P.L. homeomorphic manifolds are equivalent by elementary shellings. *European J. Combin.*, 12(2):129–145, 1991.

[Pra73] Gopal Prasad. Strong rigidity of $\mathbf{Q}$-rank 1 lattices. *Invent. Math.*, 21:255–286, 1973.

[PSS25] Anna Parlak, Saul Schleimer, and Henry Segerman. veering x.y, code for studying taut and veering ideal triangulations. https://github.com/henryseg/Veering, 2025.

[Pur20] Jessica S. Purcell. *Hyperbolic knot theory*, volume 209 of *Graduate Studies in Mathematics*. American Mathematical Society, Providence, RI, © 2020.

[PV09] Carlo Petronio and Andrei Vesnin. Two-sided bounds for the complexity of cyclic branched coverings of two-bridge links. *Osaka J. Math.*, 46(4):1077–1095, 2009.

[Riv94] Igor Rivin. Euclidean structures on simplicial surfaces and hyperbolic volume. *Ann. of Math. (2)*, 139(3):553–580, 1994.

[RST24] J. Hyam Rubinstein, Jonathan Spreer, and Stephan Tillmann. A new family of minimal ideal triangulations of cusped hyperbolic 3-manifolds. In *2021–2022 MATRIX annals*, volume 5 of *MATRIX Book Ser.*, pages 5–28. Springer, Cham, [2024] ©2024.

[Rub78] J. Hyam Rubinstein. One-sided Heegaard splittings of 3-manifolds. *Pacific J. Math.*, 76(1):185–200, 1978.

[ST80] Herbert Seifert and William Threlfall. *Seifert and Threlfall: a textbook of topology*. Pure and Applied Mathematics 89. Academic Press, New York-London, 1980. (Translated from the German edition of 1934 by Michael A. Goldman).

[SW95] Makoto Sakuma and Jeffrey Weeks. Examples of canonical decompositions of hyperbolic link complements. *Japan. J. Math. (N.S.)*, 21(2):393–439, 1995.

[Thi10] Morwen Thistlethwaite. Cusped hyperbolic manifolds with 8 tetrahedra. https://web.math.utk.edu/~mthistle/8tet/, 2010.

[Tho25] Em K. Thompson. Triangulations of the ‘magic manifold’ and families of census knots, 2025. arXiv:2503.06198.

[Thu80] William P Thurston. The geometry and topology of 3-manifolds. *Lecture Notes*, 1980. Princeton University.

[Thu86] William P. Thurston. A norm for the homology of 3-manifolds. *Mem. Amer. Math. Soc.*, 59(339):i–vi and 99–130, 1986.

[Til08] Stephan Tillmann. Normal surfaces in topologically finite 3-manifolds. *Enseign. Math. (2)*, 54(3-4):329–380, 2008.

[Tol98] Jeffrey L. Tollefson. Normal surface Q-theory. *Pacific J. Math.*, 183(2):359–374, 1998.

[Tsv14] Anastasiia Tsvietkova. Exact volume of hyperbolic 2-bridge links. *Communications in Analysis and Geometry*, 22(5):881–896, 2014.

[WS33] C. Weber and H. Seifert. Die beiden Dodekaederräume. *Math. Z.*, 37(1):237–253, 1933.